

https://dspace.org/

Removal of hydrogen fluoride from gas streams

Rampersadh, Pradish

2006-11-03T09:10:03Z
http://hdl.handle.net/10539/1601

Downloaded from a DSpace repository. https://dspace.org/

Removal of hydrogen fluoride from gas streams

Pradish Rampersadh

‘A thesis submitted to the Faculty of Science, University of Witwatersrand, Johannesburg, in fulfilment of the requirements for the degree of Doctor of Philosophy.’

Johannesburg, October 2005

DECLARATION

I declare that this thesis is my own work and that any technical and industrial assistance has been acknowledged.

It is being submitted for the Degree of Doctor of Philosophy in the University of Witwatersrand, Johannesburg. It has not been submitted before for any degree or examination in any other University.

_____
Pradish Rampersadh

_____ day of _____ 2005

Abstract

The removal of hydrogen fluoride (HF) from fluorine (F_2) and other media, *e.g.* inorganic and organic compounds, is normally achieved by adsorbing HF onto sodium fluoride (NaF). The aim of this study was to assess alternative adsorbents for the removal of HF in the gas phase. It deals more specifically with the sorption of HF by inorganic compounds, ion exchange resins, and carbon based materials. Further the study can be classified as a thermogravimetric study as this was the principle analytical tool used in this investigation. This study also aims to address some of the controversy surrounding the removal of HF by calcium salts.

Firstly, commercial calcium salts (*viz*. CaF_2, $Ca(OH)_2$, $CaCl_2$ and $CaSO_4$) were assessed for HF removal in the presence of fluorine. Other inorganic adsorbent were also investigated *e.g*. mixtures of NaF with other metal fluorides and an aluminophosphate molecular sieve. It was noted that most of the calcium salts do have a capacity for HF, but can release their anions as impurities in the gas streams. However, the other inorganic adsorbents, including CaF_2 did not have an HF adsorbtion capacity.

Secondly polymeric resins were assessed for HF removal in non-fluorine environments, in particular, a perfluorinated resin, a polyacrylate and a series of commercial ion exchange resins. Most of the polymeric material did have a HF capacity, however the weak base acrylic resins has the best capacity and kinetics for the removal of HF from organic streams.

Finally, considering pure carbon is inert with reference to HF, three types of carbon-based structures were investigated for HF uptake, *viz* activated carbon, carbon molecular sieves and nanotubes. From the results obtained, most forms of carbon do have a capacity for HF. These including impregnated activated carbons.

To my darling Shriya

For all the light you brought into my life.

Acknowledgements

I would like to thank my supervisors, Professor N. J. Coville, University of Witwatersrand and Dr. P. A. B. Carstens, South African Nuclear Energy Corporation Limited (Necsa) for their support, suggestions and guidance.

I also would like to thank the following people:

Dr. Carstens and Dr. A. A. Ponelis (Necsa) for allowing me the opportunity and time to conduct this investigation. Further, to Dr. Carstens, thank you for assisting me by removing the obstacles from my path, for this I am truly grateful.

To Benny Vilakazi, thanks for all the assistance with regard to operating the thermobalance and the insightful discussions it was really appreciated.
To my colleagues, John, Arthur, Johan, Aubrey, Danie, Piet, Carl, Vanessa and Driekus, thanks for guiding me through the World of Fluorine Chemistry. It was a difficult journey and I would not have made it without your assistance and guidance.

Thanks to Dr. A. M. Venter and Niyum for assistance with regard to running and interpretation of the powder XRD.

I would like to thank both the University of Witwatersrand and the Necsa for all assistance received, both financially and with regard to usage of facilities.

Special thanks to my parents for encouraging and supporting me throughout.

And finally, to my wife Niyum, thank you for all the encouragement, support and patience you displayed during this time, it helped carry me.

List of Abbreviations

Å	Angstrom
cm	centimeter
cm^{-1}	inverse centimetre
cm^3	cubic centimetre
CNT	carbon nanotube
eq	equivalence
g	gram
IR	infrared
kJ	kilojoule
kPa	kilopascal
l	litre
meq	milliequivalence
Meq	megaequivalence
min	minute
ml	millilitre
mmol	millimole
mmHg	millimetres of mercury
mol	mole
MPa	megapascal
PPE	personnel protective equipment
ppm	parts per million
PVC	Polyvinyl chloride
R	South African Rand
$	United States Dollar
STP	standard temperature and pressure
T	temperature
wt	weight
℃	degree Celsius
%	percentage

Table of Contents

Abstract..... i
Dedication.....ii
Acknowledgements.....iii
List of Abbreviations.....iv
Table of Contents..... v
List of Figures x
List of Tables xix

Chapter 1 1

Introduction 1
1.1. Introduction 1
1.2. Hydrogen Fluoride 2
1.2.1. Discovery of hydrogen fluoride 2
1.2.2. Industrial synthesis 3
1.2.3. Impurities in hydrogen fluoride 5
1.2.4. Recent developments in hydrogen fluoride production 6
1.2.5. Physical properties of hydrogen fluoride 8
1.2.6. Pelchem hydrogen fluoride 10
1.2.7. Uses 10
1.2.8. Handling of anhydrous hydrogen fluoride 11
1.2.9.Personnel protective equipment 12
1.3. Fluorine 12
1.3.1. Production of fluorine 13
1.3.2. Impurities in fluorine 13
1.3.3. Impurities in Pelchem fluorine 14
1.3.4. Adsorption of hydrogen fluoride onto metal fluorides 15
1.4. Removal of hydrogen fluoride from organics 16
1.5. Characteristics of ideal hydrogen fluoride adsorber 18
1.6. Checklist for suitability of adsorbers..... 18

1.7. Thermogravimetry 20
1.7.1.Modifications to the thermogravimetric analyser 21
1.7.2. Example of typical thermogravimetric result 23
1.8. References 26

Chapter 2 30

Inorganic salts and complexes 30
2.1. Introduction 30
2.2. Literature survey 31
2.2.1. Calcium fluoride – hydrogen fluoride interaction 31
2.2.2. Adsorption studies 33
2.2.3. Calcium fluoride crystal surface chemistry 36
2.2.4. Methods of activation and regeneration 37
2.2.5. Adsorption separation by zeolites 38
2.2.6. Aluminophosphate molecular sieves 39
2.2.7. Adsorption properties of aluminophosphate molecular sieves 40
2.2.8. Interaction of aluminophosphate molecular sieves with HF 40
Results and Discussion 42
2.3. Uptake of hydrogen fluoride by calcium fluoride 42
2.3.1. Assessment of commercial calcium fluoride 42
2.3.2. Influence of surface area on hydrogen fluoride uptake 46
2.3.3. Crystallization of calcium fluoride and its effect on hydrogen fluoride uptake 48
2.3.4. Fluorination of calcium and its effect on hydrogen fluoride uptake 50
2.3.5. Fluorination of calcium fluoride at different temperatures and its effect on hydrogen fluoride uptake 51
2.4. Uptake of hydrogen fluoride by fluorinated and un-fluorinated calcium salts 52

2.4.1. Calcium hydroxide 52
2.4.2. Calcium chloride 56
2.4.3. Calcium sulphate 58
2.5. Uptake of hydrogen fluoride by sodium fluoride-metal fluoride mixtures 63
2.6. Exposure of AlPO to hydrogen fluoride and fluorine 68
2.6.1. Hydrogen fluoride exposure 68
2.6.2. Fluorine exposure 71
2.6.3. HF exposure at elevated temperatures 71
2.6.4. Pre-treatment at elevated temperatures 72
2.7. Experimental 75
2.8. References 79

Chapter 3 82

Resins 82
3.1. Introduction 82
3.2. Literature survey 82
Results and Discussion 89
3.3. Uptake of hydrogen fluoride by Nafion® Superacid Resin 89
3.4. Uptake of hydrogen fluoride by sodium polyacrylate 92
3.5. Ion exchange resins 94
3.6. Initial tests 96
3.7. Uptake of hydrogen fluoride by various resins 100
3.8. Effects of changing the resin cation/ anion 104
3.9. Mechanism of hydrogen fluoride uptake 117
3.9.1. Influence of the polymeric backbone 117
3.9.2. Effect of the acidic and basic functional groups 118
3.9.3. Amine chemistry 120
3.9.4. Exchange capacity of resins 124
3.10. Stability of resins upon multiple hydrogen fluoride exposures 128
3.11. Hydrogen fluoride uptake as a function of temperature 134

3.12. Hydrogen fluoride uptake at lower acid concentrations 136
3.13. Hydrogen fluoride uptake by non-functional ion exchange resins . 142
3.14. Separation of hydrogen fluoride from organics 148
3.15. Uptake of other acidic and basic gases by ion exchange resins ... 155
3.16. Experimental 157
3.17. References 163

Chapter 4 166

Carbon structures 166
4.1. Introduction 166
4.2. Literature survey 166
4.2.1. Activated carbon 166
4.2.2. Carbon molecular sieves 170
4.2.3. Carbon nanotubes 171
Results and Discussion 172
4.3. Activated carbons 172
4.3.1. Exposure of activated carbons to hydrogen fluoride 173
4.3.2. Sodium fluoride adsorption 177
4.3.3. Sodium hydroxide adsorption 180
4.3.4. Nitric acid oxidation 182
4.3.5. Ion exchange 185
4.4. Carbon molecular sieves 189
4.5. Carbon nanotubes 191
4.6. Experimental 196
4.7. References 199

Chapter 5 201

Conclusion 201
5.1. Introduction 201
5.2. Checklist for suitability of adsorbers 201

5.3. Sodium fluoride 203
5.4. Inorganic salts 204
5.5. Aluminophosphates 205
5.6. Resins 206
5.7. Carbon structures 208
5.8. References 210

Appendix 1 211

Appendix 2 222

List of Figures

Chapter 1

Figure 1.1: Thermogravimetric curve of Amberlite IRA 68 after exposure to a 10% HF/N_2 mixture 23

Chapter 2

Figure 2.1: Interaction between CaF_2 and HF 32
Figure 2.2:Thermogravimetric curve for CaF_2 (BDH) after exposure to 10% HF/N_2 at room temperature 43
Figure 2.3:Thermogravimetric curve for CaF_2 (Saarchem) after exposure to 10% HF/N_2 at room temperature 43
Figure 2.4:Thermogravimetric curve for the decomposition product of $CaSiF_6 \cdot 2H_2O$ which is followed by the exposure of the sample to 10% HF/N_2 at room temperature 44
Figure 2.5:Thermogravimetric curve for the uptake of HF by NaF on exposure to a 10% HF/N_2 mixture 46
Figure 2.6: Uptake of HF by CaF_2 crystallized from water (50℃) 49
Figure 2.7: Uptake of HF by CaF_2 crystallized from water (Boiling) 49
Figure 2.8: Uptake of HF by CaF_2 that was exposed to F_2 50
Figure 2.9: Fluorination of $Ca(OH)_2$ with F_2 followed by HF uptake 53
Figure 2.10: Attempted fluorination of $Ca(OH)_2$ with HF 54
Figure 2.11: Uptake of HF by $Ca(OH)_2$ 55
Figure 2.12: Uptake of HF by $CaCl_2$ 56
Figure 2.13: Fluorination of $CaCl_2$ with F_2 and HF uptake 57
Figure 2.14: Uptake of HF by $CaSO_4$ 58
Figure 2.15: Uptake of HF by $CaSO_4$ possibly surface fluorinated in a Monel reactor 60
Figure 2.16: Fluorination of $CaSO_4$ by F_2 and HF uptake 61
Figure 2.17: Uptake of HF by $NaMgF_3$ 66

Figure 2.18: Uptake of HF by another $NaMgF_3$ sample 67
Figure 2.19: Thermogravimetric curve of AlPO-5 after exposure to a 10% HF/N_2 mixture 69
Figure 2.20: Thermogravimetric curve of AlPO-5 after exposure to a 10% HF/N_2 mixture 70
Figure 2.21: Thermogravimetric curve of AlPO-5 after exposure to a 10% F_2/N_2 mixture 71
Figure 2.22: Thermogravimetric curve of AlPO-5 after exposure to a 10% F_2/N_2 mixture at 250℃ 72
Figure 2.23: Thermogravimetric curve of AlPO-5, preheated to 320℃, thereafter exposure to a 10% HF/N_2 mixture 73
Figure 2.24: Thermogravimetric curve of AlPO-5, preheated to 400℃ thereafter exposure to a 10% HF/N_2 mixture 73

Chapter 3

Figure 3.1:Structure of Nafion® Superacid Resin 83
Figure 3.2: Mechanism of SO_2 uptake by FFA-1..... 87
Figure 3.3: Thermogravimetric curve for the interaction of Nafion® (Aldrich) with 10% HF/N_2 (Pre-dried at 150℃ for 2 hours).... 89
Figure 3.4: Thermogravimetric curve for the interaction of Nafion® (Ion Power) with 10% HF/N_2 (Pre-dried at 150 ℃ for 2 hours)..... 90
Figure 3.5: Thermogravimetric curve for the interaction of Nafion® with 10% HF/N_2 (Pre-dried to the 0:1 state)..... 91
Figure 3.6: Thermogravimetric curve for the interaction of Nafion® with 10% HF/N_2 (Pre-dried to the 1:1 state)..... 92
Figure 3.7: Thermogravimetric curve for the interaction of Sodium polyacrylate with 10% HF/N_2..... 93
Figure 3.8: Schematic drawing of various resins..... 96
Figure 3.9: Thermogravimetric curve of Amberlite IRC 50H after exposure to a 10% HF/N_2 mixture..... 97

Figure 3.10: Thermogravimetric curve of Amberlite IR 120H after exposure to a 10% HF/N_2 mixture 98
Figure 3.11: Thermogravimetric curve of Dowex 1x8 after exposure to a 10% HF/N_2 mixture 98
Figure 3.12: Thermogravimetric curve of Amberlite CG 400Cl after exposure to a 10% HF/N_2 mixture 99
Figure 3.13: Thermogravimetric curve of Amberlite IR 120H after exposure to a 10% HF/N_2 mixture 211
Figure 3.14: Thermogravimetric curve of Amberlite IR 120Na after exposure to a 10% HF/N_2 mixture 211
Figure 3.15: Thermogravimetric curve of Amberjet 1200H after exposure to a 10% HF/N_2 mixture 212
Figure 3.16: Thermogravimetric curve of Bio-Rad AG 50Wx4 after exposure to a 10% HF/N_2 mixture 212
Figure 3.17: Thermogravimetric curve of Dowex 50W x 8 after exposure to a 10% HF/N_2 mixture 213
Figure 3.18: Thermogravimetric curve of Dowex HCR-W2 after exposure to a 10% HF/N_2 mixture 213
Figure 3.19: Thermogravimetric curve of Amberlite IRC 50H after exposure to a 10% HF/N_2 mixture 214
Figure 3.20: Thermogravimetric curve of Amberlite IRC 86 after exposure to a 10% HF/N_2 mixture 214
Figure 3.21: Thermogravimetric curve of Lewatit CNP LF after exposure to a 10% HF/N_2 mixture 215
Figure 3.22: Thermogravimetric curve of Lewatit CNP 80 after exposure to a 10% HF/N_2 mixture 215
Figure 3.23: Thermogravimetric curve of Dowex MAC 3 after exposure to a 10% HF/N_2 mixture 216
Figure 3.24: Thermogravimetric curve of Amberlite IRA 458Cl after exposure to a 10% HF/N_2 mixture 216
Figure 3.25: Thermogravimetric curve of Bio-Rad AG 1 after exposure to a 10% HF/N_2 mixture 217

Figure 3.26: Thermogravimetric curve of Bio-Rad AG 2 after exposure to a 10% HF/N_2 mixture 217
Figure 3.27: Thermogravimetric curve of Dowex 21K after exposure to a 10% HF/N_2 mixture 218
Figure 3.28: Thermogravimetric curve of Lewatit MP 500 after exposure to a 10% HF/N_2 mixture 218
Figure 3.29: Thermogravimetric curve of Dowex Marathon A after exposure to a 10% HF/N_2 mixture 219
Figure 3.30: Thermogravimetric curve of Amberlite IRA 67 after exposure to a 10% HF/N_2 mixture 219
Figure 3.31: Thermogravimetric curve of Amberlite IRA 68 after exposure to a 10% HF/N_2 mixture 220
Figure 3.32: Thermogravimetric curve of Amberlite IR 92 RF after exposure to a 10% HF/N_2 mixture 220
Figure 3.33: Thermogravimetric curve of Lewatit MP62 after exposure to a 10% HF/N_2 mixture 221
Figure 3.34: Thermogravimetric curve of Lewatit MP 64 after exposure to a 10% HF/N_2 mixture 221
Figure 3.35: Thermogravimetric curve of Amberlite IR 120H (Na exchanged) after exposure to a 10% HF/N_2 mixture .. 105
Figure 3.36: Thermogravimetric curve of Amberlite IR 120Li after exposure to a 10% HF/N_2 mixture 106
Figure 3.37: Thermogravimetric curve of Amberlite IR 120K after exposure to a 10% HF/N_2 mixture 107
Figure 3.38: Thermogravimetric curve of Amberlite IR 120Ca after exposure to a 10% HF/N_2 mixture 108
Figure 3.39: Thermogravimetric curve of Amberlite IR 120Al after exposure to a 10% HF/N_2 mixture 109
Figure 3.40: Thermogravimetric curve of Bio-Rad 50W x 4 (Na) after exposure to a 10% HF/N_2 mixture 110
Figure 3.41: Thermogravimetric curve of Lewatit CNP LF (Na) after exposure to a 10% HF/N_2 mixture 111

Figure 3.42: Thermogravimetric curve of Dowex MAC 3 (Na) after exposure to a 10% HF/N_2 mixture 111
Figure 3.43: Thermogravimetric curve of Lewatit MP 500 (OH) after exposure to a 10% HF/N_2 mixture 112
Figure 3.44: Thermogravimetric curve of Amberlite IRA 458(OH) after exposure to a 10% HF/N_2 mixture 113
Figure 3.45: Thermogravimetric curve of Dowex Marathon A (Cl) after exposure to a 10% HF/N_2 mixture 114
Figure 3.46: Thermogravimetric curve of Dowex Marathon A (F) after exposure to a 10% HF/N_2 mixture 114
Figure 3.47: Thermogravimetric curve of Amberlite IRA 67(Cl) after exposure to a 10% HF/N_2 mixture 115
Figure 3.48: Thermogravimetric curve of Amberlite IR 120Na after exposure to a 10% HF/N_2 mixture 119
Figure 3.49: Schematic of co-ordination of water to tertiary and secondary amine. 122
Figure 3.50: Thermogravimetric curve of Amberlite IRA 67 after exposure to a 10% HF/N_2 mixture 129
Figure 3.51: Thermogravimetric curve of Amberlite IRA 68 (OH) after exposure to a 10% HF/N_2 mixture 130
Figure 3.52: Thermogravimetric curve of Lewatit MP 64 (OH) after exposure to a 10% HF/N_2 mixture 131
Figure 3.53: Thermogravimetric curve of Amberlite IR 120Na after exposure to a 10% HF/N_2 mixture. 132
Figure 3.54: Thermogravimetric curve of Bio-Rad AG 50W x 4(Na) after exposure to a 10% HF/N_2 mixture 134
Figure 3.55: Thermogravimetric curve of Lewatit CNP LF (Na) after exposure to a 10% HF/N_2 mixture 134
Figure 3.56: Graph indicating percentage uptake of HF by Amberlite IR 67 as a function of temperature 135
Figure 3.57: Thermogravimetric curve of Amberlite IRA 67 from a 0.68% HF/N_2 mixture 222

Figure 3.58: Thermogravimetric curve of Amberlite IRA 67 from a 1.2% HF/N_2 mixture 222
Figure 3.59: Thermogravimetric curve of Amberlite IRA 67 from 2% HF/N_2 mixture 223
Figure 3.60: Thermogravimetric curve of Amberlite IR 120Na from a 0.68% HF/N_2 mixture 223
Figure 3.61: Thermogravimetric curve of Amberlite IR 120Na from a 1.2% HF/N_2 mixture 224
Figure 3.62: Thermogravimetric curve of Amberlite IR 120Na from a 2% HF/N_2 mixture 224
Figure 3.63: Thermogravimetric curve of Amberlite IRA 458Cl from a 0.68% HF/N_2 mixture 225
Figure 3.64: Thermogravimetric curve of Amberlite IRA 458Cl from a 1.2% HF/N_2 mixture 225
Figure 3.65: Thermogravimetric curve of Amberlite IRA 458Cl from a 2% HF/N_2 mixture 226
Figure 3.66: Thermogravimetric curve of Amberlite IRC 86 from a 0.68% HF/N_2 mixture 226
Figure 3.67: Thermogravimetric curve of Amberlite IRC 86 from a 1.2% HF/N_2 mixture 227
Figure 3.68: Thermogravimetric curve of Amberlite IRC 86 from 2% HF/N_2 mixture 227
Figure 3.69: Graph of %HF taken up by Amberlite IRA 67 as a function of percentage delivered. 137
Figure 3.70: Graph of %HF taken up by Amberlite IRA 458 Cl as a function of percentage delivered. 138
Figure 3.71: Thermogravimetric curve of the uptake of HF by Amberlite IRA 67 from 0.059% HF/N_2 mixture 228
Figure 3.72: Thermogravimetric curve of Amberlite IRA 67 from 0.099% HF/N_2 mixture 228
Figure 3.73: Thermogravimetric curve of Amberlite IRA 67 from 0.162% HF/N_2 mixture 229

Figure 3.74: Thermogravimetric curve of Amberlite IRA 458Cl from a 0.059% HF/N_2 mixture 229
Figure 3.75: Thermogravimetric curve of Amberlite IRA 458Cl from a 0.099% HF/N_2 mixture 230
Figure 3.76: Thermogravimetric curve of Amberlite IRA 458Cl from a 0.162% HF/N_2 mixture 230
Figure 3.77: Graph of %HF taken up by Amberlite IRA 67 as a function of percentage delivered. 140
Figure 3.78: Graph of %HF taken up by Amberlite IRA 458 Cl as a function of percentage delivered 141
Figure 3.79: Thermogravimetric curve of Amberlite XAD 4 from 10% HF/N_2 mixture 143
Figure 3.80: Thermogravimetric curve of Amberlite XAD 16 from 10% HF/N_2 mixture 143
Figure 3.81: Thermogravimetric curve of Amberlite XAD 7HP from 10% HF/N_2 mixture 144
Figure 3.82: Thermogravimetric curve of Amberlite XAD 7 HP from 10% HF/N_2 mixture 145
Figure 3.83: Thermogravimetric curve of Amberlite XAD 4 from 10% HF/N_2 mixture 145
Figure 3.84: Thermogravimetric curve of Polystyrene powder from 10% HF/N_2 mixture 146
Figure 3.85: Calibration graph for HF between 0 and 70 kPa. 150
Figure 3.86: Calibration graph for HF indication quantity of HF adsorbed on window. 151
Figure 3.87: Schematic drawing of HF adsorption system 161

Chapter 4

Figure 4.1: Thermogravimetric curve of Activated Carbon F200 after exposure to a 10% HF/N_2 mixture 174
Figure 4.2: Thermogravimetric curve of Activated Carbon IVP after

exposure to a 10% HF/N_2 mixture 174
Figure 4.3: Thermogravimetric curve of Activated Carbon F200 after exposure to a 10% HF/N_2 mixture 176
Figure 4.4: Thermogravimetric curve of Activated Carbon F200 soaked in 0.1M NaF after exposure to a 10% HF/N_2 mixture 177
Figure 4.5: Thermogravimetric curve of Activated Carbon F200 soaked in 0.5M NaF after exposure to a 10% HF/N_2 mixture 178
Figure 4.6: Thermogravimetric curve of Activated Carbon F200 soaked in 1M NaF after exposure to a 10% HF/N_2 mixture 178
Figure 4.7: Thermogravimetric curve of Activated Carbon F200 soaked in 2M NaF after exposure to a 10% HF/N_2 mixture 179
Figure 4.8: Thermogravimetric curve of Activated Carbon F200 soaked in 5M NaF after exposure to a 10% HF/N_2 mixture 179
Figure 4.9: Thermogravimetric curve of Activated Carbon F200 soaked in 1M NaOH after exposure to a 10% HF/N_2 mixture 181
Figure 4.10: Reaction between surface oxygen groups on activated carbon and NaOH. 182
Figure 4.11: Thermogravimetric curve of Activated Carbon F200 treated in 0.5 M HNO_3 after exposure to a 10% HF/N_2 mixture 183
Figure 4.12: Thermogravimetric curve of Activated Carbon F200 treated in conc. HNO_3 after exposure to a 10% HF/N_2 mixture..... 183
Figure 4.13: Thermogravimetric curve of Activated Carbon F200 treated in boiling HNO_3 after exposure to a 10% HF/N_2 mixture... 184
Figure 4.14: Thermogravimetric curve of Activated Carbon F200 soaked in 1M NaF after exposure to a 10% HF/N_2 mixture..... 185
Figure 4.15: Thermogravimetric curve of Activated Carbon F200 soaked in 1M NH_4OH after exposure to a 10% HF/N_2 mixture..... 186
Figure 4.16: Thermogravimetric curve of Activated Carbon IVP after repeated exposure to a 10% HF/N_2 mixture 188
Figure 4.17: Thermogravimetric curve of Carbosieve CMS after exposure to a 10% HF/N_2 mixture 189
Figure 4.18: Thermogravimetric curve of CMS 10304 after exposure to a

10% HF/N_2 mixture 190
Figure 4.19: Thermogravimetric curve of a Herringbone carbon nanofibre after exposure to a 10% HF/N_2 mixture 192
Figure 4.20: Thermogravimetric curve of a nanotubular carbon nanotube after exposure to a 10% HF/N_2 mixture 192
Figure 4.21: Thermogravimetric curve of a Herringbone carbon nanofibre after exposure to a 10% HF/N_2 mixture at 70℃ 193
Figure 4.22: Thermogravimetric curve of a Herringbone carbon nanofibre after exposure to a 10% HF/N_2 mixture at 180℃ 194
Figure 4.23: Thermogravimetric curve of a nanotubular carbon nanotube after exposure to a 10% HF/N_2 mixture at 70℃ 195

List of Tables

Chapter 2

Table 2.1: Table of solubility of CaF_2 and NaF in HF at various temperatures 33
Table 2.2: Mass changes for the uptake in 10 % HF/N_2 by CaF_2 44
Table 2.3: Mass changes and surface areas for the uptake of 10 % HF/N_2 by CaF_2 47
Table 2.4: Table of uptake of HF, from a 10% HF/N_2 on the Thermogravimetric analyser, by CaF_2 51
Table 2.5: Percentage uptake of HF for different fluorination temperatures. 62
Table 2. 6: Surface area data for calcium salts 63
Table 2. 7: Powder diffraction data for $NaMgF_3$ 65

Chapter 3

Table 3. 1: Amount of HF present in perfluoroheptane after treatment ... 94
Table 3. 2: Summary of percentage HF taken up by various resins 101
Table 3. 3: Table of percentage HF taken up by the different ionic forms of Amberlite IR 120H 107
Table 3. 4: Table of percentage uptake of HF by the various ion exchange resins 116
Table 3. 5: pKa values for various substituted amines 122
Table 3. 6: HF uptake based on exchange capacity *vs*. actual uptake .. 126
Table 3. 7: HF uptake based on exchange capacity *vs*. actual uptake .. 128
Table 3. 8: Percentage HF adsorbed by Amberlite IRA 67 at different temperatures 135
Table 3. 9: Table of % HF uptake for low concentrations of HF 137
Table 3. 10: Table of % HF uptake for low concentrations of HF 139
Table 3. 11: Table of % HF uptake for Amberlite IRA 458 Cl 141

Table 3. 12: Table of properties and HF uptake by Ion Exchange Resins 142
Table 3. 13: Table of experimental data for HF adsorption system 161

Chapter 4

Table 4.1: Uptake of HF by oxidised ion exchanged carbons..... 186

Chapter 1

Introduction

1.1. Introduction

This study focuses on the sorption of hydrogen fluoride (HF) by various materials. It deals more specifically with the sorption of HF by inorganic compounds, polymers, ion exchange resins, carbon based materials and aluminophosphates. The study can be classified as a thermogravimetric study as this was the principle analytical tool used in the investigation.

The initial aim of this study was to assess alternative adsorbents for the removal of HF from fluorine (F_2). Although technology is in place to achieve this, certain inherent problems in this technology have warranted this investigation. Further, the removal of HF from other media, *e.g*. organics is also an important industrial problem and the study also includes the uptake of HF by materials that show promise as adsorbents for HF in non F_2 environments.

This study also aims to address, some of the controversy surrounding the removal of HF. Over the years there have been various claims by workers on HF adsorption and this study aims to verify and if possible confirm some of the earlier studies.

Chapter 1 contains an introduction to F_2 and HF chemistry and aims to introduce some of the problems that are addressed in this thesis. Hence the chapter includes information on HF synthesis, and some properties of HF. The uses and dangers of working with this material are also made explicit.

This is followed by a description of the synthesis of F_2 and problems associated with HF removal. The removal of HF from organics will also be

reviewed. The characteristics of adsorbents for gas removal in general will also be discussed. Finally, as the thermogravimetric analyser was the principle analytical tool used in this study, a discussion on the modifications to the industrial analyser used will be presented.

It is important to define two words that are used in the world of HF removal. The first is scrubber and the second adsorber. For this work, the word **scrubber** is defined as "*a material that can remove HF from a gas stream normally via an irreversible chemical reaction.*" This reaction will sometimes release other impurities into the gas stream. An **adsorber**, on the other hand, is "*a material that removes HF from a gas stream, without releasing any other impurities and that can be regenerated back to its original form.*"

Most of this work described in this thesis concentrates on HF adsorbers.

1.2. Hydrogen Fluoride

HF is called the life-blood of the modern fluorochemical industry and historically is the most important compound of F_2. HF was used to etch glass in the 17th century but was only first described in 1813 [1].

1.2.1. Discovery of hydrogen fluoride

Marggraf discovered HF in 1764 while attempting to ascertain the composition of fluorspar, (natural form of CaF_2), by heating it in a glass apparatus with H_2SO_4. He noted the formation of a white saline sublimate and that the glass apparatus was corroded, with holes in several places. In 1771 Scheele repeated Marggraf's experiment and concluded that a peculiar acid (fluor acid) was liberated which united with the lime in fluorspar. The dissolution of the glass apparatus did baffle him and other workers in the field. They did note the formation of silica (SiO_2) and fluorosilic acid (H_2SiF_6). However, it was realized that this was due to the

decomposition of the glass apparatus. This led to the usage of Pb and Sn apparatus in further work.

Later, in 1809, Gay-Lussac and Thénard reported that they had prepared pure and concentrated hydrofluoric acid by heating white fluorspar with concentrated H_2SO_4 and by collecting the vapours in a lead apparatus at 0℃. Their product fumed in air, dissolved glass, had a great affinity for water and caused extraordinary burns on contact with the skin.

In 1813 Davy, investigated the nature of this fluor acid and concluded it was a compound of H_2 with a fourth halogen (the others being Cl_2, Br_2 and I_2). The finding that F_2 was an element was clarified in 1814.

Frémy produced pure anhydrous hydrogen fluoride (AHF) in 1856 and reported that the HF produced by Gay-Lussac and Thénard contained impurities including water. He reacted the HF with KF to form a precipitate of KHF_2. This, he recrystallized several times to remove potassium hexafluorosilicate. Heating this salt produced the anhydrous HF (Equation 1.1).

$$KHF_2 \rightarrow KF + HF_{anhydrous} \qquad (1.1)$$

(AHF = $HF_{anhydrous}$)

During the next decade Gore determined the boiling point, the density and vapour pressure of AHF. Most of the work was conducted in Pt apparatus [1].

1.2.2. Industrial synthesis

Reaction of acid grade fluorspar with concentrated H_2SO_4 in a heated kiln produced AHF. The production process involves reacting fluorspar with

H_2SO_4, and kneading and heating the mixture to between 400℃ and 500℃. This produces HF in the following reaction (Equation 1.2).

$$CaF_2 + H_2SO_4 \rightarrow CaSO_4 + 2HF \qquad (1.2)$$

The product obtained is separated into a low boiling mixture, comprising mostly of HF, and a high boiling mixture comprising mostly of unreacted H_2SO_4, a little HF and water. This separation was performed in a crude gas-washing column. The low boiling fraction is introduced at the bottom of the column and the high boiling fraction in the middle; this results in the H_2SO_4 fraction trapping dust particles in the ascending high temperature HF. Liquid HF is now introduced at the top to wash any H_2SO_4 and water in the rising fraction. High purity HF (99.9%) is then withdrawn from the top of the column.

Next, SO_3 is added to the high boiling fraction. The SO_3 reacts with the residual water, to form H_2SO_4. If not enough SO_3 is added, the water present retards the reaction giving deposits and caking of fluorspar. Excess H_2SO_4 is added to the first step to ensure complete reaction with the fluorspar [2]. One of the other suggested methods to prevent ‘cake’ formation is that the reaction be conducted in a rotary tube furnace, which is divided into different heating zones [3].

Hydrofluoric acid (aqueous HF) can be produced when high purity AHF is diluted with water to the required concentration, (acid always being added to cold water). Commercial hydrofluoric acid is made in the concentration range of 48 to 70% and is shipped in 208 litre drums lined with polyethylene [1]. Necsa transports hydrofluoric that is in the concentration range greater than 60% in 22 litre high-density polyethylene containers. HF that is less than 60% concentrated is transported in 210 litre polyethylene drums [4].

1.2.3. Impurities in hydrogen fluoride

Impurities in HF pose a problem when HF is to be used in chemical reactions. The impurities mostly arise from the trace impurities present in CaF_2. Hence, it is important that one starts with “acid grade” CaF_2, *i.e*. CaF_2 that is at least 98.5 to 99% pure. Some of the impurities present are SiO_2, CaS, PbS, and $CaCO_3$. These impurities can react with H_2SO_4 or HF, to give rise to other impurities as follows (Equations 1.3 -1.5):

$$SiO_2 + 4HF \rightarrow SiF_4 + 2H_2O \qquad (1.3)$$

$$CaCO_3 + H_2SO_4 \rightarrow CaSO_4 + H_2O + CO_2 \qquad (1.4)$$

$$CaS + H_2SO_4 \rightarrow CaSO_4 + H_2S \qquad (1.5)$$

Other impurities include AsF_3, BF_3, and PF_3. In some cases the formation of HF is carried out in a steel vessel, but the steel reactor is also slowly attacked by H_2SO_4 (Equation 1.6).

$$Fe + 2H_2SO_4 \rightarrow FeSO_4 + 2H_2O + SO_2 \qquad (1.6)$$

These impurities cause numerous problems, *e.g*. the H_2O present dilutes the final product and the formation of the various fluorides removes some of the HF formed. The generation of SO_2 and H_2S yields sulphur (equation 1.7); this tends to cause blockages within the plant.

$$SO_2 + 2H_2S \rightarrow 2H_2O + 3S \qquad (1.7)$$

A distillation step removes most of these impurities and as mentioned HF with a purity > 99.9% can be made [5]. However, the removal of these impurities from HF is the subject of ongoing research.

One of the alternative HF purification techniques used is electrolysis. For example, AsF_3 can be electrochemically converted to AsF_5, which has a lower vapour pressure than AsF_3. The AsF_5 can then be separated by distillation [6, 7, 8]. OF_2 has been introduced along with an inert gas, to the HF steams. The OF_2 oxidises and removes some of the inorganic impurities [9]. Passing AHF through a fluoropolymer film can also reduce the AsF_3 content [10].

With reference to water, this can be removed by the addition of F_2, which reacts with the water to produce HF and O_2, (Equation 1.8) [11],

$$2F_2 + 2H_2O \rightarrow O_2 + 4HF \qquad (1.8)$$

1.2.4. Recent developments in hydrogen fluoride production

There has been some development work on the synthesis of HF since HF was first synthesized in the 1850's. The synthesis of HF has been commercialised and most of the synthesis information is found in patents. Some of the most recent patent literature on HF synthesis is reviewed here.

The most common method of making HF is from phosphate rock. Natural phosphate rock is delivered with preheated N_2 to a high temperature plasma. The natural phosphate rock, with a F_2 content of 2.5% is heated to 3770℃ and results in HF formation. There is about 97% fluorine recovery from the phosphate rock [12]. Lamb also invented an apparatus that was capable of extracting HF from the hot gas mixture exhausted from a phosphate rock defluorination kiln. This allows even further recovery of the desired product [13].

HF is also prepared from SiF_4. A mixture of SiF_4 and water vapour is flame hydrolysed to convert it to SiO_2 and HF. This mixture is deliberately cooled to initiate agglomeration of the SiO_2 particles. This has the two-fold effect

of allowing ease of separation and preventing the reverse reaction from taking place. About 95% conversion of SiF_4 to HF takes place [14].

Ehlig, has described an apparatus where AHF is manufactured by dropping small particles of CaF_2 through a reaction zone, counter current to a gas stream containing SO_3, H_2SO_4 and water vapour. The metal fluorides are maintained in free fall for a sufficiently long time such that the reaction can reach completion. $CaSO_4$ is recovered from the bottom and HF from the top of the reactor. This reactor has the advantage that it is of simple design, can be easily sealed and the rate of production can be easily changed without the need for significant equipment modification [15].

HF can also be produced from fluorosilicic acid (H_2SiF_6), a by-product of the manufacture of H_3PO_4 and superphosphate fertilizers. The process consists of reacting H_2SiF_6 with NH_3 to produce aqueous NH_4F and solid SiO_2. The NH_4F is hydrolysed and then converted to $NaHF_2$. Heating the $NaHF_2$, decomposed it to HF gas of 99.9% purity [16].

An alternative to produce HF is by treating fluorspar and fluorapatite with H_2SO_4 and to react the ore as a slurry in fluorosulphonic acid (FSO_3H). The reactions are as follows (Equations 1.9 and 1.10):

$$Ca_3(PO_4)_2 + 3CaF_2 + 6HSO_3F \rightarrow 6CaSO_4 + 2POF_3 + 6HF \qquad (1.9)$$

$$Ca_3(PO_4)_2 + 7CaF_2 + 10HSO_3F + 2H_2O \rightarrow 10CaSO_4 + 2PF_5 + 14HF \qquad (1.10)$$

This results in the co-generation of HF and volatile phosphorus compounds. This method has the advantage in that SiF_4 is not formed, which occurs when H_2SO_4 and SiO_2 rich ores are used (Equation 1.11).

$$2CaF_2 + SiO_2 + 2H_2SO_4 \rightarrow 2CaSO_4 + SiF_4 + 2H_2O \qquad (1.11)$$

Separation of HF and the volatile phosphorus compound is achieved by hydrolysing the phosphorus compound to H_3PO_4 [17]. Another method to remove SiO_2 is to dissolve the HF acid mixture in water, react it with $CaCO_3$ and neutralize the subsequent solution. The reaction yields CaF_2, which can be recycled back to starting material, and a colloid of silicic acid ($SiO_2 \cdot xH_2O$), which can be separated [18].

A further method of forming HF is by the reaction of fluorite with SO_3 and steam as compared to reacting fluorite with H_2SO_4. SO_3 and steam form H_2SO_4 and heat. The advantage is that the heat of reaction drives the HF production process hence removing the need for external heating. A conversion rate of 35 to 90% is achieved. Passage of the reaction mixture into a second reactor with H_2SO_4 allows the reaction to reach completion [19].

1.2.5. Physical properties of hydrogen fluoride

AHF has a freezing point of –83.6℃ and a boiling point of 19.5℃. It has a vapour pressure of 921.4 mmHg and a density of 0.9546 at 25℃. It has a very corrosive action on glass and other apparatus made of silica (Equation 1.12).

$$4HF + SiO_2 \rightarrow SiF_4 + 2H_2O \qquad (1.12)$$

This makes handling HF very difficult. Most work is carried out in a steel or Monel apparatus, making visual observation of HF reactions impossible [20].

One of the other characteristics of HF is the strong hydrogen-fluorine bond. This molecule remains intact to very high temperatures, (only 40%

dissociated at 4000℃). This results in HF having a low ionic character in water although it has a strong acid character.

In terms of acidity, HF is weakly dissociated in water. However, AHF and high aqueous concentrations of HF are very strong acids, *i.e*. HF is a strong Bronsted-Lowry proton doner and on the Hammett acidity scale, H_o approaches a value of –11. This indicates that AHF is in the class of superacids [21].

Another characteristic of HF is its ability to form secondary hydrogen bonds. These hydrogen bonds result in the formation of a polymeric type of structure in the gas, liquid and solid phase. These hydrogen bonds have a marked effect on the properties of HF, as discussed below [21].

Hydrogen bonding in inorganic and organic fluorine compounds is associated with the high electronegativity of the bound fluorine element [1]. Hydrogen bonding persists in the gas phase and results in a large deviation from the ideal gas laws. This accounts for the high boiling point; it is one of the most 'imperfect' gases known.

HF is basically monomolecular above 200℃ but as the temperature is lowered, hydrogen bonding results in chain formation. These chains have varying lengths (Equation 1.13).

$$HF + (HF)_n \rightleftharpoons (HF)_{n+1} \qquad (1.13)$$

Where n = 1 to 5.

These polymeric structures have a linear zigzag configuration and are noted across a large temperature range (-45 to 100°C). However, below 27℃, there appears to be a monomer-dimer-hexamer equilibrium (Equation 1.14).

$$6HF \rightleftharpoons 3(HF)_2 \rightleftharpoons (HF)_6 \qquad (1.14)$$

Also present are cyclic hexamer structures (Equation 1.15);

$$(HF)_6\,(chain) \rightleftharpoons (HF)_6\,(cyclic) \qquad (1.15)$$

These cyclic structures are very stable and increase in concentration in the gas phase with increasing pressure (26 to 100 kPa). However, as the concentration of each of these structures vary, it is not possible to allocate a specific formula for HF *e.g*. H_2F_2 or H_6F_6 to them [21, 22].

Lee quantified this polymerisation in HF by working out a compression factor. He indicated that there are two contributing factors to this compression factor, a chemical and a physical factor. The chemical factor is based on the ratio of associated molecules to that which would be present without association and the physical factor is dependent on critical temperature, pressure and on volume [23].

1.2.6. Pelchem hydrogen fluoride

Pelchem, the chemical manufacturing division of Necsa, which produces 3000 to 3400 tons of HF per annum, supplied the AHF used in all this work. The HF is manufactured by reacting fluorspar with H_2SO_4, on site. This HF is used mainly as an alkylating catalyst in the petrochemical industry and for the production of fluoride chemicals [24].

1.2.7. Uses

Although HF was discovered in the 17th century, the early commercial uses of HF included glass etching, polishing and foundry scale removal. The first bulk manufacture of HF was conducted by Sterling Products Company in 1931 for the manufacture of chlorofluorocarbons to be used

as refrigerants. Other uses of HF include: use as an alkylation catalyst for aviation gasoline, use in the manufacture of UF_4, and use in the synthesis of fluoropolymers and lubricants. The majority of HF produced is used by the fluorocarbon and aluminium industries [1].

1.2.8. Handling of anhydrous hydrogen fluoride

HF inflicts very serious damage to skin and underlying tissue and shortened the lives of many of the original workers who were exposed to HF [1]. Serious inhalation hazards arise when solutions containing greater than 60% HF are used. Symptoms include a burning sensation of the eyes, intolerable burning sensation of the mouth, nose and throat and a deep substernal pain. However, HF can be detected by smell at sub harmful levels and a TLV of 3 ppm or less is recommended. Exposure of the body to fluorides in general must be considered as exposure to HF. Body moisture hydrolyses fluorides to HF. Even F_2 forms HF when exposed to skin moisture.

Treatment of HF exposure is therefore an important criterion when dealing with HF. In the 1920s, Fredenhagen and Wellman suggested calcium gluconate therapy for HF exposure. Pre 1900s HF workers were advised to wear rubber gloves and if the skin was exposed to HF, to wash with water and aqueous NH_3 or another alkali. Plant operators protected themselves against HF fumes with respirators, tying a handkerchief over their mouths and noses and coating their faces with lanolin. Gay-Lussac and Thénard also recommended the use of an alkali wash after they were accidentally exposed to HF and also when they deliberately exposed their skin to HF.

The severe pain associated with HF burns is ascribed to the immobilisation of tissue calcium as CaF_2. Treatment includes injecting a 10% solution of calcium gluconate into and around the burn, or topical

treatment with iced alcohols, aqueous solutions of quaternary ammonium compounds or calcium gluconate gel [25, 26, 27, 28].

After application of the calcium gluconate paste to an affected area, if the area is kept moist and wrapped with, for example, paper towel for a few hours, the resultant damage caused by the HF is reduced when dealing with minor burns [29].

Apart from the visible signs of the effects of HF it is also a human health hazard, being suspected as a cardiovascular, developmental, gastrointestinal, musculoskeletal, neuro, reproductive, respiratory and skin or sense organ toxicant [30]. Chronic exposure to HF results in vomiting, nausea, loss of appetite and diarrhoea or constipation. Fluorosis and hypocalcaemia, which can result in cardiac arrhythmias and death, can be caused by extended HF exposure. However this is still a controversial subject [25, 26, 27, 28].

1.2.9. Personnel protective equipment

In terms of personnel protective equipment (PPE) it is recommended that workers wear safety spectacles, chemical safety goggles, face shields, hats, overalls with sleeves to wrists, long aprons and safety boots when working with HF. All PPE must be made of material resistant to HF *e.g*. PVC [25], or Viton® or neoprene [26].

1.3. Fluorine

Fluorine is the 13th most abundant element in the Earth's crust and was isolated by Henri Moissan on 26th June 1886. Fluorspar is the most important source of F_2 of which 40% is used as a metallurgical flux for the steel industry and most of the remainder used to produce HF [1].

1.3.1. Production of fluorine

Elemental F_2 is produced by the electrolysis of AHF. AHF itself is a non-conductor of electricity, hence, the electrolyte has KF present in it to improve electrical conductance in the form KF·2HF, (38 to 42% HF). The electrolytic cell, which is normally constructed of steel, sometimes with a Monel liner, is operated between 80 to 110℃, the molten temperature of the electrolyte. KF·2HF is used as a fluorine source, as KF·HF has the disadvantage in that it's melting point is too high at 240 - 280℃. F_2 production occurs at the anode, which is normally made of ungraphitised carbon and H_2 production at the cathode, which is made of mild steel. (Equation 1.16)

$$2HF + \text{electrical energy} \rightarrow H_2 + F_2 \qquad (1.16)$$

The use of an electrolyte also reduces the vapour pressure of HF, making it easier to work with, *e.g*. the vapour pressure of HF over KF·2HF at 100℃ is about 6 kPa, whereas HF at 100℃ has a vapour pressure of 1054 kPa [5, 31, 32].

1.3.2. Impurities in fluorine

The F_2 generated in fluorine cells contains about 10% HF. The other impurities present are CF_4, C_2F_6 and OF_2 [33]. These impurities arise from different sources, *e.g*. OF_2 is formed as a result of the moisture content in the HF feed and the carbon impurities are as a result of electrode breakdown in the fluorine cell. The OF_2 content can be kept low by ensuring sufficiently low moisture content in the feed HF. Ensuring that the carbon electrodes are changed on a regular basis controls the CF_4 content. The majority of HF is normally removed by condensation. The condensers are kept at very low temperatures by the use of dry ice (-78℃), by the evaporation of Freon 13 (-85℃), or by the use of a slush made of dry ice and trichloroethylene ($ClCH=CCl_2$) (-57℃). This normally

reduces the HF content substantially, but for some applications, further reduction of the HF content is required. This is achieved by the use of a secondary condensation column, (*e.g*. one cooled with liquid O_2 at -183℃ which removes both HF and CF_4) or a NaF column, which reduces the HF content to at least 0.05% [3, 34].

1.3.3. Impurities in Pelchem fluorine

The F_2 produced at Pelchem has about 8% HF present in it. Passing it through a series of condensers reduces the HF loading to <1%. In the first step two Freon cooled condensers reduce part of the HF load and bring the temperature of the gas mixture down to -80℃. T his mixture is then passed through a cold trap that is cooled to -145℃ with liquid N_2. The HF is thereafter recovered.

Passing this gas mixture through NaF filled columns, kept at 90℃, reduces the HF content further. The NaF is in the form of pellets and is porous to ensure maximum surface area. The exhausted F_2 gas has about 300 ppm HF present in it [35]. (This is based on the formula logP in mmHg = 11.19 – 4292/T for the vapour pressure of HF over $NaHF_2$) [36].

There are problems associated with these methods. The majority of the HF is removed in the liquid N_2 cooled traps. As HF condenses on the walls of this trap, it is coated with solid HF and this reduces the heat transfer. Hence unless the solidified HF is removed on a regular basis, column efficiency is compromised. The net result is higher HF content in the F_2 stream. A problem also arises with the NaF columns; HF reacts with NaF to form $NaHF_2$. This is a solid and heating will release the NaF. However, more HF thereafter adsorbs onto this complex, resulting in polyacid formation (Equation 1.17).

$$NaHF_2 + xHF \rightarrow NaHF_2 \cdot xHF \qquad (1.17)$$

This dissolves the $NaHF_2$ complex resulting in the column sintering. (It was noted that NaF could take up to 4.5 moles of HF per mole of NaF when exposed to a 10% HF/N_2 gas mixture, refer to Chapter 2). Hence, keeping these columns at 90℃ prevents this polyacid formation and column sintering.

A further problem is encountered when the column needs to be regenerated. This is achieved by heating the walls of this column to remove the HF. This poses a problem, as there is a temperature gradient set up from the walls of the column to the inner core. HF desorbed from close to the warmer wall section tends to migrate to the cooler core and re-adsorbs there, resulting in polyacid formation and core sintering. This is prevented by uniformly heating the column to ensure there are no cool areas [35].

1.3.4. Adsorption of hydrogen fluoride onto metal fluorides

Removal of HF can also be achieved by adsorption onto other metal fluorides. Capps studied the adsorption of HF onto metal fluorides in the presence of UF_6 [37]. His aim was to obtain an adsorbent to remove HF from UF_6. He studied the adsorption on the following metal fluorides: BiOF, BiF_3, CoF_2, CoF_3, PbF_2, LiF, MnF_2, KF, NaF and SnF_2. He found that HF adsorbed onto the following fluorides; MnF_2, NaF, LiF and BiOF, of which LiF and BiOF adsorbed HF exclusively [37]. KF is an HF adsorber as KF complexes with HF to give $KF{\cdot}xHF$, with x = 1, 2, 2.5, 3, 4 [38], but Capps mentioned KF can be used as a UF_6 adsorber [37].

The removal of HF and water from F_2 was also achieved by Otsuka who used a mixture of an alkali earth metal hydroxide *e.g*. $Sr(OH)_2$ and iron oxide *e.g*. Fe_3O_4. He found that when he passed a mixture of F_2 with HF (50 ppm) and moisture (200 ppm) through a column consisting of the above mixture, the impurities were removed. This was tested by passing the purified gas stream through a SUS 316 L-EP pipe and checking for

corrosion compared to a standard run. However, he did not quantify the impurities in the off gas. Further, no mention was made of regeneration techniques for the purifying agent [39].

1.4. Removal of hydrogen fluoride from organics

The other area considered in this thesis is the removal of HF from fluorinated organic compounds. Fluorinated organics are formed by the reaction of non-fluorinated organics with HF or F_2, sometimes in the presence of a fluorinating agent. The resultant product normally has HF associated with it and in some cases there is an azeotrope formed between the HF and the fluoroorganic. In the case where azeotropes form, normal distillation does not separate the HF very easily from the organic phase. Removal of the HF is achieved by scrubbing the product stream with water or aqueous alkali. This aqueous scrubbing liquor can then be disposed. This is a rather expensive procedure as it is preferable to recover the HF. This can be achieved for example by using an alkali metal fluoride to adsorb the HF rather than to let it react with a base. The solution used may be anhydrous or aqueous. The HF can then be distilled off [40, 41].

Other methods can also be used to remove HF from organics. These include contacting the mixture with water or with adsorbents such as acids, inorganic fluorides, molecular sieves, membranes *etc*. Some of this work is discussed in later chapters but the following is worth noting here.

Van Der Puy patented a method to separate HF from organics by contacting the organics with a HF binder. The binder was an acid salt comprising of methanesulphonic acid (CH_3SO_3H) and ammonium bifluoride (resulting in ammonium methanesulphonate). What he found was that this binder reduced the HF content of a mixture of HF/ organic from 16.9% down to 0.32 mass %. This method gives excellent results but requires that the binder does not react with the organic [42].

HF can be recovered from the organics by dissolving the HF in water if the organic is not soluble in water. The HF is removed from the water by reacting it with NaF or LiF crystals and regenerating the crystals to obtain HF [43, 44]. HF can also be recovered from an aqueous stream, by heating the stream and contacting the vapour with SO_3 dissolved in H_2SO_4 (oleum) [45, 46], or by using an amine to extract the HF [47, 48].

The separation of water and HF can also be achieved by contacting the mixture with carbon molecular sieves having a pore size of about 3.5 Å. Both HF and water are adsorbed. However, upon regeneration, water comes off at a lower temperature, followed by water free HF at a higher temperature. The carbon molecular sieve reported in the literature is derived from the pyrolysis of acrylonitrile ($H_2C=CHCN$) [49].

Another way of separating HF from organics, especially where an azeotrope is involved is to pass the HF/ organic steam through a semi permeable polymer membrane. The membrane should preferably be partially or fully fluorinated as the HF present may fluorinate it and change the membrane characteristics. Lee used such a membrane to separate HF from HCFC–22. He used a Nafion® membrane, which has SO_3H or SO_3Na functional groups [50]. Tarasenko also studied the use of membranes for HF separation and found similar results [51].

Manzer also noted that when an HF/ organic mixture is cooled to -80℃, a degree of phase separation of the organic phase and HF phase occurred. The HF phase can thereafter be separated and distilled to reduce the organic loading. This was demonstrated with 2,2-dichloro-1,1,1-trifluoroethane and 2-chloro-1,1,1,2-tetrafluoroethane as the organic samples. Manzer found that the upper HF layer contained about 7% organic components [52].

1.5. Characteristics of an ideal hydrogen fluoride adsorber

The above (section 1.4) gives an indication of some of the work that has been done on the removal of HF from F_2 and non-F_2 environments. The work in this thesis focuses on adding value to the above knowledge base.

To make the procedure quantitative, it is important that the results be measured against some benchmark. In this regard, a table of characteristics has been compiled detailing some of the more important features desired of an HF remover. The aim of this study is to assess alternatives to NaF for HF removal. However, if the alternative adsorber does not display the desired selectivity, removal from complex matrices cannot be considered for that matrix application. Another is financial cost; some solutions are just too expensive to consider. Some of the adsorbents selected for assessment will be graded against the characteristics displayed in the checklist below.

1.6. Checklist for suitability of adsorbers

When assessing the suitability of an adsorber or comparing two adsorbers for gas effluent removal, various factors need to be considered.

1) Selectivity

a) Does the adsorber display the desired selectivity?
b) What is the effect of the product matrix on the adsorber?
c) Does the adsorber introduce impurities into the product stream and if so are they acceptable in the product stream?

2) Effectiveness

a) Is it possible to remove the effluent gas down to the desired concentration?
b) Does the adsorber have a highly accessible surface area and/or a high density of active sites?

3) Kinetic and thermodynamic considerations

a) Is the adsorption process fast?
b) Ensure that $|\Delta H_{rxn}|$ is not large.

4) Physical characteristics

a) Is the adsorber present in a form that allows efficient adsorption *e.g*. pellets, sieves *etc*. or does it lend itself easily to the formation of the above that can result in the formation of a high surface area material?
b) Does the adsorber maintain its physical integrity? It should not sinter, form dust particles or undergo phase changes during use or regeneration?

5) Financial considerations

a) Is the total financial outlay to synthesize the new adsorber justified?

6) General

Apart from the above, other factors that need to be considered are;

a) Can the adsorber be physically regenerated *e.g.* with elevated temperature or pressure?
b) Are the products environmentally acceptable?

c) Are they reusable?

Further, when evaluating and comparing different adsorbers, the desired characteristics based on the above mentioned factors, need to be listed and the suitability of each adsorber assessed [53].

1.7. Thermogravimetry

Thermogravimetry was used as the principle analytical tool in this study. A commercial thermogravimetric analyser (TGA) was modified to permit the use of HF and hence a discussion of the instrument and on the interpretation of the results obtained in the study is warranted.

A Zero Beam thermobalance normally has two pans, one for the sample and one for the standard. The sample pan is housed in an enclosure to prevent atmospheric interference. The pan is normally a hang down type with the weighing mechanism and electronics situated above the pan.

Normally in thermogravimetry, one would monitor the change in mass experienced by a sample as a function of temperature. This mass change is indicative of some physical or chemical process that is occurring and an understanding of the chemistry of the sample is obtained by interpreting the data. Examples of mass loss include loss of waters of crystallization or the decomposition of the material. Depending on the information required, the temperature could be ramped, at different rates, stepped, or held constant.

Further, an inert gas normally flows over the sample. This has the effect of removing any decomposition products that could interfere with the sample analysis and helps cool the sample after a heating cycle. The flow of this inert gas can be varied depending on the requirement of the study.

Reactive gases, not harmful to the construction material of the balance, may also be used to study its interaction with the sample, *e.g*. CO_2, H_2O, and O_2.

1.7.1. Modifications to the thermogravimetric analyser

For this work, the TGA was not used in the classical sense of monitoring a mass change as a function of temperature, but rather was used to monitor the mass change as a function of the gas passing over the sample, while the temperature was kept constant. The results obtained from this type of study are useful especially if there is an interaction between the sample and the gas passing over the sample.

Normally the gas passing over the sample is an inert gas *e.g*. N_2. However, this gas can be changed to another inert gas or a gas that can interact with the sample, in this case HF or F_2. The TGA was modified to allow the gas stream to be easily changed from inert to interacting gas and *vice versa*. Flow regulators ensured that the gas flow remained the same irrespective of whether the inert or interacting gas was flowing. Both the inert and the interacting gas were delivered from gas cylinders. The mass change experienced by the sample was then noted on the TGA and thus provided an indication of the extent and type of interaction of HF or F_2 with the sample.

HF and F_2 are very corrosive gases hence dilute mixtures of these gases had to be used. 10% mixtures of HF or F_2 with N_2 were made up in 20 litre cylinders and introduced into the TGA. Further, all tubing used to carry these gases to the TGA had to be changed to stainless steel and stainless steel connectors were also used. This tubing was connected directly to the sample chamber of the TGA and allowed flow of the interacting gas directly over the sample. There was an outlet that removed the exit gas directly to a fume hood. Further, the entire TGA unit was housed in a glove box.

One of the problems with such an arrangement is that the corrosive HF or F_2 could diffuse up the hang down wire of the sample pan and damage the highly sensitive weighing mechanism and electronics. This was prevented by continuously purging the chamber housing the electronics, with a flow of inert gas.

For further flexibility in delivering lower concentrations of HF, down to a few hundred ppm, a Kin-Tek, 670c Precision Gas Standards Generator was also connected on-line. The source of the HF used was certified Trace Source™ LFH Permeation Tube. Variations in interacting gas concentrations could have been achieved by other means, *e.g*. varying the gas flow. However, to prevent the introduction of other variables into the HF adsorbtion process and for ease of operation it was decided to use the Kin-Tek gas generator. N_2 was used as a carrier gas to deliver the HF to the sample and once again the flow rate was not changed.

The normal temperature functions present on a TGA were still present and were used as such in most cases. Further, an Instrument Specialists Inc. Temperature Programmer Interface (TPI-PE-2) was installed to ensure proper temperature control. As, adsorption is a temperature dependent phenomenon, the cooling system of the sample chamber of the TGA, which normally had water flowing through it was changed to a circulating system that passed through a Neslab, Endocal Refrigerated Circulating bath. By varying the bath solution, the temperature of the sample chamber could theoretically be reduced to below freezing. However, for this work it was only reduced to a few degrees above 0℃. One of the biggest problems with working at lower temperatures is that HF liquefies below 19.5℃ and when working at lower temperatures it is difficult to ascertain if a mass fluctuation is due to HF uptake or HF condensation on the sample pan.

These modifications were introduced over time on a trial and error basis. Information on the thermobalance is obtainable in the experimental section of the various chapters and from a publication by Sanderson [54].

1.7.2. Example of typical thermogravimetric result

With reference to the interpretation of data, the following example will assist in this regard.

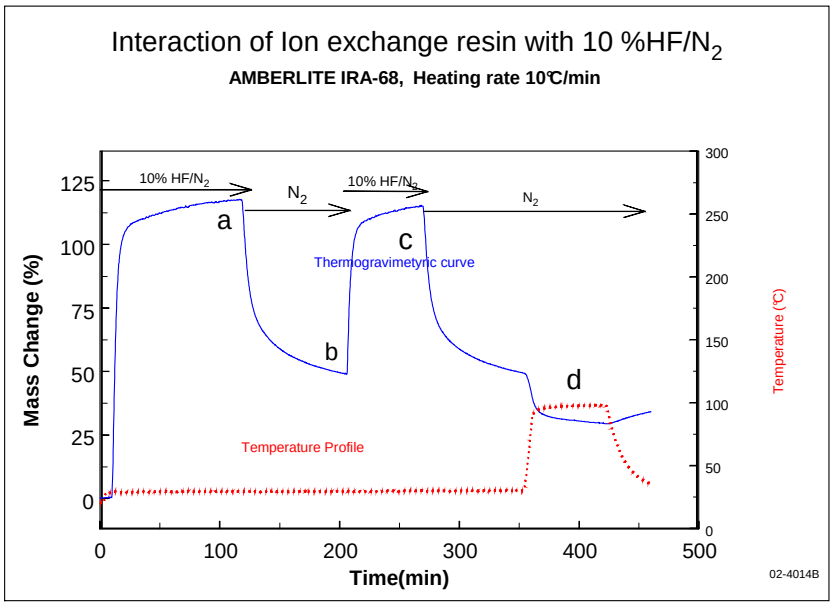


Figure 1.1: Thermogravimetric curve of Amberlite IRA 68 after exposure to a 10% HF/N_2 mixture

Figure 1.1 is a typical thermogravimetric trace that was obtained in this work. In this example the interaction of an ion exchange resin, Amberlite IRA 68 with HF is shown. The solid line indicates the thermogravimetric curve and the mass variations associated with this changes are indicated on the left hand axis. This curve is a plot of % mass change as a function of time. Time was selected as the other factor. The temperature profile is indicated by the dotted line, with the temperature indicated on the right

hand axis. Arrows above the thermogravimetric curves indicate the gas mixtures. The gas used was either an inert gas (N_2) or one of the HF or F_2 mixtures. In most cases the sample was dried in the TGA prior to being exposed to the interacting gases. For further clarity, the thermogravimetric curve is broken up into four regions and more details of these regions and the terminology used in subsequent discussions are given below.

- **(%) HF adsorbed 1** refers to the uptake of HF by a pre-dried sample (start of experiment to point a).
- **(%) HF desorbed 1** refers to the loss of HF by the same sample once the HF gas stream is closed off and an inert gas flowed over the sample. The percentage given, in reference to this point, does not refer to the HF lost but to the amount of HF remaining on the ion exchange sample based on the original pre-dried mass (point a to point b)
- **(%) HF adsorbed 2** refers to the amount of HF vapour now taken up by the same sample again, using the pre-dried mass as the starting reference (point b to point c).
- **(%) HF desorbed initially by inert gas and then at 100℃** refers to the amount of HF remaining on the sample after the HF gas stream has been turned off and the sample exposed to a temperature ramp up to 100℃. (from point c to poin t d).

A summary of the thesis is given below.

Chapter 2 focuses on inorganic compounds, more specifically calcium salts, where the uptake of various calcium salts (and sodium complexes) will be discussed. The uptake of HF by aluminophosphates is also included in this chapter. Chapter 3 deals with the uptake of HF by ion exchange resins. This is a more extensive study into ion exchange resins by various acidic and basic resins, the effect of the functional group, the polymeric backbone and the effect of changing the cation or anion on the

gas uptake. It also covers the uptake of other acidic and basic gases and the separation of HF from organics. Chapter 4 deals with the uptake by various carbon structures including activated carbon, carbon molecular sieves and carbon nanotubes. Finally Chapter 5 assesses some of the findings of this study.

1.8. References

1 Banks, R. E., Sharp, D. W. A. and Tatlow, J. C., Fluorine, The first 100 years, Elsevier Sequoia, (1986).

2 Sota, T., Takeuchi, T. and Morioka, I., Daikin Industries Ltd., Osaka (JP), Patent US 6 350 426 B1, (2002).

3 Ring, R. J. and Royston, D., A review of fluorine cells and fluorine production facilities, Australian Atomic Energy Commission, AAEC/E281, (1973).

4 Valkenburg, E., Personnel communication.

5 Rudge, A. J., The Manufacture and Use of Fluorine and its Compounds, Oxford University Press, (1962).

6 Bulan, A. and Krancher, M., Bayer Aktiengesellschaft, Leverkusen, Fed. Rep. Of Germany, Patent US 5 164 052, (1992).

7 Barker, C. T., Freire, F. J., Howell, J. L., Motz K. and Ziegenhain W. C., E. I. Du Pont de Nemours and Company, 1007 Market Street, Wilmington, DE 19898 (US), Patent WO 91/13024, (1991).

8 Bulan, A., Weber, R., Klaeren, A. and Moretto, H-H., Bayer AG, 51373 Leverkusen, DE, Patent DE 43 03 836 C 1, (1994).

9 Bulan, A., Weber, R., Block, H-D. and Moretto, H-H., Bayer AG, Leverkusen, Germany, Patent US 5 411 726, (1995).

10 Tarasenko, V. and Edelstein, H., Allied Corporation, Morris Township, Morris County, N. J., Patent, US 4 424 067, (1984).

11 Seseke-Koyro, U., Grossmann, A. and Rudolph, W., Solvay Fluor und Derivate GmbH, Hanover, Germany, Patent US 5 585 085, (1996).

12 Mosse, A. L., Pechkovsky, V. V., Teterevkov, A. I., Burov, I. S., Vilk, J. N., Ershov, V. A., Chelnokov A. A., Yasko O. I., Bysjuk V. V., Dzjuba, E D., USSR, Patent US 4 010 241, (1977).

13 Lamb, L. J., Land of lakes, FL (US), Patent US 6 179 901 B1, (2001).

14 Reed, R. S., NJ, Patent US 4 036 938, (1977).

15 Ehlig, W. H., E. I. Du Pont de Nemours and Company, Wilmington, Del, Patent US 4 120 939 (1978).

16 Worthington, R. E., O'Neill, P. S. and Hackett, P. F. X., Goulding Chemicals Limited, Dublin, Ireland, Patent US 4 144 315 (1979).
17 Cannon, C. W. and Hall, R. N., Climax Chemical Company, Hobbs, N. Mex., Patent US 4 292 289, (1981).
18 Terase, K., Hagita, S., Yokoyama, K., Sanada, Y., Nagase, M. and Hirata, S., Asahi Glass Company Ltd, Tokyo, Japan, Patent US 5 219 551, (1993).
19 Suzuki, K., Nakaya, K., Gotoh, T., Kitasako, M. and Iwasaki, M., Asahi Glass Company Ltd., Tokyo, Japan, Patent US 4 491 571, (1985).
20 Bailar, J. R., Comprehensive Inorganic Chemistry, Pergamon Press, (1973).
21 Grayson, M., Kirk-Othmer Encyclopaedia of Chemical Technology, 3rd ed., Vol. 10, John Wiley and Sons, (1980).
22 Keller-Rudek, H., Kuhn, P., List, H., Merlet, P., Ruprecht, S., Vanecek, H. and Wagner, J., Gmelin Handbook of Inorganic Chemistry, 8th ed. Fluorine Suppl. Vol. 3, Dieter Koschel (Editor), Springer-Verslag, (1982).
23 Lee, J. and Kim, H., *Fluid Phase Equilibra*, 47, **190**, (2001).
24 http://www.pelchem.com/hydrogen_fluoride.html
25 National Occupational Health and Safety Commission report on HF, Australian Government, WAP 89/039, GS 001-1989 (1989).
26 MSDS for HF, CAS-No. 7664-39-3, Pelchem document PTC-SHE-SDS-01001.
27 The website of the Canadian Centre for Occupational Health and Safety, http://www.intox.org/databank/documents/chemical/hydroflu/cie45.htm
28 http://www.atsdr.cdc.gov/toxprofiles/tp11-c5.pdf
29 Snyders, E., Personnel communication.
30 http://www.scorecard.org/chemical-profiles/
31 Kuhn, A. T., Industrial Electrochemical Processes, Elsevier Publishing Company, (1971).
32 Braker, W. and Mossman, A. L., Matheson Gas Data Book, 6th ed. Matheson, (1980).

33 Stein, L., Rudzitis, E. and Settle J. L., Purification of Fluorine by Distillation, Argonne National Laboratory, University of Chicago, ANL-6364, (1961).

34 Froning, J. F., Richards, M. K., Stricklin, T. W. and Turnbull, S. G., *Industrial and Engineering Chemistry*, 277, (1947).

35 Carstens, P. A. B., Personnel communication.

36 Belova, L. P., and Nekrasov, Y. D., *Russian Journal of Inorganic Chemistry*, 920, **11(7)**, (1966).

37 Capps, R. H., Reaction of Gaseous UF_6 and HF with Metallic Fluorides, Carbide and Carbon Chemicals Company, Report K – 770, (1951).

38 Mootz, D. and Boenigk, D., *J. Am. Chem. Soc*., 6634, **108**, (1986).

39 Otsuka, K., Fukuda, H. and Arakawa, S., Japan Pionics Co., Ltd., Tokyo, Japan, Patent US 5 589 148, (1996).

40 Ewing, P. N., Shields, C. J. and Low, R. E., Ineos Fluor Holdings Limited, GB, Patent US 6 555 086 B2, (2003).

41 Ewing, P. N., Shields, C. J. and Roberts, C., Ineos Fluor Holdings Limited, GB, Patent US 6 660 893 B2, (2003).

42 Van Der Puy, M. and Luly, M. H., AlliedSignal Inc., Morris County, N. J., Patent US 5 632 966, (1997).

43 Keller, A. E., Conoco Inc., Ponca City, OK, Patent US 5 336 832, (1994).

44 Ryan, T. A., Allen, G. J., Schoelzel, H. M. and Pilotti, M., Imperial Chemical Industries PLC, Imperial House, Millbank, London, SW1P 3JP (GB), Patent WO 94/20412 (1994).

45 Buehler, H. J., Mallinckrodt Speciality Chemicals Co., St. Louis, Mo. Patent US 5 032 371, (1991).

46 Eicher, J., Rudolph, W. and Schulte, B., Solvay Fluor and Derivate GmbH, Hanover, Fed. Rep. Of Germany, Patent US 5 300 709, (1994).

47 Mizrahi, J., IMC Fertilizer Inc., Northbrook, Ill, Patent US 4 882 132, (1989).

48 DeVries, R. A., The Dow Chemical Company, Midland, MI, Patent US 4 640 831, (1987).

49 Chang, C-H. and Gualdron, M. A., AlliedSignal Inc., Morris County, N. J., Patent US 5 597 545, (1997).
50 Lee, K. H., Barsotti, D. J. and Sakata, E. K., E. I. Du Pont de Nemours and Company, Wilmington, Del, Patent US 5 196 616, (1993).
51 Tarasenko, V. and Edelstein, H., Allied Corporation, Morris Township, Morris County, N. J., Patent US 4 424 067, (1984).
52 Manzer, L.E., Rao, M. V. N., Rockwell, R. T., Sisk, M. A., Warwas, E. J. and Winteringham, R., E. I. Du Pont de Nemours and Company, Wilmington, Del, Patent US 4 911 792, (1990).
53 Carstens, P. A. B., Le Roux, J. P., Nelwamondo A. N. and Moolman, D, personnel communications.
54 Sanderson, R. D., du Toit, F. J., Carstens, P. A. B. and Wagener, J. B., *Journal of Thermal Analysis*, **41**, 563, (1994).

Chapter 2

Inorganic salts and complexes

2.1. Introduction

The possibility of using an alkali earth metal salt to remove HF is investigated in this chapter. There have been discussions in the literature with regard to the use of calcium salts for the adsorption of HF. The problems associated the current technology has been well documented in Chapter 1, hence, considering these problems, alternative purification technologies are being sought. One of the areas of focus is on the use of CaF_2. Over the years evidence has appeared in the literature both supporting and rejecting the usage of CaF_2 as a HF adsorber. The issue of whether or not CaF_2 is capable of removing HF from a F_2 stream has not been resolved.

In this study experiments were thus designed to assess this issue. Firstly, commercial CaF_2 was assessed for HF removal and the effect of fluorination of CaF_2 at different temperatures was investigated. Thereafter, the uptake of HF by other salts of calcium (*viz*. $Ca(OH)_2$, $CaCl_2$ and $CaSO_4$) was assessed.

The idea of mixing NaF with other metal fluorides to form a complex was also investigated. Salts of CaF_2 and MgF_2 were assessed and these results are discussed in this chapter.

Another adsorbent investigated was a molecular sieve, more specifically an aluminophosphate molecular sieve. Based on the work of Takita [1, 2, 3], it appears that aluminophosphate molecular sieves are possibly stable to both HF and F_2.

Molecular sieves have certain characteristics that are useful for HF/F_2 adsorption. Molecular sieves are porous solids with pores of 3 to 20 Å; examples include zeolites, carbons, glasses and oxides. Some are crystalline with uniform pore sizes (*e.g*. zeolites) and others are more amorphous (*e.g*. carbons). Most current commercial molecular sieves are based on zeolites. Aluminophosphates are thus similar to zeolites in that they have pores and channels [4].

Zeolites comprise of SiO_x and AlO_x units. Whereas the SiO_x unit has no charge, the presence of the AlO_x unit result in generating positive charge in the zeolite, thus making the zeolite acidic.

If other similar atoms replace the Al atoms, the new structures are referred to as zeotypes. For example, replacement of the SiO_x unit by PO_x unit results in each unit being negatively charged. In aluminophosphate structures, the aluminium and phosphorus charges cancel each other out, resulting in the generation of a neutral species.

2.2. Literature survey

This will first cover the calcium salts and next the aluminophosphate.

2.2.1. Calcium fluoride – hydrogen fluoride interaction

HF coordinates onto CaF_2 via the calcium ion in CaF_2 and the fluorine ion in HF or by interactions between the hydrogen of HF and the fluorine of CaF_2 (Figure 2.1)[5].

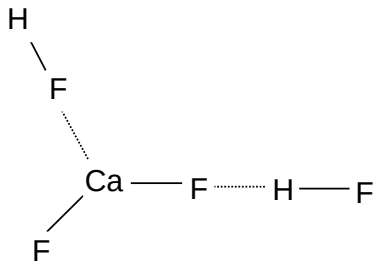


Figure 2.1: Interaction between CaF_2 and HF

The CaF_2-HF complex exists as $CaF_2 \cdot 2HF$ and was confirmed by a number of studies.

(i) Jache and Cady [6], upon doing solubility studies of CaF_2 in anhydrous HF, isolated from the matrix, a complex they characterized as $CaF_2 \cdot 1.86HF$. This they ascertained by weight loss.

(ii) In 1970, Ikrami and Nikolaev [7] isolated $CaF_2 \cdot 2HF$ as large flat hexagonal crystals (1-2 mm) from a CaF_2/HF/water mixture, the HF concentration being greater than 56%. This complex was characterized by powder XRD. Two other points noted in this paper, were that the complex $CaF_2 \cdot 2HF$ decomposed in air, with the loss of HF and that decomposition occurred upon long standing. They also noted that the $CaF_2 \cdot 2HF$ rapidly hydrolysed in water.

The solubility of CaF_2 in HF was also investigated and compared with data for NaF (Table 2.1). One of the problems experienced with NaF is its high solubility in HF and an adsorbent with a lower solubility is preferable for adsorption of HF, *e.g*. $CuSO_4$ will adsorb moisture to $CuSO_4 \cdot 5H_2O$ and stop, whereas NaF will adsorb HF till it dissolves.

Table 2.1: Table of solubility of CaF2 and NaF in HF at various temperatures

Salt	Temp. (℃)	Solubility g/l	Reference:
CaF_2	12.2	8.2	6
	0	9.8	7
	-3.3	10.6	6
	-23.0	14.4	6
NaF	11.0	301	6
	-9.8	251	6
	-24.3	221	6

As can be noted from Table 2.1, NaF is much more soluble than CaF_2 in HF. It is also interesting to note the increase in solubility of CaF_2 as the temperature decreases.

2.2.2. Adsorption studies

Colvin [8] investigated the possibility of using CaF_2 as an adsorbent for HF. Two sources of CaF_2 were used in his studies. The first source was, a commercial CaF_2 that was pelletized, crushed and screened to obtain 16 – 18 mesh granules. The second source was a 16 – 18 mesh $CaSO_4$ (Drierite) that had been fluorinated in a fixed bed reactor.

The surface area of the commercial CaF_2 was not calculated. However, the claimed increase in surface area in fluorinating $CaSO_4$ to CaF_2 was from 11.68 m^2/g to 128.6 m^2/g. This was done by passing a dilute stream of fluorine in nitrogen over the sample, slowly increasing the fluorine concentration to 100% over a few days. Further, after fluorination, the claimed SO_4 content was 0.01%.

For the CaF_2 granules, only the total loading of HF under a flow rate of 500 cm^3/min of anhydrous HF was evaluated. The average weight gain of CaF_2 was found to be about 36% for two adsorption-desorption cycles, with exposure time being 5 and 4 hours respectively. For regeneration, the CaF_2 was heated to 136℃ for 17 hours and 150℃ for 19 hours respectively.

With reference to the synthesized CaF_2, this was subjected to eight adsorption–desorption cycles with the flow rate fluctuating between 89.0 and 23.8 cm^3/min. The percentage weight gain dropped from 22.2% for CaF_2, for run one, to 11.3% for run six. For the final two runs the CaF_2 was subjected to a mixture of 30% HF and 70% F_2. Here the weight gains were 8.3 and 9.7% respectively. According to Colvin, breakthrough occurred at 11-15% by weight of CaF_2 for anhydrous HF and 8-10% for the HF/F_2 mixture in a fixed bed reactor. The regeneration times varied from 18 to 40 hours. However this could be reduced to between 2 and 4 hours if complete desorption was not desired [8]. This indicates that most of the bound HF could be easily released.

Colvin's conclusion was that CaF_2 is a good adsorbent for HF and it can be easily regenerated. He further indicated that the problems of mechanical disintegration or fusion, experienced with NaF, did not occur with these CaF_2 samples. He further indicated that CaF_2 had a usable HF capacity of 9% and hence recommended further industrial testing however no information on this was obtained.

Merchant and Hodges also investigated the removal of HF from organic gaseous mixtures by CaF_2. [9]. However, they indicated that naturally occurring CaF_2 could only adsorb 5 to 6% by weight of HF, whereas if the CaF_2 is produced *in situ* from $CaCl_2$, it could adsorb between 20 to 50% of its own weight of HF.

The authors also calculated the surface area of natural CaF_2 to be 1.8 m^2/g, whereas that of $CaCl_2$ increased from 2.0 to a maximum of 16.5 m^2/g upon fluorination.

In one example, a 2.54 cm diameter column was filled up with about 100 cm (length of column) particulate CaF_2 (particle diameter between 0.48 to 0.64 cm). This column was subjected to a gaseous mixture of about 60% organic, 10.3% HF with the rest of the mixture being HCl. The gaseous pressure was about one atmosphere with velocities ranging from 4.57 to 45.7 cm/min with the retention times between 110 to 330 seconds. The HF content was reduced from 10.3% to 0.38%.

The difference between Merchant and Colvin's work was that Colvin obtained HF loadings of 9% whereas Merchant obtained 20% under normal conditions. Further, Colvin obtained this loading with a surface area of 129 m^2/g whereas the surface area reported by Merchant was 12 to 17 m^2/g Hence this CaF_2 adsorbent removes more HF per unit mass with considerably less surface area.

Nakano [10], in his 1998 patent on the dry treatment method for HF gas, also noted the adsorption of HF on CaF_2. He scrubbed HF with $Ca(OH)_2$. The $Ca(OH)_2$ converted to CaF_2, but he noted that the percentage conversion of $Ca(OH)_2$ to CaF_2 was greater than 100-mole% under certain conditions and in one case where pure HF was used he obtained 140% conversion. The additional percentage mass increase he ascribed to adsorbed HF.

Kemnitz and Hass [11] determined the adsorption isotherm of HF on CaF_2 at 30℃ and 60℃. The CaF_2 used was synthesized and had a surface area of 1.1 m^2/g. The experiment was carried out in PTFE containers, where weight differences were determined. The maximum surface concentrations obtained for HF were, 73.1 mg/m^2 (30℃) and 71.8 mg/m^2

(60℃) for HF. The adsorption enthalpy was calculated to be –2.98 kJ/mol, which indicates a weak bond between HF and CaF_2. They also indicated that they did not find any evidence for the formation of a $CaF_2 \cdot 2HF$ complex.

Hence considering the above CaF_2 warranted further investigation, and this chapter concentrates on that investigation.

2.2.3. Calcium fluoride crystal surface chemistry

Bennewitz noted that the irradiation of CaF_2 with low energy electrons resulted in F_2 desorption from the surface and the formation of metallic clusters on the surface. It was further noted that the number of clusters increased with increasing temperature [12].

The formation of these clusters were also noted by Batzill, who exposed a CaF_2 surface to electrons emitted by a heated thoriated tungsten filament which was close but out of sight of the CaF_2 surface. He also noted that the Ca metal on the surface underwent rearrangement to form Ca wires [13].

Upon further investigation of the surface of CaF_2 crystals by photo simulation, it was noted that the surface undergoes a large atomic relaxation with the Ca^{2+} ions moving inwards by as much as 0.5 Å and the F^- ions out by about the same amount. Also noted was the depletion of fluorine atoms from the crystal surface [14].

Wu [15] noted another interesting phenomenon, when using X-ray photoelectron spectroscopy (XPS) to study the surface of CaF_2. He noted that water adsorbed to a limited extent and is present on the surface as hydroxyl and/or oxygen species. He indicated that the interactions between the adsorbed water and the substrate are sufficiently strong that

surface fluorine ions are displaced by oxygen-containing species, but he also noted that the reaction between fluorides and water is very slow.

Bermudez [16], also noted that damaged CaF_2 surfaces, *i.e*. where fluorine desorption has occurred, are highly reactive to O_2 and CO_2.

2.2.4. Methods of activation and regeneration

McVicker [17] reported that high surface area metal fluorides could be synthesized by reacting high surface area metal oxides (from a select group including Ca) with a fluorocarbon vapour. One of the oxide examples he used was alumina and he stated that when the fluorinating agent was fluoroform (CHF_3), the sample exhibited a higher surface area than samples prepared by fluorination with either HF or NH_4F.

According to Colvin [8], evacuating the CaF_2 onto which HF was adsorbed, for 3 to 4 hours at 100℃ or purging for 2 to 4 hours at 150℃ with an inert gas easily regenerates CaF_2. He also indicated that no problems of dusting, mechanical disintegration or fusion were noted in these experiments.

Merchant [9] indicated that the “spent” CaF_2 could be regenerated by one of three methods.

1) External heating of a sample between 107℃ and 177℃.
2) Heating a sample to around 93℃ or higher and passing an inert gas such as N_2, air or anhydrous HF through the solids.
3) Passing an inert gas through the solid while heating to 177℃ or higher.

Cady [6] also noted, that by heating a CaF_2-HF complex that he had formed, to 110℃ he was left with CaF_2.

Opalovsky [18], upon studying the kinetics of the thermal decomposition of $CaF_2 \cdot 2HF$ found that HF was removed at 130℃. It was a one step decomposition. He further noted that the decomposition reaction has a reaction order of 0.34, with activation energy of 114.3 kJ/mol.

2.2.5. Adsorption separation by zeolites

Selective adsorption and desorption of a desired reactant or product occurs in the channels of the zeolite. In the process there may also be an initial activation step to remove any moisture or other undesirable adsorbate from the zeolite.

Adsorptive separation by zeolites is proposed to occur by one of three mechanisms. These are referred to as steric, kinetic or equilibrium mechanisms. Any steric effect associated with adsorption is derived from the size and shape of the molecules to be separated. As zeolites have definite pore shapes and sizes, only small and particularly shaped molecules can diffuse into them. Thus separation of normal paraffins from iso-paraffins can be achieved by size exclusion. Kinetic separation is achieved when there are differences in diffusion rates between reactants. An example of this is the separation of N_2 and O_2 from air by pressure swing adsorption; N_2 adsorbs preferentially into a zeolite compared to O_2. Finally, equilibrium separation depends largely on a zeolite's characteristics *e.g*. a molecule that has a high polarizability will adsorb onto a highly polar zeolite surface. This is used for the removal of water from air by adsorption.

Product recovery is achieved by desorbing the adsorbed product from the adsorbent. This is achieved by one of the following techniques; thermal swing desorption, pressure swing desorption, purge gas stripping and displacement desorption. These techniques are sometimes used separately or in conjunction, but the deciding factor is that these techniques must not destroy the adsorbent or adsorbate [19, 20].

2.2.6. Aluminophosphate molecular sieves

Aluminophosphate molecular sieves are also similar to zeolites in that they are microporous crystalline oxides that contain pores within their framework structure. In aluminophosphates (AlPO's) Al^{3+} and P^{5+} occupy the framework sites. AlPO materials can contain aluminium in co-ordination environments other than tetrahedral. The AlPO framework is neutral. The general composition for an AlPO material is

$$xR \cdot Al_2O_3 \cdot 1.0(+/- 0.2)P_2O_5 \cdot yH_2O$$

where R is an organic amine or quaternary ammonium ion, the amounts *x* and *y* represent the amount of R and H_2O respectively, that fill the pores. No counter ion is required. The aminophosphate has to be calcined at 400 to 600℃ to remove the water and organics.

Both natural and synthetic aluminophosphates have been described in the literature. Natural aluminophosphates include berlinite (quartz analogue), variscite, metavariscite, augelite, senegalite, wavellite, trolleite, bolivarite and evansite. The synthesis of aluminophosphate hydrates was reported in 1961 and included the variscite and metavariscite structures. The materials were not pure and were thermally unstable. Irreversible structural collapse of the AlPO occurring upon heating, due to loss of coordinated water.

The more recently synthesized aluminophosphates exhibit excellent thermal and hydrothermal stability. Further, due to their neutral frameworks, they have no ion exchange capacity. However, their surface selectivity is mildly hydrophilic.

More than two-dozen structures of AlPO based molecular sieves (with two hundred compositions) have been reported, including some with zeolite like topologies. Examples of zeolite structures seen in aluminophosphates

are Linde type A, faujasite and sodalite structures. Most AlPO pore sizes are in the range from 3 to 8 Å. Some aluminophosphates have large pore sizes, *e.g*. VPI-5, has an 18-member ring channel, and a free pore diameter of 12.5 Å.

Modification of the aluminophosphates structure is possible by replacement of the AlO_x, or the PO_y units. Three other groups of molecular sieves have been identified, the silicoaluminophosphates (SAPO), the metal aluminophosphates (MeAPO) and the non-metal AlPO's (ElAPO) [21, 22, 23].

2.2.7. Adsorption properties of aluminophosphate molecular sieves

The adsorption properties of aluminophosphate molecular sieves exhibit characteristics similar to those of zeolites. The capacities for gases or liquids are dependent on the opening, pore size and the geometry of the adsorbed molecule. Water capacities range from 0.04 to 0.35 cm^3/g [4, 22].

2.2.8. Interaction of aluminophosphate molecular sieves with HF

In 1985 Kirsch claimed that he could remove low levels of HF with a zeolite from a gaseous SiF_4 stream, contaminated with 0.31 to 0.38 mole% SO_2, 0.08 to 4.55 mole% HCl and up to 0.15 mole% HF. The zeolite used in the H cation form, was a hydrated metal aluminium silicate known as mordenite. At least 90% of the impurities were removed when this gas stream was passed through a column containing this zeolite. However, he did not determine the capacities for HF or the effect of mixed contaminants versus a single contaminant. The zeolite could be regenerated using hot N_2.

With reference to the stability of this zeolite to HF, Kirsch noted that HF broke down the zeolite. However, Kirsch noted that natural mordenite broke down faster than the synthetic material and that the sodium form of the zeolite is less stable to acid than the H^+ form [24]. In another study, Foley also reported AlPOs are not useful for the separation of mixtures that contain HF, since they react with and consume the zeolite [25].

Studies on the interaction of aluminophosphates with HF by Jeon were reported. Jeon prepared an $AlPO_4$-Al_2O_3 catalyst for the conversion of CF_4 and found it was stable to HF attack. In contrast HF converted γ-alumina to the α-alumina phase. A 2.5 mol% addition of phosphate to the γ-alumina improved the durability [26].

Takita studied the decomposition of chlorofluorocarbons over metal phosphate catalysts. One of the problems he noted is that formed HF reacted with and deactivated the catalyst. Normally the catalyst is a metal oxide and reacts with the HF to form a metal fluoride, with reduced catalytic activity. However when the catalyst is an AlPO, no reaction between the AlPO and HF was observed during 1000 hours of reaction at 400℃. This was confirmed by running an XRD before and after a short catalytic test [1, 2, 3].

The sample used in this investigation was obtained from Naydenov, and was a mesoporous Me-AlPO-5 material with spherical morphology, (Me is vanadium). The spheres were prepared by a multi-step procedure using a cation exchange resin as a template. In the process, an Al exchanged resin was hydrothermally treated with H_3PO_4, tetraethylammonium hydroxide ($(C_2H_5)_4NOH$) and H_2O to produce the resin-AlPO-5 composite. This was ion exchanged with V or Cr and calcined to produce the Me-AlPO-5 spheres. The final product was similar in appearance to cation exchange resin beads and consisted of nano-sized particles as AlPO-5 formed within the constraints of the exchange resin chain. The advantage

of producing AlPO-5 by this method is that the template determines the macro-shape and the secondary porosity. With reference to crystallinity, the formation of AlPO-5 was confirmed by XRD. [27].

Results and Discussion

2.3. Uptake of hydrogen fluoride by calcium fluoride

2.3.1. Assessment of commercial calcium fluoride

Three CaF_2 samples of different origins were investigated with reference to the uptake of gaseous HF at room temperature in a thermogravimetric analyser. They were, CaF_2 from BDH, CaF_2 from Saarchem and CaF_2 as a decomposition product of $CaSiF_6$.

A mass increase was noted when all three of the samples were exposed to 10% HF/N_2 mixture in a thermogravimetric analyser. The adsorbed HF was not strongly bonded, as some HF desorbed, as soon as the HF mixture was replaced with a N_2 carrier gas (see Table 2.2). Thermogravimetric curves for the interaction of HF with the three CaF_2 samples are shown in Figures 2.2 to 2.4.

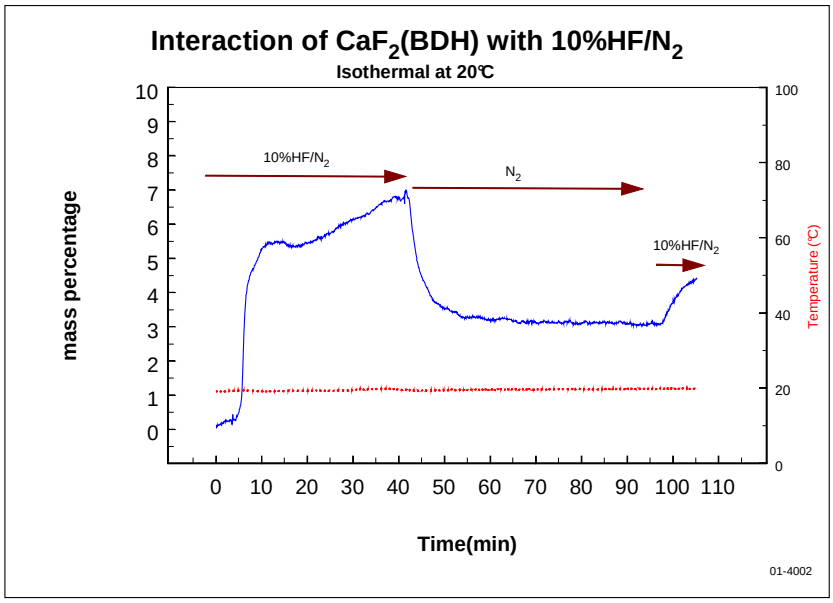


Figure 2.2:Thermogravimetric curve for CaF_2 (BDH) after exposure to 10% HF/N_2 at room temperature

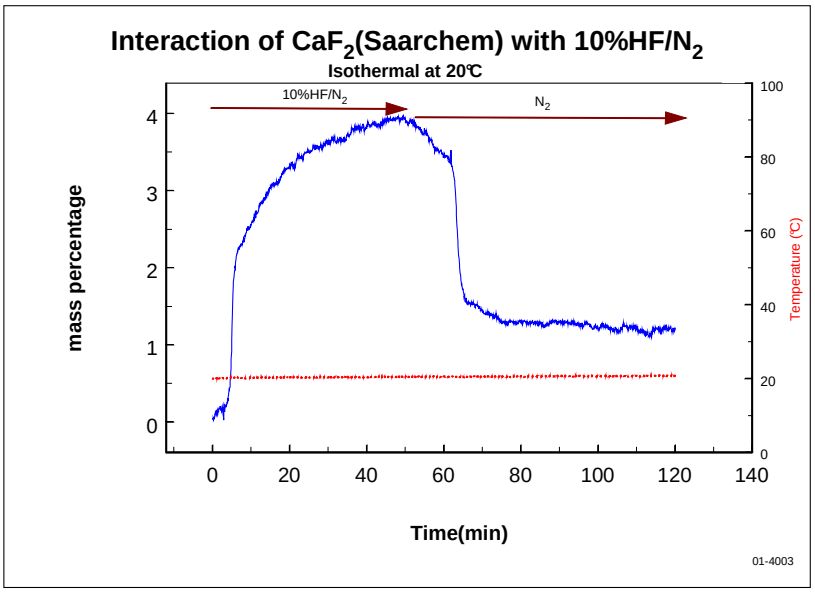


Figure 2.3:Thermogravimetric curve for CaF_2 (Saarchem) after exposure to 10% HF/N_2 at room temperature

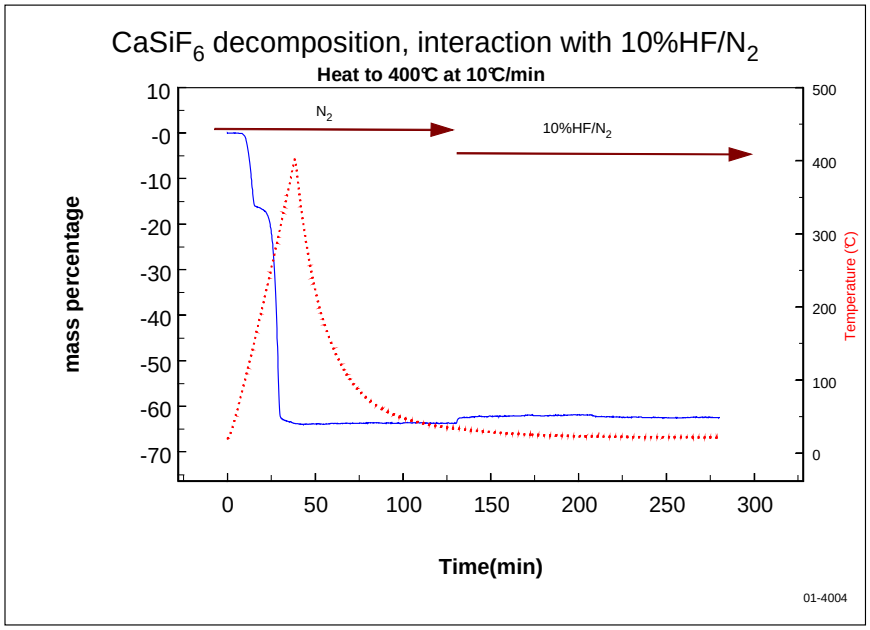


Figure 2.4:Thermogravimetric curve for the decomposition product of $CaSiF_6 \cdot 2H_2O$ which is followed by the exposure of the sample to 10% HF/N_2 at room temperature

Table 2.2: Mass changes for the uptake in 10 % HF/N_2 by CaF_2

Sample	**Thermogravimetric curve**	**Mass change (%)**
CaF_2 (BDH)	Figure 2.2	+7
CaF_2 (Saarchem)	Figure 2.3	+4
CaF_2 from $CaSiF_6$	Figure 2.4	+3
NaF (pellet)	Figure 2.5	+210

As noted the uptake of HF by the calcium salts is extremely low. The CaF_2 sample from BDH (Figure 2.2) was a freshly obtained sample. This sample took up 5.5% HF before reaching a plateau, before taking up a maximum of 7% HF. This is assumed to be secondary HF adsorption. The initial uptake is due to direct uptake by the CaF_2 and the rest is due to

multiplayer adsorption of HF [28]. Only half the adsorbed HF was retained upon removal of the HF source, indicating that the remainder of the HF does bond at room temperature to CaF_2. From the thermogravimetric curve, it will be also noted that exposure of this sample to more HF once again, results in an uptake of HF to a lesser extent (Figure 2.2).

The CaF_2 from Saarchem, took up only 3.9% HF, a lower uptake than that of the sample from BDH (Figure 2.3). The difference in uptake may be due to various reasons, e.g. industrial synthesis, different levels of crystallinity or impurities. However in both cases the uptake is low. This sample also retained some HF (~1.5%) upon removal of the HF source.

Finally, a freshly produced sample of CaF_2 synthesized by decomposing $CaSiF_6$ to produce CaF_2, was used (Equation 2.1).

$$CaSiF_6 \xrightarrow{\triangle} CaF_2 + SiF_4 \qquad (2.1)$$

The uptake was found to be even lower than that determined for the commercial samples (Figure 2.4).

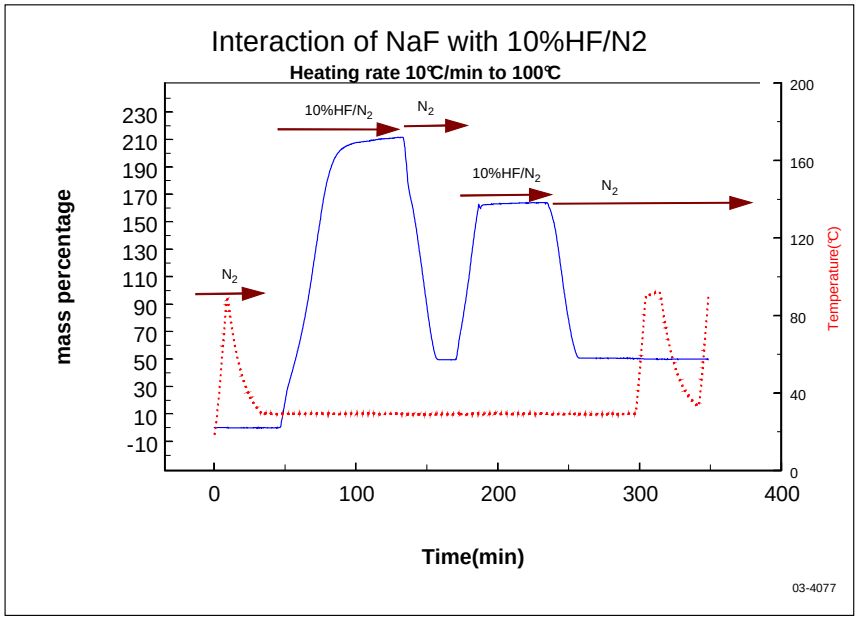


Figure 2.5:Thermogravimetric curve for the uptake of HF by NaF on exposure to a 10% HF/N_2 mixture

For comparative purposes HF uptake by NaF was determined. The uptake of HF by NaF is extremely high at 210 mass % (approximately, NaF·4.5HF) (Figure 2.5). The main contributing factor to this high uptake is the solubility of NaF in HF. This solubility tends to aid the HF hydrogen bonding and results in the NaF liquefying. [29].

From the above it is clear that CaF_2 has limited capacity as a HF adsorption chemical.

2.3.2. Influence of surface area on hydrogen fluoride uptake

It is expected that the surface area and surface characteristics of a potential adsorbent would influence the adsorption of HF. If the surface area of the adsorbent controls the HF adsorption, a higher surface area would lead to a higher degree of HF uptake. Powdering the sample,

chemical activation or using samples from different origin *e.g*. precipitation or formation as a result of decomposition, can modify the surface area [30]. Due to the natural octahedral cleavage planes of CaF_2 a ground sample will have more octahedral crystal faces than a precipitated sample, as the crystals will now be eight faced octahedral crystals instead of the six-faced cubic crystals [30]. Surface area measurements were then performed on the three samples listed in section 2.3.1. above and the values measured are report in Table 2.3.

Table 2.3: Mass changes and surface areas for the uptake of 10 % HF/N_2 by CaF_2

Sample	**Thermogravimetric curve**	**Mass change (%)**	**Surface area (m^2/g)**
CaF_2 (BDH)	Figure 2.2	+7	4.02
CaF_2 (Saarchem)	Figure 2.3	+4	1.04
CaF_2 from $CaSiF_6$	Figure 2.4	+3	85.29

From the above results, the sample from BDH (Figure 2.2) took up 7% HF and had a surface area of 4.02. m^2/g and the CaF_2 sample from Saarchem took up 4% HF for a surface area of 1.04 m^2/g. It appears that the Saarchem sample, which was not crushed, has a higher capacity for HF, per surface area compared to the crushed BDH sample.

The CaF_2 sample, synthesized from the thermal decomposition of $CaSiF_6$, which has the highest specific surface area, has the lowest HF capacity. This result is surprising, considering the extremely high surface area of the CaF_2 compared to the other CaF_2 samples. Further, this was freshly synthesized CaF_2 and according to Colvin [8], freshly synthesized CaF_2 had a higher capacity than commercial CaF_2. Colvin synthesized his CaF_2 by direct fluorination of $CaSO_4$ whereas the CaF_2 used in this experiment was synthesized by the thermal decomposition of $CaSiF_6$. This suggests

that the surface deactivation of CaF_2 may occur upon heating of CaF_2 to elevated temperatures.

2.3.3. *Crystallization of calcium fluoride and its effect on hydrogen fluoride uptake*

Another method of generating crystalline CaF_2 is to re-crystallize it from a solvent. Thus, samples of CaF_2 were crystallized from aqueous solutions and the uptake of HF on this material assessed. This experiment consisted of making up saturated solutions, of CaF_2 and allowing the CaF_2 to crystallize out overnight. Samples were thus prepared by dissolving CaF_2 in (i) rapidly boiling and (ii) warm (±50 ℃) wate r and allowing natural crystal growth as the samples cooled. The uptake of HF, as measured by TGA, from a 10% HF/N_2 mixture, was once again found to be very low, *i.e*. about one percent, indicating that even freshly crystallized CaF_2 has a low capacity for HF adsorption (Figures 2.6 and 2.7)

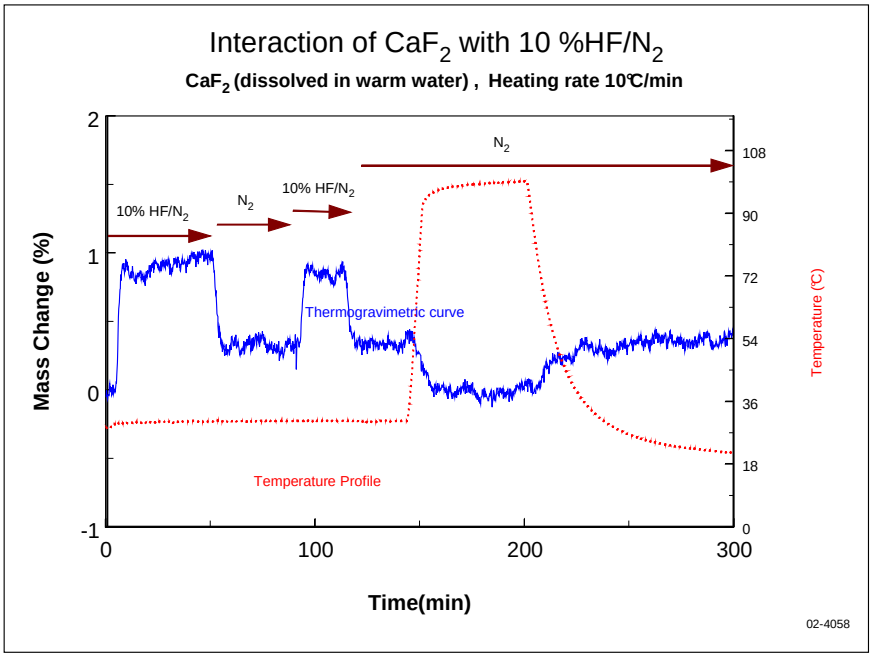


Figure 2.6: Uptake of HF by CaF_2 crystallized from water (50℃)

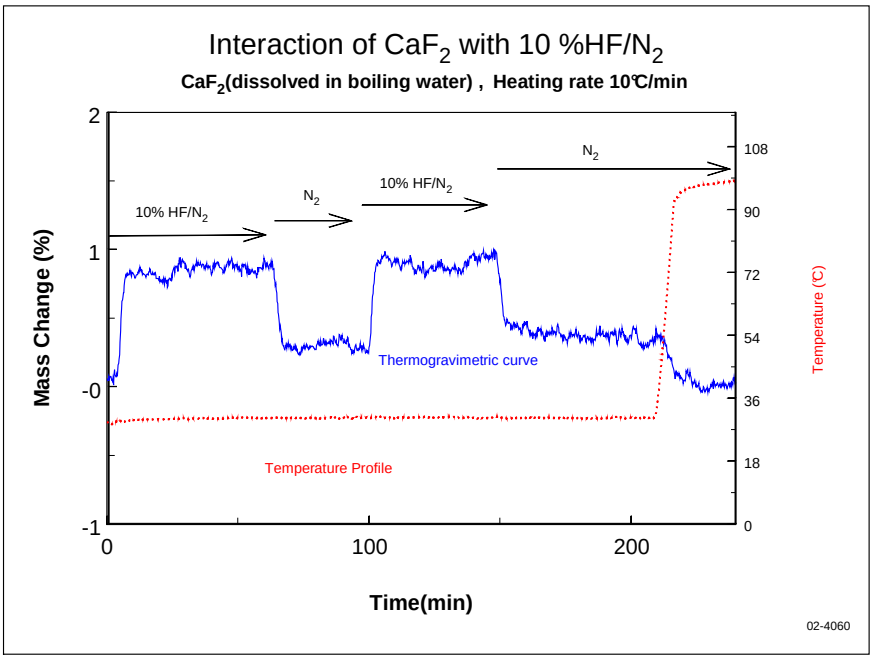


Figure 2.7: Uptake of HF by CaF_2 crystallized from water (Boiling)

2.3.4. Fluorination of calcium fluoride and its effect on hydrogen fluoride uptake

Irradiation studies by Song [14] suggest that depletion of fluorine atoms may occur from the crystal surface. Considering the very low uptake of HF by CaF_2 noted in the earlier studies, it is possible that surface fluorine depletion may have occurred over time. Hence, co-ordination of fluorine to the surface should generate a fully fluorinated CaF_2 sample. This can be achieved by exposure of a sample of CaF_2 to F_2. Thus a sample of CaF_2 was powdered and fluorinated at 1 bar pressure and room temperature for 72 hours, and the HF uptake assessed. The uptake results obtained are shown in Figure 2.8:

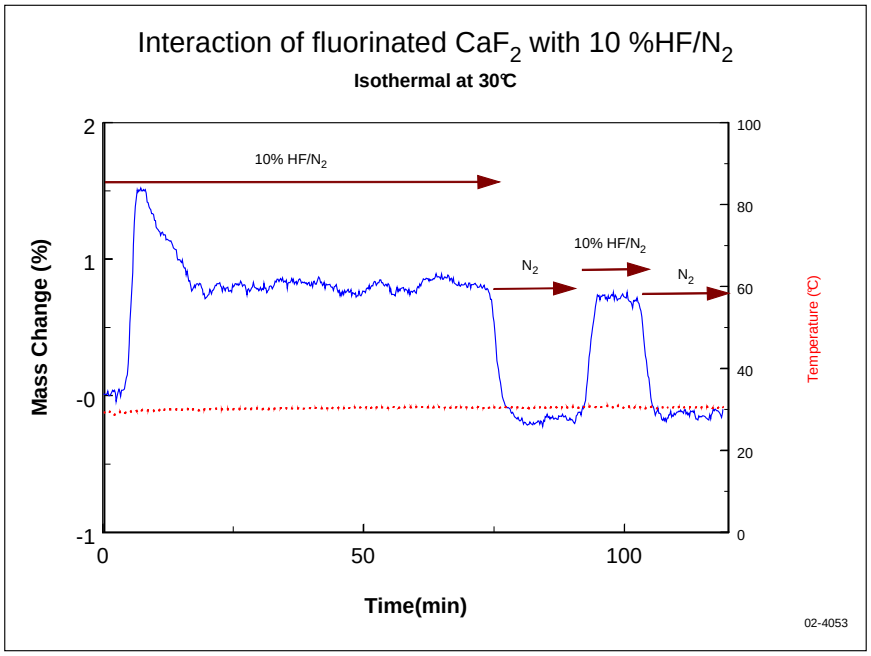


Figure 2.8: Uptake of HF by CaF_2 that was exposed to F_2

From Figure 2.8, it can be noted that this fluorinated CaF_2 sample also has a low capacity for HF as it took up <2% HF from a 10% HF/N_2 mixture. Removal of the HF stream resulted in the loss of the adsorbed HF.

2.3.5. Fluorination of calcium fluoride at different temperatures and its effect on hydrogen fluoride uptake

To investigate the effect of temperature on HF uptake by CaF_2, a freshly ground CaF_2 sample was fluorinated at different temperatures (25 to 270℃).

This reaction was conducted in a Monel reactor. This reactor was evacuated and charged with one bar F_2. It was then left overnight, hence ensuring an exposure time of at least sixteen hours. This experiment was repeated at different temperatures, ranging from room temperature to 270℃. The results obtained are as follows:

Table 2.4: Table of uptake of HF, from a 10% HF/N_2 on the Thermogravimetric analyser, by CaF_2

Sample	**% HF uptake**
CaF_2 fluorinated at room temperature	1
CaF_2 fluorinated at 50℃	1
CaF_2 fluorinated at 140℃	4
CaF_2 fluorinated at180℃	2
CaF_2 fluorinated at 270℃	1

What is evident from the above results is that fluorination of the above samples does not result in an increase in the uptake of HF. Based on the above it is evident that the uptake of HF by CaF_2 cannot be increased by direct fluorination.

2.4. Uptake of hydrogen fluoride by fluorinated and un-fluorinated calcium salts

The uptake of HF by other calcium salts was also assessed. $Ca(OH)_2$, $CaCl_2$ and $CaSO_4$ (Drierite) were fluorinated to form CaF_2 and the HF

uptake, from a 10%HF/N_2 mixture, thereafter assessed. This experiment was an attempt to repeat the work of Colvin [8], Merchant [9] and Nakano [10]. This experiment was conducted on the thermogravimetric analyser with the fluorinations being done with either the 10% HF/N_2 mixture mentioned above or a 10% F_2/N_2 mixture.

2.4.1. Calcium hydroxide

The reaction of $Ca(OH)_2$ with F_2 generates CaF_2 (equation 2.2),

$$Ca(OH)_2 + 2F_2 \rightarrow CaF_2 + 2HF + O_2 \qquad (2.2)$$

This reaction was monitored by TGA (Figure 2.8). The molar mass of $Ca(OH)_2$ is 74.1 g/mole and CaF_2, 78.1 g/mole. Hence the calculated mass gain, due to the fluorination of $Ca(OH)_2$ was 5.4%.

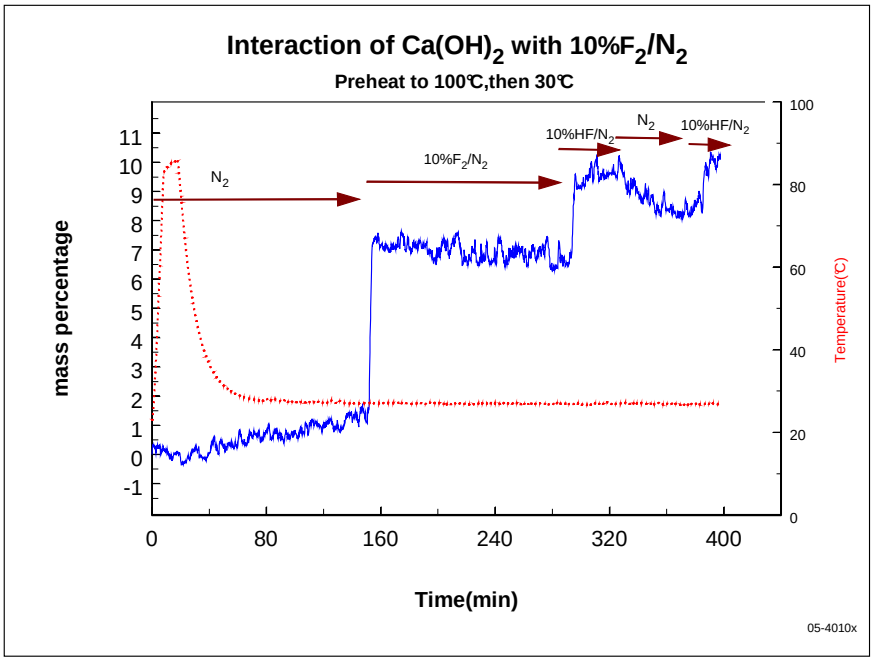


Figure 2.9: Fluorination of $Ca(OH)_2$ with F_2 followed by HF uptake

As noted from Figure 2.9, when a sample of $Ca(OH)_2$ was exposed to a 10% F_2/N_2 mixture the experimental mass gain was as expected. As seen in Figure 2.9, the sample was pre-dried at 90℃ in a flowing N_2 stream prior to fluorination; hence the mass variation is not due to adsorbed water. This sample when exposed to HF thereafter took up 3% HF. This is line with what is expected that the CaF_2 (which is now formed) will have a low HF capacity. Further, removal of the source of HF resulted in a small mass loss.

The interaction of $Ca(OH)_2$ with HF (equation 2.3) was also investigated and the TGA data is shown in Figure 2.10.

$$Ca(OH)_2 + 2HF \rightarrow CaF_2 + 2H_2O \qquad (2.3)$$

In the reaction, HF must first fluorinate the $Ca(OH)_2$ and thereafter adsorb onto the CaF_2 formed.

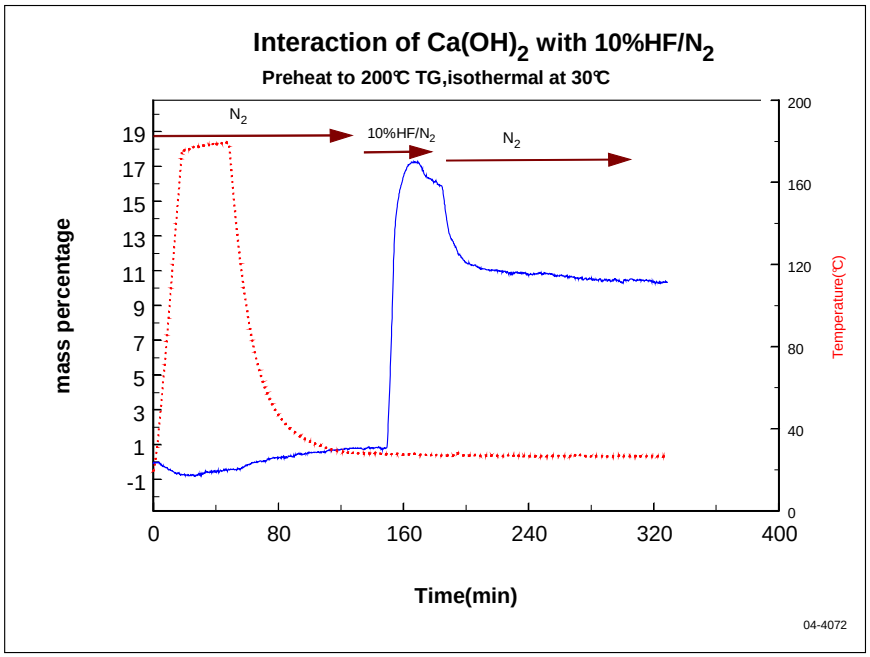


Figure 2.10: Attempted fluorination of $Ca(OH)_2$ with HF

As can be noted from Figure 2.10 exposure of $Ca(OH)_2$ to HF resulted in a 17% mass increase. Once again it is difficult to ascribe individual percentages to conversion to CaF_2 and HF uptake. However in a HF stream, the $Ca(OH)_2$ would be converted to CaF_2 and would release H_2O as a possible contaminant into the gas stream. The formation of CaF_2 was confirmed by X-ray diffraction and with no residual $Ca(OH)_2$ being noted (as verified by the JCPDS standards 35-0816). Considering that the $Ca(OH)_2$ was converted to CaF_2, upon changing the gas stream from HF to N_2, the mass change should be about 5%. The residual mass increase is however about 11%. This could indicate that the formed CaF_2 has about a 6% capacity for HF or there also could be water adsorbed (equation 2.3) onto the formed CaF_2.

The re-adsorption capacity of the formed CaF_2 was also assessed and the results are shown in Figure 2.11.

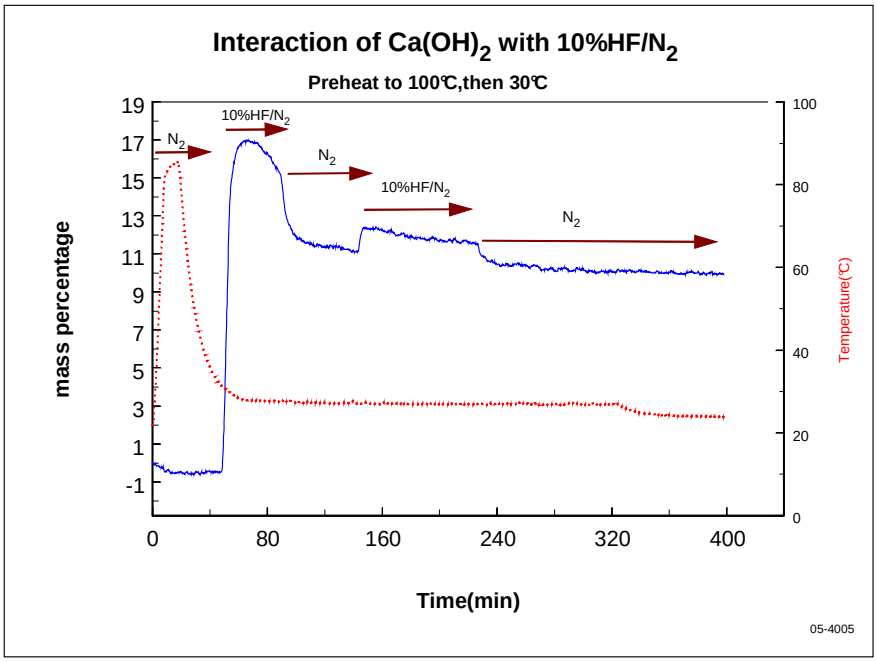


Figure 2.11: Uptake of HF by $Ca(OH)_2$

As can be noted from Figure 2.11 re-adsorption does occur but at a lower capacity. The initial uptake of HF was 17% and this decreased to 12% when the HF stream was changed to a N_2 stream. Re-exposure to HF resulted in the re-adsorption capacity going to 13%. Considering that a portion of this mass increase is due to the conversion of $Ca(OH)_2$ to CaF_2, this sample has overall a low capacity for HF.

2.4.2. Calcium chloride

$CaCl_2$ was also exposed to HF and the reaction monitored by TGA, (Figure 2.12).

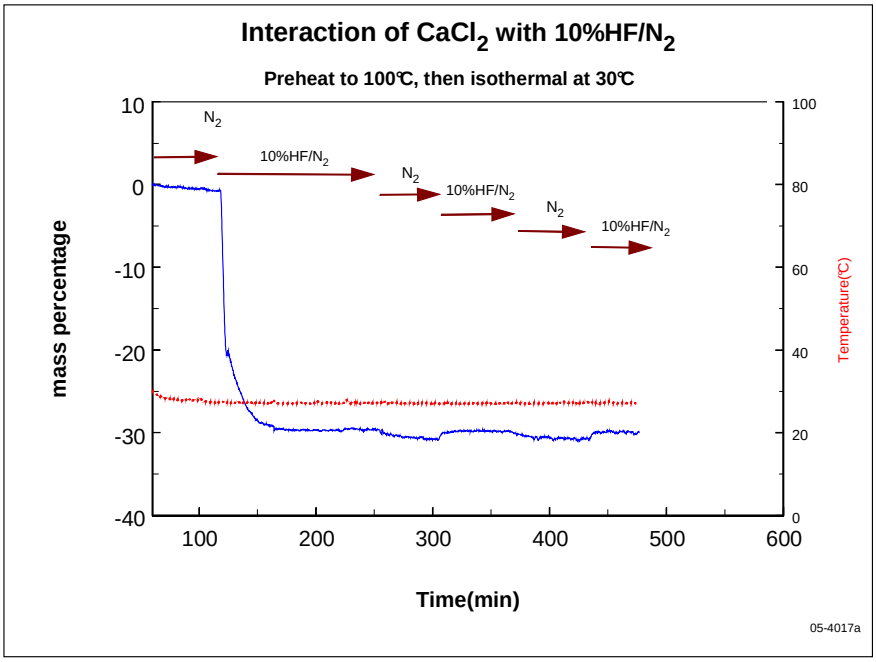


Figure 2.12: Uptake of HF by $CaCl_2$

$$CaCl_2 + 2\,HF \rightarrow CaF_2 + 2HCl \qquad (2.4)$$

As noted this sample is fluorinated in a HF environment. Hence it is not very suitable as a HF adsorber as Cl_2 gas will be released as an impurity. When this sample was re-exposed to HF it had almost no capacity. The 30% mass loss corresponds to complete fluorination, hence resulting in CaF_2 being formed. From previous data CaF_2 has a very low capacity for HF and this was seen above.

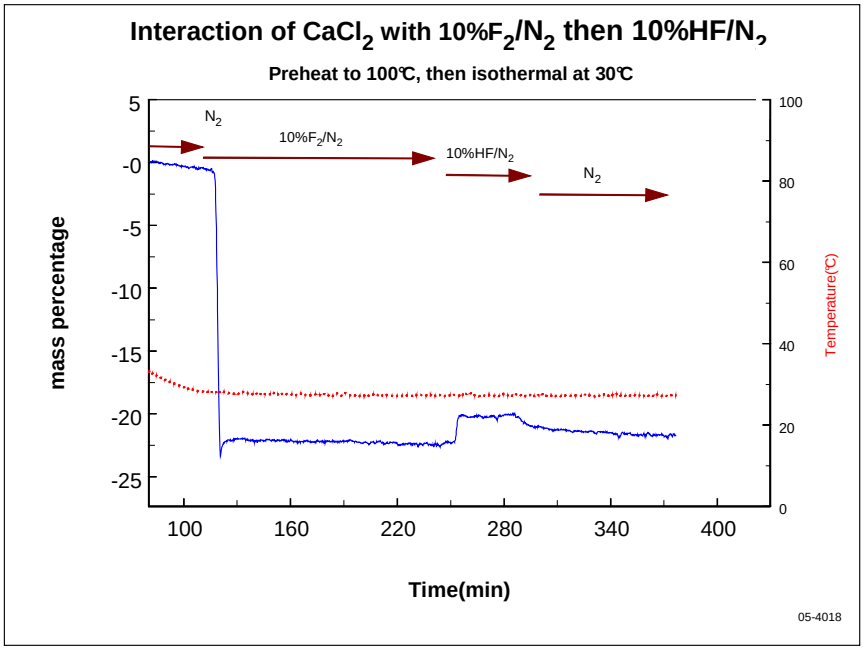


Figure 2.13: Fluorination of $CaCl_2$ with F_2 and HF uptake

From Figure 2.13, the sample was fluorinated in fluorine gas stream and thereafter exposed to a HF stream. Fluorination of $CaCl_2$ will result in a theoretical mass loss of 29.7%, but a 22% mass loss was noted experimentally for the conditions used, (see experimental). This sample thereafter has a low capacity for HF and hence cannot be used for HF adsorption.

2.4.3. Calcium sulphate

Finally, the behaviour of $CaSO_4$ (Drierite) in the presence of F_2 and HF was assessed (Figure 2.14).

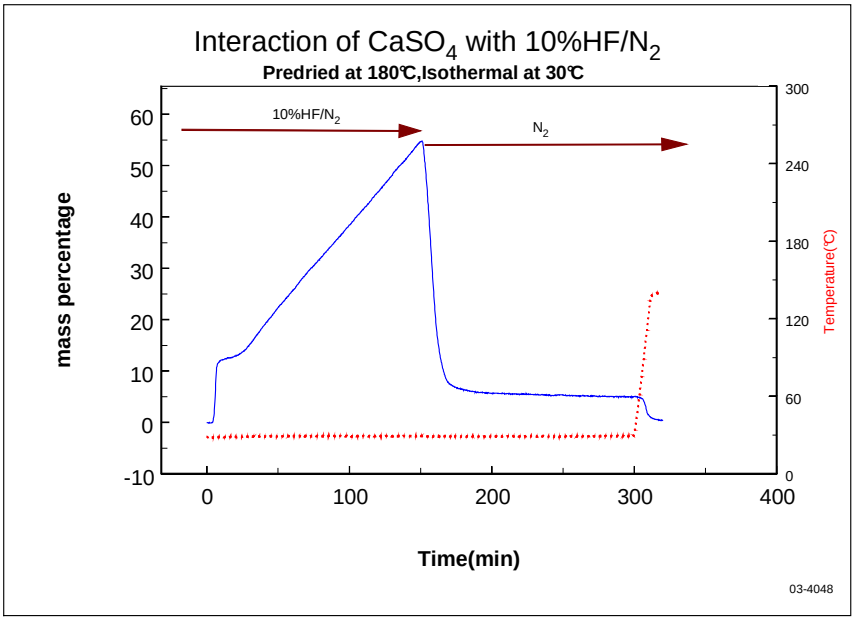


Figure 2.14: Uptake of HF by $CaSO_4$

As noted $CaSO_4$ has a high capacity for HF, after two and a half hours 55% of HF was taken up with no change in the uptake rate. Once again the initial 12% HF uptake was possibly due to monolayer cover and the rest of the uptake due to HF polymerisation. The other possible mechanism for HF uptake is *via* interaction with the $CaSO_4$. $CaSO_4$ is a drying agent that removes water by forming $CaSO_4 \cdot xH_2O$, and this same bonding may apply to HF resulting in the formation of $CaSO_4 \cdot yHF$.

The HF desorbed relatively quickly once the HF stream was removed, hence indicating that no formal interaction between the HF and $CaSO_4$

occurred for the majority of the HF taken up. The remaining HF was removed by heating.

As the aim of the experiments was to produce CaF_2 that has a high capacity for HF, after $CaSO_4$ fluorination and evaluation of HF uptake, the reaction was repeated in a Monel reactor (Figure 2.15). $CaSO_4$ (5 g) and 2.5 bar F_2 was introduced into the reactor and left for 65 hours at room temperature. The F_2 was evacuated and a further 1.5 bar introduced for 24 hours. After the first fluorination a gas sample was analysed by FTIR and the presence of SO_2F_2, one of the gaseous products of the fluorination, was confirmed (equation 2.5).

$$CaSO_4 + 2F_2 \rightarrow CaF_2 + SO_2F_2 + O_2 \qquad (2.5)$$

XRD confirmed the presence of CaF_2 and $CaSO_4$, (as verified by the JCPDS standards 35-0816 and 37-1496 respectively) [31], whereas no CaF_2 was detected in the starting material. This indicates that the sample was not fully fluorinated, possibly only surface fluorinated. The uptake of HF by this sample was thereafter assessed on the thermogravimetric analyser.

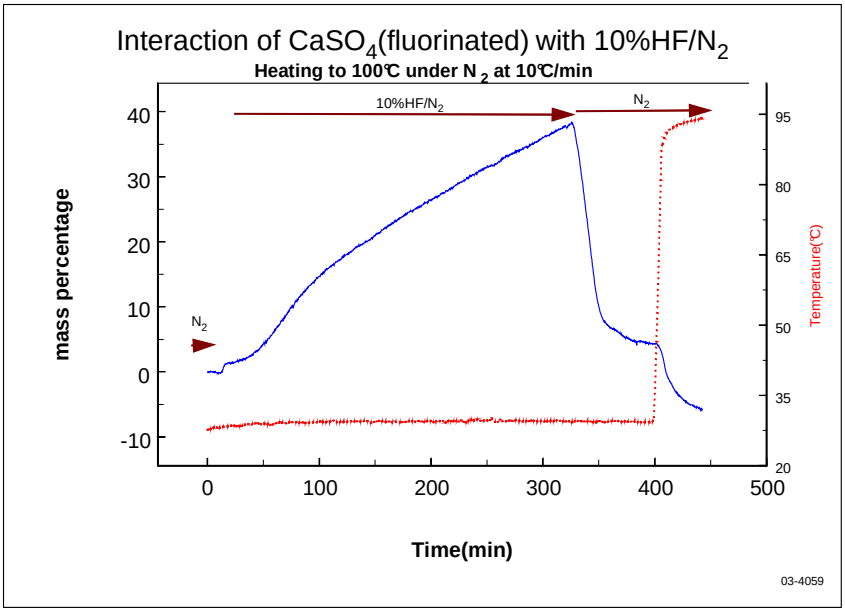


Figure 2.15: Uptake of HF by $CaSO_4$ possibly surface fluorinated in a Monel reactor

As noted this sample took up 38% HF in five and a half hours. This was a very high uptake for CaF_2, but lower than that of $CaSO_4$, (Figure 2.14). This result is similar to that obtained by Colvin [8] when he assessed the uptake of the CaF_2 from $CaSO_4$, (37% HF in five hours). The similarity of these results indicates that Colvin only observed surface fluorination of his $CaSO_4$ sample. To further evaluate the result, it was decided to repeat the fluorination (with F_2) and HF uptake experiment, on the thermogravimetric analyser. A sample of $CaSO_4$ was fluorinated with 10% F_2/N_2 mixture, at 180℃.

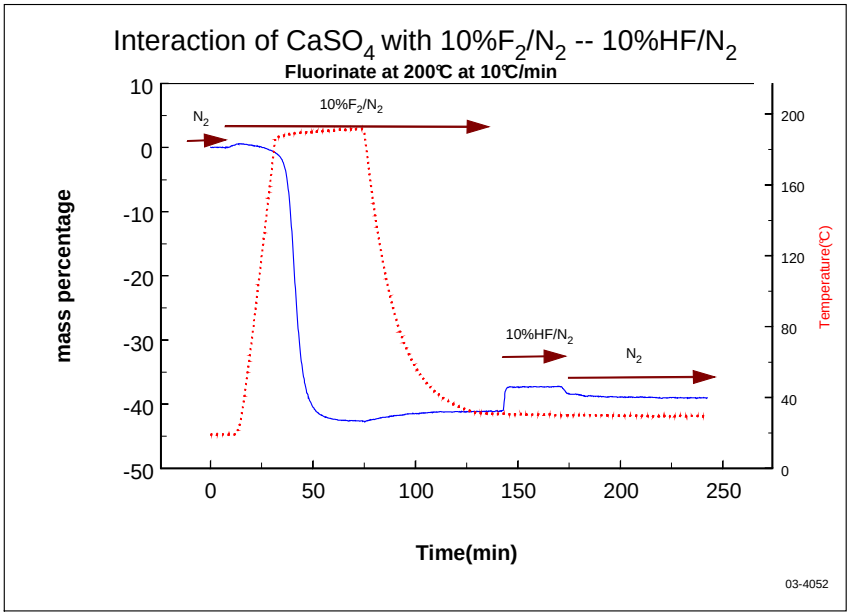


Figure 2.16: Fluorination of $CaSO_4$ by F_2 and HF uptake

As noted the sample did experience the theoretical mass loss (43%) indicating complete fluorination. No further mass loss was noted after this point even though the sample was held at the elevated temperature in the F_2 environment for a while longer, indicating completion of reaction. This sample when exposed to HF at room temperature took up only 4% HF. This shows that a fully fluorinated $CaSO_4$ sample *i.e.* CaF_2 has a very low capacity for HF adsorption when compared to $CaSO_4$. This serves as further evidence that Colvin reported data on a partially fluorinated $CaSO_4$ sample and not a CaF_2 sample.

The effect of the temperature of fluorination of $CaSO_4$, on the uptake of HF was also explored. It is also not clear if as to whether the fluorination would affect the crystal structure integrity and hence the HF uptake. As mentioned above, when the fluorination is done at 180℃, complete fluorination is achieved; hence temperatures above and below 180℃ were selected for experimentation. The results are shown in Table 2.5 below.

Table 2.5: Percentage uptake of HF for different fluorination temperatures.

Sample	**Fluorination temperature (℃)**	**Mass loss due to fluorination (%)**	**Amount HF adsorbed (%)**
1	280	43	3
2	180	42	4
3	170	43	3
4	160	37	3

It can be noted from Table 2.5 above for temperatures 170 to 280℃ the mass loss due to fluorination was 43% and the mass gain due to adsorbed HF was 3%. Hence irrespective whether a temperature of 170℃ or higher is used the result is the same. When the sample was fluorinated at 160℃, the mass loss was below expectation, indicating incomplete fluorination, yet this made no difference to the overall HF uptake. If the HF is taken up on the crystal surface then this can be expected as initially the crystal surface would be fluorinated.

As noted earlier, variations of the fluorination temperature did not have an effect on the uptake of HF by the fluorinated $CaSO_4$ samples, but the lowest fluorination temperature that ensured complete fluorination, in the earlier study was 170℃. Hence to achieve complete fluorination the crystal integrity may have been compromised. This is not desired, as it will result in adsorption column break-up, when $CaSO_4$ is used on an industrial scale. At temperatures below 170℃, incomplete fluo rination is also not desired, as sulphonated gases will be released into the F_2 gas stream.

The surface areas of the $CaSO_4$ samples were also determined (Table 2.6).

Table 2. 6: Surface area data for calcium salts

Sample	**Surface area (m^2/g)**
$CaSO_4$	9.3
$CaSO_4$ fluorinated in monel reactor	12.1

The interesting result is the surface area of the $CaSO_4$ sample that was fluorinated in the Monel reactor. This sample has a surface area of 12.1 m^2/g and 9.3 m^2/g prior to fluorination. This sample took up 38% HF in just over five hours, (see Figure 2.15), Colvin noted a similar HF uptake however his claimed surface area after fluorination was 128 m^2/g from 11.68 m^2/g prior to fluorination. This massive increase in surface area was not realized in this work. It is assumed that unreacted $CaSO_4$ participates in the adsorption process. Assuming Colvin did fully fluorinate his $CaSO_4$ sample, this would indicate that a high surface area CaF_2 has a high capacity for HF.

2.5. Uptake of hydrogen fluoride by sodium fluoride-metal fluoride mixtures

The possibility of using a mixture of CaF_2 and NaF, for the removal of HF, was also investigated. In 1912 Edeleanu [32], investigated the properties of a mixture of sodium chloride and $CaCl_2$ as a drying agent for gases. He indicated that a melt of these salts did not deliquesce upon adsorption of water.

One of the main problems experienced with the current NaF technology, is that it deliquesces in the presence of excess HF. Hence a way to overcome this problem is possibly to use a combination of NaF and CaF_2, which will result in a more stable system, *i.e*. one that does not deliquesce due to the interactions between the salts, in the presence of HF.

From the phase diagram of a CaF_2 and NaF mixture, the eutectic mixture occurs at about a third mole ratio CaF_2 and two-thirds mole ratio NaF, with the melting point being 818℃ [33]. Based on the ab ove, three CaF_2-NaF mixtures were made up by mixing NaF and CaF_2 as follows;

$$NaF + CaF_2 \rightarrow NaCaF_3 \qquad (2.6)$$

- The eutectic mixture (CNF0100) (Note: the melting point of CaF_2 is 1418℃ and that of NaF 996℃)
- A CaF_2 rich mixture (CNF0200), based on the eutectic mixture, consisting of 0.5 mole fraction CaF_2 and 0.5 mole fraction NaF and
- A NaF rich mixture (CNF0300), consisting of 0.2 mole fraction CaF_2 and 0.8 mole fraction NaF.

These mixtures were heated to 850℃ in a tube furna ce for a period of 30 minutes. After cooling these mixtures appeared to have melted, indicating some interaction between the salts. Further, the samples took on a slightly off white to grey appearance and the outer layer was extremely hard. Force was required to separate the samples from the sample boat, although the samples had not bonded to the sample boats. To verify whether or not the melting was due to the eutectic mixture being formed, a sample of NaF was subjected to the same treatment referred to above. This sample appeared to only harden and not melt. Further, the mass losses from the samples were low with CNF0100 and CNF0200 loosing about 0.4 and 0.5 mass% respectively and sample CNF0300 loosing 1.3 mass%.

Complexes of MgF_2 and NaF were also synthesized. It was hoped that magnesium, being very close to calcium in the periodic system of elements, might exhibit similar behaviour to calcium in the fluoride form. Further, if a stable complex of MgF_2 and NaF is found, this synthetic procedure may be adapted to synthesize CaF_2-NaF complexes. A

complex, sodium magnesium fluoride ($NaMgF_3$), a mineral known as Neighborite has been reported in the XRD database [31], Neighborite ($NaMgF_3$) has been synthesized from NaF and MgF_2 [34].

$$NaF + MgF_2 \rightarrow NaMgF_3 \qquad (2.7)$$

The synthetic procedure used consisted of heating a stoichiometric mixture of NaF and MgF_2 in an alumina crucible. The published XRD spectra were compared to known spectra of neighborite (in the mineral form) and found to match.

Hence, the bimetallic salt complex, $NaMgF_3$ (from NaF and MgF_2) was synthesized in this study, according to the reported synthetic procedure (see experimental) [34]. The complex synthesized, was verified by XRD analysis (with JCPDS standard 13-0303), Table 2.7 [31].

Table 2. 7: Powder diffraction data for $NaMgF_3$ [*]

hkl	d_{cal}(Å)	d_{obs}(Å)	$100I/I_o$
020	3.85	3.83(2)	24
121	2.71	2.71	51
202	2.41	2.41	17
211	2.30	2.31(1)	39
022	2.23	2.23	28
220	2.20	2.20	20
040	1.918	1.918	100
141	1.713	1.716(3)	12
042	1.575	1.575	17
321	1.556	1.555(1)	38

[*]*peaks with intensity greater than 10% are listed*

With regard to the $NaMgF_3$ complex, the surface area was found to be 0.25 m^2/g; these samples were then subjected to thermogravimetric analysis to assess the HF vapour uptake. The results however, were poor. As can be noted from the thermogravimetric curves below (Figures 2.17 and 2.18), the mass uptake of HF was 1%.

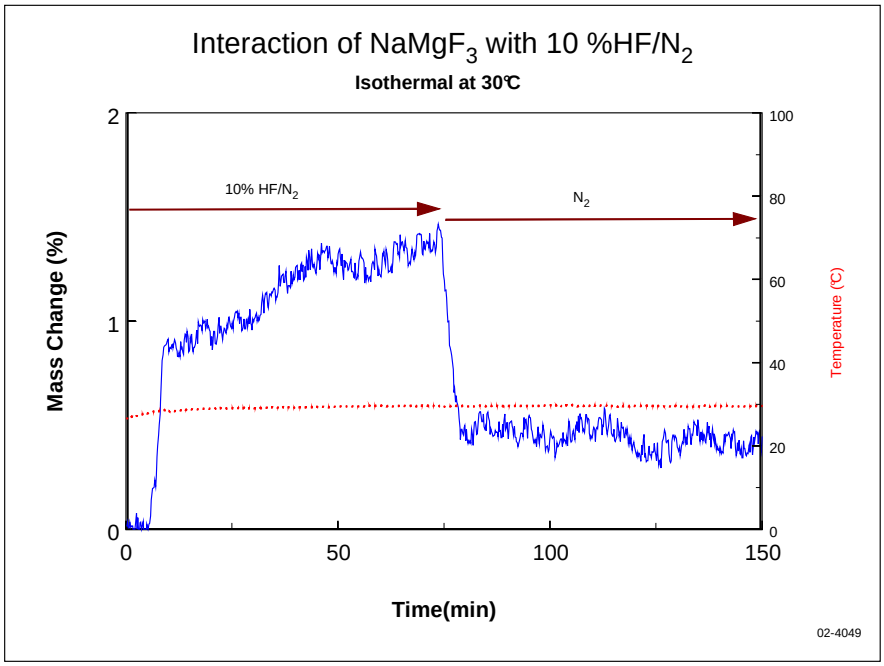


Figure 2.17: Uptake of HF by $NaMgF_3$

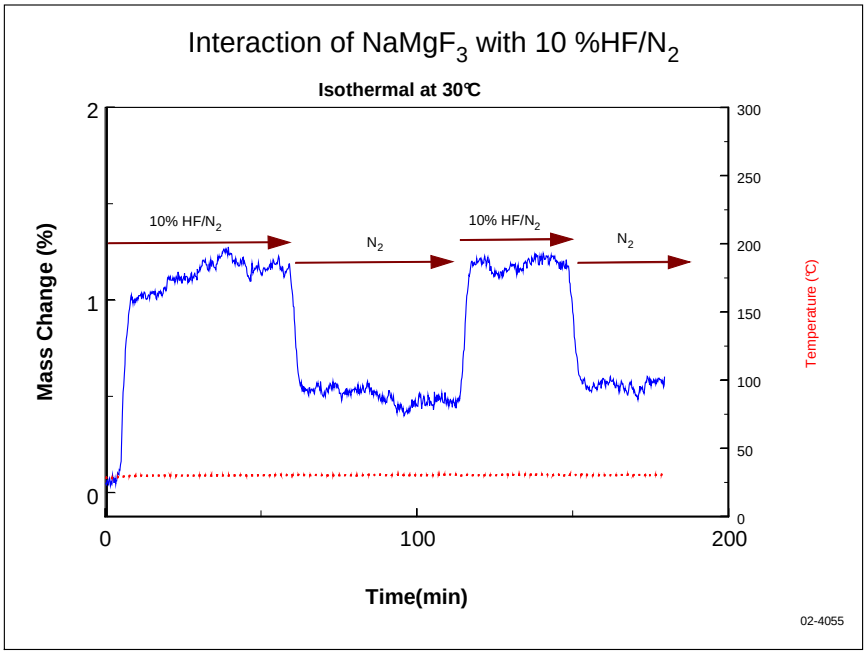


Figure 2.18: Uptake of HF by another $NaMgF_3$ sample

It was hoped that CaF_2 would react with NaF, similarly to the reaction with MgF_2. Only publications referring to the modelling of the Ca analogue *i.e*. $NaCaF_3$ have been reported [33, 35, 36]. However, the $NaMgF_3$ synthetic procedure was attempted on the CaF_2–NaF analogue. Firstly, the synthesis procedure was followed as stipulated for the $NaMgF_3$ complex. This was not successful as no new complex was identified by X-ray analysis. Attempts were also made to synthesize the CaF_2–NaF analogue at higher temperatures but using the same $NaMgF_3$ synthesis procedure *i.e*. at 1100 and 1400℃ but this was also unsuccessful .

As is evident from these results, the $NaMgF_3$ samples have a very low capacity for HF. However, the idea of using other complex salts and inorganic complexes to take up HF should not be discarded. If the co-ordination between HF and NaF is clearly understood, this will assist in finding another complex that does not deliquesce in the presence of HF.

2.6. Exposure of AlPO to hydrogen fluoride and fluorine

The AlPO-5 sample is the only AlPO sample that was tested for chemical resistance. It is not commercially available and hence was not easy to obtain. The tests were conducted as follows; The AlPO-5 sample was exposed to either a 10% HF/N_2 mixture or a 10% F_2/N_2 mixture, at various temperatures in the TGA. The variations in mass, as the sample was heated, were then noted. Some samples were thereafter sent for XRD analysis.

2.6.1. Hydrogen fluoride exposure

The AlPO-5 was exposed HF on the thermogravimetric analyser (Figure 2.19). When the AlPO-5 sample (dried at 100℃) was exposed to a 10% HF/N_2 mixture, the sample took up about 120 mass % of HF. When this stream was changed to one of only N_2 the sample lost most of its mass (the HF taken up) and the uptake dropped to about 20% greater than the starting mass. However when the HF stream was re-introduced into this sample, the mass increased by only a further 10%. Hence the sample only took up a total of 30 mass% HF compared to 120 mass% for the first HF exposure.

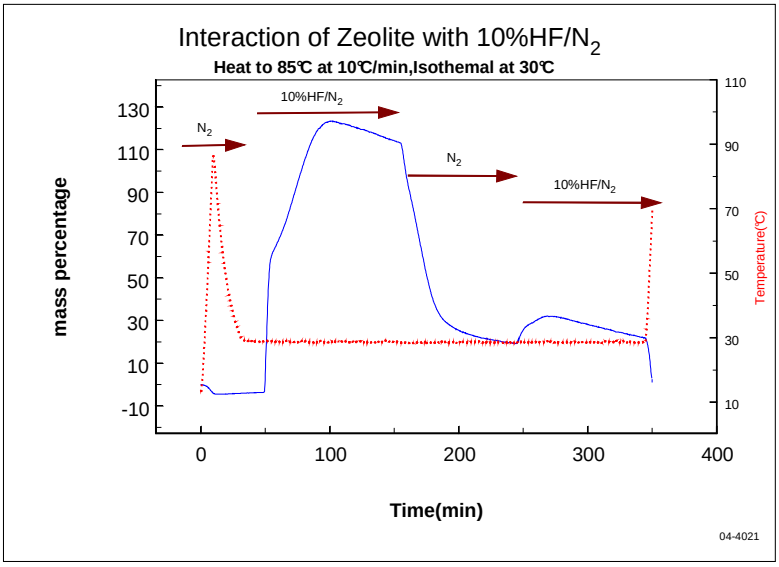


Figure 2.19: Thermogravimetric curve of AlPO-5 after exposure to a 10% HF/N_2 mixture

As can be seen from Figure 2.19 the sample took up HF relatively quickly (120%), and then the mass began to decrease. This decrease could be due to HF desorbing from the sample or it could indicate breakdown of the zeolite with the release of some volatile component, for example the sample contains some V and upon reaction with HF it could form volatile VF_5. Further, as can be seen from Figure 2.19, this sample has a very low capacity for HF upon re-exposure to the HF/N_2 stream. This type of result is indicative of a sample that has decomposed upon exposure to HF.

To determine if decomposition of the AlPO had occurred, a sample was exposed to the 10% HF mixture (Figure 2.20), and after HF removal, analysed by powder XRD.

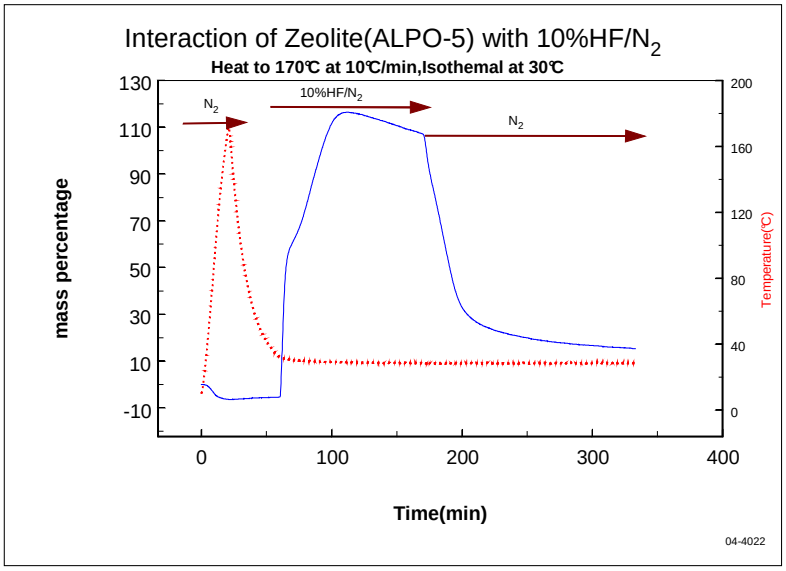


Figure 2.20: Thermogravimetric curve of AlPO-5 after exposure to a 10% HF/N_2 mixture

From the XRD results obtained the AlPO-5 peaks (as verified by the JCPDS standards 44-0044) were no longer present. Only one broad peak, centred where an AlF_3 peak would normally be found, and verified by the JCPDS standards 20-0006, was observed. This indicates that the Al_2O_3 in the AlPO was fluorinated to AlF_3.

Naydenov has suggested that high initial gas uptake is due to the porous structure of AlPO material, but that it decomposes to amorphous aluminophosphate [37]. Based on the above results it is evident that the sample studied has also been fluorinated.

2.6.2. Fluorine exposure

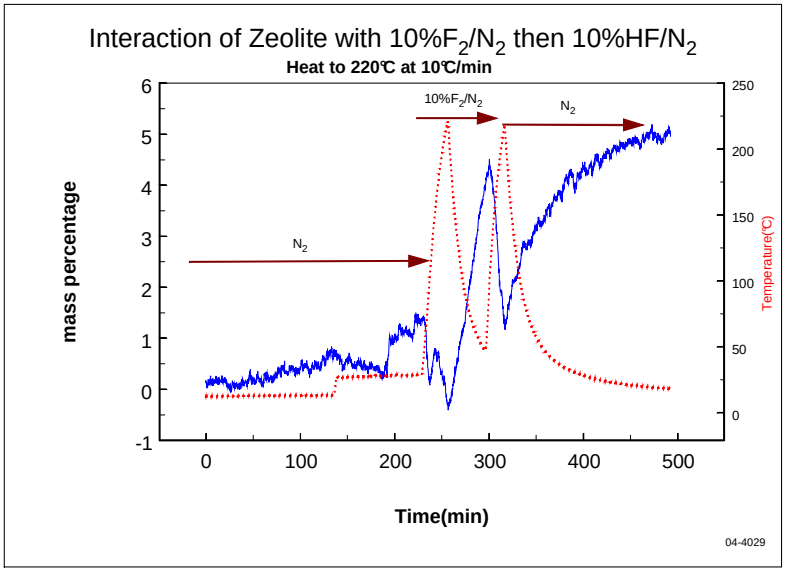


Figure 2.21: Thermogravimetric curve of AlPO-5 after exposure to a 10% F_2/N_2 mixture

The AlPO was also exposed to F_2, (Figure 2.21). This sample was exposed to a 10% F_2/N_2 stream with the temperature being taken up to 220℃ (to accelerate any decomposition if present). Thereafter the sample was analysed by XRD. From the TGA result it appears as if this sample does not have much capacity for F_2. However, the XRD results indicate that the sample appeared to have lost crystallinity as the diffraction peaks all disappeared except for a broad band at about 2θ peak 20°.

2.6.3. HF exposure at elevated temperatures

The AlPO-5 sample was also exposed to HF at an elevated temperature, (Figure 2.22). It is possible that the AlPO-5 sample dissolves in HF (similar to a hydroscopic salt taking up atmospheric moisture; it dissolves after a while) before being fluorinated. If however the adsorption is done at a high temperature, it would prevent any dissolution of the AlPO-5 sample.

However, the XRD results indicate that treatment of the AlPO-5 sample with HF at 250℃ resulted in product destruction. No crystalline phase present after reaction on the XRD.

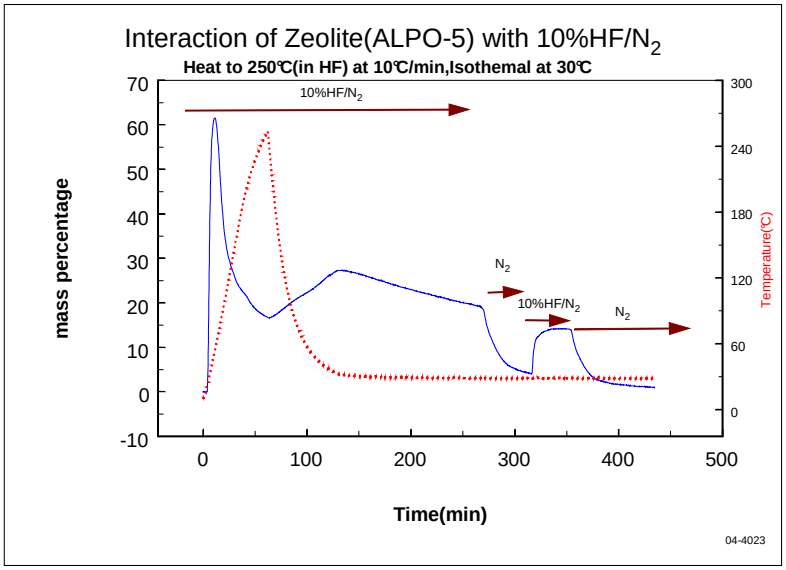


Figure 2.22: Thermogravimetric curve of AlPO-5 after exposure to a 10% F_2/N_2 mixture at 250℃

2.6.4. Pre-treatment at elevated temperatures

In a final experiment the AlPO was heated to a higher temperature to drive off any remaining water and thereafter it was exposed to HF. According to Naydenov, AlPO-5 strongly adsorbs water and this water would assist in the dissolution of AlPO-5 by the HF. He suggested heating the sample to 400℃ [37]. The HF uptake experiments consisted of heating AlPO samples overnight at 320℃ and 400℃ respectively, before exposing the sample to HF.

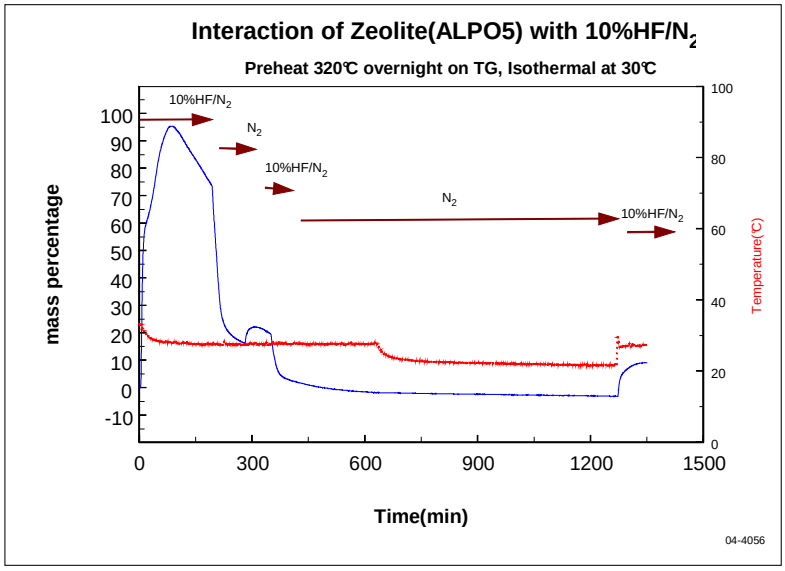


Figure 2.23: Thermogravimetric curve of AlPO-5, preheated to 320℃, thereafter exposure to a 10% HF/N_2 mixture

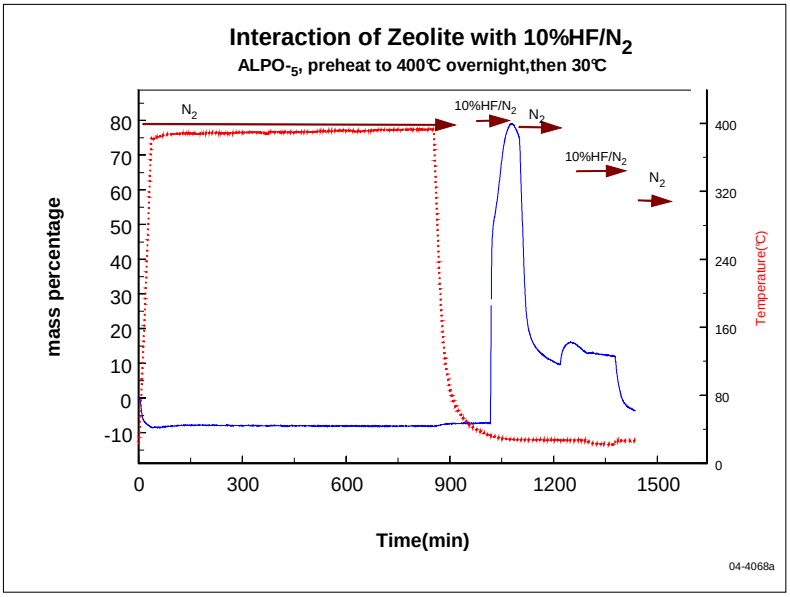


Figure 2.24: Thermogravimetric curve of AlPO-5, preheated to 400℃ thereafter exposure to a 10% HF/N_2 mixture

As can be noted from Figures 2.23 and 2.24, this sample still decomposed upon exposure to HF; hence it appears that the adsorbed water does not play a role in the decomposition of the AlPO sample. It is possibly a reaction between the AlPO and HF. Further, the initial HF capacity decreased from 120% to 100% for the sample heated to 320℃ and 80% for the sample heated to 400℃. Hence heating the sample to these temperatures, damages it.

2.7. Experimental

General experimental procedures

Materials

The CaF_2 used was supplied by BDH, (GPR grade 97% pure), as well as from Saarchem. Delta F, Peldev, supplied the $CaSiF_6$. The $Ca(OH)_2$ (96%) was from BDH and the NaF (GR, 99%) from Merck. The Drierite ($CaSO_4$) 10 to 20 mesh was obtained from Aldrich and the $CaCl_2$ 3 to 8 mesh, fused granular from BDH. The Drierite and $CaCl_2$ was reduced to 16 –18 mesh, (grinding then using sieves) prior to any experiments being conducted. The mesoporous Me-AlPO-5, (where Me is V) sample spheres used for this investigation was obtained from Naydenov, V. and used without further purification.

All the above chemicals were used as received, without further purification except for the processing mentioned above. The anhydrous HF was 99.9% pure as supplied by Pelchem. This was used as received, or in some cases to make a 10% vapour mixture with N_2 up to a maximum total pressure of six bar. This 10% mixture was used as the HF feedstock for the TGA. The F_2 (nominally 98%, as supplied by Pelchem) was used as is, and diluted to 10% with N_2 up to a maximum total pressure of three bar for the thermogravimetric fluorination.

Thermogravimetry

The process of HF adsorption was monitored with an in-house assembled thermobalance, by measuring the mass increase experienced by a sample over a period of time as a function of temperature, with the fluorinations being conducted by F_2 or HF and the fluorinations being monitored by the mass change experienced by the sample due to anion substitution. Thermal analysis is usually conducted in an inert atmosphere. Use of a

reactive atmosphere required a weighing mechanism for the thermobalance protection using a N_2 blanket that flowed directly over the weighing mechanism. The flow rate of the inert/reactive gas used was 28.8 ml/min at STP with sample masses normally in the range of 3 to 5 mg. Further, the gas streams could be changed from inert (N_2) to reactive gas and back easily. The thermobalance has a resolution of 1 µg. Further, cooling of the circulating water, used for the low temperature thermogravimetry work was achieved using a Neslab, Endocal Refrigerated Circulating bath. More information on the thermobalance can be obtained from a publication by Sanderson [38].

Surface Area

Surface area analysis was conducted on a Micromeritics Flowsorb 2300 single point surface area analyser, using the classical BET technique. N_2 was used as the adsorbate from a 25% N_2/He mixture. All samples were degassed for at least 30 minutes at between 150 and 200℃ prior to analysis. The limit of detection is 0.1 m^2/g with a reproducibility of 0.5%.

FTIR

FTIR was done on a Hartman and Braun Bomen MB-100 spectrometer with the data being processed on the Bomen IR software.

X-ray Powder diffraction

Powder X-ray data were collected at 298K using a Siemens D500 diffractometer with copper radiation giving a wavelength of 1.5406Å. The X-rays were generated at 40kV and 30 mA. The data collection conditions were $10° \leq 2\theta \leq 110°$, $\Delta 2\theta = 0.05°$ and $t = 5$s.

Precipitation of CaF_2 from aqueous solutions

Saturated solutions of CaF_2 (BDH) in 50 ml distilled water were made up in rapidly boiling and warm (±50℃) water. These solut ions were left at room temperature overnight to allow complete precipitation and fine crystalline CaF_2 formed in the bottom of both beakers. The supernatant liquids were thereafter decanted and the crystals dried under a stream of N_2.

Fluorination of CaF_2

CaF_2 (BDH) was finely powdered and dried at 100℃ for a t least two hours. The sample was then re-powdered for a few minutes and 1 g of this sample was placed in a 400 ml cylindrical Monel vessel. This vessel was degassed and one bar F_2 introduced. The vessel was left at the desired temperature for 16 to 72 hours (depending on the requirements of the experiment) where after it was degassed and flushed five times with N_2.
The fluorinations were conducted at various temperatures, from room temperature to 270℃. Temperature control was obtai ned using a clamp-on-heater with a Rkc temperature controller.

Fluorination of Drierite ($CaSO_4$)

Drierite, 10 – 20 mesh (Aldrich) was reduced to 16 – 18 mesh, (by grinding and sieving), and dried at 180℃ for 24 hours. 5 g of this sample was placed in a 400 ml cylindrical Monel vessel. The vessel was degassed and 2.5 bar F_2 introduced into the vessel. This vessel was left for 65 hours at room temperature. A gas sample was extracted and the presence of SO_2F_2 was confirmed by FTIR spectroscopy, IR (SO_2F_2); *v* 1515, 1501, 1409, 1283, 1269, 1268, 1161, 898, 884, 863, 847 cm^{-1}. The vessel was then evacuated and thereafter 1.5 bar F_2 introduced into the reaction vessel. This was left for 24 hours at room temperature where after it was

degassed and flushed five times with N_2. This sample was subjected to powder XRD, which confirmed the presence of both CaF_2 and $CaSO_4$.

NaF – CaF_2 mixtures

Three oven-dried mixtures of CaF_2 (BDH) and NaF (Merck) were made up which consisted of; (i) the eutectic mixture; 26.0 g CaF_2 and 28.0 g NaF. (ii) an equimolar ratio mixture, 39.0 g CaF_2 and 21.0 g NaF and (iii) a mixture of 0.2 mole fraction CaF_2 (15.6 g) and 0.8 mole ratio NaF (33.6g). Each of these mixtures were well powdered and mixed in a pestle and mortar for at least 30 minutes. 5 g of each mixture was there after placed in alumina crucibles and heated in a Carbolite tubular furnace at a rate of 10℃/min up to 850℃. The samples were held there f or 30 minutes and allowed to cool slowly to room temperature. Some samples were subjected to longer heating times at 850℃.

Synthesis of $NaMgF_3$

Stochiometric amounts of NaF (Merck) and MgF_2 (98%, Aldrich) were used in the synthesis. NaF (21.0 g) and MgF_2 (31.2 g) were oven dried and mixed in a pestle and mortar for at least 30 minutes. They were there after heated in an alumina crucible at 750℃ in a C arbolite tubular furnace for 7 hours. The samples were removed and re-ground once they had cooled sufficiently. They were then re-heated to 800℃ for 12 hours. These reactions were conducted under a stream of N_2. The product was verified using powder XRD.

2.8 References

1 Takita, Y., Li, G-L., Matsuzaki, R., Wakamatsu, H., Nishiguchi, H., Moro-oka, Y. and Ishihara, T., *Chemistry letters*, 13, (1997).

2 Takita, Y. and Ishihara, T., *Catalysis Surveys from Japan*, 165, **2**, (1998).

3 Takita, Y., Ninomiya, M., Matsuzaki, R., Wakamatsu, H., Nishiguchi, H. and Ishihara, T., *Phys. Chem. Chem. Phys*., 2367, **1**, (1999).

4 Szostak, R., Molecular Sieves, Principles of Synthesis and Identification, van Nostrand Reinhold, (1989).

5 Wu, P.; Wu, J.; Li, C. and Yang, W., *Chin. J. Geochem.*, 229, **18**, (1999).

6 Jache, A. W. and Cady G. H., *J. Phys. Chem.*, 1106, **56**, (1952).

7 Ikrami, D. D. and Nikolaev, N. S., *Russ. J. Inorg. Chem*., 1313, **15**, (1970).

8 Colvin W. L., AEC (US) report number K-1117, (1953).

9 Merchant, D. R. and Hodges, J. R., Penwalt Corporation, Philadelphia, Pa., Patent US 3 976 447, (1976).

10 Nakano, H.; Matsuoka, N.; Ueda, T.; Nogami, C. and Odajima, H., Japan, Patent Hei 10-128061,(1998).

11 Kemnitz, E. and Hass, D., *Z. Chem.*, 384, **20**, (1980).

12 Bennewitz, R.; Smith, D. and Reichling, M., *Phys. Rev. B. Condens. Matter Mater. Phys.*, 8237, **59**, (1999).

13 Batzill, M. and Snowdon, K. J., *Appl. Phys. Lett.*, 1955, **77**, (2000).

14 Cai, Y. and Song, K. S., *Nucl. Instrum. Methods Phys. Res. Sec. B*, 115, **101**, (1995).

15 Wu, Y.; Mayer, J. T.; Garfunkel, E. and Madey, T. E., *Langmuir*, 1482, **10**, (1994).

16 Bermudez, V. M., *Applied Surface Science*, 227, **161**, (2000).

17 McVicker, G. B. and Eggert, J. J., Exxon Research and Engineering Co., US patent 4 402 924, (1983).

18 Opalovsky, A. A.; Fedorov, V. E. and Fedotova, T. D., *Journal of Thermal Analysis*, **1**, 301, (1969).

19 Yang, R. T., Adsorbents, Fundamentals and Applications, Wiley-Interscience, (2003).

20 Jasra, R. V. and Bhat, S. G. T., *Separation Science and Technology*, 945, **23(10 and 11)**, (1988).

21 http://www.iza-online.org., The web page of the International Zeolite Association.

22 van Bekkum, H., Flanigen E. M. and Jansen J. C., Introduction to Zeolite science and practice, Vol. 58, Studies in Surface Science and Catalysis, Elsevier, (1991).

23 McCusker, L. B., Liebau, F. and Engelhardt, G., *Pure Appl. Chem*., 381, **73(2)**, (2001).

24 Kirsch, W. B. and Laurent, S. M., Ethyl Corporation, Richmond, Va, Patent, US 4 557 921, (1985).

25 Foley, H. C. and Mariwala, R. K., University of Delaware; E. I. Du Pont de Nemours Co., Both of Wilmington, Del., US Patent 5 261 948, (1993).

26 Jeon, J. Y., Xu, X-F., Choi, M. H., Kim, H. Y. and Park, Y-K., *Chem. Commun.*, 1244, (2003).

27 Naydenov, V., Tosheva, L. and Sterte, J., Poster presented at the 14th International Zeolite Conference, Cape Town, South Africa, 25 April 2004.

28 Deane, A. M., AERE – R 3261, Atomic Energy Research Establishment, Harwell, Berkshire, H. M. Stationary Office, (1960).

29 As noted in a separate experiment in our laboratories where a NaF pellet was exposed to HF vapour in a clear polyethylene container.

30 Dana, E. S. and Ford, W. E., *A Textbook of Mineralogy*, 4th Ed, John Wiley and Sons, 462, (1949).

31 JCPDS-ICDD, PDF-2 sets 1-41 database (1991).

32 Edeleanu, L., Patent US 1041608, 15th Oct. (1912).

33 Xu, Q.;Yu, Y. and Qiu, Z.; *Jinshu Xuebao*, **30(4)**, B150, (1994).

34 Chakhmouradian, A. R., Ross, K., Mitchell, R. H. and Swainson, I., *Phys Chem Minerals*, **28**, 277, (2001).

35 Hara, S., Shibaike, H. and Ogino, K., *ISIJ International*, **30(4)** 298, (1990).

36 Cheng, Z., Jia, Z., Xu, L. and Chen, N., *Wuli Huaxue Xuebao*, **10(8)**, 676, (1994).

37 Naydenov, V., Personnel communication.

38 Sanderson, R. D., du Toit, F. J., Carstens, P. A. B. and Wagener, J. B., *Journal of Thermal Analysis*, **41**, 563, (1994).

Chapter 3

Resins

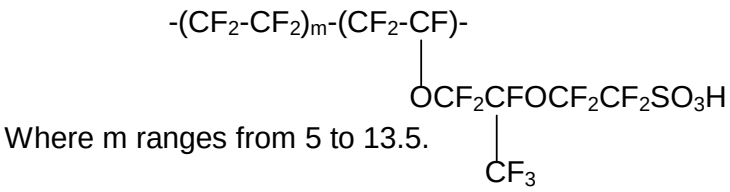
3.1. Introduction

This chapter deals with the uptake of HF by polymeric structures. In this regard both functionalised and non-functionalised polymeric structures will be discussed. In particular, (i) a perfluorinated resin, Nafion® Superacid Resin, (ii) sodium polyacrylate and (iii) a series of commercial ion exchange resins will be investigated

3.2. Literature survey

This work has as its basis, a 1995 patent by Barsotti [1] in which he used Nafion® Superacid Resin to remove HF from organic materials, even in cases where azeotropes were formed. This polymer was used by Barsotti to separate organics from HF in both the liquid and vapour phase. He reported that the polymer had a high sorption rate for HF; and that it was also highly resistant to HF attack [2]. Sorption of 10 to 15% of the polymer weight was reported before the polymer needed to be regenerated; a heated nitrogen stream was used to remove essentially 100% of the HF.

Nafion® Superacid Resin is a strongly acidic resin which is a co-polymer of tetrafluoroethylene and perfluoro-3,6-dioxa-4-methyl-7-octenesulfonyl fluoride (ratio approx 7:1), with the sulphonyl fluoride group (SO_2F) normally converted to the acid form (SO_3H). The chemical structure is shown in Figure 3.1 [3, 4]:



Where m ranges from 5 to 13.5.

Figure 3.1:Structure of Nafion® Superacid Resin

One of the properties that makes Nafion® unique is its ability to take up very high ratios of water to sulphonic acid groups. Amounts as high as 22 water molecules per sulphonic acid group for liquid uptake and 14 for vapour uptake have been reported [5], and this high uptake cannot be explained only by hydrogen bonding. Further, considering the backbone of the Nafion® is hydrophobic, the possibility that it has a high water capacity is not expected. With reference to cations, changing the cation from H^+ to Li^+ or Na^+ resulted in a decrease in water capacity for both vapour and liquid uptake indicating that the high capacity is influenced by the cation [6].

Further investigation into the structure of Nafion®, indicated distinct ionic clustering occurred and that it possessed discrete hydrophilic and hydrophobic regions [7]. The hydrophobic region is composed of the polymer backbone and the hydrophilic region of the sulphonic acid groups and their counter ions. However, interfacial regions of polymer backbone and ionic sites, not involved in clustering, do exist in the resin [7]. Further investigations into these hydrophilic regions reveal clusters that are 40Å in diameter linked by channels that are 10Å in diameter. Pretreating the polymer, for example by boiling it in water, generally forms these clusters known as micelles [8].

The second polymeric structure that was assessed in this thesis study was the sodium salt of polyacrylic acid *i.e.* sodium polyacrylate. In a 1998 patent by Luly, he claimed that this polymer has a higher capacity for

separating HF from a chemical mixture [9]. One of the reasons given for the higher capacity was that this polymer is water-soluble or at least able to swell to twice its dry volume. He quoted 28 examples where the HF content was partially removed from both organics and inorganics and in both the liquid and vapour phase [9].

The third material type investigated was the ion exchange resins. It was reasoned that if sodium polyacrylate is soluble in water then it might also be soluble in HF thus making it difficult to work with on an industrial scale. The cross-linking present in ion exchange resins would render the polymer insoluble in HF.

Ion exchange resins have been used in many applications that include water softening and decolourisation, separation and recovery of rare earth metals, organic and inorganic separation, catalysis, esterification and treatment of sugars, amino acids, enzymes, *etc*. [10, 11]. The majority of the above applications are carried out in an aqueous or liquid medium. In this study however, the intended application is a gas phase application for removal of HF from a gas mixture. A survey of publications relating to gas phase use of ion exchange resins is given below.

Richter appeared to be the first to note that ion exchange resins can be used industrially for the removal of acidic and basic vapours from gases. He studied the uptake of NH_3, HCl, SO_3 and CH_3COOH by various resins. He noted that moist resins have a higher capacity for gases than dry resins; *e.g*. 100 cm^3 of a moist amine resin took up 39 g of CH_3COOH as compared to 1.6 g by the dry resin. Washing with water can regenerate these resins [12].

Since then, the uptake of acidic gases viz. CO_2, CO, SO_2, NO_2, H_2S *etc*. have be assessed by many workers [13 -21]. Some work of interest is as follows:

Vaidyanathan studied the uptake of SO_2, H_2S and NO_2 by various polymeric ion exchange resins. He noted that there was a low sorption rate of SO_2 on a tertiary amine resin. There was an initial rapid uptake but it was followed by a period of slow uptake.

In terms of mechanism, he indicated the initial quick uptake is due to surface adsorbtion and some adsorbtion into the polymer matrix, causing it to swell. However, due to elastic forces within the polymer matrix, this uptake within the polymer stops. However, slowly the elastic forces relax and more sorption takes place until the forces decay completely. It is only at this point that equilibrium is reached. This can produce a wide variety of sorption curves as the complex behavior of polymer relaxation below its glass transition temperature has to be factored in, so too must the diffusion coefficients and the immobilization of the diffusing species.

With reference to desorption, there was a rapid initial desorption, accounting for 15 to 40% of the initial mass followed by a slow desorption step. He ascribed the initial step to macropore desorption and the remainder to slow diffusion of the adsorbate from the polymer matrix. However not all the SO_2 desorbed, as about 1.9 meq/g resin remained; he indicated the exchange capacity of the resin was 6.5 meq/g, hence he could draw no conclusion as to why this percentage SO_2 remained on the polymer.

For H_2S, he used a quaternary amine resin in the chloride form. Again he noted slow adsorption. He tried to influence this rate by varying the pressure but with no success. The uptake characteristics were similar to that for SO_2. With regard to NO_2, here he noted excellent kinetics for uptake on Amberlyst A27 and good equilibrium loading, however he gave no details as to characteristics of this resin. He noted also that the sorption was irreversible indicating some sort of reaction between the exchange sites and NO_2 [22].

Cole also studied the uptake of SO_2 by ion exchange resins and found that the chloride quaternary amine functionalized resins appeared to have the greatest capacities, more specifically Dowex 21K, which was a high porosity resin. Amberlite IRA 400 a medium porosity resin however had the highest adsorption rate. He also compared these results with Molecular sieves (5Å) and activated carbon and found the molecular sieve rivaled the resin in terms of capacity but the resin showed the highest desorbtion [23].

With reference to the uptake of HF by resins, Bulikh reviewed some of the work on the sorption of gases including wet HF and HCl from air. With regard to HCl, he found that a weak base resin with 57 mass% moisture takes up 24 parts by mass HCl per 100 parts by volume of which most is adsorbed by the water. This allows immediate regeneration and reuse.

In terms of HF, the resin used was a strongly basic resin in the fluoride form. It took up 12.5 to 13.5 mmole of HF per gram resin before any was detected in the off gas. The resin took up a total of 22 mmole of HF at equilibrium from a moisture saturated air mixture with 4 mg HF per litre. As for the weak base resin, this took up 16-16.5 mmole of HF until it was detected and 42 mmole at equilibrium. The uptake mechanism is as a solvate between the functional group and HF, and the water present is replaced. He also indicated that washing with water could regenerate the resins.

With reference to ammonia, Bulikh has indicated that the proton form of a strong acid resin can take up ammonia, however it is heavily dependent on the moisture content of the resin. The resin can be regenerated with an acid resulting in an ammonium salt [24].

With reference to the removal of HF from other gases, Vulikh developed a method to remove HF and HCl by adsorption from air. It comprised of

passing the gas mixture through an anion exchange fibre. The fibre consisted of vinyl pyridine or aliphatic amino groups and was made up into a non-woven cloth 6 mm thick. This allowed faster flow through of gases compared to a column. He indicated the cloth could be regenerated and reused numerous times, by washing with water. He did also indicate that the adsorption capacity is dependent on the humidity of the gas flow and that reduced moisture contents resulted in reduced capacity [25].

Low concentrations of HF or HCl could also be removed by adsorption from SO_2 by contacting the gas mixture with a weak or strong base anion exchange resin with an amine fluoride or chloride functional group. The degree of removal of HF from SO_2 was greater than 99.98% [26]. Strong base resins can also be used to remove HF from HCl [27].

Siguo reported, that FFA-1 ion exchange fibre has the capacity to adsorb acid gases including SO_2, HF and HCl [28]. Based on the description given in the paper, FFA-1 has a polymeric backbone (not specified) containing a NH_2 functionality. The up take of acid gases was described as a chemical adsorption process *e.g*. the uptake of SO_2 is shown in Figure 3.2:

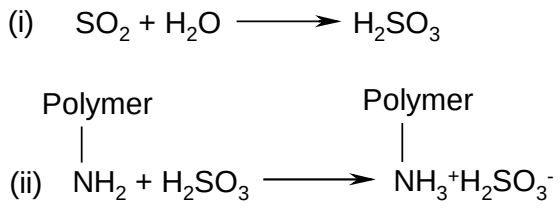


Figure 3.2: Mechanism of SO_2 uptake by FFA-1

Figure 3.2 indicates the formation of an acid (i) that is then taken up by the polymer (ii). Siguo also noted that this fibre had a higher capacity for HF than for the other acidic gases studied. Most of the HF can be eluted by water but the rest (8 mmol/g) can only be removed using an alkaline solution. A further interesting point was that he reported the saturation

adsorption capacity of HF at 25℃ to be 22 mmol/g for gaseous HF and 7.27 mmol/g for liquid HF. With reference to the mechanism, it was proposed that HF initially reacted with the alkaline functional group on the fibre. The HF is then removed by base and the rest of the HF uptake is due to HF polymer formation onto the initial HF adsorbed by the functional group. He also indicated that FFA-1 was to be developed for use in gas masks [28].

A follow up paper appeared in 2000, where the adsorption and filtration of hazardous fluoride dust and acidic gas by FFA-2 ion exchange fabrics was discussed [29]. FFA-2 (which is assumed to be different from FFA-1) is described as a low alkaline non-woven fabric with an exchange capacity of 5.5 – 6.5 meq/g, which is produced by his institute for industrial trial runs. He indicated that the adsorption capacity for HF of this fabric is 11 mg/g. However, increasing the moisture content of the fibre or relative humidity, the HF volume can be increased to 50 mg/g. This increase in uptake is due to swelling and unfolding of the fibre in moisture and the adsorption of a gas in ionised form. Finally this fibre was incorporated into protection masks.

Hence based on the above it was decided to do a more comprehensive study into the uptake of HF by the various resins. This includes Nafion® superacid resin, sodium polyacrylate and various ion exchange resins. However this study focuses on the ion exchange resins as one of the problems associated with Nafion® is it's extremely high cost making it impractical for some industrial applications. Factors considered included uptake by acid and basic ion exchange resins, both strong and weak, the effect off the functional group, polymeric backbone, the cation or anion, stability of the resins in an HF environment, the effect of temperature and HF concentration. The mechanism of uptake was also investigated and so too the uptake by non-functional ion exchange resins, the uptake of other acidic and basic gases and the separation of HF from organics.

3.3. Uptake of hydrogen fluoride by Nafion® Superacid Resin

The uptake of HF after exposure of a resin to a 10% HF/N_2 mixture was assessed by thermogravimetric analysis. Nafion® NR50 beads were pre-treated with dilute H_2O_2 and H_2SO_4 to produce the micelles [30, 31] and the data is shown is Figures 3.3 and 3.4.

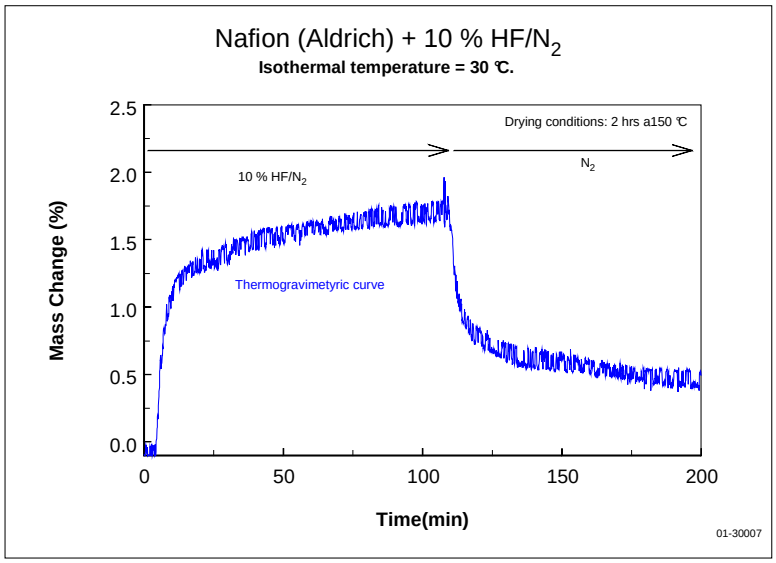


Figure 3.3: Thermogravimetric curve for the interaction of Nafion® (Aldrich) with 10% HF/N_2 (Pre-dried at 150℃ for 2 hours)

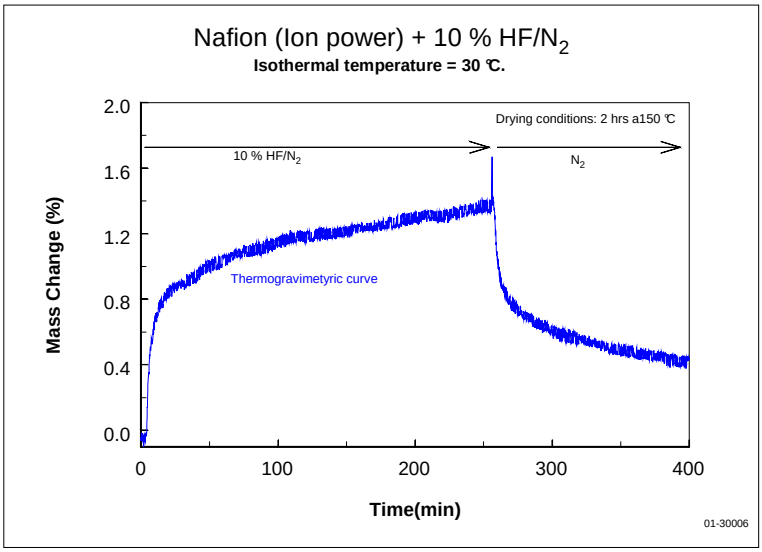


Figure 3.4: Thermogravimetric curve for the interaction of Nafion® (Ion Power) with 10% HF/N_2 (Pre-dried at 150 ℃ for 2 hours)

Nafion® shows a relatively low adsorption/reaction capacity with respect to HF vapour at 30℃. It is also evident from the curves that some of the adsorbed HF is released when the carrier gas was changed to a stream of N_2. The maximum % uptake for the Aldrich and Ion Power samples for the duration of this investigation was 1.7 and 1.3% respectively. The reason for this low HF uptake compared to what was obtained by Barsotti [1] is unknown.

However from work done on the H_2O uptake of Nafion® it is evident that there are two dry states, one that has a high H_2O capacity and one with a low capacity. For Nafion® to retain it's high water capacity, the micelle integrity must be maintained. When the micelles are hydrated, electrostatic factors govern the internal morphology, due to the ionisation of the sulphonic acid moieties. As Nafion® dries, the micelles shrink but maintain integrity. However upon complete drying, the electrostatic barriers to reorientation are removed, hence micelle disintegration occurs, when

Nafion® is dried to this state it is known as the 0:1 state *i.e*. zero H_2O molecules per SO_3H moiety. The net result is that when drying Nafion®, it must not be completely dry (generally known as the 1:1 state *i.e*. one H_2O per SO_3H moiety) in order to maintain its H_2O capacity [5].

To assess if this applies to the HF capacity, Nafion® was pretreated to activate the micelles [5], then dried to the 0:1 state and 1:1 state and the HF vapour capacity determined for both states. (Figures 3.5 and 3.6)

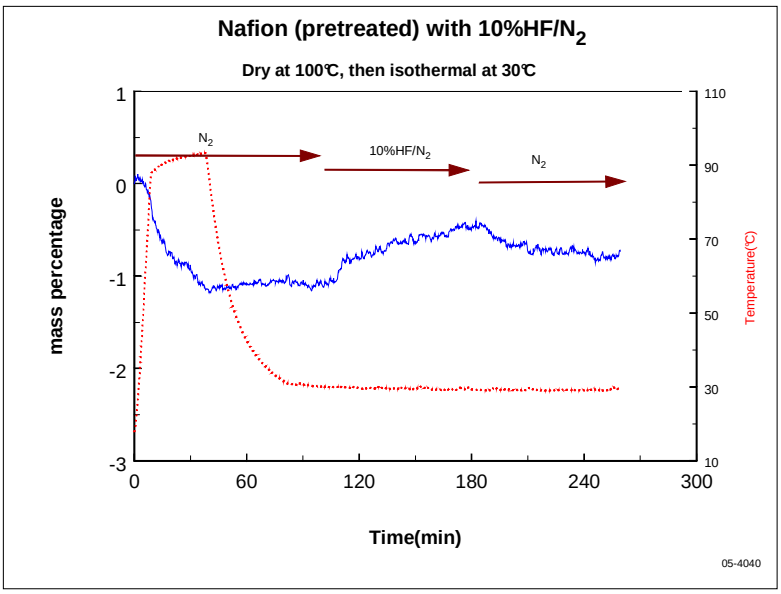


Figure 3.5: Thermogravimetric curve for the interaction of Nafion® with 10% HF/N_2 (Pre-dried to the 0:1 state)

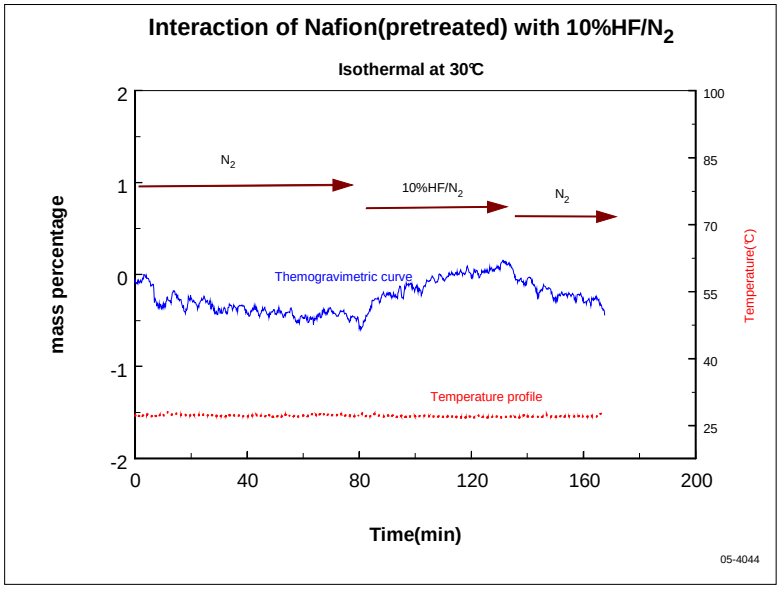


Figure 3.6: Thermogravimetric curve for the interaction of Nafion® with 10% HF/N_2 (Pre-dried to the 1:1 state)

It appears as if Nafion® does not have a capacity for HF vapour under the conditions of this experiment. Barsotti [2] mentioned that Nafion® has a high capacity for HF, hence it is postulated that the organic matrix swells the polymer and assists in HF uptake. This will be discussed in more detail later.

3.4. Uptake of hydrogen fluoride by sodium polyacrylate

The thermogravimetric curve for the interaction of HF with sodium polyacrylate is shown in Figure 3.7.

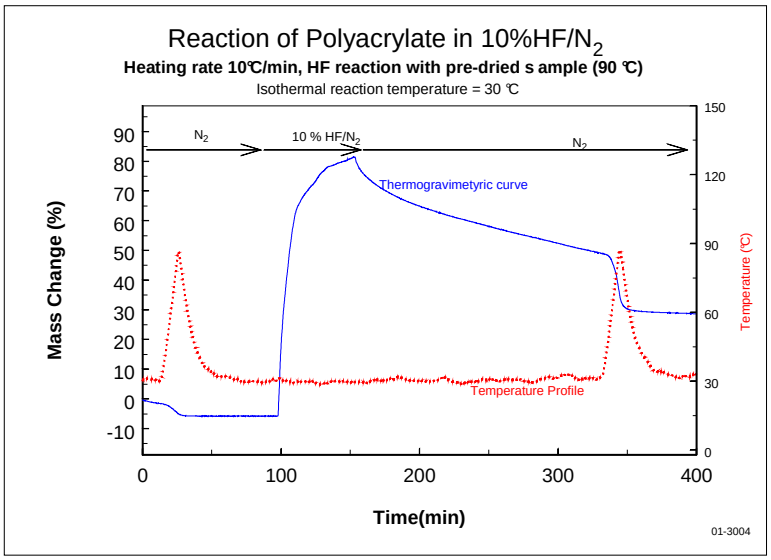


Figure 3.7: Thermogravimetric curve for the interaction of Sodium polyacrylate with 10% HF/N_2

A high absorption capacity for HF vapour (± 90%) is shown by sodium polyacrylate. An initial loss of water (± 6% mass loss) is noted when the sample was heated to 90℃. Some of the HF is also d esorbed when the 10% HF/N_2 atmosphere was replaced with the N_2 carrier gas. A further desorption event was noted when the sample was heated to 90℃. Examination of the sample at the end of the reaction revealed that it had dissolved in the HF in the thermogravimetric analyser. This could limit the use of the resin in any application *e.g.* use in a packed column.

However, it was decided to conduct one liquid phase practical test with this sample. In the experiment, perfluoroheptane, traces of HF and sodium polyacrylate were mixed together, the sample allowed to separate and the HF content analysed. The results obtained are indicated in Table 3.1:

Table 3. 1: Amount of HF present in perfluoroheptane after treatment

Sample No:	**Perfluoroheptane (g)**	**Sodium polyacrylate (g)**	**ppm F^-**
Blank 1	194.54	0.00	38
1	194.88	0.51	51
2	194.59	1.02	41
3	197.94	1.52	39
4	196.87	2.00	42
5	196.36	2.56	38
Blank 2	206.90	0.00	17
6	195.87	40.35	22

As can be seen in Table 3. 1, sodium polyacrylate is unable to remove the HF present in the perfluoroheptane sample used.

3.5. Ion exchange resins

The limited success of using Nafion® superacid resins and sodium polyacrylate, suggested that the samples were not suitable for HF removal It was thus decided to investigate a third polymeric type material *i.e*. ion exchange resins.

An ion exchange resin is a polymer with certain chemically bound functional groups [10, 11]. Ions from these functional groups can be exchanged for other ions in solution and generally these resins are used to remove undesirable ions from certain environments. The possibility that there could be adsorption of HF on these functional groups was indicated by the work on Nafion® resins. Certain ion exchange resins have the same functional group as the Nafion® resins *i.e*. the SO_3H group. Our interest in these resins is not in their exchange capacity but rather on their

adsorption capacity. This adsorbtion capacity is a factor of both the polymeric backbone and the functional group.

Ion exchange resins can be broadly classified into two groups and four main categories [10, 11]. The two groups are cation exchange resins and anion exchange resins and the four categories are strong acid, strong base, weak acid and weak base categories. The acids are the cation exchange resins and the bases are the anion exchange resins. The above classification has as a variable the functional group however there is also a dependency on the polymeric backbone (Figure 3.8). Generally the strong acid resins have a sulphonic acid (SO_3H) group, attached to a styrene/divinylbenzene backbone. The weak acid resin consists of a polymerized methacrylic acid with a carboxylic acid functional group (COOH) sometimes crosslinked with divinylbenzene. The acid functionality is sometimes exchanged with other cations. The strong base resin usually has a trimethylamine ($CH_2N(CH_3)_3Cl$) functional group and the weak base resin has a dimethylamine ($CH_2NH(CH_3)_2Cl$) functional group. The anion in the resin need not necessarily be the chloride ion. The backbone can be either styrene/divinylbenzene or acrylic. With reference to the resin exchange capacity this is normally given as milliequivalents of functional groups per gram of dry resin (meq/g) or milliequivalents per milliliter of wet resin (meq/ml).

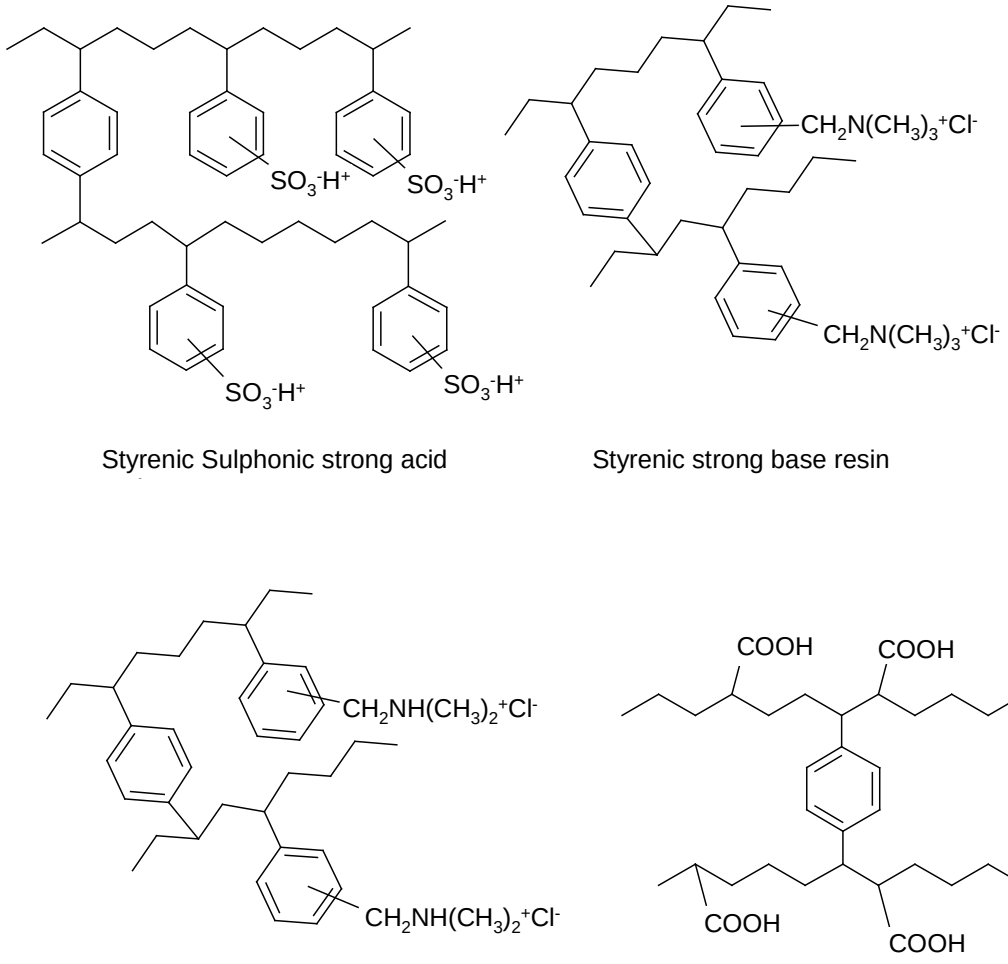


Figure 3.8: Schematic drawing of various resins

3.6. Initial tests

A range of resins was used in the initial analysis, these are, Amberlite 120H (a strong acid cation exchange resin), Amberlite IRC 50H (a weak acid cation exchange resin), Dowex 1x8 (a strong base anion exchange resin) and Amberlite CG 400Cl (a strong base anion exchange resin).

The interactions of these ion exchange resins with a 10% HF/N_2 mixture were then investigated on a thermobalance. The ion exchange resins were pre-dried at 100℃ before they were subjected to th e HF mixture.

The thermogravimetric curves for the resins under discussion are shown below in Figures 3.9 – 3.12.

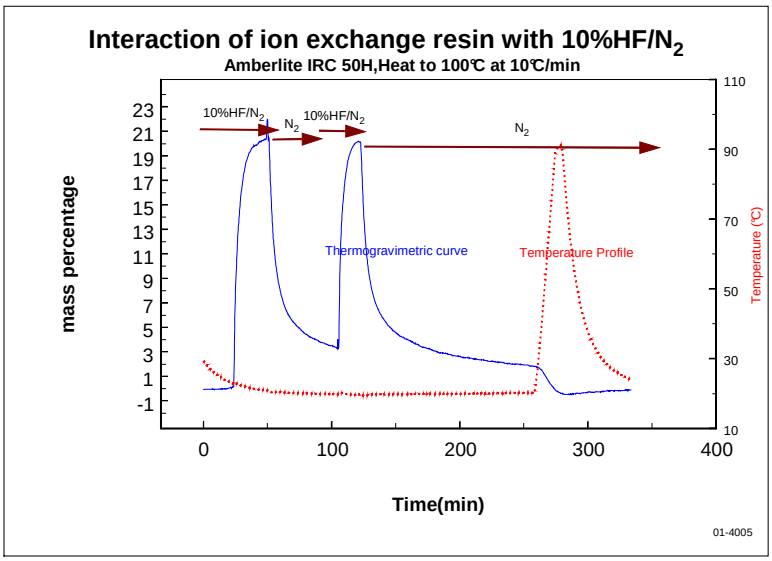


Figure 3.9: Thermogravimetric curve of Amberlite IRC 50H after exposure to a 10% HF/N_2 mixture

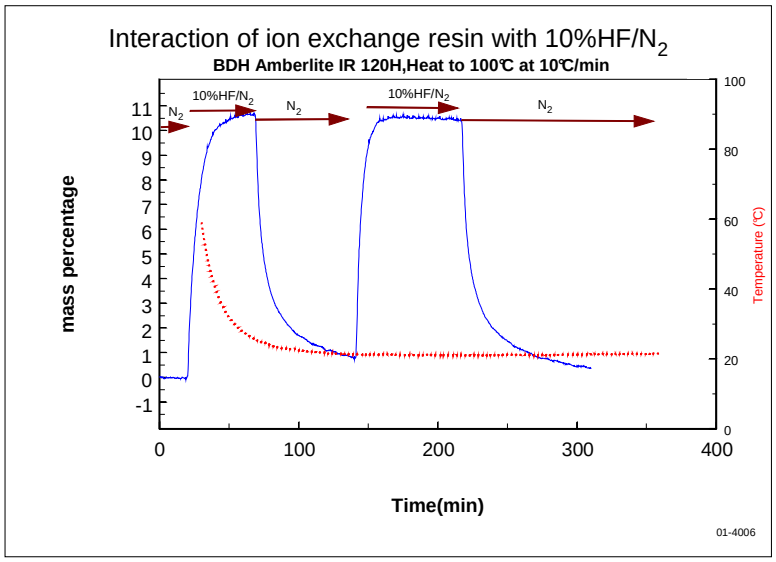


Figure 3.10: Thermogravimetric curve of Amberlite IR 120H after exposure to a 10% HF/N_2 mixture

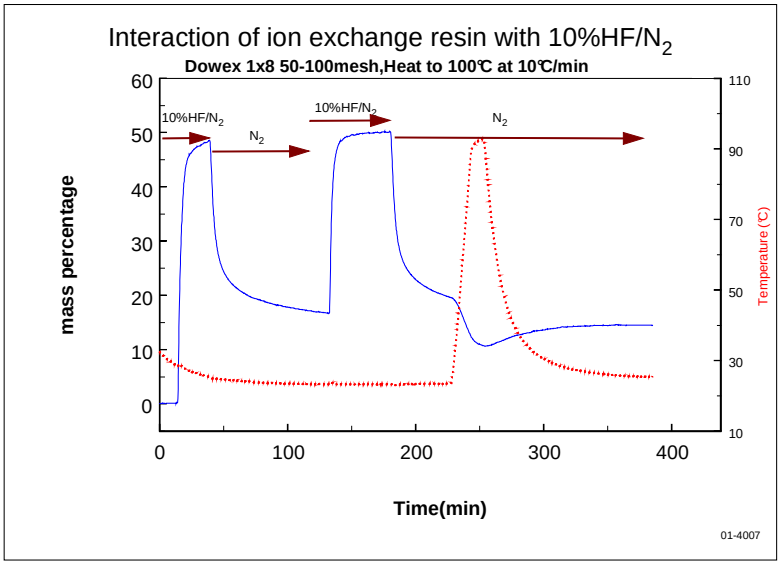


Figure 3.11: Thermogravimetric curve of Dowex 1x8 after exposure to a 10% HF/N_2 mixture

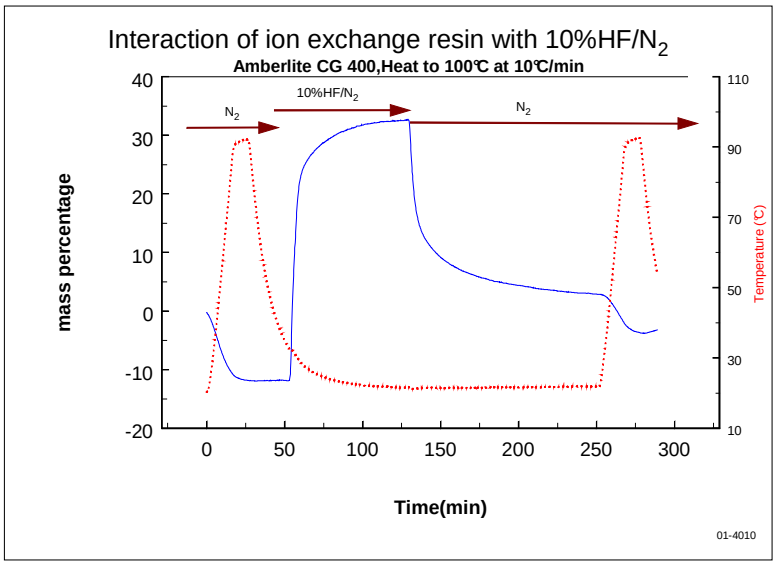


Figure 3.12: Thermogravimetric curve of Amberlite CG 400Cl after exposure to a 10% HF/N_2 mixture

The ion exchange resins showed some mass increase with HF uptake and the anion exchange resins showed the highest mass increases (Figures 3.11 and 3.12). The cation exchange resins showed some ability to adsorb HF, but the HF was easily removed in a stream of N_2 or under heating conditions (Figures 3.9 and 3.10). It was noted that part of the adsorbed HF is desorbed when the HF containing carrier gas was switched to a N_2 carrier gas. Most of the remaining adsorbed HF was removed with heating.

The actual reactions between HF and the acidic ion exchange resins are proposed to occur as shown in equation 3.1 and 3.2.

Strong acid: $SO_3H + nHF \rightarrow SO_3H\cdot(HF)_n$ ..... *(3.1)*

Weak acid: $COOH + mHF \rightarrow COOH\cdot(HF)_m$ ..... *(3.2)*

It is possible this is a physical rather than a chemical interaction.

For basic resins an acid base reaction is proposed to occur, (equation 3.3a). When the basic resin has OH^- as the counter ion, the following reaction occurs:

$$B^+OH^- + HF \rightarrow B^+F^- + H_2O \quad \text{.....(3.3a)}$$

$$BF + (HF)_x \rightarrow BF(HF)_x \quad \text{.....(3.3b)}$$

In this case both ion exchange and adsorption occurs. Ion exchange initially involves exchange of OH with F ions. Upon resin regeneration, water is given off and the resin can be reused. However the resin is now a BF resin, (equation 3.3a and b).

When the basic functionality has a halide counter ion, the follow reaction is envisaged (equation 3.4):

$$BCl + (x + y)\,HF \rightarrow BCl.(HF)_y + BF\,(HF)_{x-1} \quad \text{.....(3.4)}$$

The chloride ion can also be ion exchanged with the fluoride ion.

Hence, based on the above, a more intensive evaluation of the commercially available ion exchange resins was conducted, by selecting more representatives of the four categories.

3.7. Uptake of hydrogen fluoride by various resins

A series of commercial resins were selected for further testing (Table 3. 2).

Table 3. 2: Summary of percentage HF taken up by various resins

Resin	**Functional group**	**Backbone**	**(%) HF adsorbed**	**Figure**
Strong Acid Cation				
Amberlite IR 120H	SO_3H	PS/DVB	9	3.13
Amberlite IR 120Na	SO_3Na	PS/DVB	42	3.14
Amberjet 1200H	SO_3H	PS/DVB	9	3.15
Bio-Rad AG 50W x 4	SO_3H	PS/DVB	10	3.16
Dowex 50W x 8	SO_3H	PS/DVB	10	3.17
Dowex HCR-W2	SO_3Na	PS/DVB	44	3.18
Weak Acid Cation				
Amberlite IRC 50H	COOH	PA/DVB	17	3.19
Amberlite IRC 86	COOH	PA/DVB	20	3.20
Lewatit CNPLF	COOH	PA/DVB	21	3.21
Lewatit CNP80	COOH	PA/DVB	20	3.22
Dowex MAC 3	COOH	PA/DVB	19	3.23
Strong Base Anion				
Amberlite IRA 458 Cl	Quart. Amine (Cl)	PA/DVB	72	3.24
Bio-Rad AG1 x 4	Quart. Amine (Cl)	PS/DVB	51	3.25
Bio-Rad AG2 x 8	Quart. Amine (Cl)	PS/DVB	46	3.26
Dowex 21K	Quart. Amine (Cl)	PS/DVB	38	3.27
Lewatit MP 500	Quart. Amine (Cl)	PS/DVB	46	3.28

Dowex Marathon A	Quart. Amine (OH)	PS/DVB	48	3.29
Weak Base Anion				
Amberlite IRA-67	Tert. Amine (free base)	PA/DVB	114	3.30
Amberlite IRA-68	Tert. Amine (free base)	PA/DVB	116	3.31
Amberlite IR 92 RF	Tert. Amine (free base)	PS/DVB	58	3.32
Lewatit MP62	Tert. Amine (free base)	PS/DVB	67	3.33
Lewatit MP64	Tert./Quart Amine (free base/Cl)	PS/DVB	71	3.34

The thermogravimetric traces representing these results are to be found in Appendix 1.

As can be noted, all four resin categories are represented in this list. It will also be noted that strong acid cation resins have the sulphonic acid functional groups and two of these, Amberlite IR 120Na and Dowex HCR-W2, are the sodium salts. They all have a polystyrene/divinylbenzene backbone. The weak acid resins all have the carboxylic acid functionality and the polyacrylic/divinylbenzene backbone. Hence the weak and strong acids differ not only in functionality but also in the backbone. The strong base anionic resin was obtained in the chloride form of the quaternary amine functionality and had a polystyrene/divinylbenzene backbone. The exceptions were Amberlite IRA 458 Cl, which had a polyacrylic backbone, and the Dowex Marathon A, which has a hydroxide quaternary amine functionality. The weak base resins contained a chloride or a free base

tertiary amine functionality with the backbone being either polyacrylic or polystyrene, crosslinked with divinylbenzene.

The following thermogravimetric curves, Figures 3.13 to 3.34 (Appendix 1), show the results of this investigation. The ion exchange resins were pre-dried at 100℃ in a stream of N_2. The investigation involved measuring the mass change of the resin as a function of time when it was subjected to a stream of 10% HF/N_2. After adsorption of HF, the HF stream was replaced with a stream of N_2 to determine the extent of the desorption. Some samples were also subjected to a final heating step to 100℃ in a N_2 stream to obtain an indication of the uptake reversibility.

What is immediately evident from the data (Table 3.2) is that all the resins have a capacity for HF. These capacities range from 9 mass % to over 110%, with the basic resins having a higher overall uptake than the acidic resins. Further, within different resin categories there is variation in uptake for the various resins.

For the strong acid resins (Figures 3.13 to 3.18), it is evident that the results can be broken down into two groups; those with the sulphonic acid functionalities, which took up about 10% HF and those that contained the sodium salt of the sulphonic acid functionalities, which took up about 40%. For the acid functionalities, the 10% uptake is independent of the resin source. For the sodium-exchanged form, the high uptake (four times the amount of HF compared to the acid form) is surprising. This will be discussed later.

With reference to the weak acid resins (Figures 3.19 to 3.23), the HF uptake is about 20%. Slight variations in uptake for the different samples is expected; different manufacturers synthesize resins for different applications and these resins are normally fine tuned to the application. This is achieved, for example, by varying the number of functional groups

or the degree of cross-linking of the polymer backbone. All these effects will result in variations in HF uptake.

For the strong base anion exchange resins (Figures 3.24 to 3.29), the uptake is between 40 to 50%, the only exception being Amberlite IRA 458 Cl which has a greater than 70% uptake. The only major difference between this and the other strong base resins is the backbone. Further changing from the chloride to the hydroxide form does not influence capacity, (Figure 3.29 *vs*. 3.25 – 3.28).

The weak base resins (Figures 3.30 to 3.34), show the greatest variation across a category, ranging from 58% to over 110% uptake. What is immediately evident, when comparing the backbones, is that the acrylic resins have a much higher uptake compared to the styrene resins (Figures 3.30 and 3.31 *vs*. 3.32 to 3.34). This is further evidence that the backbone also plays an important role in the uptake of HF. Also evident is that the weak base resins have overall the highest uptake for HF in the gas phase. Even when the HF uptake of the styrenic backed weak base resins is compared to its strong base counterparts, this trend of acrylic backboned resins have a higher capacity, is still evident. The weak base styrenic resins take up between 60 to 70% HF, whereas the strong base resins take up between 40 to 50% HF. The high uptake of the weak base acrylic resins will be discussed later.

3.8. Effects of changing the resin cation/ anion

Based on the results found for Amberlite IR 120H and 120Na (Table 3.2), it was decided to investigate the effect of changing the resin counter ion on the uptake of HF.

$$R\text{-}SO_3^-H^+ + NaOH \rightarrow R\text{-}SO_3^-Na^+ + H_2O \qquad (3.5)$$

As the cation changes from H^+ to Na^+ in Amberlite IR 120H there is a drastic increase in HF uptake.

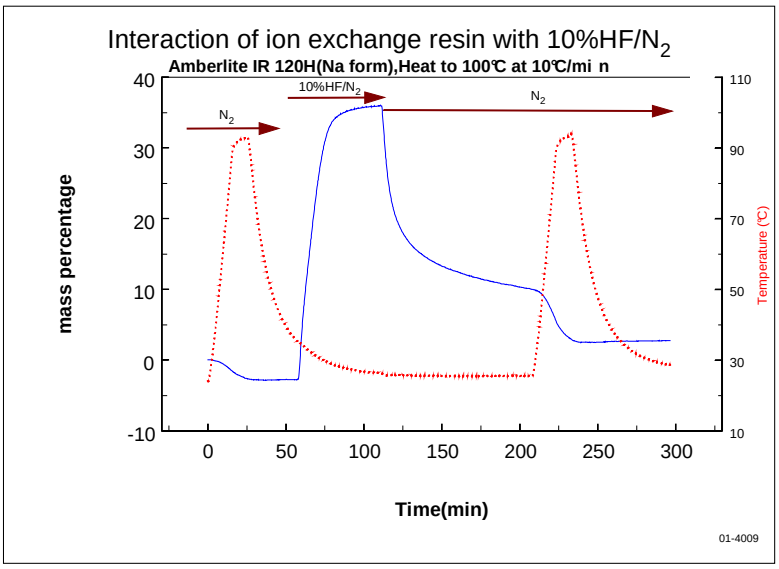


Figure 3.35: Thermogravimetric curve of Amberlite IR 120H (Na exchanged) after exposure to a 10% HF/N_2 mixture

As noted in Figure 3.35, the uptake is almost 40% and is very close to the uptake found for commercial Amberlite IR 120Na (Figure 3.14).

The ability of the sodium form of a resin to take up more water than the protonated form, is a known phenomenon For example, Dowex HCR-W2 by the Dow Chemical Company, is a sodium exchanged strong acid resin, used as a desiccant for organics. The potassium form of the resin is also known to have a high water uptake [32]. It was thus decided to ion exchange the proton form to the lithium and potassium forms and assess their HF uptake abilities.

$$R\text{-}SO_3^-H^+ + KOH \rightarrow R\text{-}SO_3^-K^+ + H_2O \qquad (3.6)$$

$$R\text{-}SO_3^-H^+ + LiCl \rightarrow R\text{-}SO_3^-Li^+ + HCl \qquad (3.7)$$

The following results were obtained (Figures 3.36 and 3.37). The key data is summarised in Table 3.3.

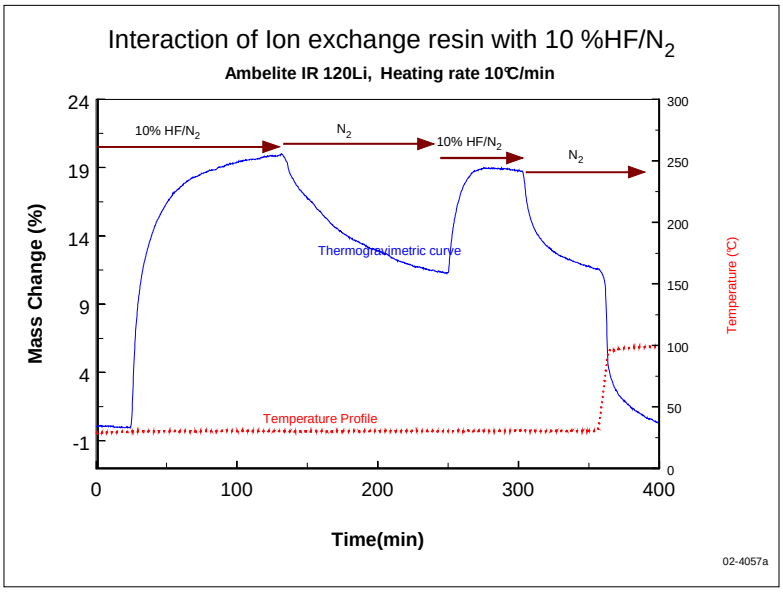


Figure 3.36: Thermogravimetric curve of Amberlite IR 120Li after exposure to a 10% HF/N_2 mixture

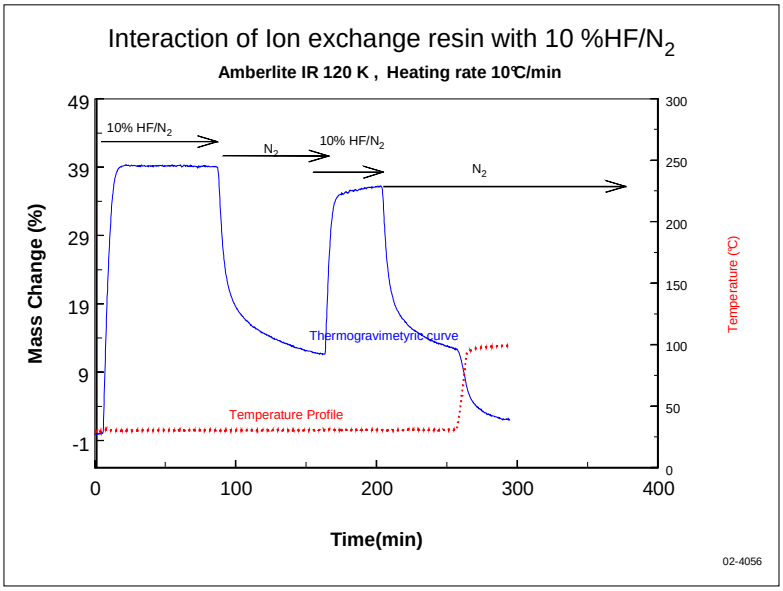


Figure 3.37: Thermogravimetric curve of Amberlite IR 120K after exposure to a 10% HF/N_2 mixture

Table 3. 3: Table of percentage HF taken up by the different ionic forms of Amberlite IR 120H

Name of Resin	**% HF Uptake**	**Figure**
Amberlite IR 120 H	9	3.13
Amberlite IR 120 Li	19	3.36
Amberlite IR 120 Na	42	3.14
Amberlite IR 120 K	40	3.37

As can be seen there is an increase in uptake in going from the proton form to the Na^+ form. The uptake for the Na^+ and K^+ exchanged materials is the same. It is possible that Na^+ and K^+ are more easily polarisable cations, due to their larger size, hence the higher capacity.

Another issue considered, was that of the charge density and its modification by ion exchange. In this instance, Amberlite IR 120H was ion

exchanged with calcium and aluminium ions to evaluate this effect, (Figures 3.38 and 3.39).

$$2R\text{-}SO_3^-H^+ + Ca(OH)_2 \rightarrow (R\text{-}SO_3)_2Ca + 2H_2O \qquad (3.8)$$

$$3R\text{-}SO_3^-H^+ + AlCl_3 \rightarrow (R\text{-}SO_3)_3Al + 3HCl \qquad (3.9)$$

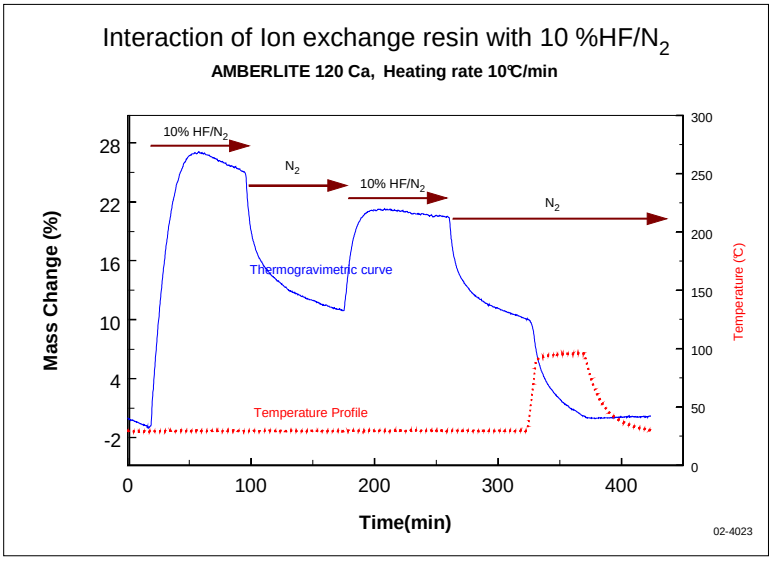


Figure 3.38: Thermogravimetric curve of Amberlite IR 120Ca after exposure to a 10% HF/N_2 mixture

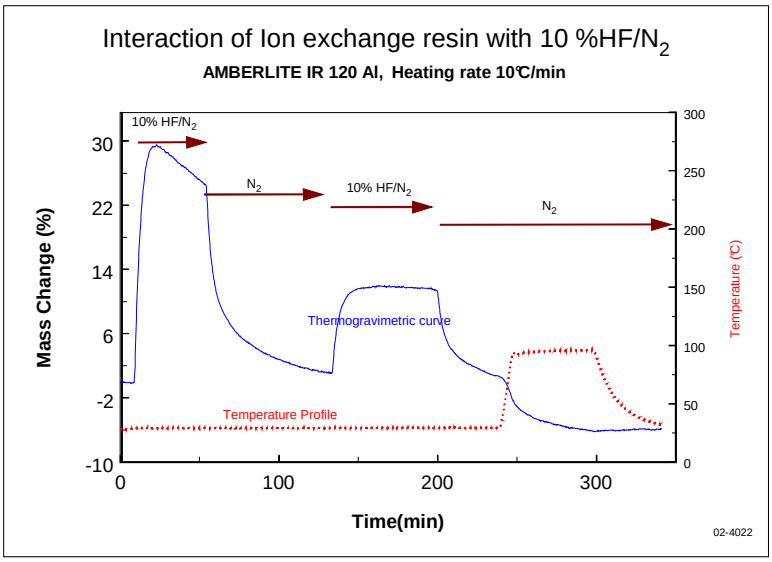


Figure 3.39: Thermogravimetric curve of Amberlite IR 120Al after exposure to a 10% HF/N_2 mixture

The calcium material took up 27% HF whereas the aluminium analogue took up 29%. Hence increasing the charge density, in going from divalent to trivalent ions, does not increase the HF uptake.

A further test conducted, was to assess whether the 42% uptake of HF by the sodium exchanged strong acid resins was a function of the material used. Another commercial sample, Bio-Rad AG 50WX4 was thus sodium exchanged and the HF uptake assessed (Figure 3.40).

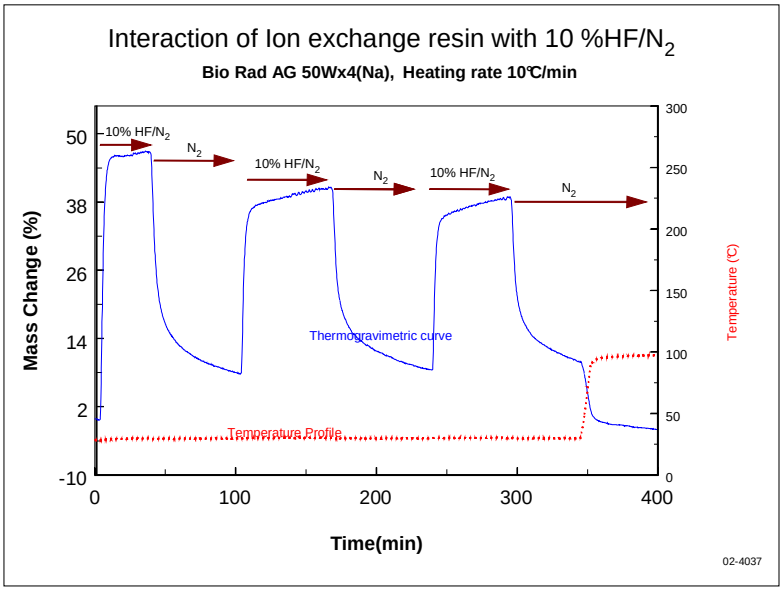


Figure 3.40: Thermogravimetric curve of Bio-Rad 50W x 4 (Na) after exposure to a 10% HF/N_2 mixture

It was found to take up 47%, which indicates that HF uptake is not determined by the different commercial samples available.

Weak acid resins, were found to have an HF uptake of between 17 and 21%. However, it is noted that all samples tested were in the protonated form. Hence to assess if the weak acid resins follow the same trend as the strong acid resins, when ion exchanged with sodium, two representative samples were ion exchanged with sodium and their HF capacities assessed.

$$R\text{-}COOH + NaOH \rightarrow R\text{-}COONa + H_2O \qquad (3.10)$$

The samples selected were Lewatit CNPLF and Dowex Mac 3 (Figures 3.41 and 3.42).

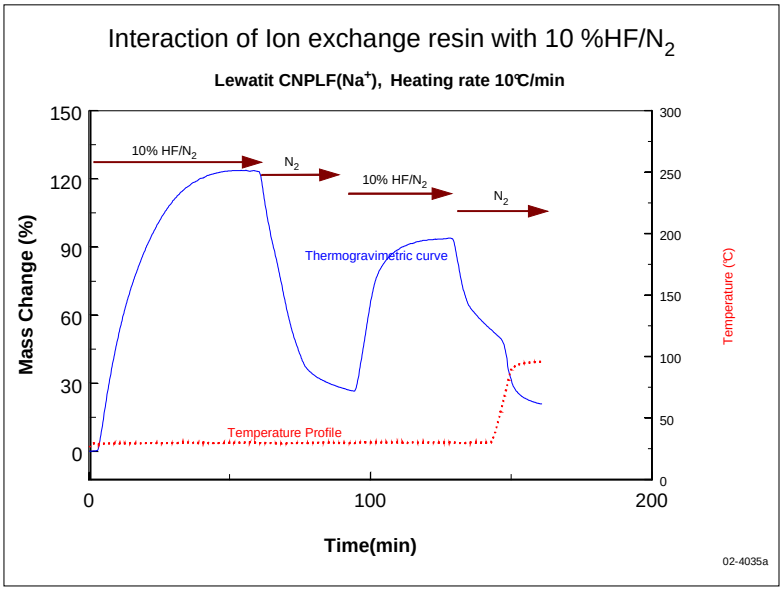


Figure 3.41: Thermogravimetric curve of Lewatit CNP LF (Na) after exposure to a 10% HF/N_2 mixture

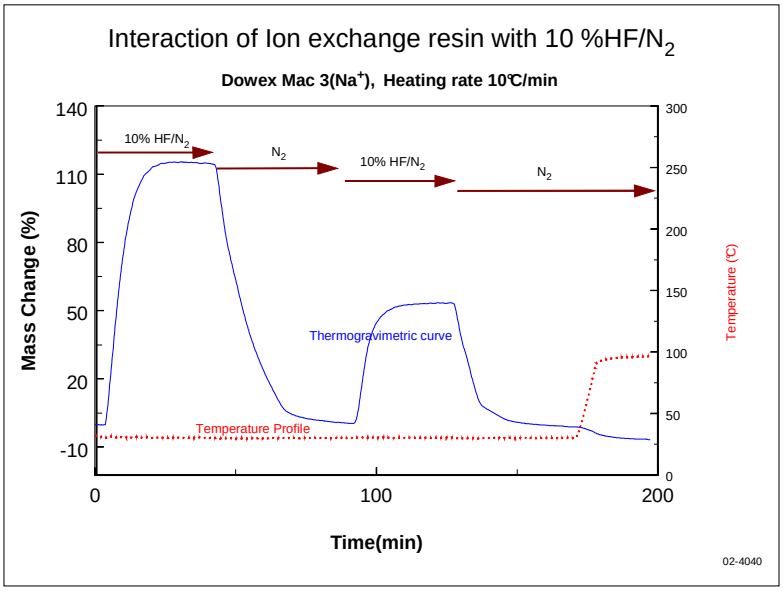


Figure 3.42: Thermogravimetric curve of Dowex MAC 3 (Na) after exposure to a 10% HF/N_2 mixture

Prior to being sodium exchanged, Lewatit CNPLF had a HF capacity of 21% (Figure 3.21); after being ion exchanged, this increased to above 120%. The Dowex Mac 3 resin capacity also increased from 19% (Figure 3.23) to almost 120%, this is greater than the four fold increase noted for the strong acid forms. These results are not totally unexpected as previous experiments on sodium polyacrylate, a non cross-linked analogue of the sodium exchanged weak acid resins, takes up about 90% HF. However upon re-adsorption, the capacity decreases significantly.

Experiments were also performed on basic resins, Lewatit MP 500, a strong base resin was converted from the chloride (Cl^-) form to the hydroxide (OH^-) form.

$$R\text{-}N(CH_3)_3^+Cl^- + NaOH \rightarrow R\text{-}N(CH_3)_3^+OH^- + NaCl \qquad (3.11)$$

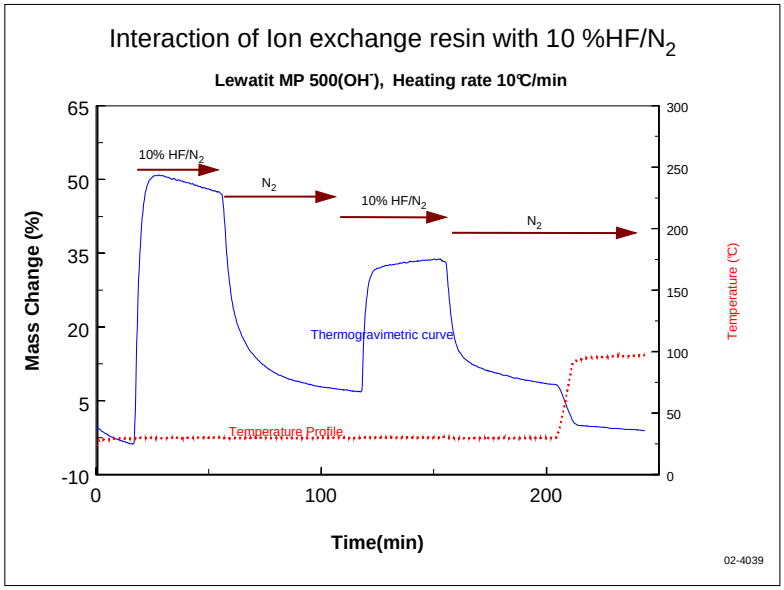


Figure 3.43: Thermogravimetric curve of Lewatit MP 500 (OH) after exposure to a 10% HF/N_2 mixture

There appears to be little difference in the uptake of HF whether in the chloride (Figure 3.28; 46%) or hydroxide form, (Figure 3.43, 52%). This is also evident from the results obtained for Dowex Marathon A (Figure 3.29), a commercially obtained strong base hydroxide resin where the uptake was found to be about 48%.

Amberlite IRA 458 Cl, also a strong base resin was converted to the hydroxide form and the uptake assessed; this sample was investigated as it is the only strong base resin studied in this thesis that has an acrylic backbone, the others have a styrenic backbone.

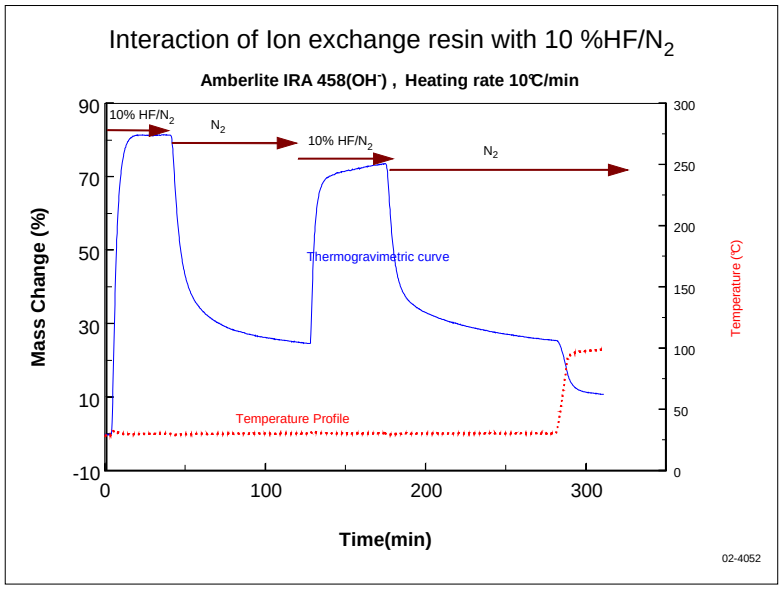


Figure 3.44: Thermogravimetric curve of Amberlite IRA 458(OH) after exposure to a 10% HF/N_2 mixture

The uptake of the hydroxide form of the resin was about 81%, (Figure 3.44), whereas the uptake of the chloride form was about 72% (Figure 3.24). As expected the HF uptake increased in going from the chloride to the hydroxide form. This was expected as the hydroxide form first undergoes ion exchange to the fluoride form (taking up additional HF) compared to the chloride form.

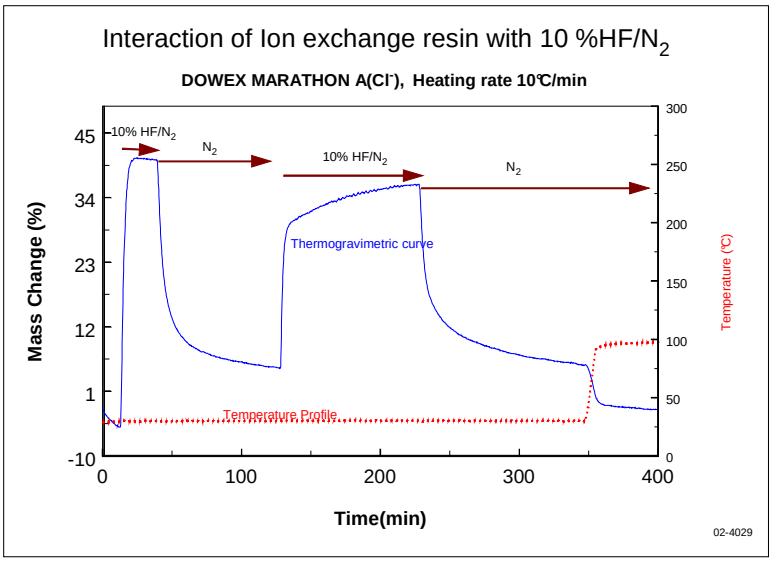


Figure 3.45: Thermogravimetric curve of Dowex Marathon A (Cl) after exposure to a 10% HF/N_2 mixture

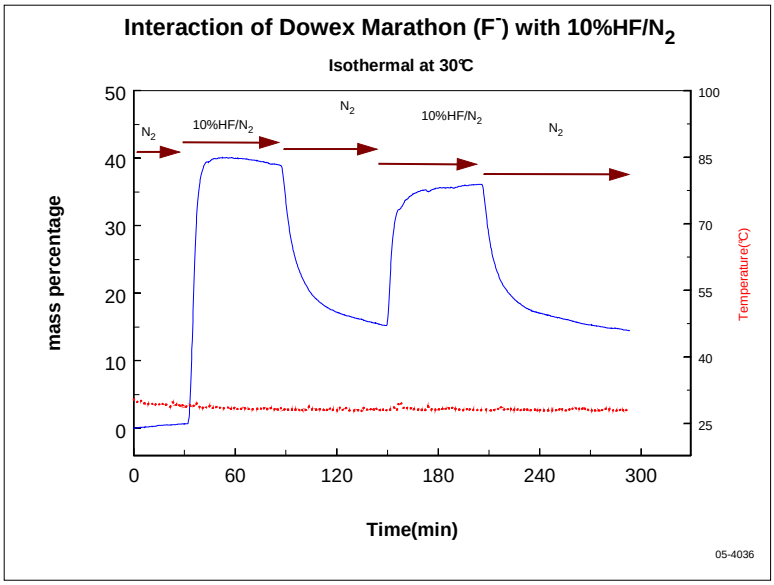


Figure 3.46: Thermogravimetric curve of Dowex Marathon A (F) after exposure to a 10% HF/N_2 mixture

This uptake test was also performed on Dowex Marathon A(OH). Here, the hydroxide form of Dowex Marathon A (Figure 3.29) was converted to the chloride form (Figure 3.45) and the fluoride form (Figure 3.46) as with the above case there was a slight decrease, *i.e*. from 48% uptake to 42%, in going to the chloride form and 41% in going to the fluoride form. Once again the additional uptake of the hydroxide form (*i.e*. the 48% noted) is due to ion exchange of the hydroxide functionality with fluoride ion.

With reference to the weak bases, Amberlite IRA 67 was converted to the chloride form (equation 3.12) and its uptake assessed. This resin should now be similar to Amberlite IRA 458 Cl except for the functional group (Figure 3.24, 72% uptake).

$$R\text{-}N(CH_3)_2 + HCl \rightarrow R\text{-}NH(CH_3)_2^{+}Cl^{-} \qquad (3.12)$$

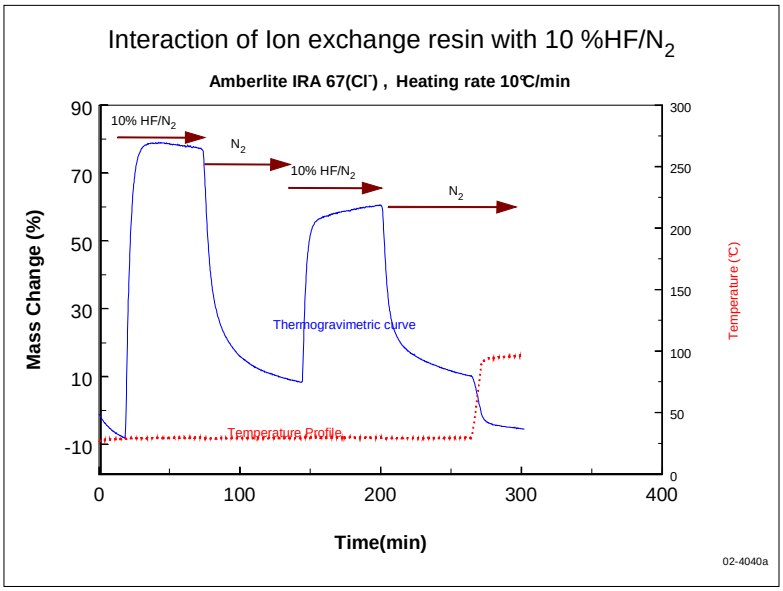


Figure 3.47: Thermogravimetric curve of Amberlite IRA 67(Cl) after exposure to a 10% HF/N_2 mixture

The mass percentage HF uptake dropped from above 110% to about 78% when the free base form was converted to the chloride form (Figure 3.47). This provides evidence that the tertiary amine functionality has an additional HF uptake mechanism compared to the quaternary amine, due to the higher uptake values.

Table 3.4 provides a summary of the results obtained for HF uptake on the ion-exchanged samples.

Table 3. 4: Table of percentage uptake of HF by the various ion exchange resins

Strong acid					
Cation	H^+	Na^+	Ca^{2+}	Al^{3+}	
% Uptake	9	42	27	29	
Backbone	PS/DVB				
Weak acid					
Cation	H^+		Na^+		
% uptake	21		123		
Backbone	PA/DVB				
Strong Base					
Anion	OH^-	Cl^-	OH^-	Cl^-	F^-
% uptake	81	72	48	42	41
Backbone	PA/DVB		PS/DVB		
Weak Base					
Anion	Free Base	Cl^-	Free Base		
% uptake	114	79	67		
Backbone	PA/DVB		PS/DVB		

As can be seen in Table 3. 4, the uptake of HF varies quite considerably across the different types of ion exchange resins. For the acids, the effect of changing the cation from H^+ to Na^+ increases the HF capacity significantly. With reference to the basic resins, the free base form does have a much higher capacity than the anion exchanged resins. Overall although the free base weak base resin has a lower capacity (114%) compared to the sodium exchanged weak acid resin (123%). The weak base is the preferred resin for HF uptake, as it does not lose capacity to the same extent on re-adsorption.

3.9. Mechanism of hydrogen fluoride uptake

The above data allows for a consideration of the influence of the resin material on the HF uptake. This influence can provide a basis for proposing HF uptake mechanisms. Two areas to be investigated are the backbone and functional groups.

3.9.1. Influence of the polymeric backbone

As noted the strong acid resins have a polystyrene-divinylbenzene (PS/DVB) backbone and the weak acid resins a polyacrylic-divinylbenzene (PA/DVB) backbone. The basic resins have both types of backbones. The protonated forms of the strong acid resins take up about 10% HF, whereas the weak acid resins take up about 20%. As both the functional group and backbones are different in these cases it is difficult to ascribe the difference in uptake to the backbone, hence basic resins were considered for comparative purposes.

When the results for the strong bases are investigated, it can be noted that the acrylic base *i.e*. Amberlite IRA 458 Cl has a greater uptake of HF than the rest of the strong base, styrenic backed resins, (72% *vs.* 50%). As the

functional groups are identical for all the strong base resins, it appears as if the backbone plays a role.

It was ascertained from the supplier of two of the styrene-based resins tested, that they are supplied as a mixture in the free base/Cl^- form. This would indicate that some of the functional groups of these resins are in the chloride ($–N(R)_2H^+Cl^-$) form and hence would result in a difference in uptake compared to the free base ($–N(R)_2$) form. This would account for the variations in HF uptake.

Further, ion exchange resins are available as gels or macroporous. The gels are generally less crosslinked and swell more easily, whereas the macroporous structures are more rigid. For desiccant applications, the gels are preferred as swelling results in a higher water uptake. However, for HF uptake, this trend is not evident for most of the resins. Thus Amberlite IR 120H a strong acid resin has a HF uptake of 9% and a gel type backbone. Bio-Rad AG 50W x 4 also has a 10% uptake and is a macroporous type resin. The acrylic based resins Amberlite IRC 86, a gel resin and Lewatit CNPLF, a macroporous resin, both weak acids, have the same uptake at about 20%.

3.9.2. Effect of the acidic and basic functional groups

It is important to note here that these resins are classified into groups based on properties, as it was observed that HF capacity is a function of resin properties.

The sodium form of the strong acid resins has the highest HF capacity at 42% when compared to the proton form at 10%. This makes this resin the most promising among the strong acid resins studied. Importantly, this resin retained 14% of HF after the HF/N_2 vapour stream was changed to a

N_2 stream. The holding capacities of the other resins were lower, with that of the proton form dropping to *ca.* 0%.

The sodium form of this resin can only be considered as a fine scrubber as prolonged exposure to HF vapour results in a breakdown of this resin. Both the backbone and the functional group broke down, resulting in the formation of NaF·HF. This was ascertained via measurement of HF uptake. Amberlite IR 120 Na (strong acid-sodium form) after exposure to 50KPa HF for 3 hours followed by desorbtion under vacuum. This sample normally takes up 42% HF whereas after this extended HF exposure, this dropped to 32% (Figure 3.48).

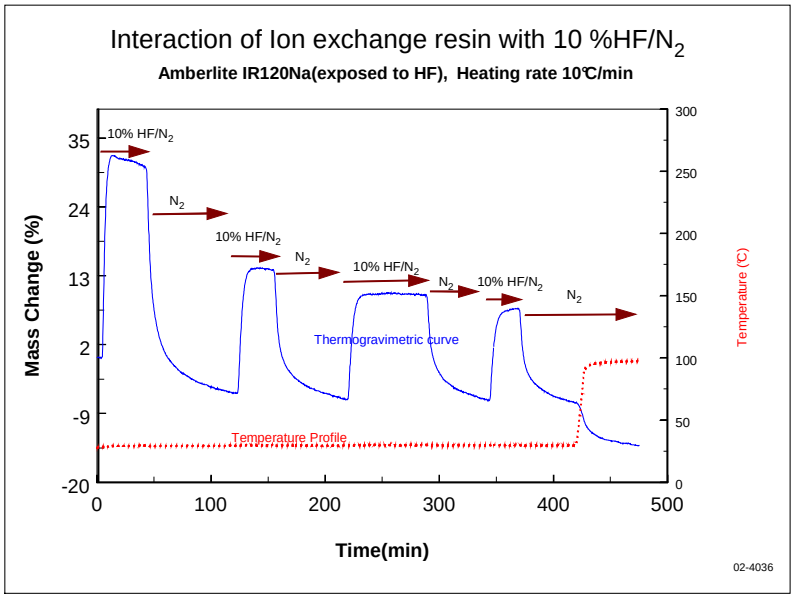


Figure 3.48: Thermogravimetric curve of Amberlite IR 120Na after exposure to a 10% HF/N_2 mixture

At the end of the experiment a white residue was noted on the sample and the sample appeared to have broken down. Upon analysis by powder XRD, the white material was found to correspond to sodium hydrogen fluoride (NaF·HF). The following gas phase reaction is thus postulated:

$$R\text{-}SO_3Na + 2HF \rightarrow R\text{-}SO_3H + NaF{\cdot}HF \qquad (3.13)$$

(R = polymeric backbone of ion exchange resin)

The above reaction compromises not only the polymer integrity, but also the polymer capacity, as the acid form of the resin has a lower capacity than the sodium form. While the NaF formed will have a high capacity for HF, however the NaF could leach out if the HF loading gets too high. However it must be noted that the NaF·HF could have formed after the polymeric backbone broke down.

Studies on the weak acid resins revealed that the proton form has an uptake of 21% whereas the sodium form has an uptake of 123% (see Table 3.4). The proton form has almost no capacity for HF vapour, once the HF stream is replaced with a N_2 stream. Studies on the sodium form also revealed NaF formation, (equation 3.14). Hence there will be eventual breakdown of this resin on prolonged HF exposure.

$$R\text{-}COONa + 2HF \rightarrow R\text{-}COOH + NaF{\cdot}HF \qquad (3.14)$$

It was also noted that the sodium form of this resin loses capacity on repeated HF adsorption. This could be due to sodium leaching out of the resin or the breakdown of the polymer.

3.9.3. Amine chemistry

The strong and weak bases, both have styrene and acrylic backbones but they have different functional groups. The strong base has a quaternary amine functionality ($-NR_3$) and the weak base has a tertiary amine functionality ($-NR_2$); (R = alkyl group).

The weak base ion exchange resins are normally of the free base type with a functional group $-N(CH_3)_2$. When this resin is used in normal aqueous applications, it has to be activated by acid washing with HCl to generate $-N(CH_3)_2H^+Cl^-$. Presumably the reaction with HCl is equivalent to the reaction with HF (equation 3.15).

$$R\text{-}N(CH_3)_2 + HF \rightarrow R\text{-}N(CH_3)_2H^+F^- \qquad (3.15)$$

$R\text{-}N(CH_3)_2$ has a higher capacity than $R\text{-}N(CH_3)_2H^+Cl^-$ for HF, as the free base form has the additional HF uptake mechanism of forming the fluoride salt (equation 3.15). Whereas the chloride resin is already in the salt form, hence does not have this additional mechanism open to it. The uptake of HF is thereafter similar for both groups, *i.e*. $R\text{-}N(CH_3)_2H^+F^-$ and $R\text{-}N(CH_3)_2H^+Cl^-$. It must be noted that there is also the possibility that the chloride can be ion exchanged for the fluoride. The extent of this substitution will depend on the relative affinities of the resins for the anions and the relative concentrations in the gas phase. This scenario is not desired, as it will release HCl into the gas phase as an impurity.

When this is compared to the strong base scenario, the functional group is normally in the salt form $-N(R)_3H^+X^-$, where X^- is a halide or hydroxide. Hence as in the above case, does not have the additional mechanism that the free base functional groups have. The strong base functional group will take up HF by hydrogen bonding. To summarize, the free base, weak base ion exchange resin has an additional mechanism *i.e*. the formation of the fluoride salt.

Dowex Marathon A is a strong base with a hydroxide active group and a styrene backbone, and an HF uptake of 48%. Exposure of the resin to N_2 led to a drop in the HF capacity to 7%. When the sample was exposed once again to HF it took up a total of 30%. When the results of all the other strong base ion exchange resins are considered, the other resins only

showed about a 2% difference when going from the first to the second HF uptake run.

The basicity of an amine in water is actually a function of two factors, the inductive effect of the alkyl groups and the solvation effect of water. The strength of an amine base is assessed on the availability of the unshared electron pair on the nitrogen to take up a proton [33]. An increase in base strength from $NH_3 \rightarrow RNH_2 \rightarrow R_2NH \rightarrow R_3N$ (R being an alkyl group) is expected, due to the increasing inductive effect of the successive alkyl groups. However, amines are found to have the following pKa values:

Table 3. 5: pKa values for various substituted amines [33]

Amine	**pKa**
NH_3	9.25
$MeNH_2$	10.64
Me_2NH	10.77
Me_3N	9.80

This arises since cation formed by the uptake of a proton can undergo solvation and become stabilized.

Further, the more hydrogen atoms attached to the nitrogen in the amine cation, the greater is the possibility of powerful solvation, via hydrogen bonding between the protons on the amine and water. See Figure 3.49.

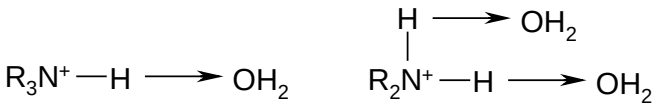


Figure 3.49: Schematic of co-ordination of water to tertiary and secondary amine [33].

The weak base resins have a higher affinity for HF than the strong base resins. HF lends itself to hydrogen bonding and behaves like water and acts as a solvent for the resin amine functionalities. The result of this is two fold, (i) the strong base resins do not have a proton available on the amine for hydrogen bonding ($R\text{-}N(CH_3)_3^+Cl^-$), but the weak base resins do once in the salt form, ($R\text{-}NH(CH_3)_2^+Cl^-$). This provides a mechanism for HF uptake and (ii) the tertiary amine of the weak base resin will actually be a stronger base than the quaternary amine functionality of the strong base resin (Table 3.5) [33].

In conclusion, the weak base resins should have a higher capacity for HF than the strong base resins for the following reasons:

1. The free base has an additional HF uptake mechanism due to the conversion of the free base form to a fluoride form.
2. Weak base resins have an additional proton for hydrogen bonding to HF.
3. Due to the solvating properties of HF, the tertiary amine (of the weak base resins) should be a stronger base.

A fourth possibility is a gas phase ion exchange if the amine is already in a salt form *e.g.* the exchange of a chloride for a fluoride, but this was not assessed.

A further point to consider is the interaction between the alkyl groups on the amine functionality and HF, these protons could easily hydrogen bond with HF resulting in the high uptake seen for the basic compared to the acidic resins. Finally, it must be noted, when separating HF from an organic or inorganic, the bulk matrix in which the HF is in cannot be ignored. The solubility or interaction of the matrix with the polymer backbone will also determine whether a styrene or acrylic based resin is used.

3.9.4. Exchange capacity of resins

When a resin is assessed for a particular application, one of the fundamental factors considered is the exchange capacity of that resin. This is usually expressed in equivalents per litre (eq/l) of resin. An equivalent is the molecular weight in grams of the ion to be exchanged, divided by its electrical charge or valence [34].

The above definition applies if a resin is being used in the classical application of ion exchange. For the uptake of HF it is not only the exchange capacity but also the adsorption capacity of the resins that are being assessed.

It must also be remembered that the exchange capacity in eq/L, applies to the volume of the resin used. However, the resins used for this application are dried prior to use, to ensure optimum HF uptake. Hence, the volume change on addition of HF needs to be measured or the resin uptake needs to be evaluated in terms of mass changes. For example, Amberlite IR 120H, this is a strong acid resin (SO_3H functional group), which has a wet exchange capacity of 1.9 meq/ml and a dry capacity of 5.0 meq/g.

It was found experimentally that Amberlite IR 120H resin has a 9% mass uptake capacity for HF. Since the resin has a capacity of 5 eq/kg it can adsorb five moles of HF per kilogram resin. Since the molar mass of HF is 20 g/mol, 100 g of HF is taken up. This implies a 10% mass increase if every resin functional group adsorbs one HF molecule, (equation 3.16).

$$R\text{-}SO_3H + HF \rightarrow R\text{-}SO_3H \cdot HF \qquad (3.16)$$

This corresponds to the experimental value of 9%. The uptake verses exchange capacity of other strong acid (protonated) resins was also evaluated. Amberjet 1200H has a dry capacity of 4.7 meq/g and a HF

uptake of 9%, Bio-Rad AG 50Wx4 has a dry capacity of 5.2 meq/g and an uptake of 10%, Dowex 50Wx8 has a dry capacity of 4.8 meq/g and an uptake of 10% and Nafion® has a capacity of 0.9meq/g and an uptake of between 1.3 and 1.7%.

The weak acid resins also show similar behaviour. Amberlite IRC 50H, has a wet capacity of 3.5 meq/ml and a dry capacity of 10 meq/g. Theoretically this translates to a 20% mass uptake and experimentally the uptake of this resin was found to be 17%.

Calculations were also performed on the sodium form of these resins. Amberlite IR 120Na has the same exchange capacity as it's protonated counterpart of 1.9 meq/ml wet and 5.0 meq/g dry. Hence theoretically should also take up 10% HF, but this resin takes up 42% of HF. This would indicate that each functional group takes up four HF molecules.

Lewatit CNPLF and its sodium exchanged counterpart should have the same exchange capacity, but Lewatit CNPLF has a HF uptake of 21% for the protonated form and 123% for the sodium form; the same applies to Dowex MAC 3, which has a 19% uptake for the proton form and an uptake of 115% for the sodium form. This would indicate an uptake of six HF molecules per functional group. An example is shown in Table 3.6.

Table 3. 6: HF uptake based on exchange capacity vs. actual uptake

Resin	Theoretical capacity (%)	Actual capacity (%)
Strong acid		
Amberlite IR120H	10	9
Amberlite IR120Na	10	42
Weak Acid		
Lewatit CNPLF (H)	20	21
Lewatit CNPLF (Na)	20	123

This high HF uptake of the resin can be explained as follows; (i) the sodium ion functional group takes up more than one HF molecule, via a solvating or "waters of crystallization" type of mechanism (equations 3.17 and 3.18).

$$R\text{-}SO_3Na + 4HF \rightarrow R\text{-}SO_3Na\cdot 4HF \qquad (3.17)$$

$$R\text{-}COONa + 6HF \rightarrow R\text{-}COONa\cdot 6HF \qquad (3.18)$$

(ii) The HF reacts with the sodium ion and forms NaF, which on it's own has a very high capacity for HF (equations 3.19 and 3.20).

$$R\text{-}SO_3Na + xHF \rightarrow R\text{-}SO_3H\cdot HF + NaF\cdot (x\text{-}2)HF \qquad (3.19)$$

$$R\text{-}COONa + yHF \rightarrow R\text{-}COOH\cdot HF + NaF\cdot (y\text{-}2)HF \qquad (3.20)$$

This mechanism involves, firstly ion exchanging the sodium for a proton and the subsequent adsorbtion of HF on the acid functionality and on NaF.

One of the aims of this project was to obtain a medium where NaF could be immobilized with its high uptake capacity. NaF pellets deliquesce when exposed to too high a concentration of HF. Immobilizing NaF on a resin in this way would have the duel effect of dispersing the NaF, allowing high uptake without deliquescence. However, from Figures 3.53 and 3.54, it is evident that these resins lose capacity with successive HF uptake, due either to the NaF leaching out of the resin or of resin breakdown.

Bio-Rad AG1x4 is a strong base resin, with a quaternary amine functional group, which has a wet capacity of 1.2 meq/ml and a dry capacity of 3.5 meq/g. Theoretically if this resin takes up one mole of HF per functional group then the resin will take up 7% HF.

$$R\text{-}N(CH_3)_3^+Cl^- + xHF \rightarrow R\text{-}N(CH_3)_3^+Cl^- \cdot xHF \qquad (3.21)$$

The actual uptake however, is 52%. Bio-Rad AG2x8 has a dry capacity of 3.2 meq/g and should theoretically take up 6.4%, but it takes up 47%. Dowex 21K takes up 38% HF with an exchange capacity of 4.5 meq/g.

With reference to the weak base resins a similar situation is observed, Amberlite IRA 67 has a dry exchange capacity of 5.6 meq/g. Theoretically if it took up one mole of HF per mole of functional group, this would result in a 11% HF uptake. This sample takes up 115%, more than 10x the expected uptake. An example is shown in Table 3.7.

Table 3. 7: HF uptake based on exchange capacity vs. actual uptake

Resin	Theoretical capacity (%)	Actual capacity (%)
Strong base		
Bio-Rad AG 1x4	7	52
Weak base		
Amberlite IRA 67	11	115

However, as mentioned previously, the weak base resins do have additional mechanisms open to it to take up more HF, equations 3.22 and 3.23.

$$R\text{-}N(CH_3)_2 + HF \rightarrow R\text{-}NH(CH_3)_2^+F^- \qquad (3.22)$$

$$R\text{-}NH(CH_3)_2^+F^- + xHF \rightarrow R\text{-}NH(CH_3)_2^+F^-.xHF \qquad (3.23)$$

This however does not explain the high capacity seen here. It is assumed however that the acidic HF is solvating the basic amine functionality, hence leading to the additional uptake.

Overall it appears as if the exchange capacity of a resin is an indication of the HF adsorption capacity for some resins but this is not so in all cases.

3.10. Stability of resins upon multiple hydrogen fluoride exposures

To assess resin stability, the gas passing across the ion exchange resin was alternated between the 10%HF/N_2 mixture and N_2. It was noted that when the ion exchange resins were exposed to N_2, not all the HF desorbed, even after heating up to 100℃. Above 100℃ polymer breakdown occurs.

Amberlite IRA-67 was exposed to five HF adsorption-desorption cycles on the corrosive thermogravimetric analyzer.

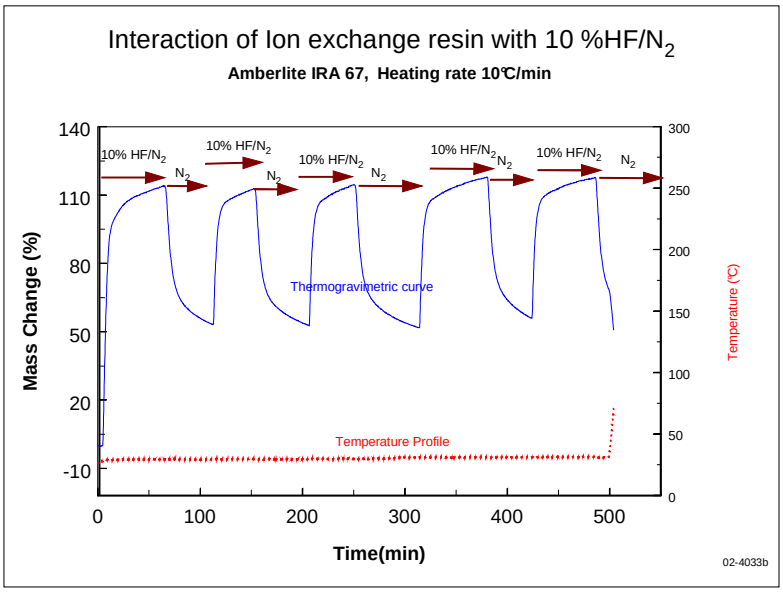


Figure 3.50: Thermogravimetric curve of Amberlite IRA 67 after exposure to a 10% HF/N_2 mixture

Based on the results obtained, it is evident that this sample is relatively stable to HF uptake and desorption cycles (Figure 3.50). No decomposition of the sample was evident. It is also noted that the HF was not desorbed totally under the experimental conditions used.

Amberlite IRA 68 was exposed to 50KPa HF for three hours and the HF pumped off. Washing twice with 0.5M NaOH regenerated the resin. The HF uptake was then reassessed and found to be 89% (Figure 3.51).

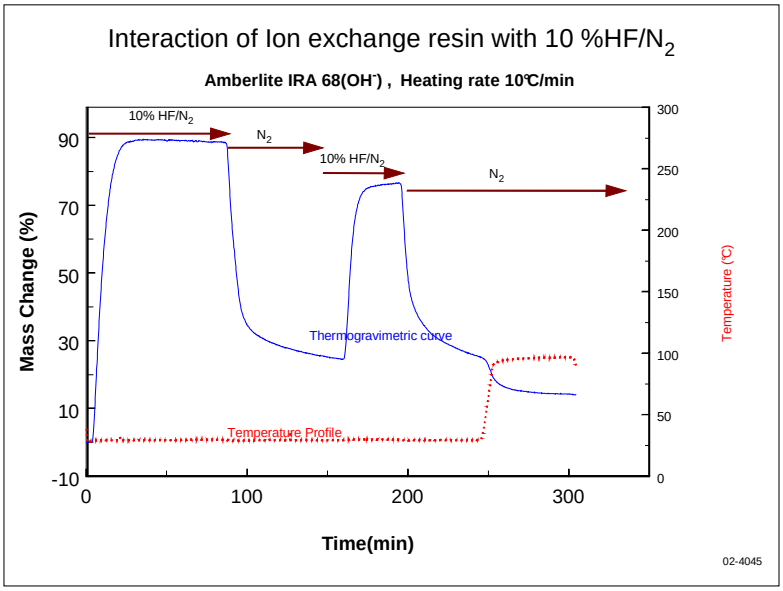


Figure 3.51: Thermogravimetric curve of Amberlite IRA 68 (OH) after exposure to a 10% HF/N_2 mixture

This indicates that the resin can be partially regenerated with sodium hydroxide.

Lewatit MP 64, a weak base, with a styrenic backbone, was also subjected to five adsorption-desorption cycles.

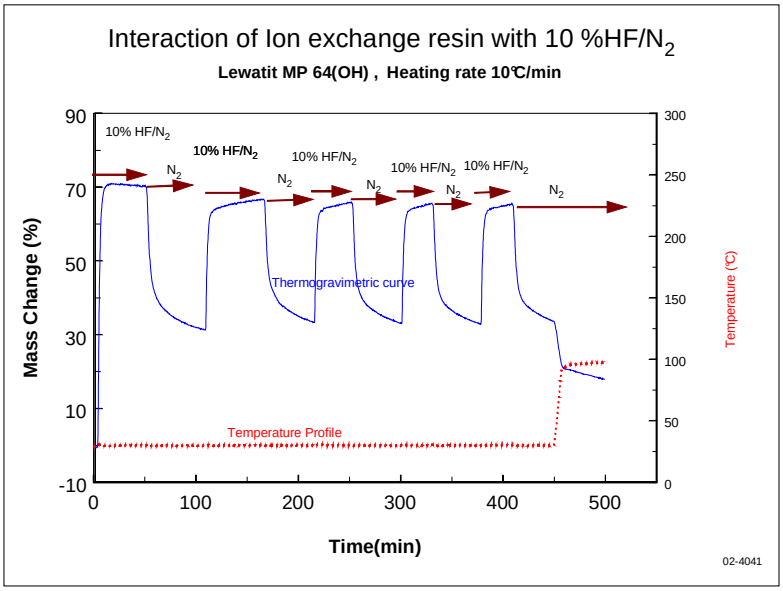


Figure 3.52: Thermogravimetric curve of Lewatit MP 64 (OH) after exposure to a 10% HF/N_2 mixture

It appears as if this sample lost a total of about 5% capacity over the five successive adsorptions (Figure 3.52).

Amberlite IR 120Na (a strong acid, polystyrene resin) marketed as a desiccant gave results as indicated in Figure 3.53.

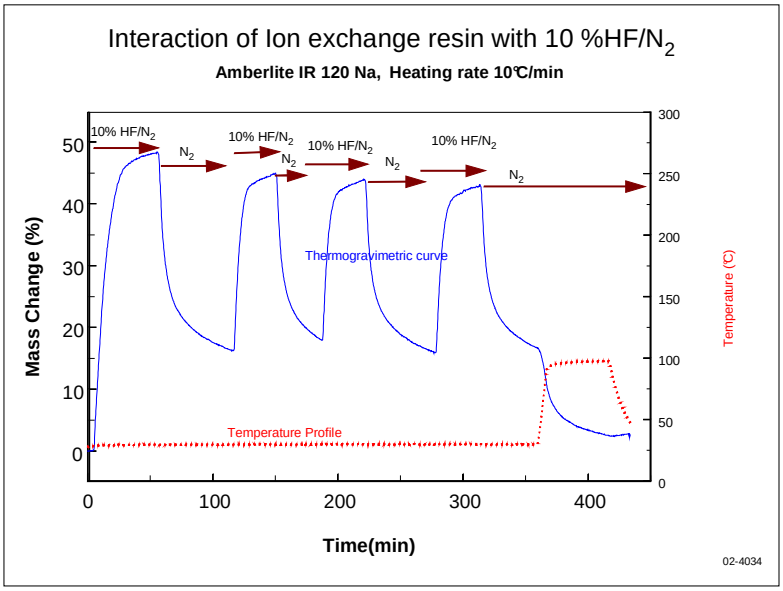


Figure 3.53: Thermogravimetric curve of Amberlite IR 120Na after exposure to a 10% HF/N_2 mixture.

In this case it would be noted that the HF uptake decreases by a total of 5% with successive cycles. The sodium form of Bio-Rad AG 50Wx4 was also tested with similar results, dropping by about 7%, (Figure 3.54).

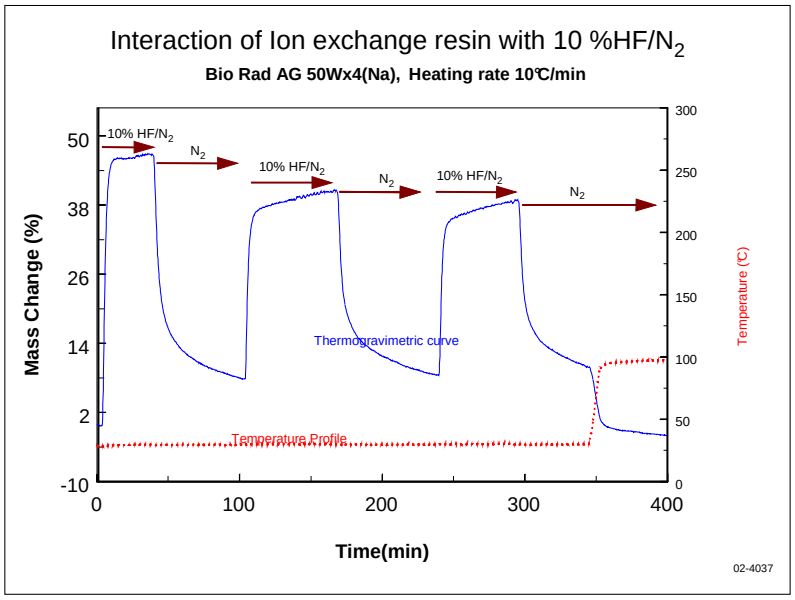


Figure 3.54: Thermogravimetric curve of Bio-Rad AG 50W x 4(Na) after exposure to a 10% HF/N_2 mixture

This is an indication of possible ion exchange breakdown upon successive HF exposure. As previously noted, Amberlite IR120Na was exposed to 50kPa HF for a period of about 3 hours, resulting in a white residue, found by XRD to be NaF·HF. However, it was noted some polymer fragments also did separate out. This indicates that the styrene/divinylbenzene backbones of the strong acid resins are not stable in an HF environment.

The solubility of some of these resins in HF was also investigated. When Bayer Lewatit CNP LF(Na) (a weak acid, polyacrylic resin) was exposed to HF, the following resulted (Figure 3.55):

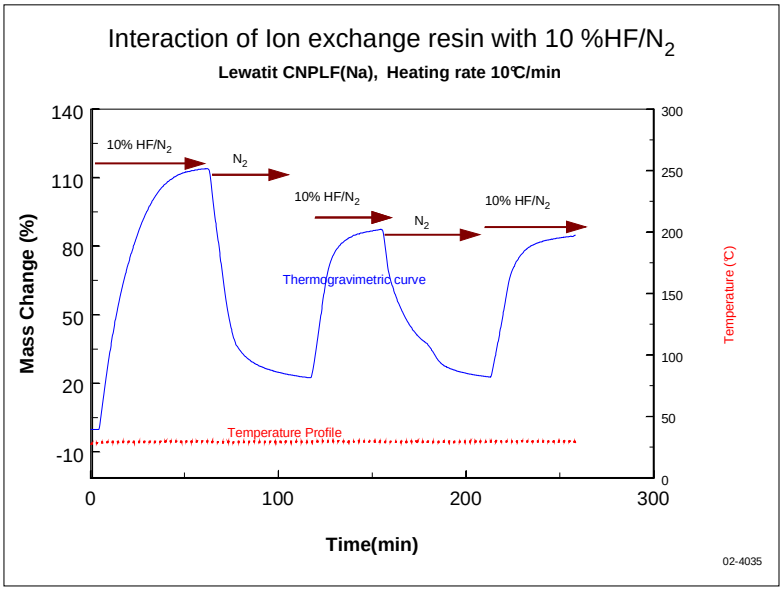


Figure 3.55: Thermogravimetric curve of Lewatit CNP LF (Na) after exposure to a 10% HF/N_2 mixture

As can be seen, this sample has a very high uptake of greater than 110% (based on the mass of the dry polymer). However upon repeat cycles the uptake decreased by about 30%. The physical appearance of the sample did change when exposed to HF and appeared to have dissolved in the HF.

3.11. Hydrogen fluoride uptake as a function of temperature

One of the desired characteristics of the adsorbents is that they must be able to adsorb at different temperatures. Although adsorbent columns can generally be heated or cooled, this is normally energy intensive.

The uptake of HF by Amberlite IRA 67 was assessed at different temperatures. These experiments were conducted on the TG using a 10%HF/N_2 mixture. Results obtained are as follows (Table 3. 8):

Table 3.8: Percentage HF adsorbed by Amberlite IRA 67 at different temperatures

Temperature (℃)	% HF adsorbed
10	167
30	114
60	79
100	55
150	43
200	33

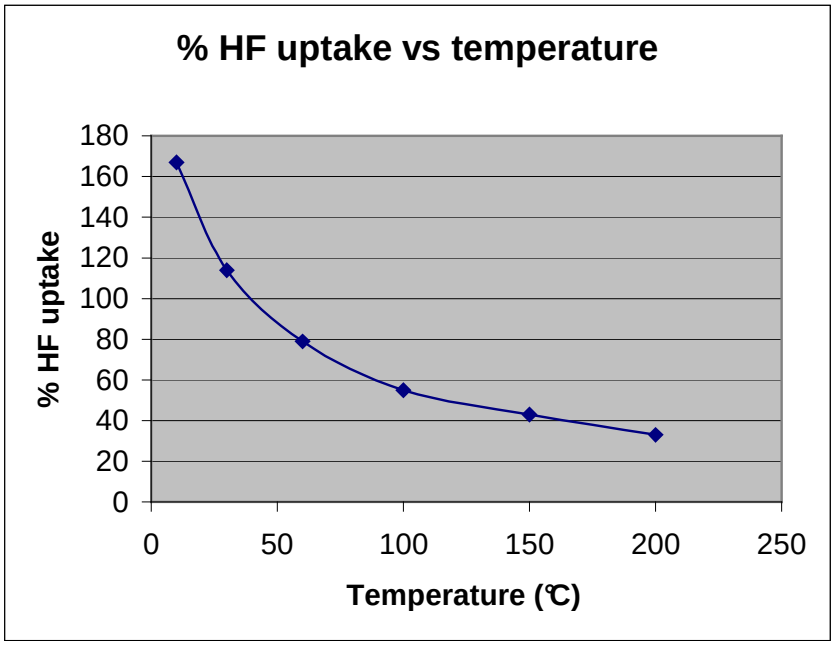


Figure 3.56: Graph indicating percentage uptake of HF by Amberlite IRA 67 as a function of temperature

The relationship for the amount (%) of HF adsorbed as a function of temperature is illustrated above (Figure 3.56). As can be seen there is a significant increase in adsorption on lowering the temperature. This

indicates that a significant capacity advantage can be gained by working at a lower temperature. HF boils at 19℃ and hence there will also be a high degree of condensation below this temperature. Considering this experiment was conducted in a flowing N_2 environment, the condensed HF must be held by some force *e.g.* hydrogen bonding.

At the high temperature end, this sample has a 33% capacity for HF at 200℃. indicating very stable bonds between HF and the resin.

3.12. Hydrogen fluoride uptake at lower acid concentrations

Although most of the work on the uptake of HF by ion exchange resins on the thermogravimetric analyser was done using a 10% HF/N_2 mixture, most possible applications for these resins will involve the removal of far smaller concentrations of HF, normally in the ppm range. The thermogravimetric analyser was thus modified to deliver lower concentrations of HF, *i.e*. in the ppm range, using a permeation cell to the resins.

The HF concentrations in N_2 were 6815 ppm (0.68%), 11846 ppm (1.2%) and 19897 ppm (2.0%). Lower levels are possible, however these concentrations were easily achievable, using the instrument default purge gas flow rate, which was 28.8 ml/min at STP.

Four resins were selected for this study, one each from the four resin categories. The results obtained are shown in Figures 3.57 to 3.68 (Appendix 2).

What was noted is that the acidic resins (Figures 3.60 to 3.62 and 3.66 to 3.68) have a far lower capacity than the basic resins (Figures 3.57 to 3.59 and 3.63 to 3.65) for HF uptake. This was expected as the same trend

was noted when a 10% HF/N_2 mixture was used. A summary of the results obtained is as indicated in Table 3. 9.

Due to the low loading levels and the slow kinetics displayed by the Amberlite IR 120Na, it was decided not to study the acidic resins further. For the basic resins, Amberlite IRA 67 and Amberlite IRA 458 Cl showed the most promise, especially with reference to capacity.

Table 3. 9: Table of % HF uptake for low concentrations of HF

Sample	**% HF adsorbed with the permeation cell set to deliver**			**% HF uptake from 10% HF/N_2**
	0.68%	**1.2%**	**2.0%**	
Amberlite IRA 67	51	53	58	114
Amberlite IRA 458 Cl	22	27	34	72

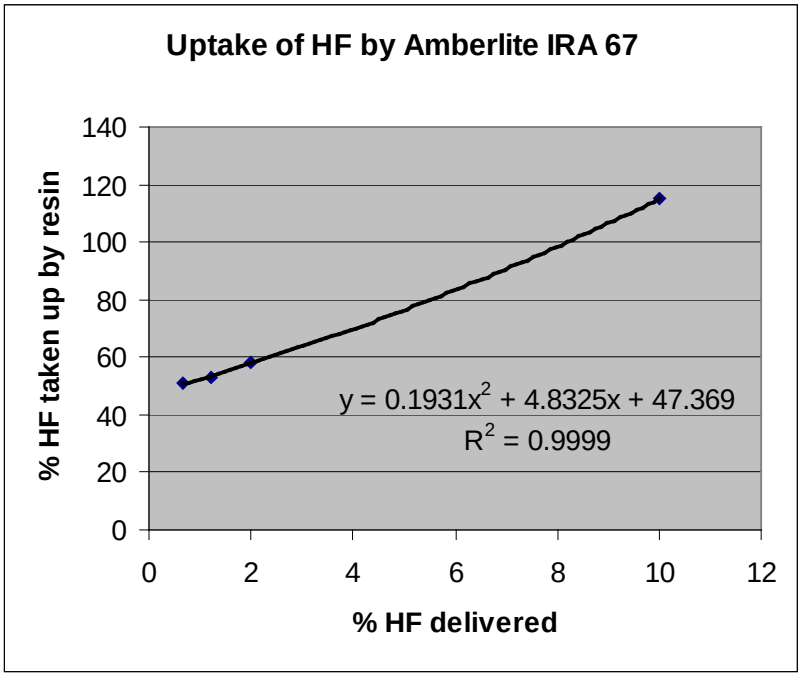


Figure 3.69: Graph of %HF taken up by Amberlite IRA 67 as a function of percentage delivered.

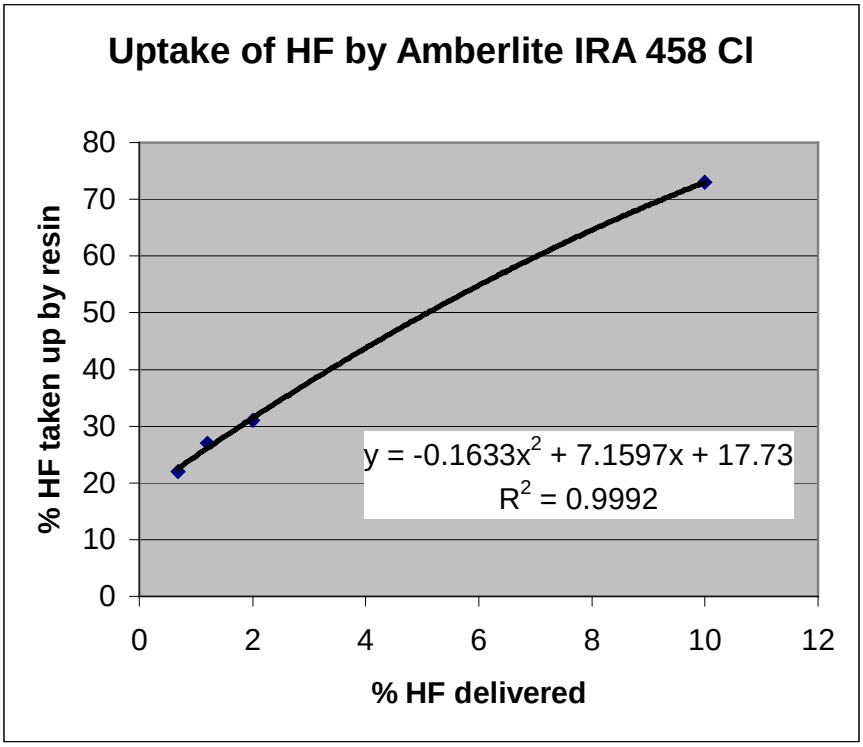


Figure 3.70: Graph of %HF taken up by Amberlite IRA 458 Cl as a function of percentage delivered.

Considering these results (Figures 3.69 and 3.70), a second permeation cell, which permeates in the order of 0.1%, was used to assess the uptake of HF of the two basic resins. At very low concentrations, difficulties are introduced in the assessment of HF uptake on the thermogravimetric analyser. Due to the tendency of HF to hydrogen bond to the walls of the tubing that feeds the HF to the sample chamber, each time the HF concentration is changed, time has to be allowed for a dynamic equilibrium to be established between the HF in the gas stream and that, adsorbed on the walls of the tubing. Use of high concentrations of HF (10%) leads to rapid establishment of its dynamic equilibrium. Below 1% it can take a few days to reach equilibrium, dependent on the concentration of HF used in the previous run. This issue was resolved by using low HF concentrations in a series of consecutive runs. HF concentrations of 0.059, 0.099 and

0.162% were used and the results are presented in Figures 3.71 to 3.76 (Appendix 2).

From the results (Figure 3.71), it can be noted that when Amberlite IRA 67 was exposed to 0.059% HF, it appeared to reach saturation after more than three hours of exposure at 34%, whereas when the resin was exposed to 0.099 and 0.16% HF, HF uptake was still occurring after 5 to 6 hours of exposure. This indicates that even with very low HF concentrations, Amberlite IRA 67 has a significant capacity for HF. This same trend of continuous uptake is also noted for Amberlite IRA 458 Cl.

For Amberlite IRA 67, the samples exposed to 0.099% and 0.162% HF were still adsorbing HF when the experiments were stopped (Figures 3.72 and 3.73). Hence there is no indication as to what the final HF capacity of the resin would be when exposed to the indicated concentrations. Considering that only the sample exposed to 0.059% HF reached saturation (Figure 3.71) it was decided to add this data to the data in Table 3.9 and Figure 3.69 as this is a table of saturated HF capacities for Amberlite IRA 67.

Table 3. 10: Table of % HF uptake for low concentrations of HF

Sample	**% HF adsorbed with the permeation cell set to deliver**				**% HF uptake from 10% HF/N_2**
	0.059	**0.68**	**1.2**	**2.0**	
Amberlite IRA 67	34	51	53	58	114

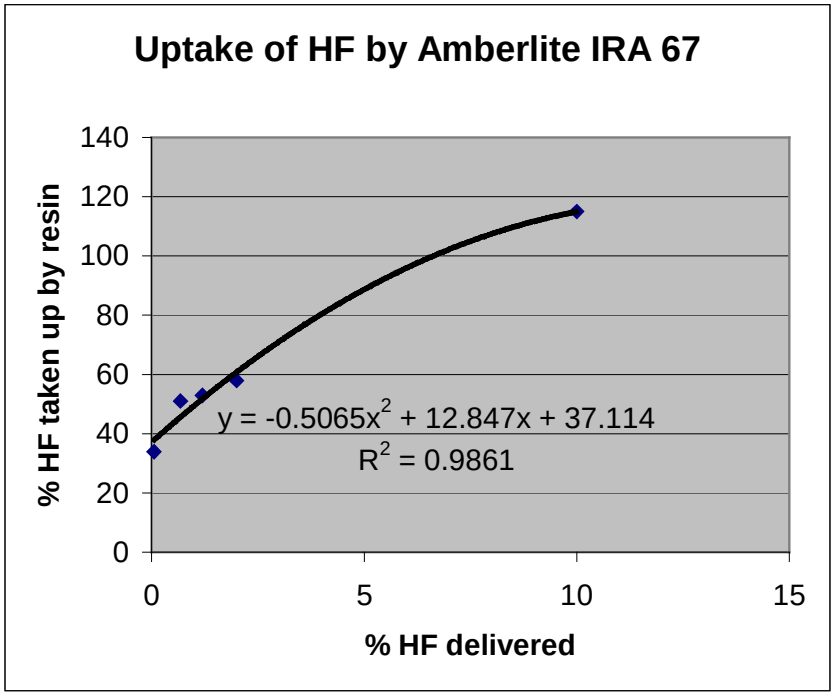


Figure 3.77: Graph of %HF taken up by Amberlite IRA 67 as a function of percentage delivered.

The results indicated above (Figure 3.77) will give some way of quantifying the capacity of Amberlite IRA 67 for different HF concentrations should the resin be used as a HF adsorber for different HF concentrations.

For Amberlite IRA 458 Cl, these resins did not reach saturation when exposed to HF during exposure time, however out of interest it was decided to add this data to the data in Table 3.9 and Figure 3.70. The result obtained is as follows.

Table 3. 11: Table of % HF uptake for Amberlite IRA 458 Cl

% HF delivered	Approx uptake (mass%)
0.059	8
0.099	10
0.16	15
0.68	22
1.2	27
2.0	34
10	72

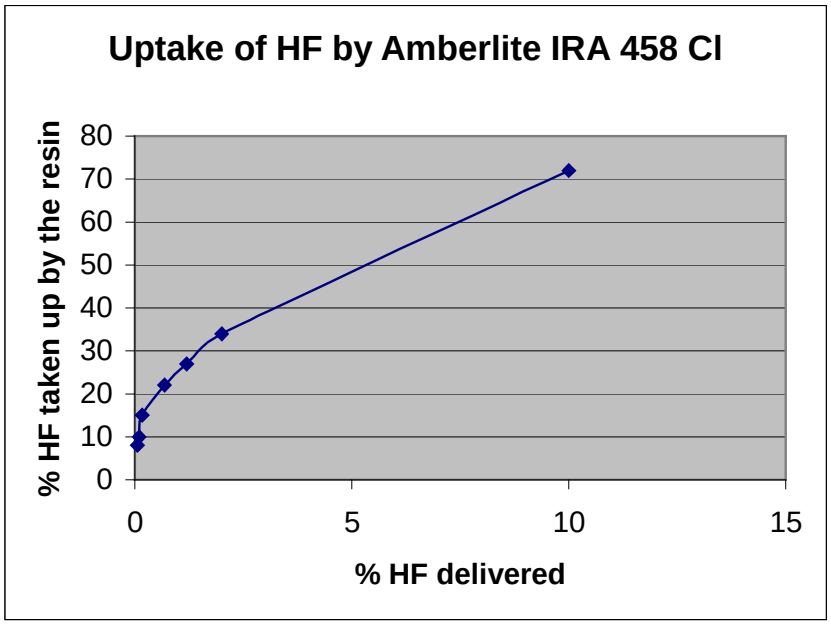


Figure 3.78: Graph of %HF taken up by Amberlite IRA 458 Cl as a function of percentage delivered

As can be noted from Figures 3.77 and 3.78, these resins have a capacity for HF even at lower concentrations; hence can be used to remove low concentrations of HF from the vapour phase.

3.13. Hydrogen fluoride uptake by non-functional ion exchange resins

Unfunctionalized ion exchange resins were also investigated for HF uptake. Samples were obtained from Rohm and Haas (Table 3. 12).

Table 3. 12: Table of properties and HF uptake by Ion Exchange Resins

Sample	**Backbone**	**Pore diam (Å)**	**Surface area (m^2/g)**	**% HF uptake**
XAD4	Aromatic	120-160	750	16
XAD16	Aromatic	240-320	800	25
XAD7HP	Acrylic	300-450	380	30

These resins do not have functional groups but instead pores to increase the surface area. The XAD resins have a styrene/divinylbenzene backbone with the XAD4 having a smaller pore size than the XAD16. The XAD7HP not only has a different backbone *i.e*. an acrylic type one, but also the largest pore size.

These samples were exposed to 10% HF vapour in the TG to evaluate their behavior. (See Figures 3.79 to 3.81 and Table 3.12).

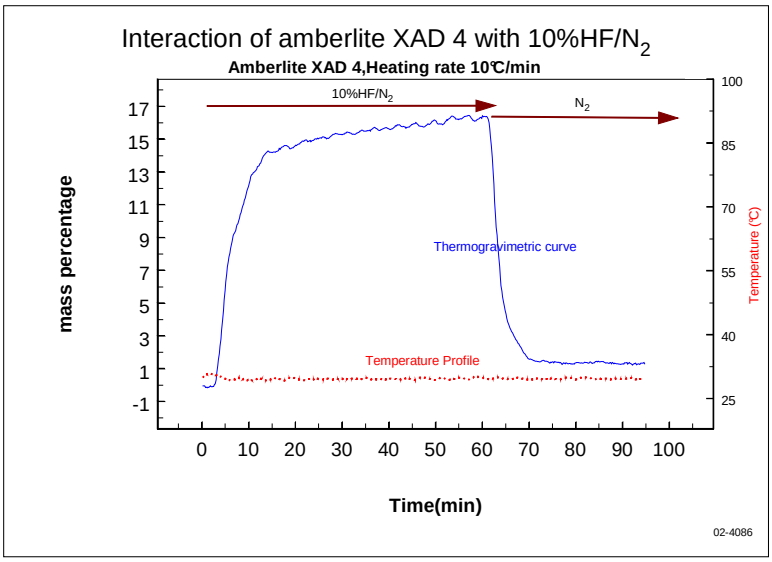


Figure 3.79: Thermogravimetric curve of Amberlite XAD 4 from 10% HF/N_2 mixture

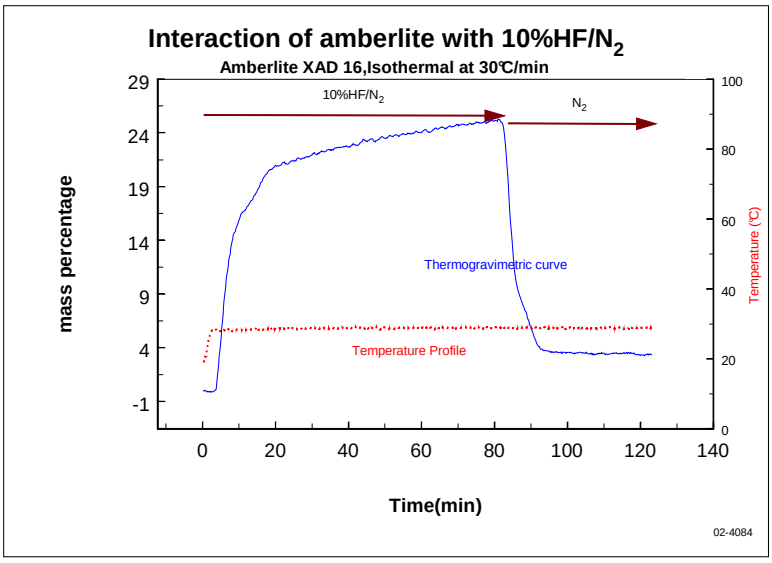


Figure 3.80: Thermogravimetric curve of Amberlite XAD 16 from 10% HF/N_2 mixture

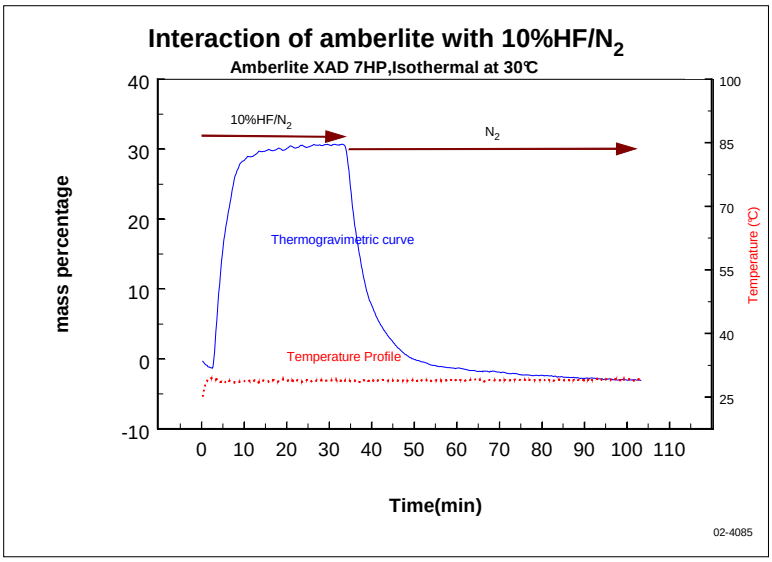


Figure 3.81: Thermogravimetric curve of Amberlite XAD 7HP from 10% HF/N_2 mixture

The results indicate that as the pore diameter increases, the HF uptake increases. The XAD 7HP with the aliphatic backbone and large pore diameter has a higher HF uptake. The acrylic as compared to the styrenic functionalized resins gives higher HF uptake (Table 3.2).

It is also interesting to note the stability of the acrylic resin to repeated exposures to HF (Figure 3.82). This is as seen for Amberlite IRA 67, the functionalized acrylic resin. The Amberlite XAD 4 (Figure 3.79) also displays stability to repeated HF exposure. Amberlite IR 120Na (Figure 3.14), which also has a styrenic backbone, breaks down on repeated exposure. Hence it appears as if introduction of functionality to a resin backbone does weaken the structure.

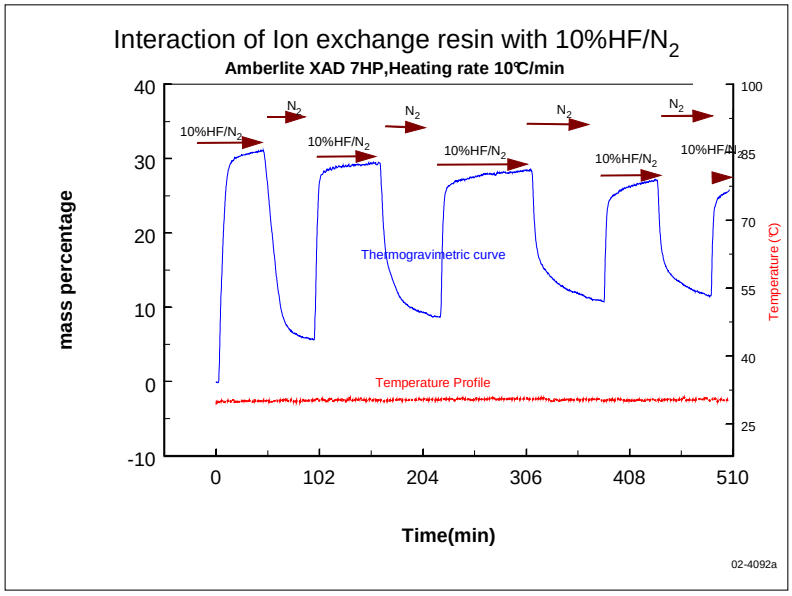


Figure 3.82: Thermogravimetric curve of Amberlite XAD 7 HP from 10% HF/N_2 mixture

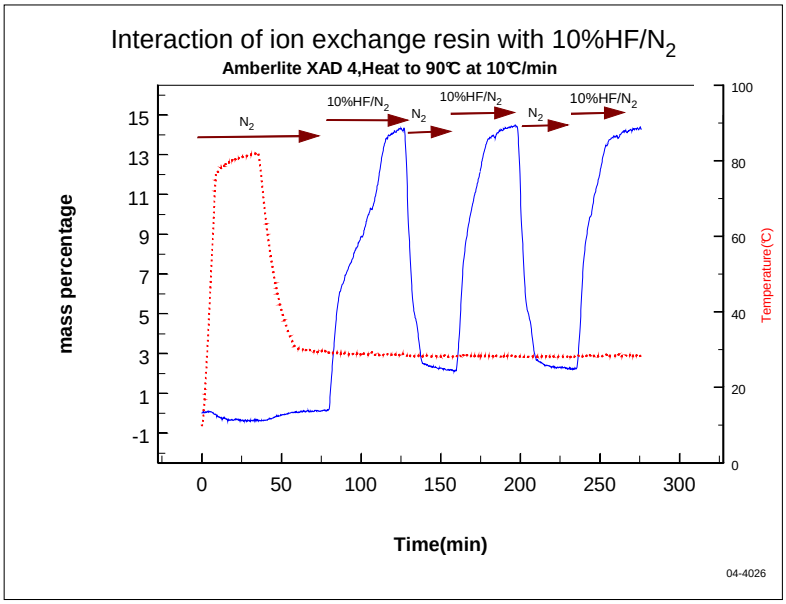


Figure 3.83: Thermogravimetric curve of Amberlite XAD 4 from 10% HF/N_2 mixture

The uptake of polystyrene was also studied (Figure 3.84). This sample has a two to three percent HF uptake indicating that the pores of the styrenic resins also play a role in the uptake of HF.

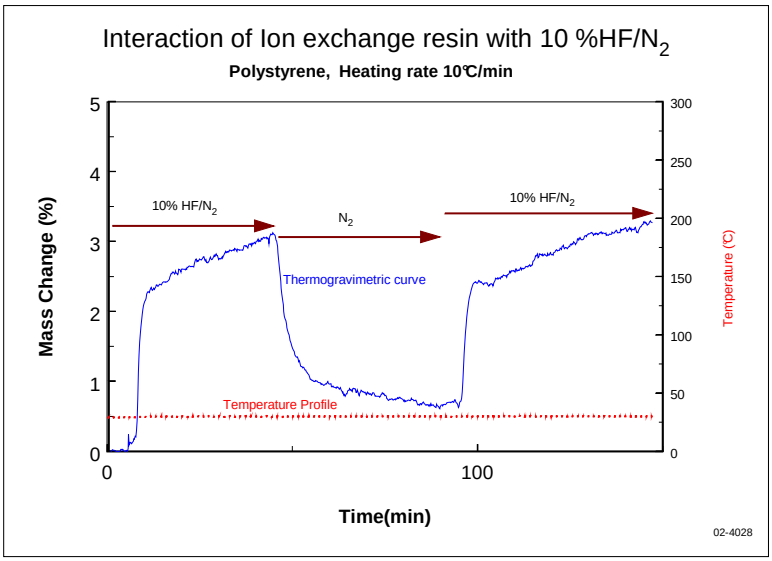


Figure 3.84: Thermogravimetric curve of Polystyrene powder from 10% HF/N_2 mixture

Other factors like backbone and surface area affect the HF capacity of a resin. The backbone may also have a capacity for HF adsorbtion. The resin backbone is either acrylic or styrenic. To quantify the uptake of HF by the resin backbone, the HF uptake by an unfunctionalized resin needs to be quantified. Amberlite XAD resins are unfunctionalized resins, however the HF uptake of these resins cannot be taken as the uptake by the resin backbone as, the Amberlite XAD resins have porosity in them. This will influence the HF uptake positively. Amberlite XAD4, which has an aromatic surface and has an HF uptake of 16% is much higher than that of another aromatic surface, polystyrene which takes up about 2 to 3% HF.

With regard to surface area, the total area is taken as being the external area and the area within the pores. Another factor is the total HF adsorbed

as a function of surface area. It is assumed the HF is taken up as a monolayer on the internal and external surface. The kinetic diameter of an HF molecule is 3.148Å [35]. Hence the area of an HF molecule, πr^2 = $\pi(3.148/2)^2$ $Å^2$. However when four HF molecules are placed together the area between them also has to be factored in as part of the total occupied area, hence the area occupied by the HF molecules was taken as d^2 *i.e.* $(3.148)^2$ $Å^2$ or 9.91 x 10^{-20} m^2. Now if Amberlite XAD 4 has a 16% mass uptake then a 1 g sample of this resin takes up 0.16 g of HF, which calculates out to being 0.16/20 moles of HF (20 g/mol being the molar mass of HF). Using Avogadro's number of 6.022 x 10^{23} molecules per mole there is a total of 4.82 x 10^{21} molecules of HF that cover the surface of this resin. Now considering that each molecule of HF covers a surface area of 9.91 x 10^{-20} m^2, we can calculate the total area covered by all the HF molecules adsorbed on 1 g of the resin. This comes out to being 477 m^2. Hence considering that the surface area of Amberlite XAD 4 is 750 m^2/g, this means we have a surface coverage of 64% assuming a monolayer cover of HF, both in the pores and on the surface.

A further complication arises due to the bond angles between the HF molecules, this was found to be as follows; θ_{HFH} = 104° and θ_{FHF} = 165° [36]. This coupled with the fact that HF has a tendency to form polymers results in a rather complicated structure, the surface coverage of which can most likely only be calculated by molecular modelling.

Considering these results, the next question asked is why not a 100% surface coverage? The surface area is normally determined by nitrogen adsorption on a surface. Nitrogen is an inert gas in that two nitrogen molecules next to each other will not interact; this however is not the case with HF. HF has a tendency of hydrogen bonding hence the HF molecules will not "sit" next to each other without interacting and this interaction has to be factored into any surface area calculations. The van der Waal's radii of hydrogen was found to be 1.2 Å and that of F_2 to be 1.35 Å [37]. Hence

the distance of closest approach was calculated to be 2.55 Å, however due to hydrogen bonding this was found to be 1.6 Å [36].

However to simplify this, it is now advantageous to consider the surface coverage of Amberlite XAD 16 which is also an aromatic resin, as possibly a factor can be calculated which when added to the surface area of HF, will account for the above factors. As noted from Table 3.12, this sample has a 25% uptake, further it has a surface area of 800 m^2/g. When the above exercise as for Amberlite XAD 4 is carried out for this sample, the coverage is calculated out to be 93%, which does not comply with what was found for Amberlite XAD 4, hence indicating that the HF uptake may not be linked to surface area.

Amberlite XAD 4 and 16 have very similar surface areas of 750 and 800 m^2/g respectively but the pore diameters vary. The pore diameter of Amberlite XAD 4 is 120-160 Å and has an HF uptake of 16%; and that of Amberlite XAD 16 is 240-320 Å and it has an uptake of 25%. Considering that these resins are identical except for pore size distribution the difference in HF uptake can only be ascribed to this difference in pore size distribution.

The result for Amberlite XAD 7HP cannot be factored into the above discussion as the backbone is not the same as that of Amberlite XAD 4 and 16. However it is interesting to note that this resin has the largest pore size distribution and the highest HF uptake, with the smallest surface area. This indicates that surface area does not play a role in uptake of HF, with regard to these resins but pore size distribution.

3.14. Separation of hydrogen fluoride from organics

The thermogravimetric analyser used, was an excellent tool to assess the uptake of HF by ion exchange resins. However there are certain limitations

associated with its use. Firstly it cannot be used to assess the uptake of HF from gas mixtures as it may be difficult to assess which gas is being taken up by the resin and secondly, as it is used exclusively for fluorine containing gases it can not be used for other acidic and basic gases.

To overcome this problem, an in-house designed gas circulating adsorption system was constructed, (see Figure 3.87 in Experimental), which basically consisted of an in-line pump, a 10 cm infrared cell and a chamber to hold the ion exchange resin. This allowed the circulation of the gas mixtures through the adsorbent and via the infrared cell. This system was constructed to assess the uptake of HF from both functionalised and unfunctionalised organics and for the uptake of other gases *e.g*. HCl and NH_3, which could not be tested on the thermogravimetric analyser. In this case an infrared spectrometer was selected as the analytical tool of preference as both organics and the acid and basic gases can be assessed both quantitatively and qualitatively with this technique.

The HF concentrations were quantified using, the integrated area under a peak of one of the representative HF peaks at 4040 cm^{-1}.

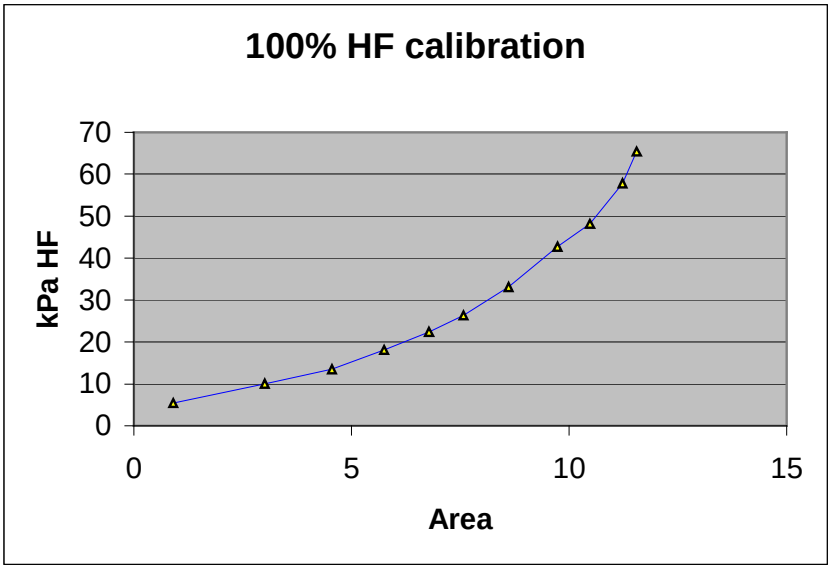


Figure 3.85: Calibration graph for HF between 0 and 70 kPa.

As can be seen the calibration curve of HF vapour pressure *vs*. integrated area, is not a straight line presumably due to polymer formation [38]. It is this polymer formation that also leads to errors in the quantification of HF in the gas phase from pressure readings [39].

A further complication with quantifying HF is the presence of residual HF in the system. This is due to adsorption of HF on the walls of the tubing and on the sapphire windows, and the efficiency of the vacuum pump. This residual HF leads to incorrect area readings, as it results in a stronger HF signal than is expected for the HF in the gas phase. Further, a dynamic vacuum did not remove all the HF from the system even after 24 hours of pumping. To quantify this effect, an experiment was conducted where the HF remaining in the system after vacuum desorption, as a function of the initial HF pressure, was quantified.

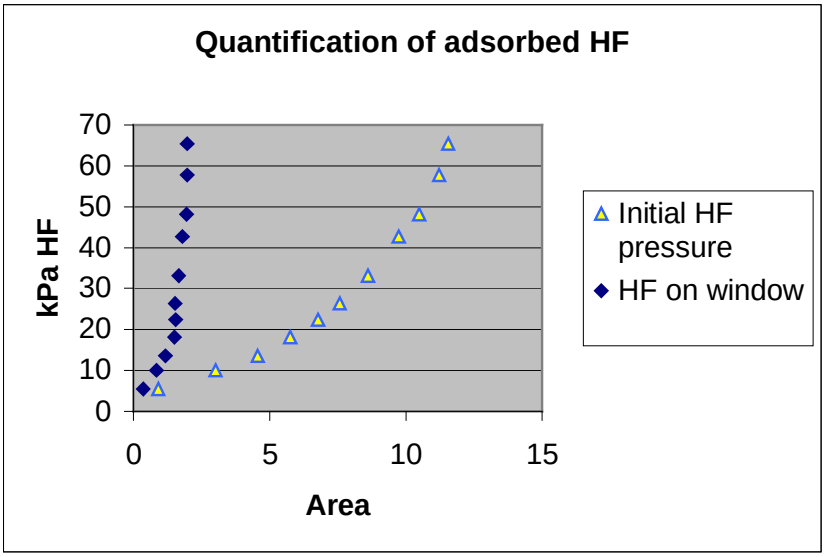


Figure 3.86: Calibration graph for HF indicating quantity of HF adsorbed on window.

From the above, Figure 3.86, it is evident that as the pressure of the HF in the system increased so did the residual HF in the system. However, it was noted that cycle purging (repeatedly introducing a gas into the system then pumping it down with vacuum), the system with a neutral gas *e.g*. N_2 removed this adsorbed layer, thus this effect could be neglected.

The limit of detection is taken as being < 0.5 kPa although from experiments conducted a much lower level was obtained. This is to compensate for adsorption of HF on the walls and windows on the system. Further separate calibration curves were established for the different gas mixtures.

Based on the excellent results obtained for the uptake of HF by Amberlite IRA 67 on the thermogravimetric analyser, it was decided to test 1 g of this resin for the uptake of HF in the presence of a non-functionalised organic material. Perfluoroheptane (a perfluorinated non-functional organic), was selected and a mixture of 50% perfluoroheptane and 50% HF was made

up. The total pressure of the synthesized mixture was 20 kPa, and 10 kPa was introduced into the system. This pressure increased to 11.9 kPa when the circulator pump was switched on and dropped to 6.4 kPa when exposed to the ion exchange resin. This drop in pressure is not due to the volume expansion of the gas into the resin chamber as this was compensated for. Upon exposure of the resin to the gas mixture the infrared data revealed no HF. The organic fraction was still visible in the infrared spectrum.

The next non-functional organic compound investigated was perfluorohexane, as the vapour pressure of this organic compound is higher at room temperature allowing a larger sample to be introduced into the adsorption system. Here 20 kPa perfluorohexane was made up to 66 kPa with HF. Of this mixture, 21.4 kPa was introduced into the circulating chamber and the pressure dropped to 7.5 kPa immediately after exposure to the ion exchange resin. No HF peaks were seen in the infrared spectrum. This pressure continued to drop slowly and should have theoretically dropped to 6.5 kPa. No breakdown of organic material was noted in the infrared spectrum.

This resin can remove HF from non-functionalised organic material with no apparent damage to the organic fraction. This indicates that this resin could be used for the removal of HF from these types of mixtures. However, another application could be the removal of HF from HF/ functionalised organic mixtures.

One of the problems that could be encountered is the reaction of the organic functionality of the organic material with the resin. An experiment was thus performed with trifluoroacetyl fluoride (CF_3COF). The mixture consisted of HF (47 kPa), CF_3COF (19 kPa) and N_2 (130.6 kPa), which gave a total pressure of 196.6 kPa. Nitrogen is included in this mixture as the acetyl fluoride was obtained as a mixture in nitrogen. The resin used

once again was Amberlite IRA 67. With reference to the uptake of HF from these mixtures, between 1 to 2 g of resin was used and the pressures of the gas mixtures introduced ranged between 40 and 60 kPa. From the infrared spectra once again it was noted the resin took up the HF rapidly and reduced the HF concentration till it was virtually undetected in the infrared spectrum. However according to the calibration curves this residual concentration ranged between –1 and 0 kPa of HF. (The negative value is possibly due to the adsorption of HF on the infra-red cell window during calibration). The organic material did not breakdown, as there were no changes to the COF peak centred at 1896 cm^{-1}, after adsorption. There was a doublet, centred at about 1800 cm^{-1}, which disappeared. This is ascribed to the hydrolysed product, CF_3COOH, formed in the presence of moisture, which was adsorbed by the resin (equation 3.24).

$$CF_3COF + H_2O \rightarrow CF_3COOH + HF \qquad (3.24)$$

It was also decided to repeat this test with a strong base resin, which has a tertiary amine functional group instead of a secondary amine functional group. The gas mixture was made up of 21% HF, 39.5% N_2 and 39.5% CF_3COF to a total pressure of 230 kPa. The ion exchange resin used in this case was Amberlite IRA 458 Cl. From the results obtained, the strong base ion exchange resin was able to take up HF from CF_3COF. However, in terms of rate, the reaction was much slower than observed for the weak base resin. It was noted that although the weak base resin took up HF immediately, the strong base resin took up HF more slowly and there was still residual HF in the system after 5 minutes of exposure to the strong base resin. Hence it appears as if this resin is unable to remove HF to very low levels.

An interesting observation made at this point was that there was a change in the infrared spectrum. While there was no change to the -COF peak, centred at 1896 cm^{-1} the CF_3COOH peak disappeared and changed in the

intensity. The positions of the $-CF_3$ peaks also varied between 1000 and 1400 cm^{-1}.

1,1,1,2 tetrafluoroethane (HFA 134a) was also tested on the resins. This organic compound is known to form an azeotrope with HF [40]. It was hoped that the weak base ion exchange resin would be capable of breaking organic-HF azeotropes without damaging the organic fraction. Current technology normally involves distillation columns that are expensive to operate.

The mixture was made up as follows, HF was introduced to a pressure of 77 kPa and this was made up to 231 kPa with the HFA 134a. Batches of 30 to 40 kPa of this gas mixture were introduced into the system, loaded with 2 g Amberlite IRA 67, and once again as with the other samples, the uptake of HF was immediate and the HF concentration reduced to below its detection limit in the infrared spectrometer. This was repeated a few times with the same ion exchange sample, with the same results.

No apparent breakdown of the organic material was noted in the infrared spectra. Further, HFA 134a is a partially fluorinated organic and partially fluorinated organics can react with secondary amines (the functional group of the weak base resin). The proton on the carbon is highly acidic and can react with the electron rich amine nitrogen, resulting in a tertiary amine. This amine will now behave as a strong base amine and have a reduced HF attraction compared to a weak base resin. However no evidence for this was noted as the HF was taken up quickly and to the levels noted with other organics.

Finally, Nafion® Superacid Resin, was also tested for the uptake of HF from the HF-HFA 134a mixture. The Nafion® beads were pretreated as indicated in the experimental section.

The Nafion® sample (1 g), although activated showed very little capacity for HF compared to the ion exchange resins and was only able to reduce the HF concentration to about a quarter of the original concentration and normally after 5 minutes of exposure. It was noted that uptake of organics may increase the uptake of HF due to the swelling of the Nafion® beads. A resin sample was then left overnight with 50 kPa of the gas mixture to activate the Nafion®. However, this procedure did not influence the uptake of HF.

3.15. Uptake of other acidic and basic gases by ion exchange resins

The uptake of HCl and NH_3 vapour was also assessed.

A 50% HCl/N_2 mixture was made up. Amberlite IRA 67 (2 g) was used in the experiment and the experimental procedure was as described for the HF organic mixtures. In the initial run 48.5 kPa of this mixture was exposed to the resin and after about 30 minutes the concentration of HCl was reduced from about 24 kPa to 1.9 kPa. This batch of resin was regenerated and the experiment repeated with a 54.5 kPa sample HCl/N_2. In this case the HCl concentration dropped to 6.5 kPa after about 30 minutes. This experiment was repeated with 5 g Amberlite IRA 67. Here a 51.5 kPa sample with about 26 kPa HCl was used, and the HCl concentration dropped to 1.3 kPa after 30 minutes. The resin batch was once again regenerated and the adsorption repeated and the HCl in a similar sample to the above was reduced to 7.3 kPa after 15 minutes.

As this resin does not appear to have a high affinity for HCl, it was decided to repeat this test with Amberlite IRA 458 Cl, a strong base resin. A sample batch consisting of 24 kPa HCl was added to 4 g of this resin. This resin immediately took up the HCl and reduced the concentration to almost zero in about 5 minutes. The resin was regenerated and a fresh HCl batch introduced. Here a slower reaction gave a similar HF uptake.

Hence the strong base resin is far more efficient at removing HCl than the weak base one.

A 50% NH_3/N_2 mixture was used to test the adsorption of NH_3 on all four types of resins, *viz*. the strong base, strong acid, weak base and weak acid.

The first experiment consisted of adsorbing NH_3 onto 2 g of Amberlite IRA 67, a weak base resin. 59 kPa of the gas mixture was introduced into the system and this resin reduced the NH_3 concentration down to 11.5 kPa after 15 minutes. A repeat adsorption reduced the NH_3 concentration, in a sample size of 53 kPa, down to 10.5 kPa after 15 minutes. The next resin assessed was Amberlite IRA 458 Cl, a strong base resin. A 2 g sample was also used in this case. It was noted that this resin reduced the NH_3 concentration in a 51.5 kPa sample to 11.4 kPa, and upon a repeat test, the NH_3 concentration in a 50.5 kPa sample was reduced to 10.9 kPa after 15 minutes.

Dowex MAC 3 (2 g), a weak acidic resin was also assessed. The NH_3 concentration in a 50.4 kPa and a 38.8 kPa sample was reduced to 10.2 kPa and 8.3 kPa respectively in presence of the resin. Finally Amberlite IR 120 H, a strong acidic resin was assessed. The resin (2 g) reduced the NH_3 concentration in a 47.9 kPa sample to 1.1 kPa after 15 minutes and to 2.8 kPa from a 58.7 kPa sample.

Hence it appears as if the strong acidic resin has the best capacity for NH_3. However, overall it appears as if the results obtained for HF in terms of resin capacity and kinetics is not mirrored when other acidic or basic gases are used.

3.16. Experimental

General experimental procedures

Materials

The ion exchange resins used in these experiments were obtained from the following suppliers; Amberlite and Amberjet was obtained from Rohm and Haas South Africa (Pty), Bio-Rad from Bio-Rad Laboratories, Bayer Lewatit from Vivendi Water Systems and Dowex from CH Chemicals.

Some of the resins were used as is and some were ion exchanged for other counter ions. The procedure used is as follows, these resins (normally 100 ml) were washed continuously with a 10% base or salt solution, for 20 to 25 minutes (total volume about 300 ml), they were then rinsed with 500 ml distilled water. Dowex Marathon A was converted from the OH form to the Cl from by passing 5% NaCl for a minimum of 60 minutes through the resin. The resin was left overnight and the exchange repeated the next day. The resin was then rinsed with 10 times the bed volume with demineralised water [41]. These resins were dried at 80 to 100℃ under a flowing nitrogen atmosphere.

The anhydrous HF was 99.9% pure as supplied by Pelchem. This was used as is and in some cases was used to make a 10% vapour mixture with N_2 (maximum total pressure of six bar). This 10% mixture was used as a HF feedstock for the use in the thermogravimetric analyser. The trifluoroacetyl fluoride (99.5% pure) was obtained from ABCR GmbH and Co KG, while the perfluorohexane and perfluoroheptane were obtained from Pelchem. The 1,1,1,2 tetrafluoroethane (99% pure) was obtained from Aldrich Chemical Company Inc. The sodium polyacrylate was obtained from Aldrich and the Nafion® NR50 beads were obtained from The BOC group and Ion Power Inc. All salts used for ion exchange were

obtained from Merck and were at least 99% pure. All chemicals were used without further purification.

Nafion® Superacid Resin

The Nafion® pre-treatment was carried out as follows; Nafion® was boiled in 20 ml of 3% H_2O_2 for one hour, washed in 3 x 20 ml distilled boiling water, boiled in 20 ml of 0.5M H_2SO_4 for one hour and again washed in 3 x 20 ml distilled boiling water. The sample was stored in distilled water until required [30, 31].

HF uptake by sodium polyacrylate from liquid perfluoroheptane

Mixtures of perfluoroheptane, with traces of HF, and sodium polyacrylate were made up and shaken on an electronic shaker at 271 rpm for 4 hours (quantities as indicated in Table 3.1). After shaking, the mixtures were allowed to settle and a sample of the liquid was analysed for fluoride, being an indication of the HF content

Thermogravimetric Analysis

The process of HF adsorption was monitored with an in-house assembled thermobalance, by measuring the mass increase of a sample over a period of time as a function of temperature. Thermal analysis was usually conducted in an inert atmosphere. The weighing mechanism of the thermobalance was protected using a nitrogen blanket that flowed directly over it. The flow rate of the inert/reactive gas used was 28.8 ml/min at STP with sample masses normally in the order of 3 to 5 mg. The gas streams could be changed from inert (N_2) to reactive and back again. The thermobalance has a resolution of 1 µg. Cooling of the circulating water, used for low temperature thermogravimetry work was achieved using a Neslab, Endocal Refrigerated Circulating bath.

The use of low HF concentrations was achieved using a Kin-Tek, 670c Precision Gas Standards Generator. The source of the HF was a certified Trace Source™ LFH Permeation Tube and was normally used as a primary standard. The concentration of the HF being delivered to the system was calculated from the formula.

$C = E/F$

Where C is the concentration of HF is ppm
E is the emission rate of the LFH standard as given and
F is the flow of the diluent gas in ml/min at STP.

F was taken as 28.8 ml/min at STP.

Surface Area Analysis

Surface area analysis was conducted on a Micromeritics Flowsorb 2300 single point surface area analyser, using the classical BET technique. Nitrogen was used as the adsorbate contained in a 25% N_2/He mixture. All samples were degassed for at least 30 minutes at between 150 and 200℃ prior to analysis. The limit of detection is 0.1 m^2/g with a reproducibility of 0.5%.

X-ray Powder diffraction

Powder X-ray data were collected at 298K using a Siemens D500 diffractometer with copper radiation at a wavelength of 1.5406 Å. The X-rays were generated at 40 kV and 30 mA. The data collection conditions were $10° \leq 2\theta \leq 110°$, $\Delta 2\theta = 0.05°$ and $t = 5s$.

Adsorption System

Adsorbtion was conducted on an in-house designed gas circulating adsorption system that was designed and built for these experiments (Figure 3.87), which consisted of an in-line pump (P2), a 10 cm infrared cell and a column to hold the ion exchange resin. The system allowed the circulation of gas mixtures through the resin (in the resin column) and the infrared cell. The experimental set-up consisted of two separate sections, firstly, the pump, IR cell and tubing (called the circulating chamber) and secondly, the cylindrical resin column. The pump used was a mini bellows pump with a pumping capacity of 6 to 8 l/min at atmospheric pressure. The gas mixture was first introduced into the circulating chamber (up to a maximum pressure of 100 kPa) and then into the resin column where adsorption took place. Access points for vacuum (V10), nitrogen (V9) and sample introduction (S1) were also included and the IR spectrometer used was a Bruker Vector 22 FT-IR. More details on the physical characteristics of the system can be found in Table 3.13.

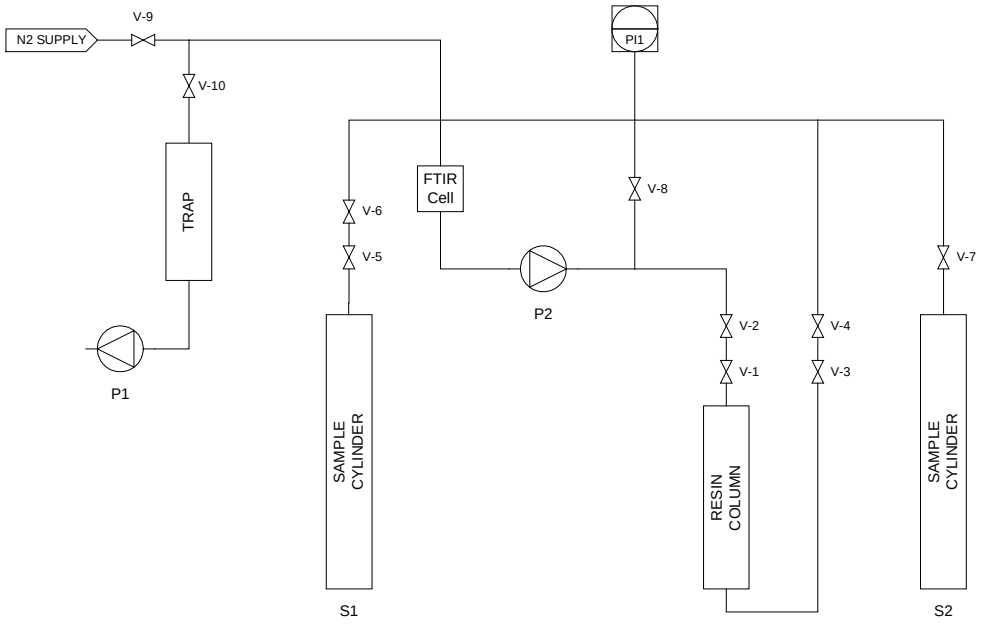


Figure 3.87: Schematic drawing of HF adsorption system

Table 3. 13: Table of experimental data for HF adsorption system

Resin chamber volume	135.2 cm^3
Circulating chamber volume	163.3 cm^3
Total volume	298.5 cm^3
Resin chamber diameter	3.4 cm
Resin chamber length	13 cm
Amount of resin used per run	1 – 5 g
Linear flow of gas thro' ¼ inch pipe	6.3 m/s
FTIR limit of detection for HF	< 0.5 kPa

The experimental procedure used was as follows: the HF-organic or other gas mixtures were introduced into the circulating chamber from the sample cylinder (S1). The sample pressure was recorded. This was allowed to equilibrate for a minute and an infrared spectrum of the sample recorded. The gas mixture was then introduced into the resin column and the gas

was circulated via this column and the infrared cell. Infra red spectra were then collected continuously for a few minutes.

FTIR Spectroscopy

FTIR spectra were recorded on a Bruker Vector 22 spectrometer with the data being processed with OPUS-NT software, version 3.1. As the samples were gaseous, a 10 cm gas infra red cell with sapphire windows was used. One of the advantages of using IR as an analytical tool is that this instrument can quantify both HF and organics. However, accurate analytical measurements are not possible in all cases.

HF has a tendency to form dimers, trimers and polymers in the gas phase as the vapour pressure increases. These polymeric structures exhibit different IR spectra from the monomer making it difficult to accurately quantify HF concentrations at partial pressures greater than a few kPa. The limit of detection for HF on an FTIR is normally much lower than specified above. However, for the experiments that followed, the number of scans on the FTIR were reduced, increasing the noise-to-signal ratio overall and reducing the limit of detection. This was done to reduce the time elapsed from the first to last scan for each FTIR run as adsorption on the resin occurred very quickly. A pressure drop was noted within seconds.

The fluorinated organics exhibited intense IR peaks in the gas phase that resulted in a flooding of the signal at low vapour pressures. Further, minor changes in the IR signal are difficult to track when the signal is flooded. However, IR revealed whether or not HF was removed from the gas phase by the ion exchange resin and whether there were any changes in the IR spectrum, indicating breakdown of the organic compounds.

3.17. References

1 Barsotti, D. J., E. I. Du Pont De Nemours and Co, United States, Patent WO 95/06021 (1995).

2 Barsotti, D. J., E. I. Du Pont de Nemours and Company, Wilmington, Del, Patent US 5 900 044, (1999).

3 DuPont Product Information, Nafion® Superacid Resins NR-50 and NR-40, DuPont Fluoroproducts, USA, NAE 105 (Oct 2000).

4 DuPont Product Information, Nafion® Resins R-1100 and R-1000, DuPont Fluoroproducts, USA, NAE 102 (Oct 2000).

5 Zawodzinski, T. A., Jr., Derouin, C., Radzinski, S., Sherman, R. J., Smith, V. T., Springer, T. E. and Gottesfeld, S., *J. Electrochem. Soc.*, 1041, **140(4)**, (1993).

6 Steck, A. and Yeager, H. L., *Anal. Chem*., 1215, **52**, (1980).

7 Payne, J., Mauritz, K. A., Nafion® Perfluorosulphonate Ionomer, http://www.psrc.usm.edu/mauritz/nafion.html, (June 2001).

8 Heitner-Wirguin, C., *Journal of Membrane Science*, 1, **120**, (1996).

9 Luly, H. M., *et al*, AlliedSignal Inc., Morristown, NJ, Patent US 5766483 (1998).

10 Ion Exchangers, ed. Konrad Dorfner, Walter deGruyter and Co, (1990).

11 CRC Handbook of Ion Exchange Resins: Their applications to inorganic analytical chemistry, vol 6, Ed Johann Korkisch, CRC Press.

12 Richter, A., Patent GB 805 853 (1958).

13 Quinn, R., Air Products and Chemicals, Inc., Allentown, Pa., Patent US 5 797979, (1998).

14 Chen, T-W. and Pinto, N. G., *Ind. Eng. Chem. Res*., 440, **29**, (1990).

15 Diaf, A., Garcia, J. L. and Beckman, E. J., *J. of Applied Polymer Science*, 857, **53**, (1994).

16 Spiegler, K. S., Calif, R. and Routsis, K., United Aircraft Corporation, East Hartford, Conn., Patent US 3 466 138, (1969).

17 Govind, R., University of Cincinnati, Cincinnati, Ohio, Patent US 4 713 091, (1987).

18 Quinn, R., Laciak, D. V., Appelby, J. B. and Pez, G. P., Air Products and Chemicals, Inc., Allentown, Pa., Patent US 5 336 298, (1994).

19 Clarke, R. G., Groth, R. H., Windham, S. and Duzak, E. J., United Aircraft Corporation, Hartford, Conn., Patent US 3 141 729, (1964).

20 Messinger, H. and Daly, J. F., Annapolis and Suitland, Md., Patent US 3 498 026, (1970).

21 Cotter, R. J. and Keogh, M. J., Union Carbide Corporation, New York, N. Y., Patent US 3 917 469, (1975).

22 Vaidyanathan, A. S. and Youngquist, G. R., *Ind. Eng. Chem. Prod. Res. Develop.,* 288, **12(4)**, (1973).

23 Cole, R. and Shulman, H. L., *Industrial and Engineering Chemistry*, 859, **52(10)**, (1960).

24 Bulikh, A. I., Bogatyrev, V. A. and Alovyainikov, A. A*., J. Mendeleev Chem*., 81, **15**, (1970).

25 Vulikh, A. I., Zagorskaya, M. K., Fokina, N. A., Nikandrov, G. A., Reznichenko, L. A., Zverev, M.P., Barash, A. N., Surkova, V. I., Mavrin, A. M., Troyan, N. V., Kalyanova, N. F., Shimko, I. G., Alovyainikov, A. A. and Pechalin, L. I., USSR, Patent US 4 157 376, (1979).

26 Zagorskaya, M. K., Volikh, A. I., Mekler, L. I. and Ksenzenko, V. I., USSR, Patent US 3 653 811, (1972).

27 Aho, C. E., Ky, L., Murray, W. S. and Sloan, W. J., E. I. Du Pont de Nemours and Company, Wilmington, Del, Patent US 2 829 028, (1958).

28 Yuan Siguo, Wang Yi, Lan Shuqin, Lin Kunhua, Lu Yun and Zeng Hanmin, *Ion Exchange and Adsorption*, 60, **13(1)**, (1997).

29 Yuan Siguo, Wang Yi, Lin Kunhua, Liu Tiemin and Zheng,Liandi, *China Safety Science Journal (CSSJ),* 43, **10(1)**, (2000).

30 Zeng, R., *et al, J Electroanal Chem*, 102, **490**, (2000).

31 Yoshida, N., *et al, Electrochemica Acta*, **43**, 3749-3754, (1998).

32 Dowex Ion Exchange Resins, Product Information, Dowex resins as organic solvent dessicants, May (1997).

33 A Guidebook to Mechanisms in Organic Chemistry, 5Th Ed. Peter Sykes, Longman, (1981).

34 http://www.remco.com/ix.htm

35 The Properties of Gases and Liquids, 4th Ed., R. C. Reid, J. M. Prausnitz and B. E. Poling (1987).

36 Sylvia E McLain, Chris J Benmore, Joan E Siewenie, Jacob Urquidi and John FC Turner, Angew. Chem. Int. Ed., **43**, 1952-1955, (2004).

37 CRC Handbook of Chemistry and Physics, 56th Ed., CRC Press, (1975).

38 Matheson Gas Data Handbook, 6th Ed., by W. Braker and A. L. Mossman, Matheson, (1980).

39 Grayson, M., Kirk-Othmer Encyclopaedia of Chemical Technology, 3rd ed., Vol. 10, John Wiley and Sons, (1980).

40 Ryan, T. A., *et.al*., Imperial Chemical Industries PLC, Great Britian, Patent US 5800795, (1998).

41 Ion exchange procedures obtained from Stephen Wrigley, Dow Chemical Company, personnel communication.

Chapter 4

Carbon structures

4.1. Introduction

The aim of this study is to investigate the removal of HF from various media, both organic and inorganic, by adsorption processes. To this end a range of potential adsorbents were investigated. These included carbon-based structures. Three types of carbon-based structures were investigated: activated carbon, carbon molecular sieves (CMS) and nanotubes. All three forms of carbon have been used extensively over the years for gas adsorption. Hence it was decided to assess and compare these adsorbents for HF adsorption. There have been extensive studies done on the gas adsorption capabilities of these materials and a review of some of the pertinent literature is given below.

4.2. Literature survey

4.2.1. Activated carbon

Active or porous carbons have been used for thousands of years for water purification, but it was only in World War I that porous carbon was used for gas phase applications *i.e*. in gas masks. Today granular activated carbon is extensively employed for gas adsorption and separation. This form of carbon is produced from natural products like wood, coal, and coconut shells, but also from synthetic materials like polymers and synthetic resins [1].

The surface area on activated carbons is increased as a result of an activation process [2]. This can be achieved by either a chemical or physical activation. Chemical activation is achieved by treating the carbon with compounds like phosphoric acid followed by carbonising the product.

Physical activation is achieved by gasification of the carbon with carbon dioxide or steam in the range 700 to 1100℃. The second method is more widely used as it creates more porosity.

In terms of porosity, a convenient classification of pores is based on the average width of a cylindrical pore and is based on the characteristic adsorption effect as manifested in the isotherm. Porous materials are classified according to the size of the pores: microporous are pores with width less than 2 nm; mesopores are pores with widths between 2 and 50 nm and macropores are pores with widths >50 nm. For micropores the interaction potential is higher than the wider pores and this results in a higher uptake. In mesopores capillary condensation occurs whereas macropores are considered as being part of the external surface. It has been found that some activated carbons contain all three types of pores [1].

The surface chemical structures on activated carbon are important and influence the adsorption capacity of the carbon. The structures are dependent on the impurities that were present in the carbon prior to activation and in some cases are removed during activation. The elements of interest are typically oxygen and hydrogen. It was found that carbon can chemisorb oxygen when exposed to air or oxygen at 400 to 500℃. Chemically bonded hydrogen is also present on the surface of activated carbon. Also, it was noted that carbons have an acid-base character that is developed as a result of surface oxidation and this character is dependent on the history and oxidation conditions of the activated carbon. Other functional groups postulated to be present on the surface of carbon include carboxyls, aldehydes, ketones, anhydrides and ethereal structures [3 -6].

Antal suggests that the formation of these surface active sites arise from “dangling bonds”. These bonds result from the fracture of chemical bonds

during the carbonisation process. These dangling bonds become oxidised resulting in a carbon-oxygen complex that can act as a Lewis base. Further, the carbon can be hydrophilic and adsorb water [7].

The oxidation process can control these surface oxides; oxidation of the carbon with hot air results in relatively weak acidic surface functional groups *i.e*. phenolic groups, whereas nitric acid produces a greater amount of carboxylic groups. These carboxylic groups are of interest since the surface acidity of these carbons is stronger than that of commercial polymeric carboxylic acid ion exchange resins [8].

With reference to water vapour uptake, Brennan has noted that adsorption of water vapour varied depending on the adsorption method used and that carbon strongly oxidised with nitric acid had the highest adsorption capacity for water vapour [5]. Further, Beck indicated that for non-polar adsorbate an increase in surface oxygen functional groups results in a significant decrease in adsorption performance, when the carbons treated under humid conditions. This possibly arises from the formation of bulky oxygen functionalities on the surface that may partially block the pore entrances in some cases [9]. Li has given an alternative explanation to this phenomenon. He has suggested that this decrease is due to an increase in polarity of the surface, resulting in increased water uptake and increased water clustering. It is these water clusters that block the adsorption sites [10].

This is an interesting proposal since Patrick has indicated that activated carbons generally have a low affinity for water. However some polar groups on the internal carbon surface, interact more strongly with water molecules, and hydrogen bonding comes into play as the partial pressure increases. Further, clustering of water molecules around particular active sites leads to quantitative micropore filling [1, 4]. This characteristic of

polar activated carbons holds promise for HF uptake as HF also displays hydrogen bonding and polymerisation activity [11].

Li also indicated that enhanced water uptake results in a smaller adsorption capacity for trace organic compounds compared to less polar activated carbons with similar micropore volumes [10]. This poses an advantage for HF removal from organics, as the HF should be taken up in preference to organics when separating HF from a mixture.

However, in terms of gas uptake, activated carbons generally have a higher uptake for aliphatics than functionalised organics *e.g*. alcohols. This is due to the non-polar character of carbons in general. Further, molecules with higher molecular weight have a better adsorption rate than smaller molecules. The smaller molecules tend to be driven out of the pores by larger molecules. [2].

Apart from oxidising the activated carbon to enhance HF uptake, another method to achieve high loadings is to load salts onto the activated carbon that have a high capacity for HF, *e.g*. NaF. Here the activated carbon is merely acting as a support for the salt and is not actively involved in the uptake process. To this end Lee used activated carbon supported sodium hydroxide for the removal of HCl gas. The carbon-supported alkali adsorbent was prepared by soaking the activated carbon in a NaOH solution. This carbon is known as impregnated activated carbon (IAC) and is a carrier for the base. The HCl gas was then passed over the surface at this point, resulting in the NaOH being converted to NaCl and the HCl being removed [12]. This will have no re-adsorption capacity as NaOH has reacted. However if HF gas is used, the NaOH will react with HF forming NaF. The NaF should have a re-adsorption capacity.

NaOH loaded carbon has also been used for the removal of other acidic gases like H_2S. However one problem with salt (or base) loaded carbons

is that the salts can block the pores in activated carbon, resulting in reduced uptake capacity [13].

4.2.2. Carbon molecular sieves

Carbon molecular sieves (CMS) are adsorbents for gas separation and reproducible CMS can only be manufactured using initial material with uniform properties. The process consists of grinding and oxidising coal to produce oxicoal. Thereafter a binder is added and the oxicoal shaped and carbonised to produce a uniform initial material. The final step consists of steam activation although there are modifications to produce CMS's for different applications [14].

Because of their microporosity, CMS's are able to separate molecules on the basis of size and shape although they are globally amorphous and lack long-range order. The surface chemistry of CMS's can be varied from basic to acidic and essentially can provide molecular separation on the basis of rates of adsorption rather than extent of adsorption. CMS's also do not have waters of adsorption as a result of their structure and hence this makes them thermally stable. What makes them of interest in this study is that they are resistant to acids including HCl and HF [15]. Foley has reported that acid gases including HF can be separated from fluorocarbons. He found that the fluorocarbon was preferentially retained however when the separation was conducted at 200℃ using an in-house prepared CMS (from polyfurfuryl alcohol resin), the reverse was noted [16].

Evidence for the ability of CMS to adsorb HF has been reported by Hong. He passed a mixture of 97% 1,1,1,2 tetrafluoroethane (HFA-134a) and 3% HF over activated carbon (Carbosieve G) and a poly(furfuryl alcohol) derived CMS. The study revealed that 134a was more strongly bound to the activated carbon than HF and hence HF was eluted first from a column

of Carbosieve G. However when the CMS was used, HFA-134a was not adsorbed and hence was eluted first from this column. It was found that the process of separation was related to the shape selectivity of HF over HFA-134a. The pore structure placed a limit on the diffusive transport of HFA-134a on the basis of its molecular size. This is not observed with Carbosieve G, which has larger pores. The mode of separation for the CMS is kinetic, while that for Carbosive G is thermodynamic in nature [17].

To further reveal the ability of CMS to adsorb HF, Chang used a CMS with an average pore size of 3.5 Å to separate HF, HCl and a chlorofluorocarbon. What he found was that HF was the strongly retained complex, followed by HCl. Regeneration was easily achieved by passing a stream of He over the column at 140℃ [18]. Later, using the same CMS he separated water and HF. The study indicated that both molecules adsorbed but that on regeneration, water was eluted first followed by HF, at a higher temperature [19].

4.2.3. Carbon nanotubes

Carbon nanotubes (CNT) are graphite cylinders. They are normally closed at one or both ends with pentagonal ring caps. Iijima first reported the materials in 1991 while he was studying the material deposited on a cathode during the arc-evaporation synthesis to prepare fullerenes [20]. The CNT's can be opened by oxidation with carbon dioxide or oxygen at elevated temperatures [21].

Different types of CNT's *viz.* stacked, herringbone and nanotubular and can be produced by different procedures, including arc discharge, laser ablation, chemical vapour deposition and flame synthesis. CNT's have shown possible applications in energy storage, molecular electronics, nanomechanical devices and composite materials. Due to their cylindrical and hollow geometry, they can store a liquid or gas in their inner cores

through a capillary effect. The US Department of Energy has set a storage requirement for CNT's of 6.5% by weight if they are to be used in hydrogen fuel cells. Here, a H/C ratio of 2 is expected to yield the maximum (>14 mass%) and most hydrogen is stored either in or on the carbon nanotubes. Generally on carbon surfaces the adsorption of hydrogen is about 2% [22, 23].

A theoretical study, has suggested that the intercalation of polarizable HF into nanotubes is energetically favourable. The calculations were based on a finite length tube of 144 molecules with two HF molecules approaching each other within the tube. It was found that the energy of interaction was lower for these two molecules when compared to the bare interaction of a pair of HF molecules [24]. Further, carbon nanotubes can be functionalised with F_2, using HF at about 325℃. These fluorinated CF_2 groups can be removed by washing the sample with hydrazine [25].

Kleinhammes found that ethane and methane can be adsorbed by carbon nanotubes but only once the tubes were cut. The capacity for methane was about 2 mmol/g at a pressure of 0.2 MPa. Further, he found that oxygen had no effect on the adsorption of any organics, which he ascribed to a low energy of adsorption. He observed that whereas helium atoms could access the interstitial sites of CNT's at room temperature and atmospheric pressure, gases like H_2, CO_2 and N_2 could not [26].

Results and Discussion

Activated carbons, CMS and nanotubes were investigated for HF uptake.

4.3. Activated carbons

With regard to the activated carbons the HF uptake of commercial activated carbons was investigated. Further they were also modified and

the HF uptake investigated. One of the modifications was the adsorbtion of NaF, from different concentration solutions, onto the surface of an activated carbon. These samples were then assessed for HF uptake. Further the uptake of HF by acid and base treated activated carbons was also investigated.

4.3.1. Exposure of activated carbons to hydrogen fluoride

The activated carbon used for these investigations was Chemviron carbon Filtrasorb F200. This is a granular activated carbon, which is steam activated with a high proportion of high-energy pores. It is suitable for removing chlorinated hydrocarbons from water that contains low levels of dissolved organic carbon. The surface area is 900 m^2/g.

The other was Chemviron Carbon IVP a highly impregnated activated carbon used for vapour phase application. The impregnation is NaOH.

The HF uptake of Chemviron carbon Filtrasorb F200 and Chemviron Carbon IVP is shown in Figures 4.1 and 4.2;

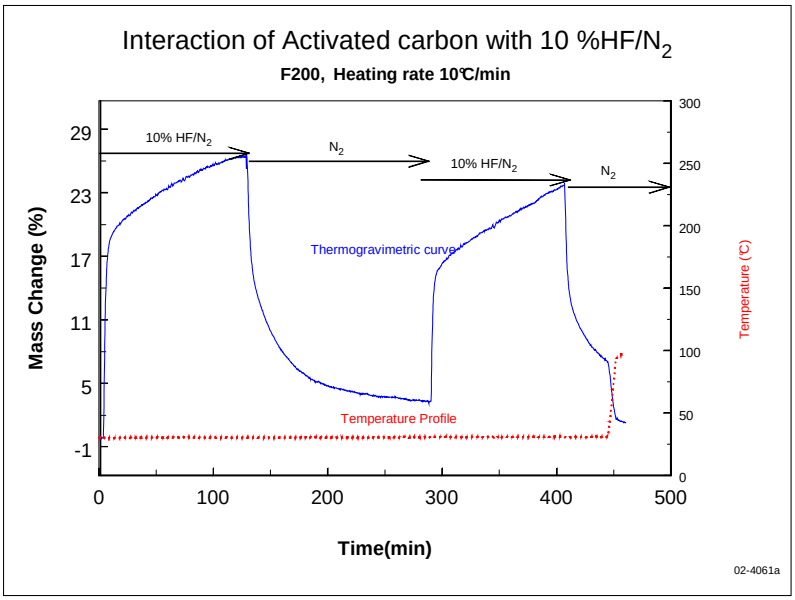


Figure 4.1: Thermogravimetric curve of Activated Carbon F200 after exposure to a 10% HF/N_2 mixture

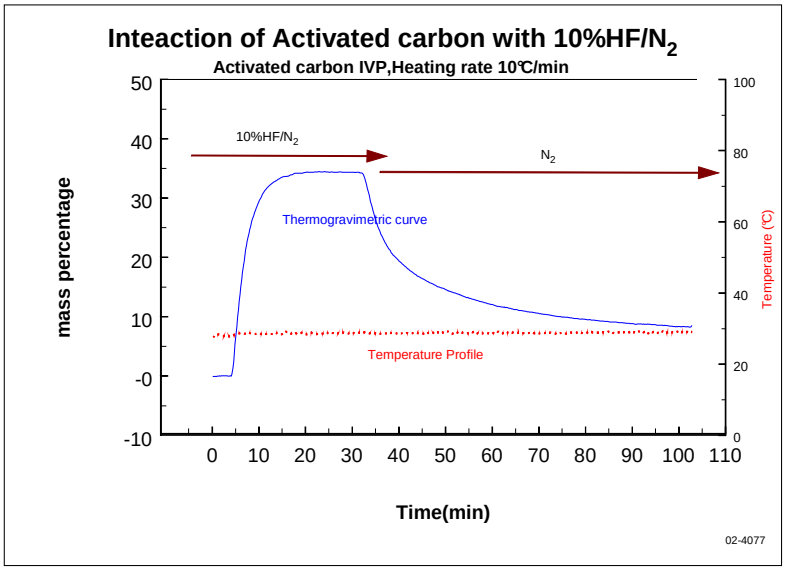


Figure 4.2: Thermogravimetric curve of Activated Carbon IVP after exposure to a 10% HF/N_2 mixture

As is noted from Figures 4.1 and 4.2, the activated carbon samples have a high capacity for HF. Chemviron Carbon Filtrasorb F200, is a granular activated carbon, which is steam activated, hence contains a high proportion of high-energy pores. From the results obtained, it is evident that there is an initial rapid uptake of HF up to about 18 mass% followed by a slower HF uptake stage. The uptake was 27 mass% after two hours and considering the surface area of this sample is 900 m^2/g; this translates to an uptake of 0.3 mg/m^2. Considering that none of the experimental conditions were changed, this change in uptake kinetics is a function of the activated carbon itself.

Chemviron Carbon IVP, on the other hand, is a NaOH impregnated activated carbon. Here, the activated carbon takes up HF at a constant rate, till it reaches about 34 mass%, then stabilises. The mechanism of uptake for this sample appears to be very different from the F200 sample.

An explanation for this different behaviour can be proposed based on studies of water uptake on these carbons [1]. This uptake relates to the presence of polar groups on the internal carbon surface of the F200 sample. These groups interact strongly with HF, due to hydrogen bonding. Clustering of HF molecules around these active sites also leads to quantitative micropore filling. Thus, the rapid initial uptake is proposed to be due to HF hydrogen bonding to these surface-active groups and the change in uptake kinetics is due to the second mode of HF uptake *i.e*. clustering around these groups and micropore filling [1].

The HF uptake of Chemviron carbon IVP is due to a neutralization reaction between HF and NaOH adsorbed on the surface (equation 4.1).

$$HF + NaOH \rightarrow NaF + H_2O \qquad (4.1)$$

Further, from the thermogravimetric trace, it appears as if this sample displays only one type of HF uptake (Figure 4.2 *vs*. 4.1). It has been proposed that the adsorbed base would block the pores and reduce the overall HF uptake capacity [13], The second slow diffusion into pores noted for F200 will not occur here due to the NaOH blocking the pores.

The thermogravimetric experiment for Chemviron Carbon Filtrasorb F200, was repeated, but with a longer HF exposure period. (Figure 4.3)

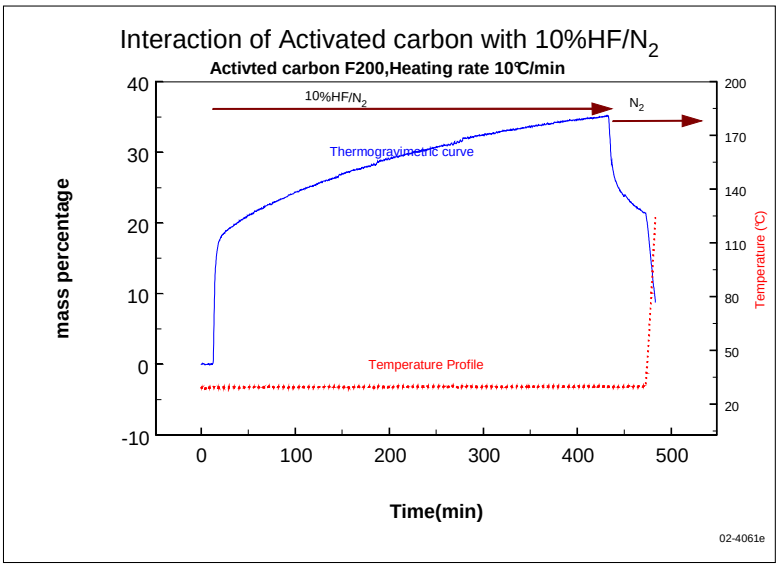


Figure 4.3: Thermogravimetric curve of Activated Carbon F200 after exposure to a 10% HF/N_2 mixture

This sample was allowed to take up HF for more than seven hours but even then still did not reach a point of maximum adsorption. However from the above result, two separate uptake mechanism are evident. If the first is surface adsorption then the second is possibly pore filling. McCallum indicated that this pore filling occurs at relatively higher pressures [4]. However, from Figure 4.3, if the second mechanism is pore filling then indications are that it does occur at atmospheric pressure, but at a much lower rate.

4.3.2. Sodium fluoride adsorption

From the above results it is evident that commercial activated carbon samples have a good capacity for HF. It was thus decided to modify the surface of Chemviron carbon Filtrasorb F200 with varying amounts of NaF and evaluate the HF capacity.

This was achieved by soaking the 0.5 g of carbon in 100 ml of different concentrations of NaF for 20 hours. The excess NaF was washed off so that only the capacity of NaF that is physically bound is assessed. The sample was dried for 24 hours. The results are shown in Figure 4.4 to 4.8.

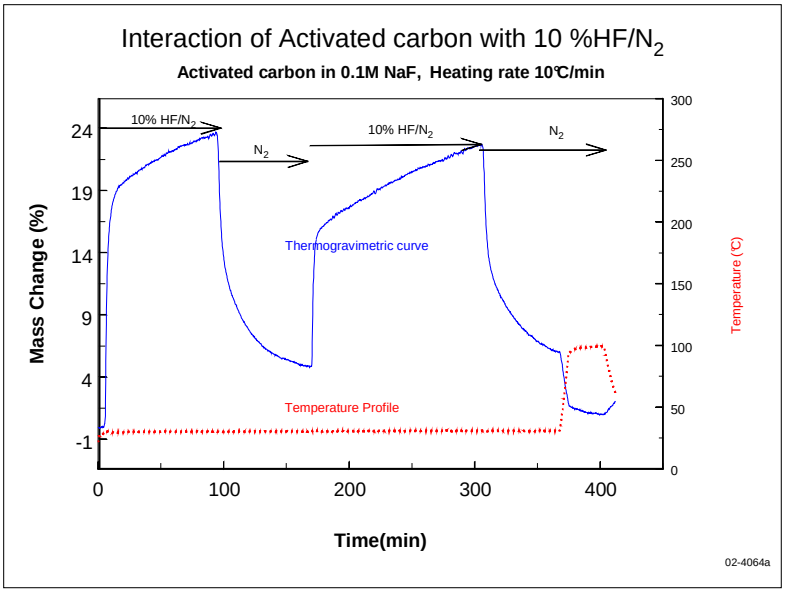


Figure 4.4: Thermogravimetric curve of Activated Carbon F200 soaked in 0.1M NaF after exposure to a 10% HF/N_2 mixture

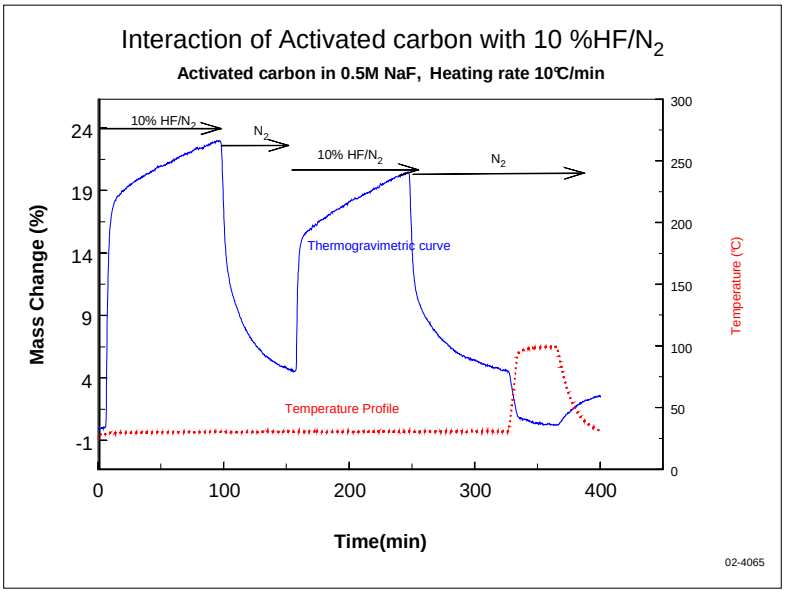


Figure 4.5: Thermogravimetric curve of Activated Carbon F200 soaked in 0.5M NaF after exposure to a 10% HF/N_2 mixture

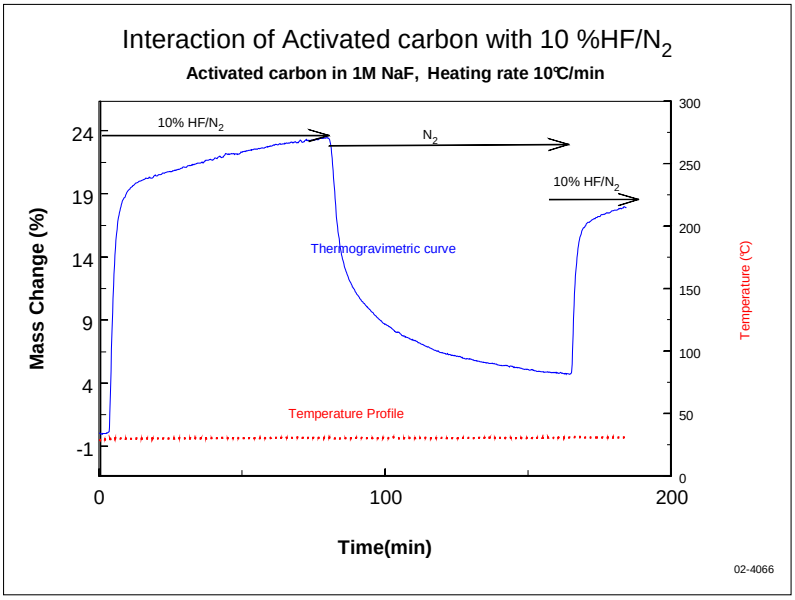


Figure 4.6: Thermogravimetric curve of Activated Carbon F200 soaked in 1M NaF after exposure to a 10% HF/N_2 mixture

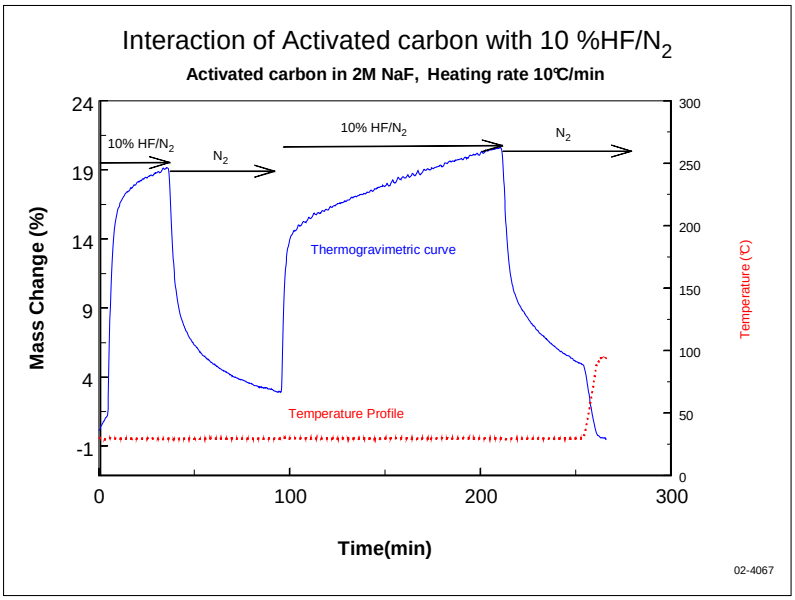


Figure 4.7: Thermogravimetric curve of Activated Carbon F200 soaked in 2M NaF after exposure to a 10% HF/N_2 mixture

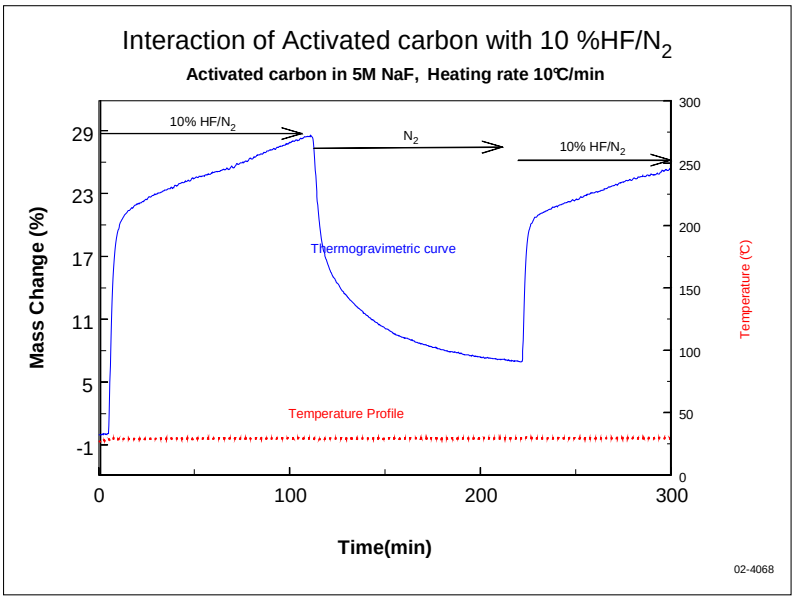


Figure 4.8: Thermogravimetric curve of Activated Carbon F200 soaked in 5M NaF after exposure to a 10% HF/N_2 mixture

The uptake of these samples is similar to the non-treated sample (see Figure 4.1) Hence, it is evident that NaF did not adsorb appreciably on the surface of the activated carbon. NaF was possibly removed in the wash step. This method of impregnation does not work as there has to be some sort of interaction between the NaF and the carbon for there to be impregnation. The fact that the NaF washed off so easily with water implies that it will be easily leached off with HF if this sample was used for HF adsorbtion.

4.3.3. Sodium hydroxide adsorption

Next it was decided to impregnate activated carbon F200 with NaOH. Considering the result obtained for NaF, it was decided to try a basic solution to impregnate the sample and assess the difference in uptake compared to the non-impregnated sample. Hence, a 1 M NaOH solution was used to impregnate activated carbon F200. The HF uptake results are as follows (Figure 4.9).

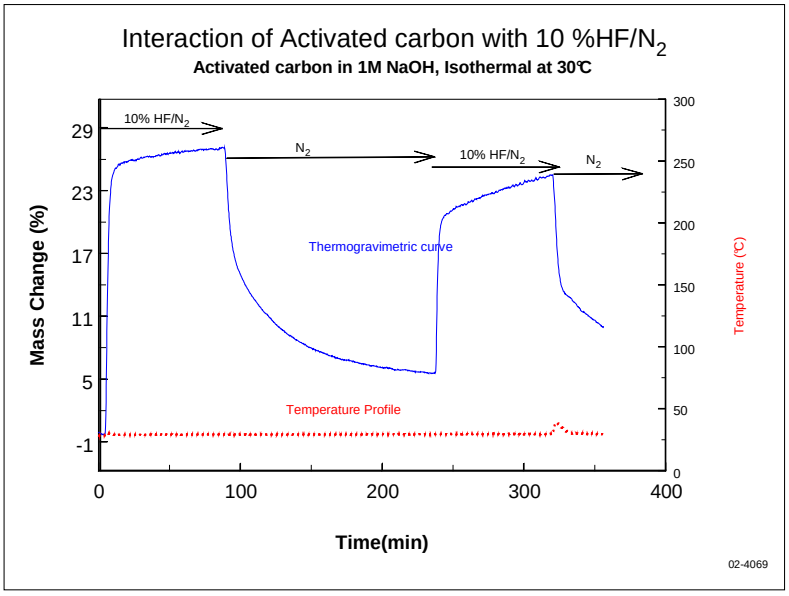


Figure 4.9: Thermogravimetric curve of Activated Carbon F200 soaked in 1M NaOH after exposure to a 10% HF/N_2 mixture

F200, when treated with NaOH, took up about 26% of HF initially (Figure 4.9). When this is compared to that obtained for untreated sample, Figure 4.1, this sample had an 18 mass% uptake initially. Comparing these results to the NaF treated samples *e.g.* Figure 4.8, it took up about 20 mass% initially which is similar to the untreated F200 sample, Figure 4.1. Hence it appears as if NaOH was able to modify the surface of the activated carbon, increasing the HF uptake capacity whereas NaF could not.

One of the reasons for the difference in uptake between the NaOH treated sample and the NaF treated sample is the reaction of NaOH with the surface oxygen groups. An example of the interaction, as indicated by Bansal, on the surface of activated carbon between NaOH and surface oxygen groups, is shown in Figure 4.10 [3].

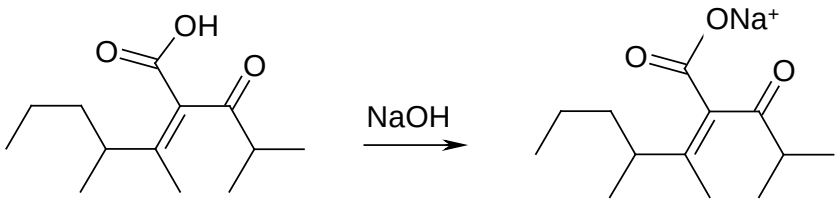


Figure 4.10: Reaction between surface oxygen groups on activated carbon and NaOH [3].

This will result is a higher percentage of Na^+ remaining on the surface after washing and hence a higher HF uptake, due to the interaction between HF and Na^+ ion. Interestingly, this high uptake was also seen with Chemviron carbon IVP, the commercial NaOH impregnated sample. This sample has a 34% HF capacity, (Figure 4.2).

4.3.4. Nitric acid oxidation

It was also decided to investigate the effect of increasing the surface-active groups on HF uptake. From the literature it is known that this is normally achieved by oxidising the activated carbon with HNO_3. The polarity of carbon surfaces can be modified by oxidation of the carbon surfaces. This oxidation is normally carried out by treating the surface with oxygen at high temperature or by an oxidising agent *e.g*. HNO_3. This results in a series of CO_x type structures being generated on the surface, including COO^-. [3]. Hence it was decided to treat Chemviron carbon Filtrasorb F200 with dilute HNO_3, concentrated HNO_3 and boiling concentrated HNO_3 respectively. Results obtained are shown in Figures 4.11 to 4.13.

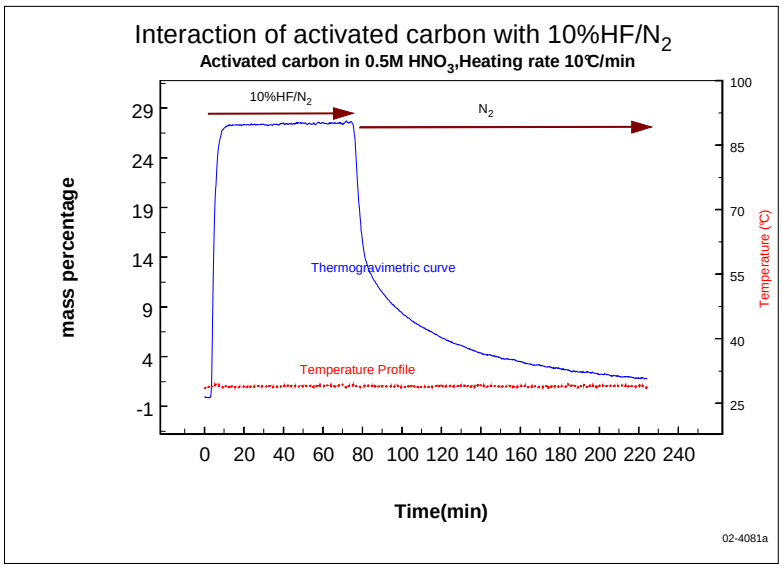


Figure 4.11: Thermogravimetric curve of Activated Carbon F200 treated in 0.5 M HNO_3 after exposure to a 10% HF/N_2 mixture

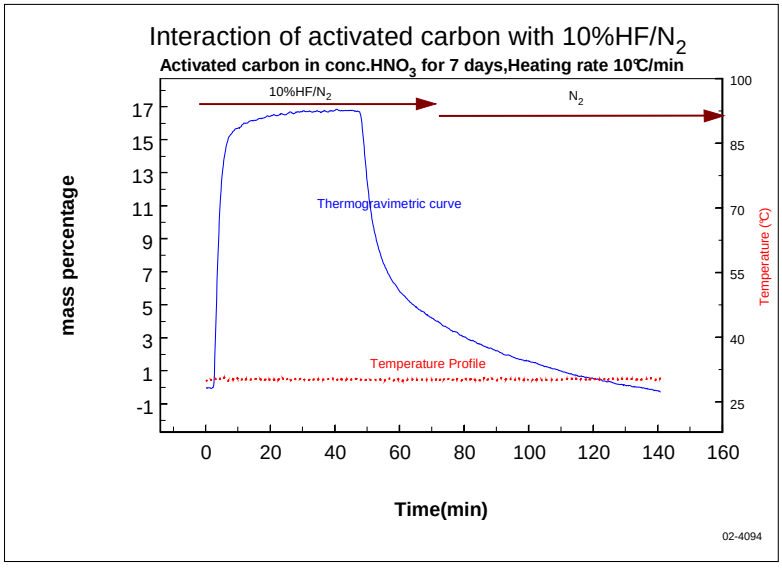


Figure 4.12: Thermogravimetric curve of Activated Carbon F200 treated in conc. HNO_3 after exposure to a 10% HF/N_2 mixture

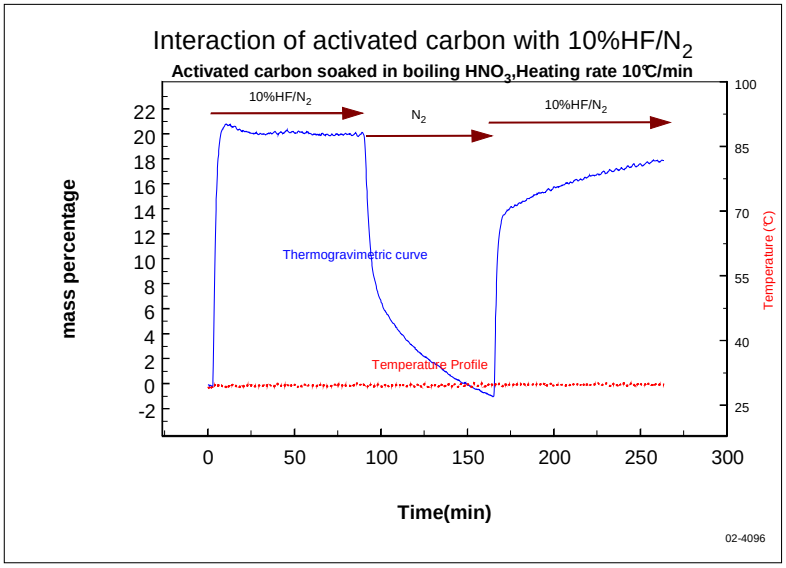


Figure 4.13: Thermogravimetric curve of Activated Carbon F200 treated in boiling HNO_3 after exposure to a 10% HF/N_2 mixture

HF uptake experiments reveal that the sample treated with 0.5 M HNO_3 has the highest uptake at about 27 mass%. It is known from the work done on ion exchange resins that acidic groups do have a capacity for HF (Chapter 3). Hence, if HNO_3 creates oxide (CO) or acid (COOH) groups on the surface, they will increase the HF adsorption capacity. Further, it can be noted that these results vary from the original sample (Figure 4.1) in that the HF uptake reaches a plateau, this could be an indication of pore blockage, either by HNO_3 or the newly created functionalities, or even pore destruction by oxidation of the lip carbons.

What is interesting however is that the capacity for HF is diminished when the activated carbon sample is treated with concentrated or boiling HNO_3. This could be due to the type of surface-active groups produced by the concentrated or hot HNO_3. They may not have a capacity for HF uptake. Hence dilute HNO_3 is more effective at increasing the HF capacity of activated carbons than concentrated acid [27].

4.3.5. Ion exchange

The acid (COOH) structures on the surface of activated carbons can be modified by ion exchange [3]. Hence it was decided to investigate the HF capacity of ion-exchanged carbon samples. Previously, the salts were adsorbed onto the surface. The activated carbon used was a 0.5 M HNO_3 oxidised Chemviron F200 sample. The carbon sample was ion exchanged with 1.0 M NaF, and then exposed to HF. The ion exchange reaction is as follows, (equation 4.2);

$$R\text{-}COOH + NaF \rightarrow R\text{-}COO^{-}Na^{+} + HF \qquad (4.2)$$

R = activated carbon

The HF uptake results are indicated in Figures 4.14

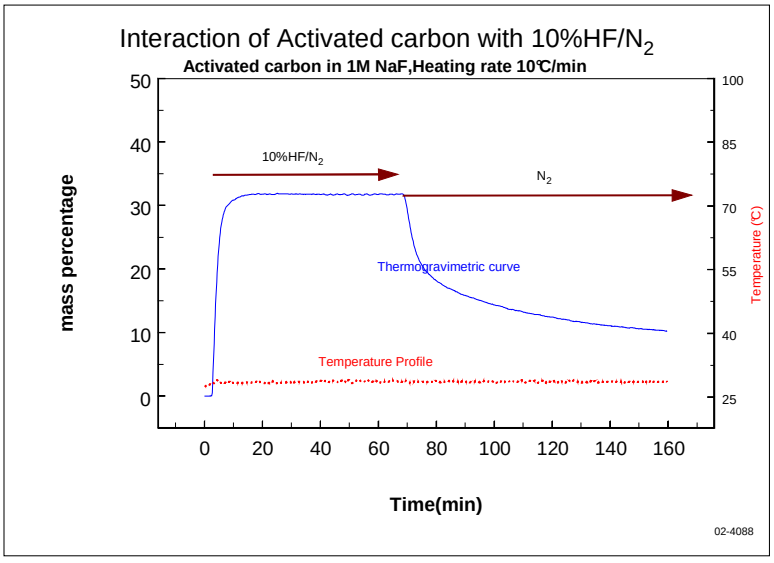


Figure 4.14: Thermogravimetric curve of Activated Carbon F200 soaked in 1M NaF after exposure to a 10% HF/N_2 mixture

Further, this oxidised sample was exposed to a base, NH_4OH; this would result in an acid-base type reaction, resulting in NH_4^+ groups on the surface (equation 4.3).

$$R\text{-}COOH + NH_4OH \rightarrow R\text{-}COO^-NH_4^+ + H_2O \qquad (4.3)$$

R = activated carbon

The HF uptake results are indicated in Figure 4.15.

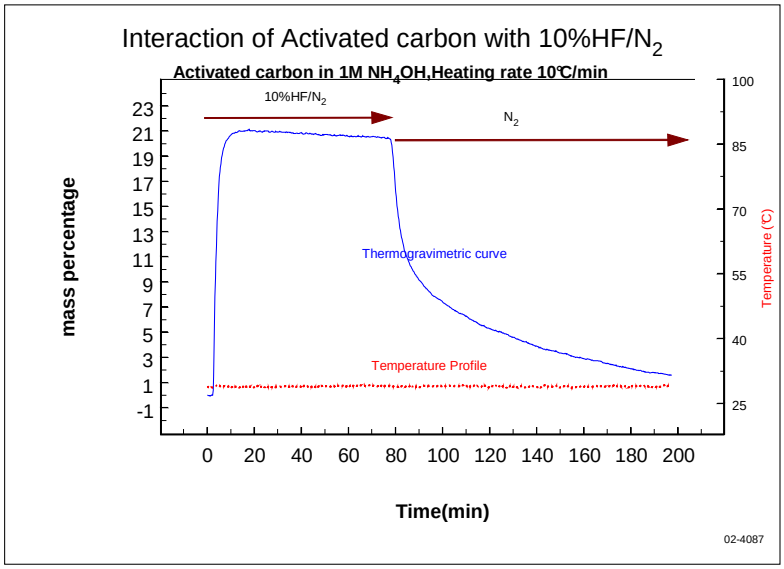


Figure 4.15: Thermogravimetric curve of Activated Carbon F200 soaked in 1M NH_4OH after exposure to a 10% HF/N_2 mixture

A summary of the results obtained is displayed in Table 4.1.

Table 4.1: Uptake of HF by oxidised ion exchanged carbons

Sample	**%HF uptake**	**Figure**
Oxid. AC in 1.0M NaF	32	4.14
Oxid. AC in 1.0M NH_4OH	21	4.15

The NaF containing sample reveals results that are interesting (Figure 4.14). When NaF is adsorbed from a 1.0M solution onto activated carbon, a 23% uptake of HF after being exposed to the gas mixture for about 80 minutes was observed. However, when the oxidised activated carbon was treated with 1.0 M NaF a 32% uptake in less than 10 minutes was obtained. This indicates that surface oxidation does increase the uptake of Na^+, (possibly as COONa) on the activated carbon samples. This as with the basic samples occurs by an ion exchange process and leaves Na^+ on the surface. From Chapter 3, when the protons on the weak acid ion exchange resins, with COOH functional groups, were ion exchanged with sodium, there was an increase in the HF capacity; hence this result is not surprising.

The NH_4OH containing sample should generate ammonium carboxylate functionality ($COONH_4$) on the carbon. It was hoped that the NH_x functionality would have a high capacity for HF as the weak base ion exchange resin, with the NHR_x functionalities, show promise as HF adsorbers. However based on the results seen here it appears as if these samples do not have a high capacity for HF as the uptake was only 21% (Figure 4.15).

Hence, it appears as if Chiang's [13] comment is valid that adsorbed ions can block the pores and reduce the HF capacity (Figure 4.15). However, the capacity is dependent on the interaction of the exchanged ion with the adsorbed gas and the sodium ion exchanged carbons shows promise for HF uptake.

The next experiment consisted of exposing Chemviron carbon IVP, the commercial NaOH impregnated sample to HF. This sample has a 34% HF capacity, (Figure 4.2), however as indicated in reaction 4.1, the HF uptake of Chemviron carbon IVP is due to a neutralization reaction between HF

and NaOH adsorbed on the surface. This will result in NaF formation on the surface of the activated carbon.

One of the initial aims of this project was to immobilize NaF on a substrate for HF adsorbtion. The NaF formed on the activated carbon IVP surface meets this aim however is only of commercial value as an adsorbent for HF from process streams, if it can be regenerated. Hence an experiment to test the above was conducted (Figure 4.16).

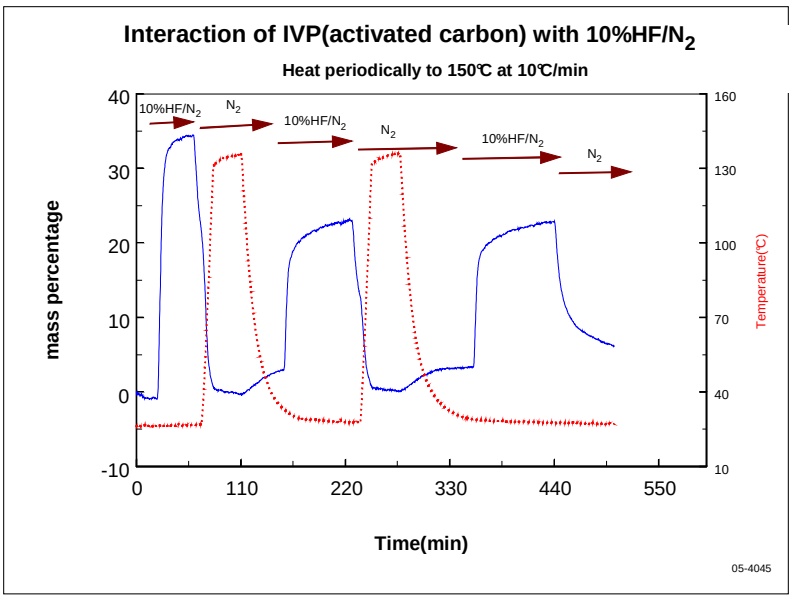


Figure 4.16: Thermogravimetric curve of Activated Carbon IVP after repeated exposure to a 10% HF/N_2 mixture

From Figure 4.16 above, the following is noted. When activated carbon IVP is exposed to HF it has a 34 mass% capacity, however upon repeated HF exposure this drops to about 25 mass%. This indicates that the impregnated NaOH has a higher capacity than the formed NaF. However once NaF is formed on the surface, heating to 150℃ can regenerate the activated carbon. This sample, upon re-exposure to HF has the same uptake kinetics and capacity as the previous exposure. Hence this is an

alternative method of immobilising NaF on an activated carbon surface and from the thermogravimetric trace above it can easily be regenerated.

Finally, as mentioned, one of the aims of this project was to immobilize NaF onto a substrate and use it as an adsorbent for HF. Further it must be possible to regenerate and reuse the adsorbent. From the results indicated in Figure 4.16 above it appears as if activated carbon IVP, after an initial exposure to HF meets these requirements.

4.4. Carbon molecular sieves

Two CMS samples were studied. The first was Superlco Carbosieve™ G, a commercial CMS used as a GC column packing for the separation of C1 – C3 hydrocarbons and the second was CMS 10304, a research sample from the BOC group, used for the separation of air. The data is shown in Figures 4.17 and 4.18.

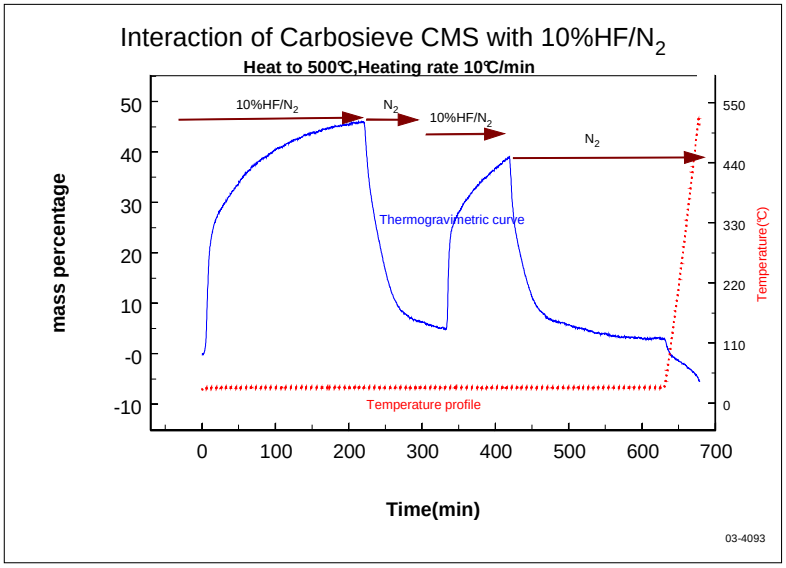


Figure 4.17: Thermogravimetric curve of Carbosieve CMS after exposure to a 10% HF/N_2 mixture

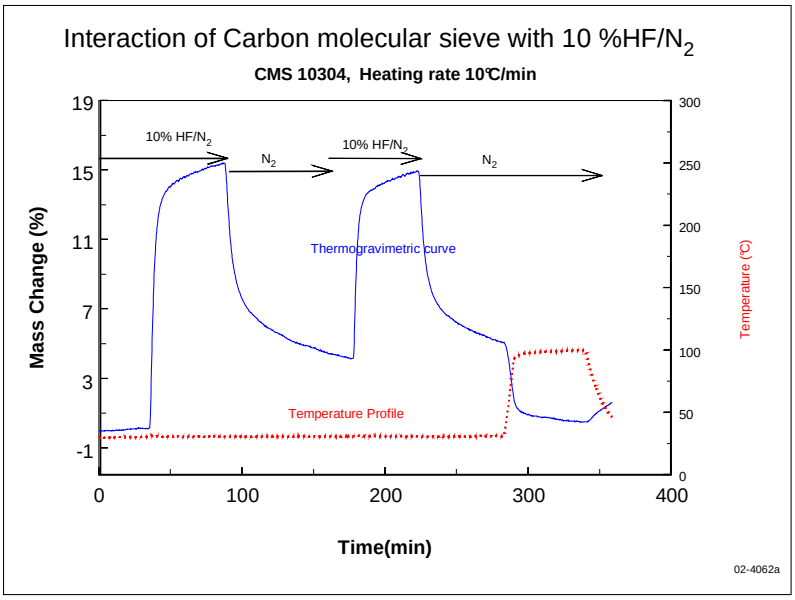


Figure 4.18: Thermogravimetric curve of CMS 10304 after exposure to a 10% HF/N_2 mixture

It can be noted that Carbosieve™ G can take up about 46 mass% of HF (Figure 4.17), whereas CMS 10304 has only a 15 mass% capacity for HF (Figure 4.18). As mentioned, Carbosieve™ G is used for the separation of C1 – C3 hydrocarbons and CMS 10304, used for the separation of air. C1 to C3 hydrocarbons are larger molecules (4.4 to 5.1 Å) than O_2 or N_2 (3.5 and 3.8 Å respectively) [28]. Hence it is expected that Carbosieve™ G will have large pores and hence a large capacity for HF (3.1 Å) than CMS 10304. The overall capacity may be larger than indicated as the smaller the pore opening, the slower the diffusion into the pores.

Further, both samples have almost no capacity for HF when the gas stream is changed to N_2 only. This also indicates that there is possibly no chemical interaction between the CMS and HF. These samples show no potential for HF adsorption.

4.5. Carbon nanotubes

There are three distinct structural types of CNT's, the stacked, the herringbone and the nanotubular. In the stacked form, the graphite platelets are perpendicular to the fibre axis; the platelets are at an angle in the herringbone form, while the nanotubular has graphite tubes parallel to the fibre axis. The stacked and herringbone forms are called nanofibers and the nanotubular are called nanotubes [22].

With regard to testing of carbon nanotubes, two samples were obtained from the University of Witwatersrand. The first was a herringbone form. It was synthesized with a Ni catalyst using $CaCO_3$ as a catalyst support. Purification involved dissolving the impurities in 30% HNO_3 [29]. The second was a multi-walled nanotube type that was synthesized with a Fe catalyst using $CaCO_3$ as a catalyst support and was also purified in HNO_3 [30]. These samples were tested for HF uptake and the results are shown in Figures 4.19 and 4.20.

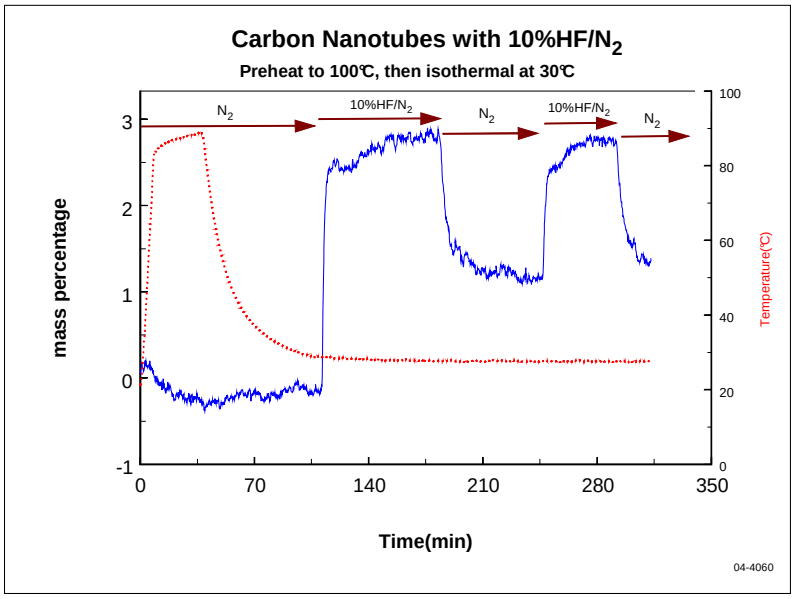


Figure 4.19: Thermogravimetric curve of a Herringbone carbon nanofibre after exposure to a 10% HF/N_2 mixture

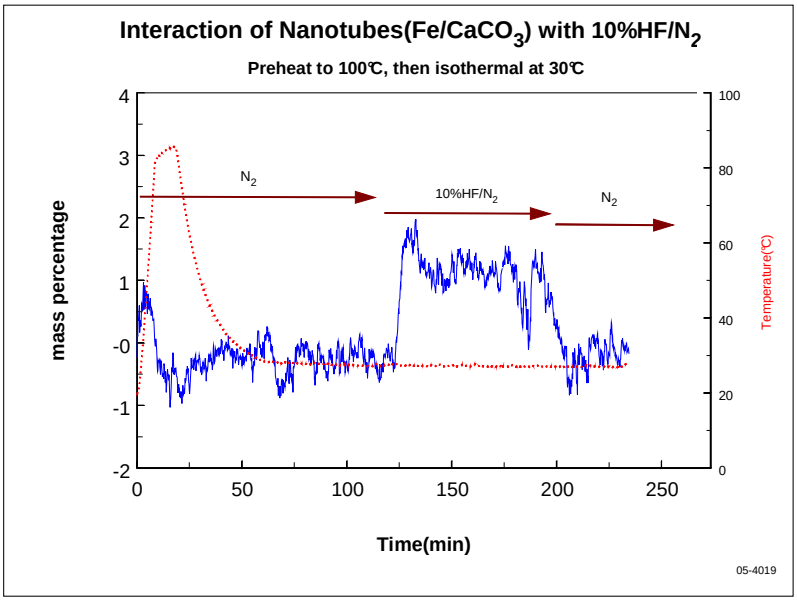


Figure 4.20: Thermogravimetric curve of a nanotubular carbon nanotube after exposure to a 10% HF/N_2 mixture

As noted from the above thermogravimetric trace (Figure 4.19), the nanofiber has a low capacity for HF. These CNT's are 95% pure [29]. Hence the above adsorption values are for relatively pure CNT. It is possible, as mentioned by Kleinhammes [26]; HF behaves like other inorganic gases and cannot be included into the interstitial sites at room temperature and atmospheric pressure. However, with the present set up of the thermogravimetric analyser, the only variable we have at our disposal is temperature. The nanotube also has a low capacity for HF, (Figure 4.20). The ends of this tube are not opened hence the uptake is on the surface only.

To increase the uptake of the nanofiber, the sample was heated during HF uptake. This was to expand the structure, creating larger spaces between the platelets for HF adsorption. The results are shown below.

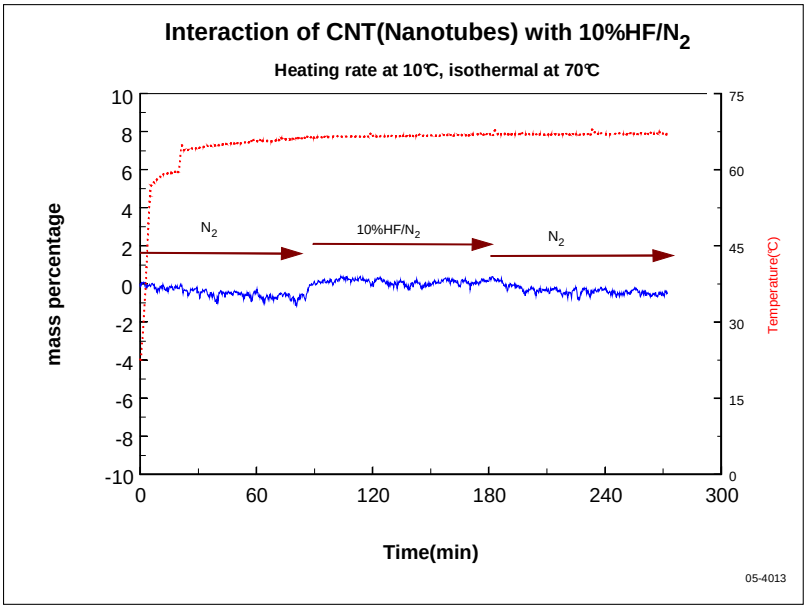


Figure 4.21: Thermogravimetric curve of a Herringbone carbon nanofibre after exposure to a 10% HF/N_2 mixture at 70℃

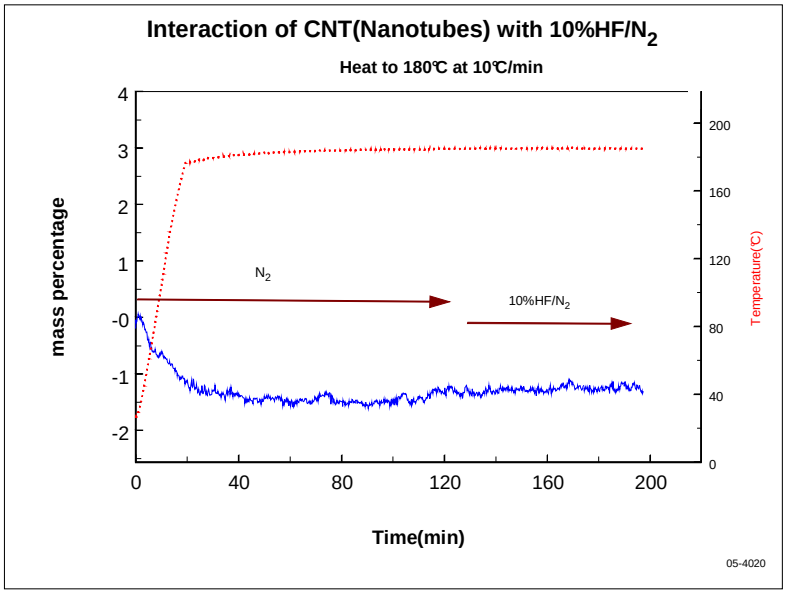


Figure 4.22: Thermogravimetric curve of a Herringbone carbon nanofibre after exposure to a 10% HF/N_2 mixture at 180℃

The results are shown in Figures 4.21 and 4.22. The HF uptake was assessed at 70℃ and 180℃. These samples have a lo wer capacity for HF at these temperatures than at 30℃ (Figure 4.19) . Hence heating the nanofibers does not increase the HF capacity.

With regard to the nanotube this sample was also heated to assess the effect on HF capacity (Figure 4.23).

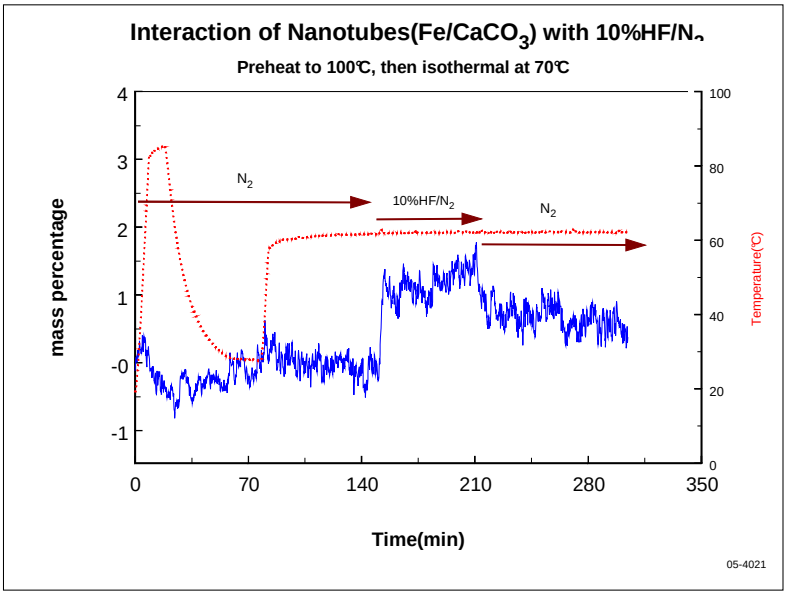


Figure 4.23: Thermogravimetric curve of a nanotubular carbon nanotube after exposure to a 10% HF/N_2 mixture at 70℃

Heating the nanotube decreased its capacity. This is expected as the adsorption takes place only on the surface in this sample.

4.6. Experimental

General experimental procedures

Materials

All commercial activated carbons were Chemviron samples, obtained from Vivendi Water Systems. The CMS samples were obtained from Aldrich Chemical Company Inc. (Superlco Carbosieve™ G 80/100 mesh) and the BOC group (CMS 10304) that was manufactured by Kuraray. The carbon nanotube samples were obtained from Mr. M C Bahome, University of the Witwatersrand. The anhydrous HF and F_2 was 99.9% pure and supplied by Pelchem. This was used to make a 10% vapour mixture with N_2 up to a maximum total pressure of six bar for HF and three bar for F_2. The 10% mixtures were used as the HF and F_2 feedstock for the thermogravimetric analyser experiments. All salts, acids and bases used were general laboratory grade chemicals obtained from either Merck or Sigma Aldrich. All chemicals were used without further purification.

Thermogravimetry

The process of HF adsorption was monitored with an in-house assembled thermobalance, by measuring the mass increase experienced by a sample over a period of time as a function of temperature. Thermal analysis was normally conducted in an inert atmosphere. Upon changing to a reactive atmosphere; the weighing mechanism of the thermobalance was protected using a N_2 blanket that flowed directly over the weighing mechanism. The flow rate of the inert/reactive gas used was 28.8 ml/min at STP with sample masses normally in the order of 3 to 5 mg. The gas streams could be changed from an inert gas (N_2) to a reactive gas and back again. The thermobalance has a resolution of 1 µg. Cooling of the circulating water,

used for the low temperature thermogravimetry work was achieved using a Neslab, Endocal Refrigerated Circulating bath.

Adsorption of NaF onto activated carbon surface

NaF solutions (100 ml) were made up as accurately as possible; 0.1 M, 0.5 M, 1 M, 2 M and 5 M. Chemviron F200 activated carbon (0.5 g) was soaked in 20 ml of each of the NaF solutions for 20 hours. The supernatant liquid was discarded the next morning and the samples were then washed with 20 ml distilled water and left to dry in air for 24 hours. The activated carbon samples were then used in the HF uptake experiments.

Adsorption of NaOH onto activated carbon surface

A NaOH solution (100 ml, 1 M) was prepared. Activated carbon Chemviron F200 (0.5g) was soaked in 20 ml of this solution overnight. The supernatant liquid was discarded the next morning and the samples were then washed with 20 ml distilled water and left to air dry. The activated carbon samples were then used in HF uptake experiments.

HNO_3 oxidation

a) Activated carbon Chemviron F200 (0.5 g) was stirred in 50 ml of concentrated HNO_3 for two hours. The sample was then removed from the HNO_3, rinsed once with 20 ml distilled water and air-dried.

b) Activated carbon Chemviron F200 (0.5 g) was stirred in 50 ml of concentrated, boiling HNO_3 for two hours. The sample was then removed from the HNO_3, rinsed once with 20 ml distilled water and air-dried.

c) Activated carbon Chemviron F200 (0.5 g) was stirred in 50 ml of 0.5M HNO_3 then left to stand for 24 hours. The sample was then removed from the HNO_3, washed once with 20 ml distilled water and air-dried.

Ion exchange

The following solutions (100 ml supplies) were made up as accurately as possible, 1.0 M NaF and 1.0 M NH_4OH. Activated carbon Chemviron F200 (0.5 g) was soaked in 20 ml of each of the solutions overnight, with occasional shaking. The supernatant liquid was discarded the next morning and the samples were then washed with 20 ml distilled water and left to air dry. The activated carbon samples were then used in HF uptake experiments.

4.7 References

1 Patrick, J. W., Porosity in Carbons, Ed., Edward Arnold, (1995)

2 The use of powder activated carbon in the chemical, pharmaceutical and agro-food industries, technical report, Ceca SA, France (1995)

3 Bansal, R.C., Donnet, J-B. and Stoeckli, F., Active Carbon, Marcel Dekker Inc, (1998)

4 McCallum C. L., *et al, Langmuir*, 533, **15**, (1999).

5 Brennan, J. K., Bandosz, T. J., Thomson, K. T. and Gubbins, K. E., *Colloids and Surfaces A, Physicochemical and Engineering Aspects*, 539, **187-188**, (2001).

6 Yang, R. T., *Adsorbents, Fundamentals and Applications*, Wiley-Interscience, (2003).

7 Antal Jr., M. J and Grønli, M., Ind. *Eng. Chem. Res*., 1619, **42**, (2003).

8 Strelko, V. Jr., Malik, D. J. and Streat, M., *Carbon*, 95, **40**,(2002).

9 Beck, N. V., Meech, S. E., Norman, P. R. and Pears, L.A., *Carbon*, 531, **40**, (2002).

10 Li, L., Quinlivan, A., Knappe D. R. U., *Carbon* 2085, **40**, (2002).

11 Gmelin Handbook of Inorganic Chemistry, 8th Ed., Koschel D, (editor), Springer Verslag Berlin-Heidelberg, (1982).

12 Lee, M-T., Wang Z-Q. and Chang J-R., *Ind. Eng. Chem. Res*. 6166, **42**, (2003).

13 Chiang, H-L., Tsai, J-H., Chang, G-M. and Hsu, Y-C., *Adsorption*, 325, **8**, (2002).

14 Jüntgen, H., Knoblauch, K. and Harder, K., *Fuel*, 817, **60**, (1981)

15 Foley, H. C., *Microporous Materials*, 407, **4**, (1995).

16 Foley, H. C. and Mariwala, R. K., University of Delaware; E. I. Du Pont de Nemours Co., Both of Wilmington, Del., US Patent 5 261 948, (1993).

17 Hong, A., Mariwala, R. K., Kane, M. S. and Foley, H. C., *Ind. Eng. Chem. Res*., 992, **34**, (1995).

18 Chang, C-H., Allied-Signal Inc., Morris County, N. J., Patent US 4 902 312, (1990).

19 Chang, C-H. and Gualdron M. A., Allied-Signal Inc., Morris County, N. J., Patent US 5 597 545, (1997).

20 Harris, P., http://www.personal.rdg.ac.uk/~scsharip/tubes.htm (2004).

21 Satishkumar, B. C., Govindaraj, A., Mofokeng, J., Subbanna, G. N. and Rao, C. N. R., *J. Phys. B: At. Mol. Opt. Phys.,* 4925, **29**, (1996).

22 Teo, K. B. K., Singh, C., Chhowalla, M. and Milne, W. I., Encyclopedia of Nanoscience and Nanotechnology, Vol X, Pg 1-22, H. S. Nalwa (Ed), American Scientific Publishers, (2003).

23 Daenen, M., de Fouw, R. D., Hamers, B., Janssen, P. G. A., Schouteden, K. and Veld, M. A. J., http://students.chem.tue.nl/ifp03/Wonderous%20World%20of%20Carbon%20Nanotubes_Final.pdf (2003)

24 Pederson, M. R. and Broughton, J. Q., *Phys. Rev. Lett*., 2689, **69**, (1992).

25 Sinnott, S. B. and Andrews, R., *Critical Reviews in Solid State and Material Sciences*, 145, **26(3)**, (2001).

26 Kleinhammes, A., Mao, S-H., Yang, X-J., Tang, X-P., Shimoda, H., Lu, J. P., Zhou, O. and Wu, Y., *Physical Reviews B*, 75418, **68**, (2003).

27 Kim, M. II., Yun, C. H., Kim, Y. J., Park, C. R. and Inagaki M., *Carbon*, 2003, **40**, (2002).

28 Reid, R.C., Prausnitz, J. M. and Poling, B. E., The Properties of Gasses and Liquids, 4th ed. (1987).

29 Couteau, E., Hernadi, K., Seo, J. W., Thiên-Nga, L., Mikó, Cs., Gaál R. and Forró, L., *Chemical Physics Letters*, 9, **378**, (2003).

30 Bohame, M. C., Jewell, L. L., Hildebrandt, D., Glasser, D. and Coville N. J., *to be published.*

Chapter 5

Conclusion

5.1. Introduction

The aim of this study was to evaluate different materials as potential sorbents for HF. The study described HF uptake by inorganic compounds, polymers, ion exchange resins, carbon based materials and aluminophosphates. The overall aim was the removal of HF from both inorganic *e.g*. F_2 and organic environments *e.g*. fluorocarbon environments. Due to the highly reactive nature of F_2, the inorganic compounds and aluminophosphates were targeted for HF removal from F_2, and the ion exchange resins and carbon based materials for the removal of HF from non-F_2 containing environments.

This chapter contains an overall evaluation of the study conducted and focuses on the suitability of the various materials investigated as possible adsorbers for HF. A checklist for the suitability of adsorbers was discussed in Chapter 1. This checklist is a measure used to evaluate the different adsorbers. Hence the adsorbers assessed in this study *e.g*. the ion exchange resins, will now be measured against this checklist. Not all points mentioned in the checklist were covered in this study. The checklist is repeated here for convenience.

5.2. Checklist for suitability of adsorbers

When assessing the suitability of an adsorber or comparing two adsorbers for gas effluent removal, various factors need to be considered.

1) Selectivity

d) Does the adsorber display the desired selectivity?

e) What is the effect of the product matrix on the adsorber?
f) Does the adsorber introduce impurities into the product stream and if so are they acceptable in the product stream?

2) Effectiveness

c) Is it possible to remove the effluent gas down to the desired concentration?
d) Does the adsorber have a highly accessible surface area and/or a high density of active sites?

3) Kinetic and thermodynamic considerations

c) Is the adsorption process fast?
d) Ensure that $|\Delta H_{rxn}|$ is not large.

4) Physical characteristics

c) Is the adsorber present in a form that allows efficient adsorption *e.g*. pellets, sieves *etc*. or does it lend itself easily to the formation of the above that can result in the formation of a high surface area material?
d) Does the adsorber maintain its physical integrity? It should not sinter, form dust particles or undergo phase changes during use or regeneration?

5) Financial considerations

b) Is the total financial outlay to synthesize the new adsorber justified?

6) General

Apart from the above, other factors that need to be considered are;

d) Can the adsorber be physically regenerated *e.g*. with elevated temperature or pressure?
e) Are the products environmentally acceptable?
f) Are they reusable?

5.3. Sodium fluoride

In terms of the current Necsa technology, NaF pellets are used for the removal of HF from both organic and inorganic environments. However, as discussed in Chapter 1 there are a number of problems associated with the use of NaF. Firstly, NaF adsorbs 4 to 5 HF molecules per NaF molecule resulting in NaF dissolving in the HF. To prevent this the adsorbtion column has to be kept at an elevated temperature resulting in a higher equilibrium vapour pressure of HF. The second problem encountered occurs when the column needs to be regenerated, as HF desorbed from close to the warmer wall section it tends to migrate to the cooler core and adsorb there. This results in polyacid formation and core sintering.

Evaluation of the use of NaF using the checklist provides the following assessment. Firstly, in terms of selectivity, this adsorbent displays the desired selectivity and introduces no impurities into the product stream. With regard to effectiveness, it reduces the HF concentration to 300 ppm under the existing operating conditions. However, a lower concentration is desired.

Further, based on laboratory trials, the uptake of HF by NaF is fast. The ΔH_{rxn} is 57.6 kJ/mol. In terms of physical characteristics, the NaF is easily compressed into a pellet into which porosity is introduced. However, in

terms of maintaining its physical integrity, it easily dissolves in HF. However, NaF pellets can be regenerated and reused.

In terms of financial considerations, if NaF is to be replaced, the costs of the alternative will have to be measured against the cost of using NaF.

5.4. Inorganic salts

Chapter 2 describes the uptake of HF by inorganic salts. This study included evaluation of CaF_2, $Ca(OH)_2$, $CaCl_2$, $CaSO_4$, and $NaMgF_2$. These salts showed varying potential as suitable adsorbers. Firstly, Colvin indicated that CaF_2 is an excellent adsorber for HF [1]. Since this salt is not very soluble in water, it was hoped that this salt would not deliquesce like NaF in the presence of excess HF. CaF_2 also is the starting material for the production of HF, and if CaF_2 could not be regenerated, it could be recycled into the HF production process.

CaF_2 displayed the necessary selectivity and did not introduce impurities into the gas stream. However, in terms of effectiveness it has a capacity of only a few percent making it inefficient as an adsorber. Even attempts to increase the surface area by recrystallisation did not assist in increasing the capacity. Hence, although CaF_2 will, according to most points on the checklist, be an acceptable adsorber for HF, the capacity is very low.

With regard to the other salts, $Ca(OH)_2$ and $CaSO_4$ showed a high capacity for HF uptake under the experimental conditions indicated in Chapter 2. $CaCl_2$ and $Ca(OH)_2$ on the other hand reacted with HF making them unacceptable for HF removal. $Ca(OH)_2$ and $CaSO_4$, if used to remove HF from F_2, will react with F_2 and introduce their anions as an impurity into the gas stream,. Hence although they display a high capacity for HF, they will not be very effective in a F_2 stream as their physical integrity would be compromised.

$CaSO_4$, in a non-F_2 environment, could be used as an alternative to NaF. However, indications are that regeneration with heat results in a decrease in uptake capacity, possibly due to decomposition, making its use less likely.

In terms of selectivity, these salts should have a preference for HF rather than organics. If inorganic materials are present, they will have to be assessed as $CaSO_4$ is a desiccant and will remove any water present. $Ca(OH)_2$, on the other hand, will react with HF and release H_2O. Hence overall, these salts show potential for use in environments where NaF can react with one of the components in a gas mixture.

$NaMgF_2$ displayed no selectivity towards HF. Hence it can be removed from the list of possible adsorbents.

5.5. Aluminophosphates

The aluminophosphate discussed in Chapter 2 has a high capacity for HF (120 mass%). However, it appears to decompose, thereafter losing capacity on re-adsorption. As mentioned in Chapter 2, one of the possible breakdown products is VF_5. The AlPO could be used for HF removal from transition metal fluorides on condition that the transition metal used in the AlPO structure does not introduce unacceptable impurities into the reactant stream. In this regard, the AlPO structure does display the desired selectivity, although HF destroys the structure and releases some volatiles into the product stream.

5.6. Resins

In Chapter 3, various resins were described. These included Nafion® Superacid Resin, sodium polyacrylate and various ion exchange resins, including the non-functional resins.

Our investigations on Nafion®, revealed that this material displayed a low capacity for HF. A dry sample was used, as regenerated Nafion® contains water which will be released as an impurity. Theoretically, if used in an organic environment, Nafion® should display the desired selectivity and not introduce impurities into the product stream. As indicated in Chapter 3, this sample was able to reduce the HF concentration to 25% of its original value when exposed to a HF-HFA 134a mixture. However this may not make Nafion® as effective an adsorbent as desired as it does not remove the effluent gas down to the desired concentration. Another problem is the financial consideration: Nafion® costs $2660 (R15600) per kg [2] which is too expensive for some industrial applications. (Based on an exchange rate of $1 = R6)

Sodium polyacrylate has a high capacity at about 80 mass% for HF but dissolves in HF. This would still be acceptable if it were possible to separate this HF-sodium polyacrylate mixture from the organic fraction. Hence depending on the application, this adsorber would meet some of the criteria on the checklist. For example, it would display the desired selectivity; removal of HF down to desired concentrations, and excellent kinetics. Problem areas would be that sodium polyacrylate may not lend itself easily to the formation of pellets or sieves and as mentioned above it dissolves in HF.

With reference to the ion exchange resins, they all display a capacity for HF and depending on the matrix, different resins can be used for HF removal. This arises since resins have different functional groups and a

resin can be selected that does not react with a component in the gas stream. For enhanced capacity, the cation on the resin can be changed to Na^+. Further the resin selected could have a backbone that is acrylic, styrenic or perfluorinated in nature. Hence the matrix and product stream has to be considered when assessing the suitability of a resin.

The resin that showed the most promise was Amberlite IRA 67, both in terms of capacity and stability in a HF environment. If the resin is measured against the checklist, the results are as follows.

Selectivity: This resin selectively adsorbs HF from the organic environments tested. Although there is some adsorption of organics the preference is for HF. One impurity that the resin can tolerate in the gas stream is H_2O as it is in the free base form.

Effectiveness: At 114 mass% it has a very high capacity hence a highly accessible surface area. The exchange capacity is 5.6 meq/g. Further, from the tests conducted, Amberlite IRA 67 removed HF from organic vapour streams to below detection limits.

Kinetic considerations; The uptake process has fast kinetics taking up 100% of its own mass in 20 minutes from a 10% HF/N_2 stream flowing at 28.8 ml/min (STP).

Physical characteristics: The resin is in the form of a bead that allows easy handling, although swelling would be expected with HF uptake. This can be factored into an adsorption column design.

Financial considerations: This resin is sold for approximately USD 183 (R 1100) per 20 kg and this outlay has to be justified in terms of the final product price, the same quantity of Nafion® will cost $ 53 200 (R 312 000).

In terms of regeneration this resin can be regenerated to 50% capacity using a nitrogen stream with mild heating or by washing using a mild basic solution. Further, based on thermogravimetric results, this resin can withstand multiple exposures to HF. In terms of environmental considerations, the resin is hydrocarbon based and hence can be eliminated via normal hydrocarbon disposal routes on condition the adsorbed HF is first removed.

Finally with reference to the non-functional resins, these can be used in applications where there is a possibility of an interaction between the organic phase and the functional groups on the resins.

5.7. Carbon structures

The carbon structures discussed in Chapter 4 (*e.g.*, activated carbons, carbon molecular sieves and carbon nanotubes) could find application in the removal of organics from HF. However, since some carbon structures also have a HF capacity, they could be used for the separation of HF from larger organic molecules by activated surface adsorption or pore size exclusion. Further, the carbons could possibly be used to separate HF from certain inorganic compounds. In terms of the checklist, this HF adsorber will have to be assessed in terms of applications and in comparison to other adsorbers.

The selectivity of the carbon material will have to be assessed as the organic fractions may adsorb on the carbon modifying the carbon structure. One of the biggest problems associated with a carbon adsorber is the release of elemental carbon or CF_4 into the product stream. Activated carbon IVP, a NaOH impregnated carbon which shows promise for HF removal will also release H_2O as an impurity, however once this is removed will take HF without releasing H_2O.

In terms of effectiveness, activated carbons may be used for bulk HF removal whereas the other structures, due to cost, will have more specialized applications.

With regards to kinetics, activated carbons take up gases by two mechanisms. These are surface adsorption and pore filling. The uptake kinetics will be very dependent on the surface characteristics and pore size of the carbon structure.

In terms of physical characteristics, activated carbons can be manufactured with high surface areas. Further the activated carbon can be compressed into a more easily usable form *e.g*. pellets. Carbon molecular sieves and nanotubes also have pore sizes and surface areas based on their synthetic route hence can be separately selected for a particular application.

Finally, the aim of this study was to assess alternative adsorbents for the removal of HF from F_2. While the study has not produced a new all-purpose adsorbent it will have laid to rest some of the conflict in the open literature on this subject. Further, with regard to the removal of HF from other media, *e.g*. organics, various possibilities were suggested by this study, some showing definite promise as alternatives to the NaF used commercially.

5.8 References

1 Colvin W. L., AEC (US) report number K-1117, (1953).

2 The web site of Ion Power Inc., suppliers of Nafion® Superacid Resin, http://www.ion-power.com/

Appendix 1

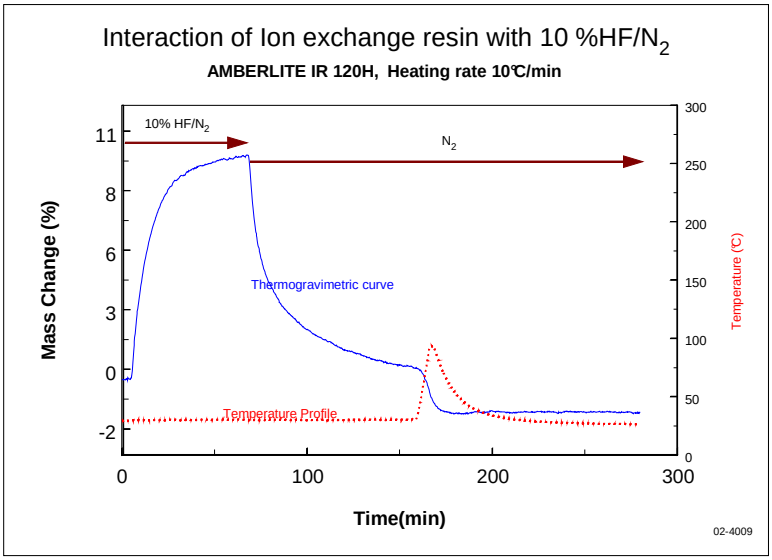


Figure 3.13: Thermogravimetric curve of Amberlite IR 120H after exposure to a 10% HF/N_2 mixture

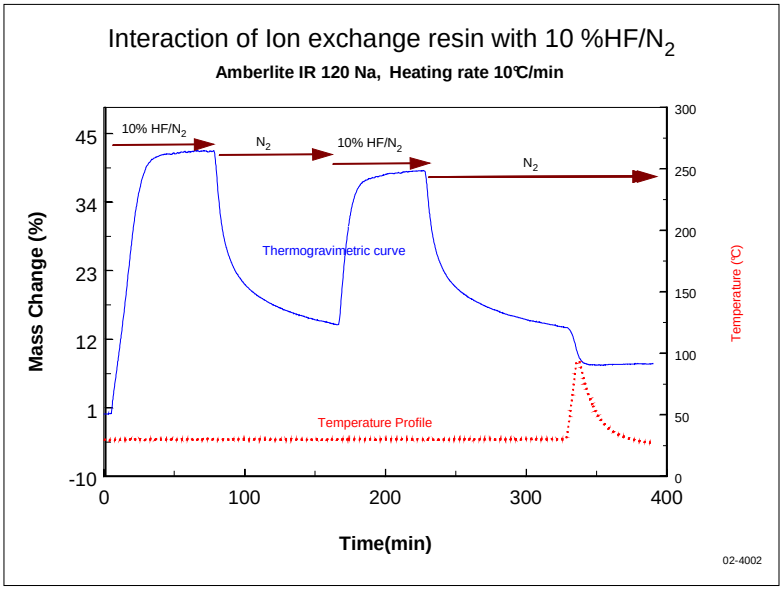


Figure 3.14: Thermogravimetric curve of Amberlite IR 120Na after exposure to a 10% HF/N_2 mixture

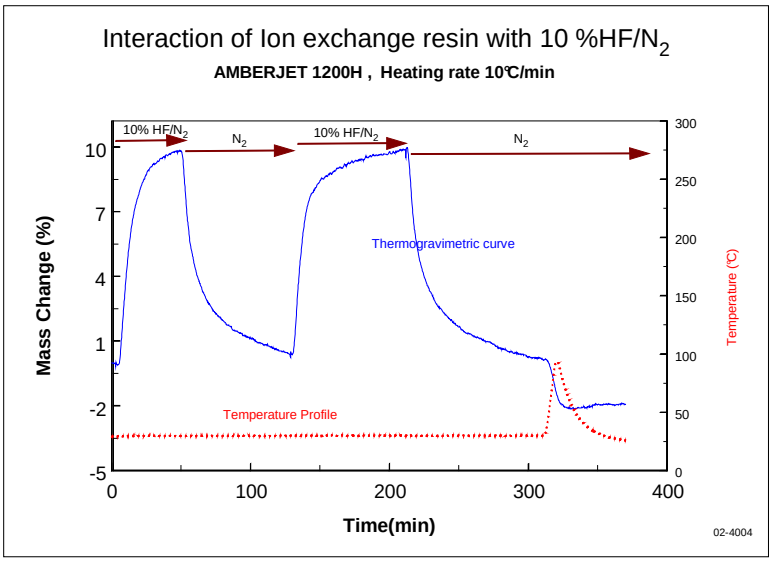


Figure 3.15: Thermogravimetric curve of Amberjet 1200H after exposure to a 10% HF/N_2 mixture

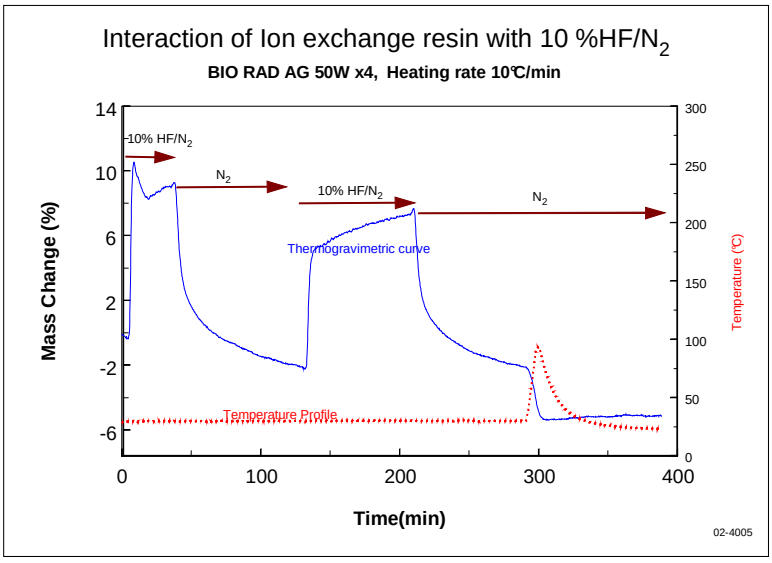


Figure 3.16: Thermogravimetric curve of Bio-Rad AG 50Wx4 after exposure to a 10% HF/N2 mixture

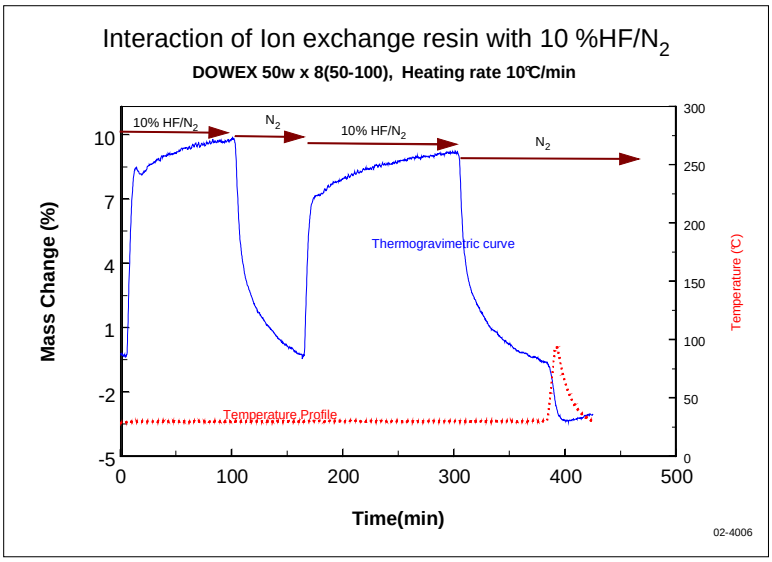


Figure 3.17: Thermogravimetric curve of Dowex 50W x 8 after exposure to a 10% HF/N_2 mixture

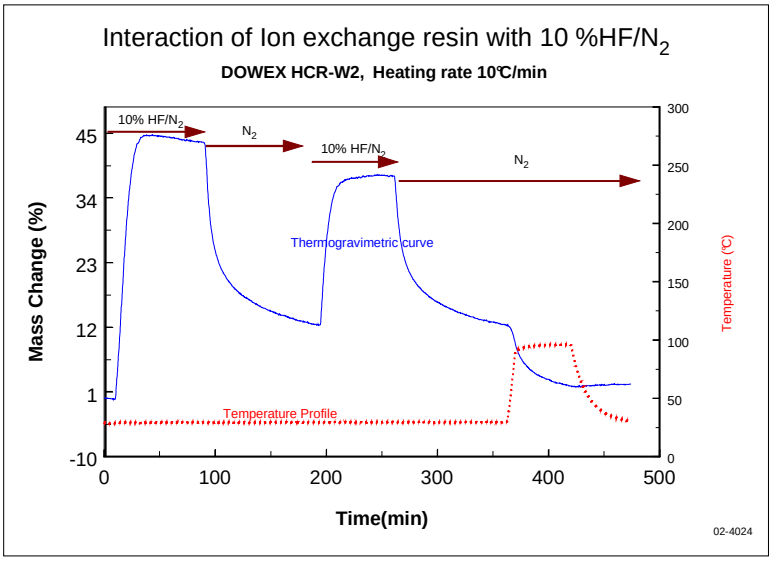


Figure 3.18: Thermogravimetric curve of Dowex HCR-W2 after exposure to a 10% HF/N_2 mixture

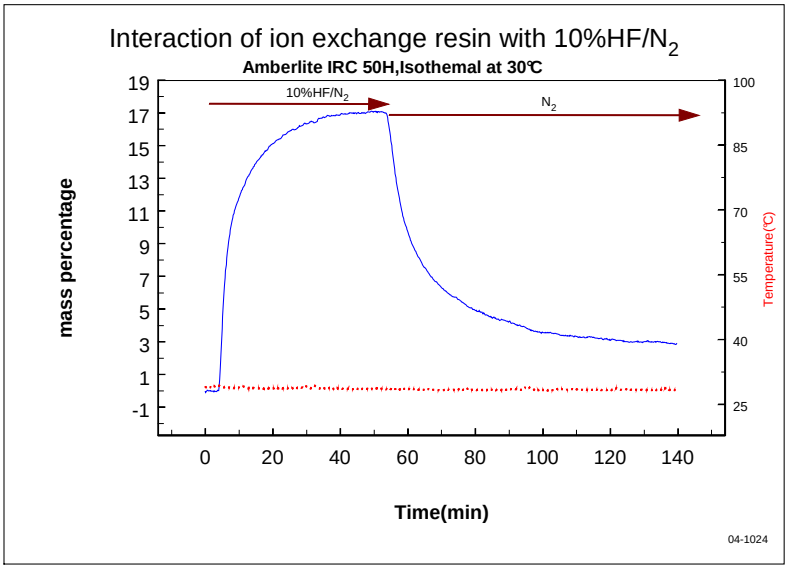


Figure 3.19: Thermogravimetric curve of Amberlite IRC 50H after exposure to a 10% HF/N_2 mixture

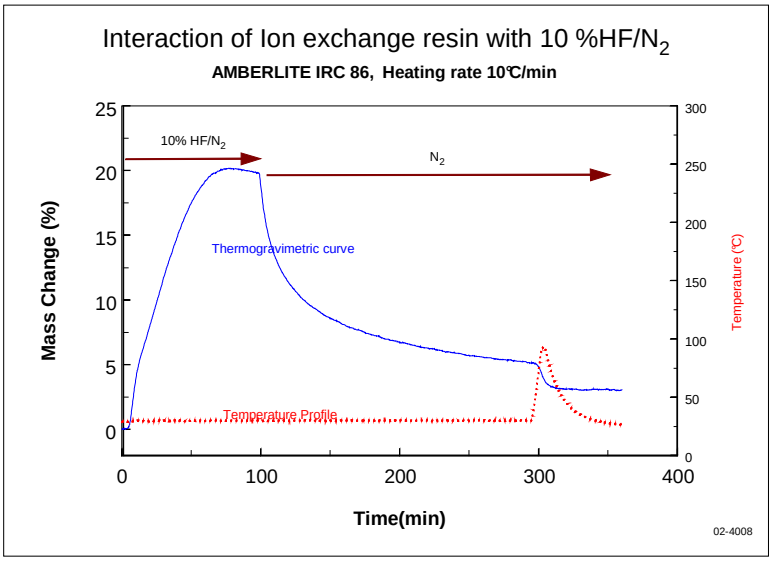


Figure 3.20: Thermogravimetric curve of Amberlite IRC 86 after exposure to a 10% HF/N_2 mixture

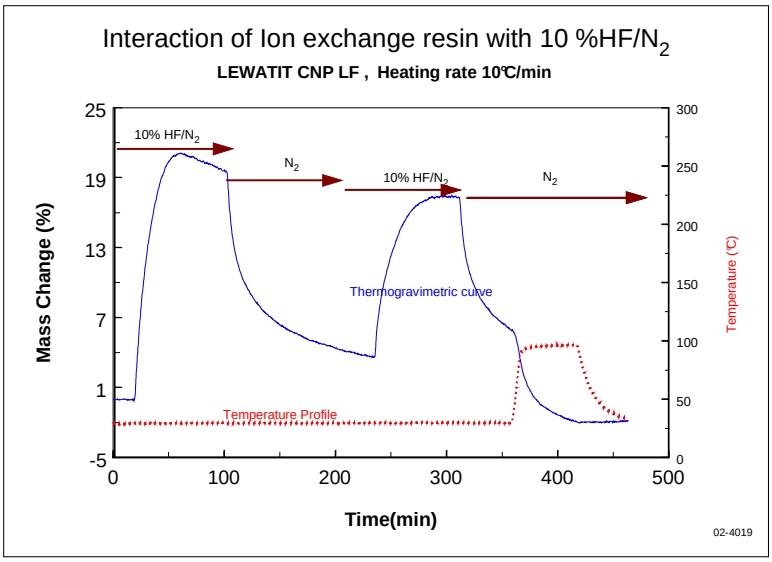


Figure 3.21: Thermogravimetric curve of Lewatit CNP LF after exposure to a 10% HF/N_2 mixture

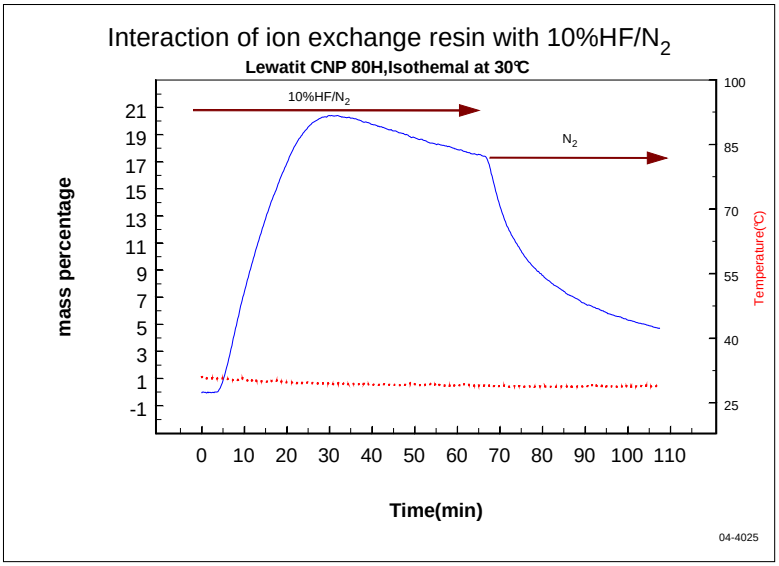


Figure 3.22: Thermogravimetric curve of Lewatit CNP 80 after exposure to a 10% HF/N_2 mixture

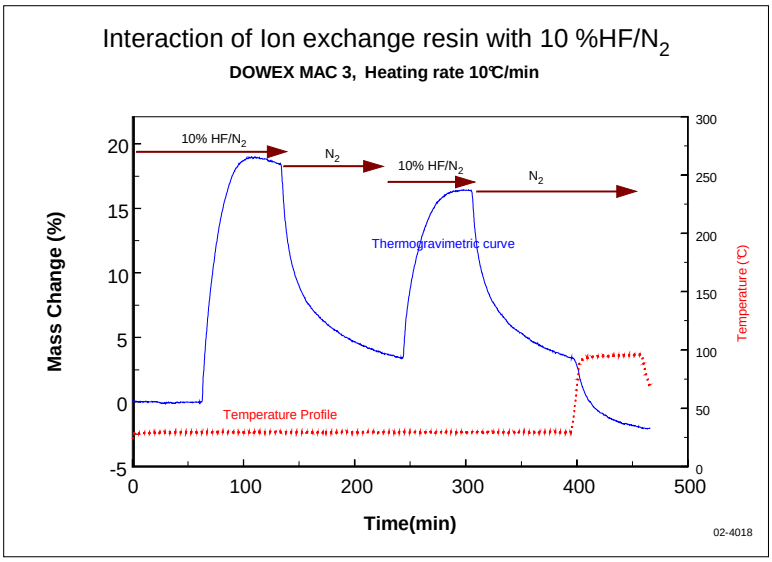


Figure 3.23: Thermogravimetric curve of Dowex MAC 3 after exposure to a 10% HF/N_2 mixture

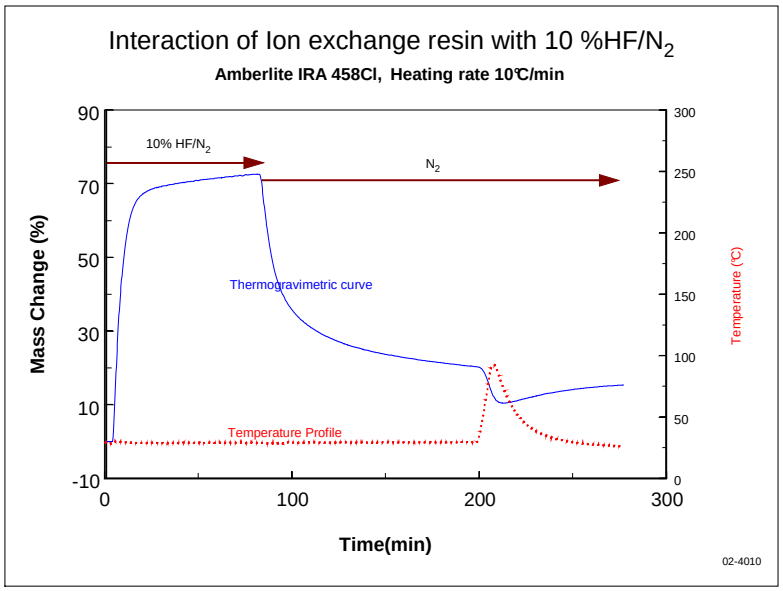


Figure 3.24: Thermogravimetric curve of Amberlite IRA 458Cl after exposure to a 10% HF/N_2 mixture

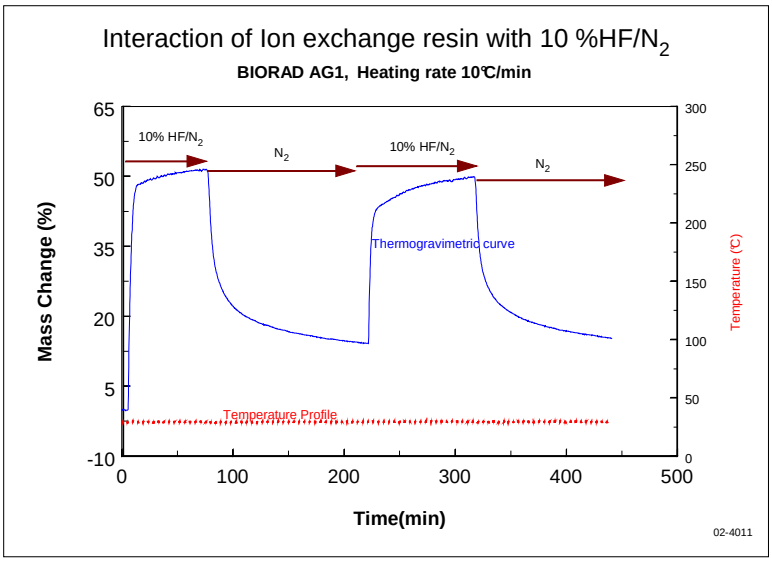


Figure 3.25: Thermogravimetric curve of Bio-Rad AG 1 after exposure to a 10% HF/N_2 mixture

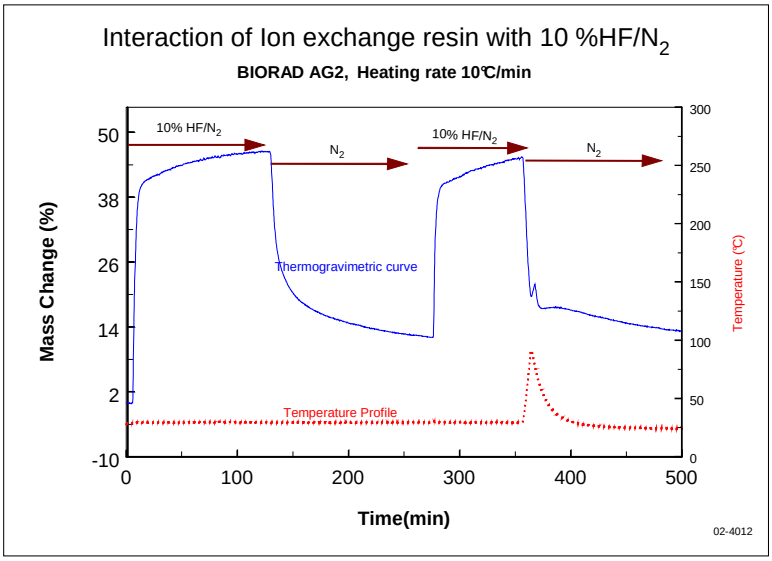


Figure 3.26: Thermogravimetric curve of Bio-Rad AG 2 after exposure to a 10% HF/N_2 mixture

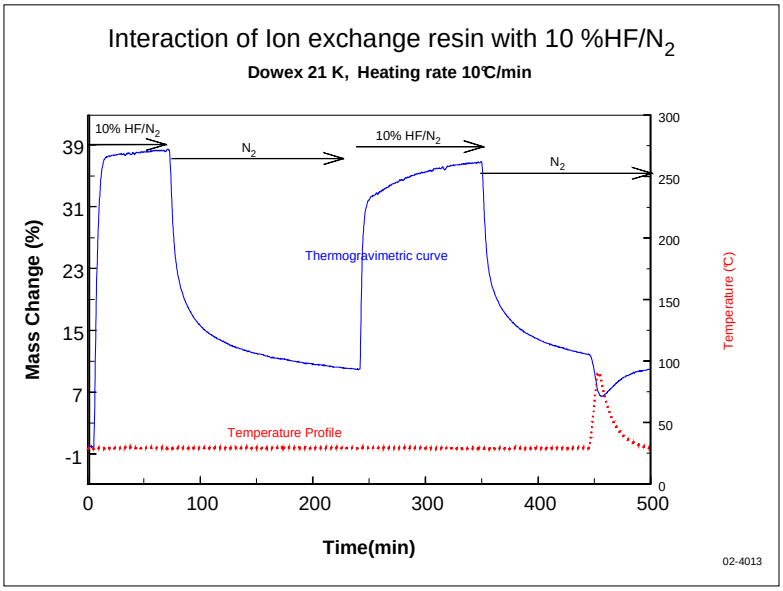


Figure 3.27: Thermogravimetric curve of Dowex 21K after exposure to a 10% HF/N_2 mixture

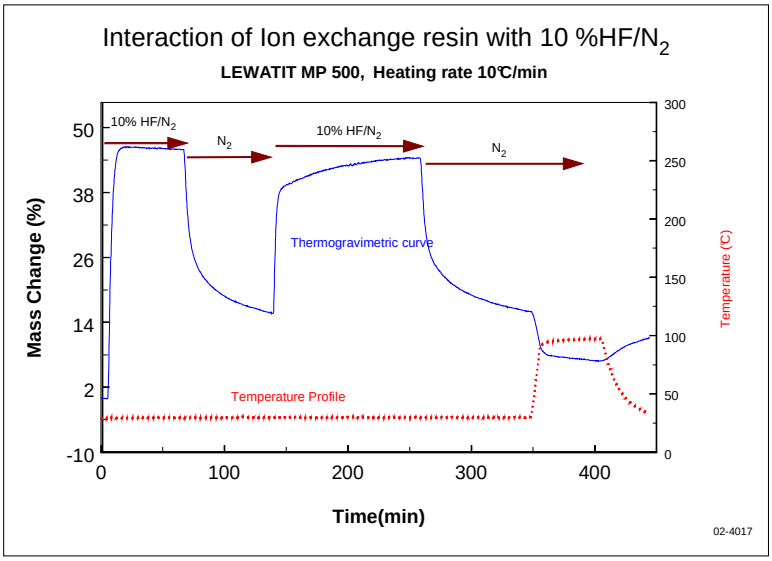


Figure 3.28: Thermogravimetric curve of Lewatit MP 500 after exposure to a 10% HF/N_2 mixture

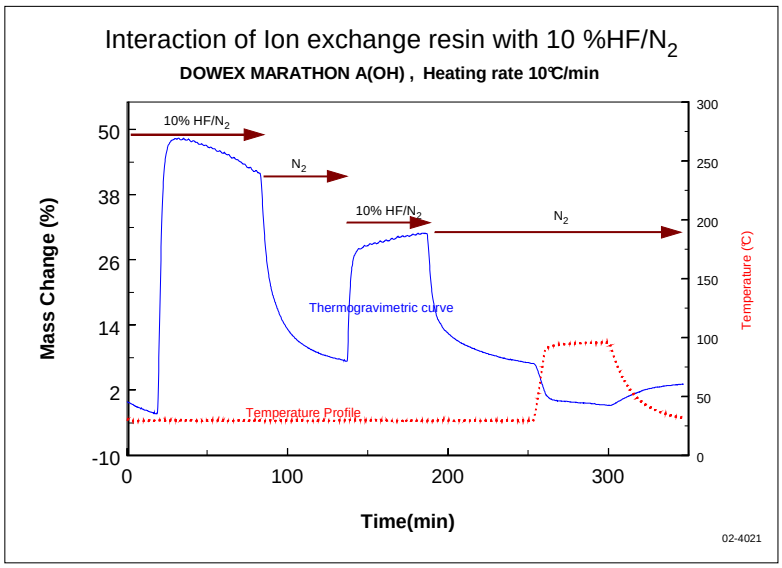


Figure 3.29: Thermogravimetric curve of Dowex Marathon A after exposure to a 10% HF/N_2 mixture

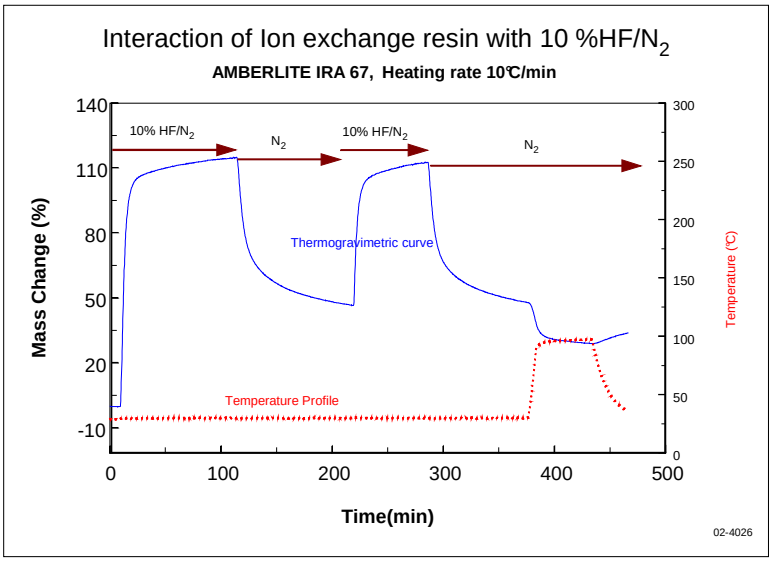


Figure 3.30: Thermogravimetric curve of Amberlite IRA 67 after exposure to a 10% HF/N_2 mixture

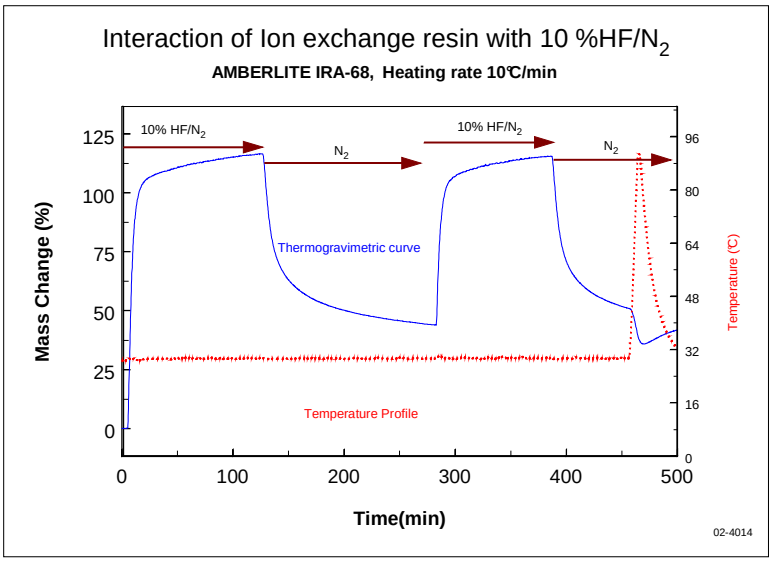


Figure 3.31: Thermogravimetric curve of Amberlite IRA 68 after exposure to a 10% HF/N_2 mixture

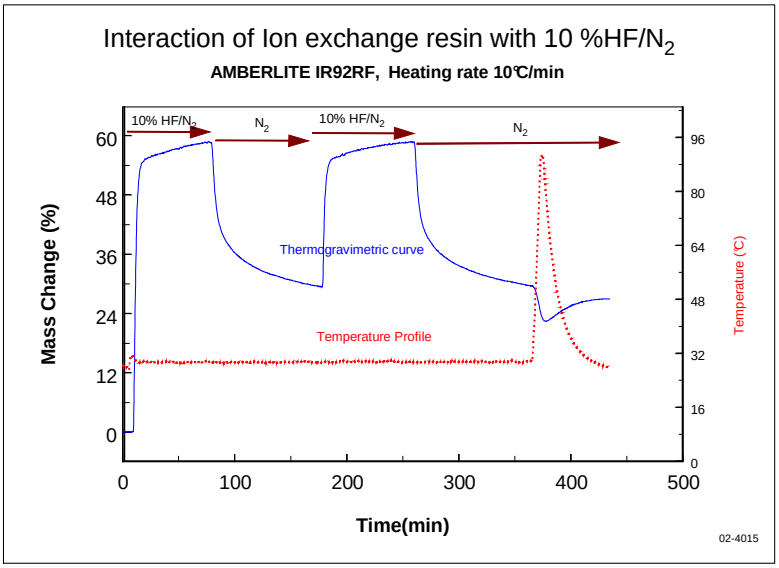


Figure 3.32: Thermogravimetric curve of Amberlite IR 92 RF after exposure to a 10% HF/N_2 mixture

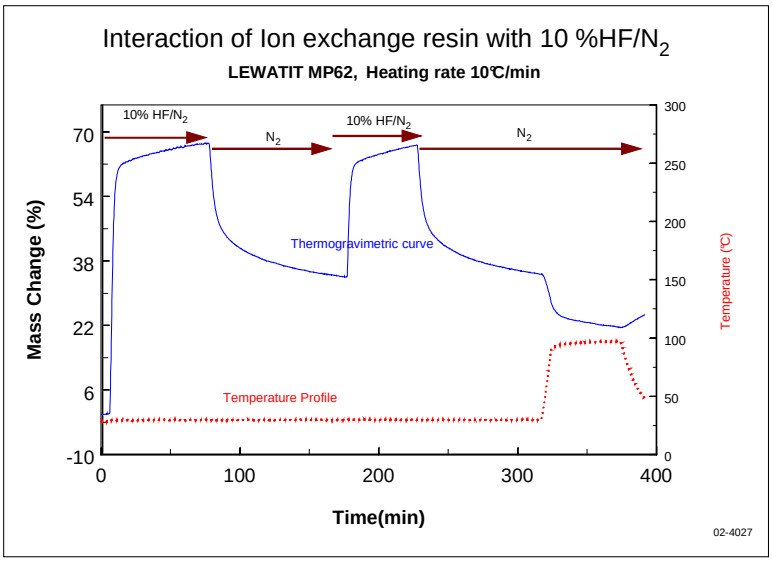


Figure 3.33: Thermogravimetric curve of Lewatit MP62 after exposure to a 10% HF/N_2 mixture

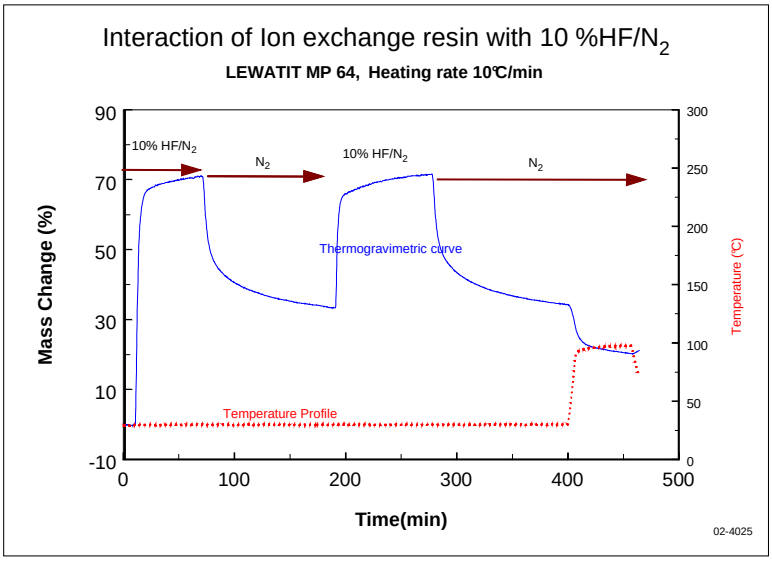


Figure 3.34: Thermogravimetric curve of Lewatit MP 64 after exposure to a 10% HF/N_2 mixture

Appendix 2

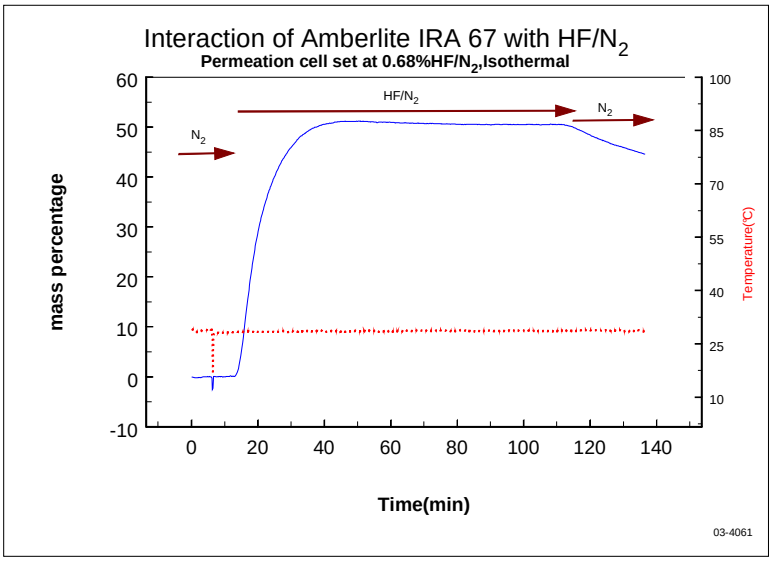


Figure 3.57: Thermogravimetric curve of Amberlite IRA 67 from a 0.68% HF/N_2 mixture

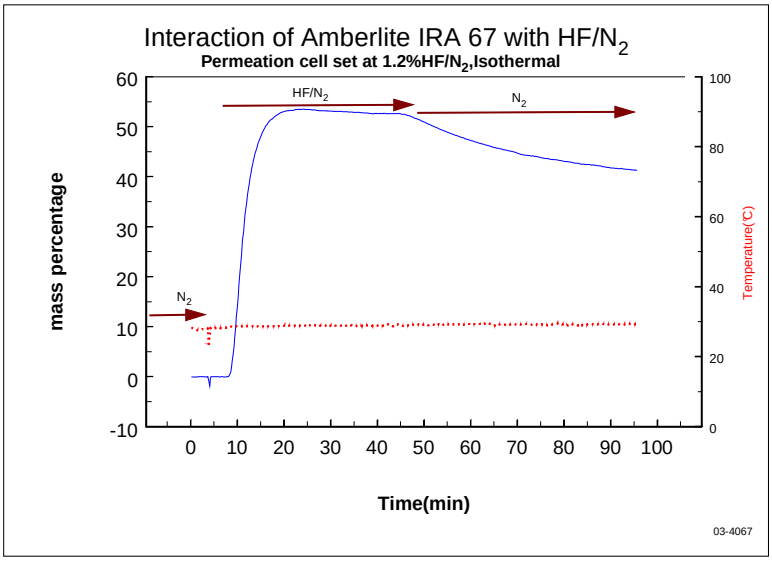


Figure 3.58: Thermogravimetric curve of Amberlite IRA 67 from a 1.2% HF/N_2 mixture

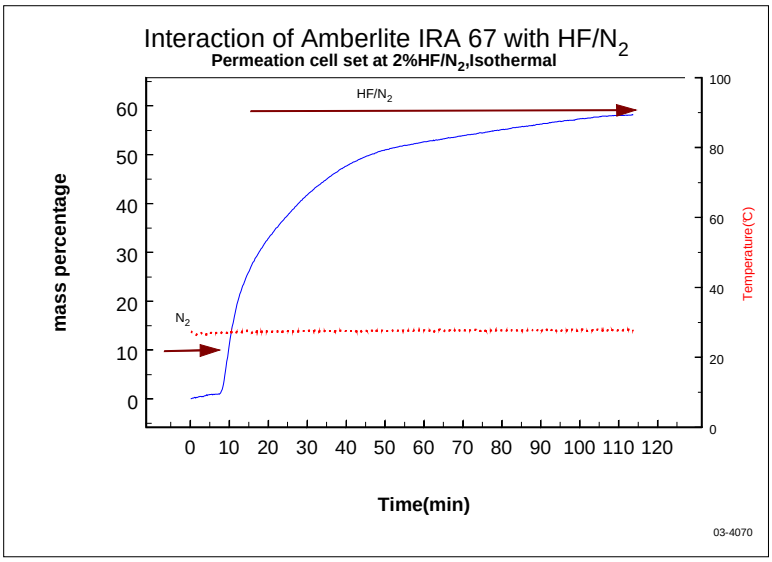


Figure 3.59: Thermogravimetric curve of Amberlite IRA 67 from 2% HF/N_2 mixture

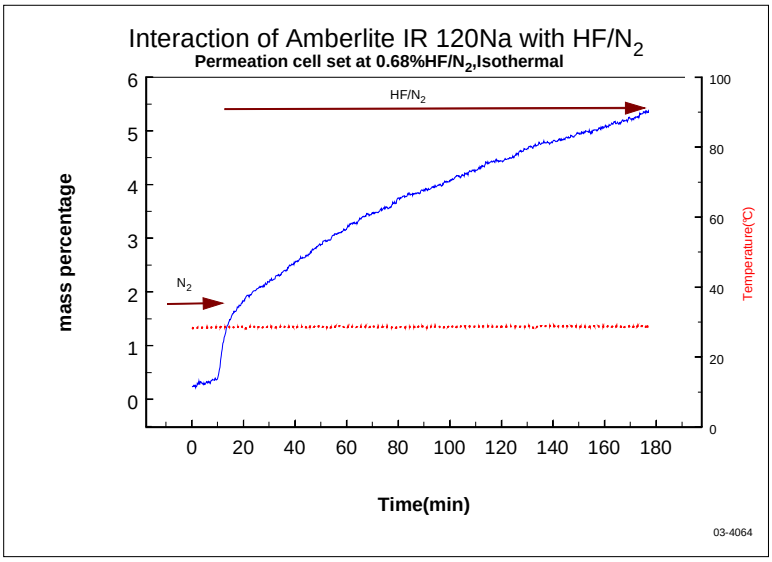


Figure 3.60: Thermogravimetric curve of Amberlite IR 120Na from a 0.68% HF/N_2 mixture

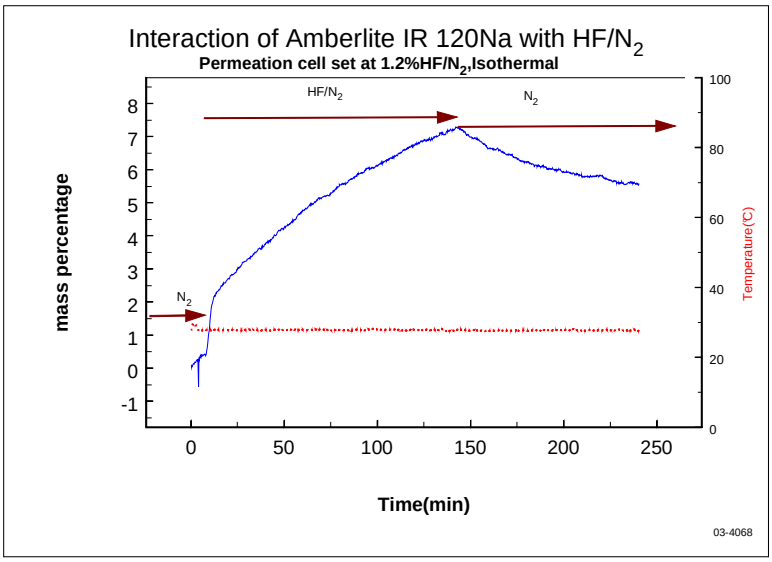


Figure 3.61: Thermogravimetric curve of Amberlite IR 120Na from a 1.2% HF/N_2 mixture

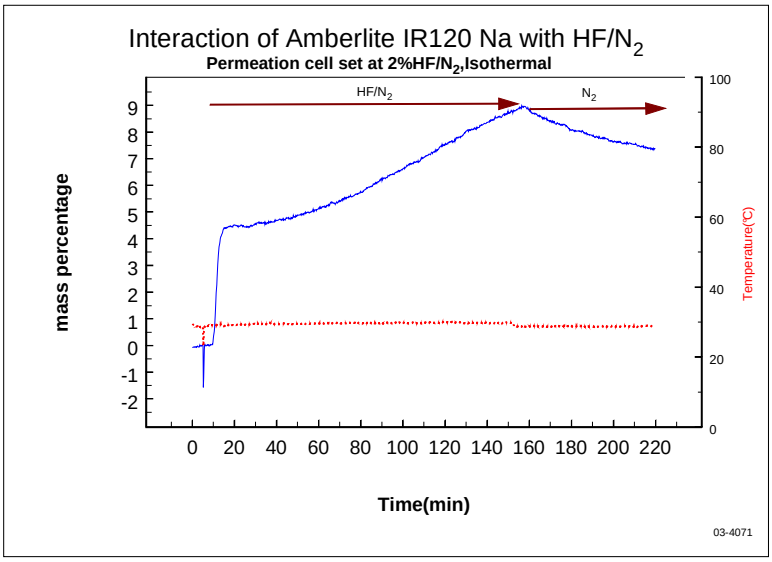


Figure 3.62: Thermogravimetric curve of Amberlite IR 120Na from a 2% HF/N_2 mixture

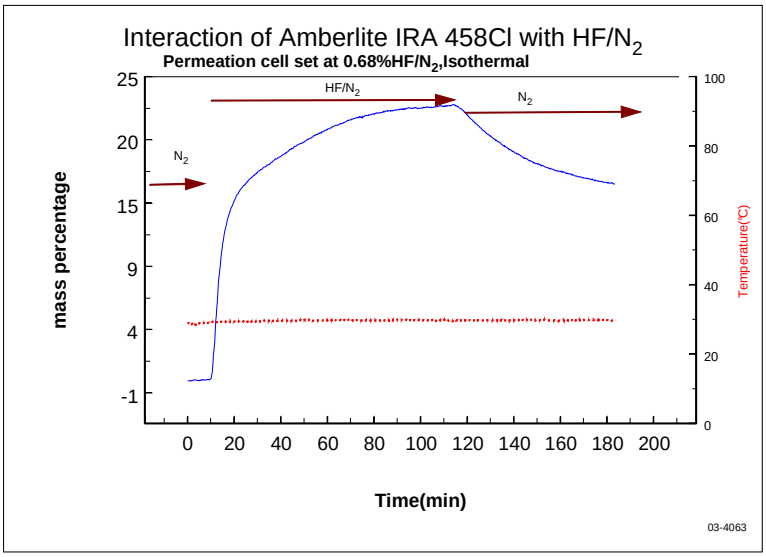


Figure 3.63: Thermogravimetric curve of Amberlite IRA 458Cl from a 0.68% HF/N_2 mixture

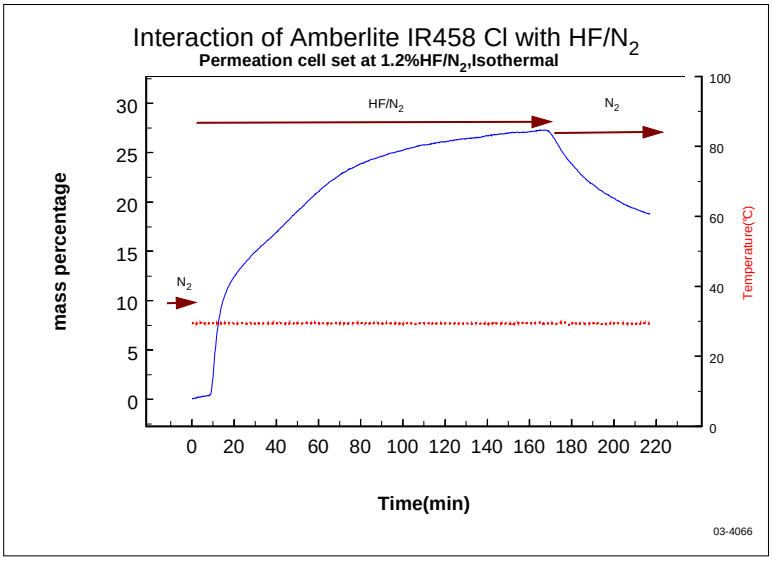


Figure 3.64: Thermogravimetric curve of Amberlite IRA 458Cl from a 1.2% HF/N_2 mixture

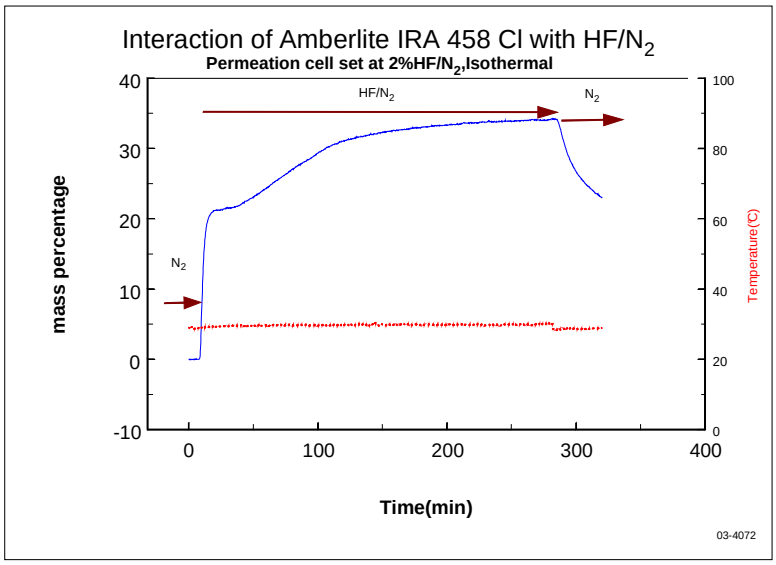


Figure 3.65: Thermogravimetric curve of Amberlite IRA 458Cl from a 2% HF/N_2 mixture

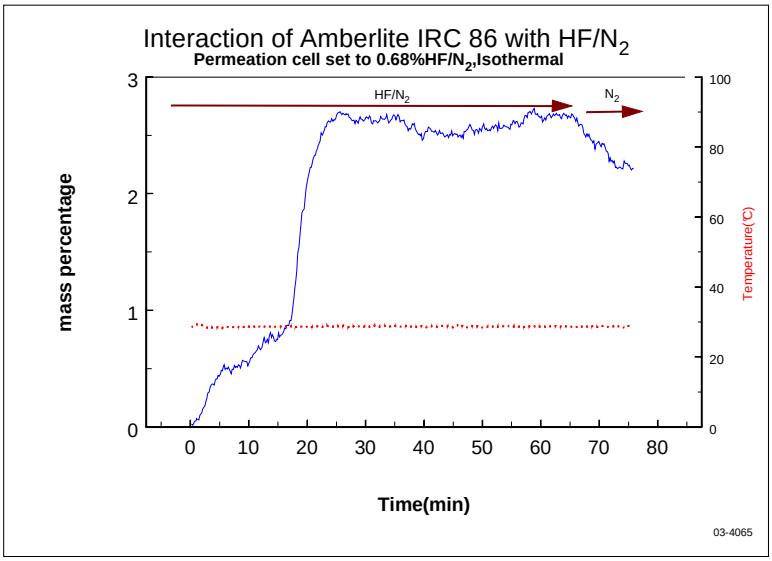


Figure 3.66: Thermogravimetric curve of Amberlite IRC 86 from a 0.68% HF/N_2 mixture

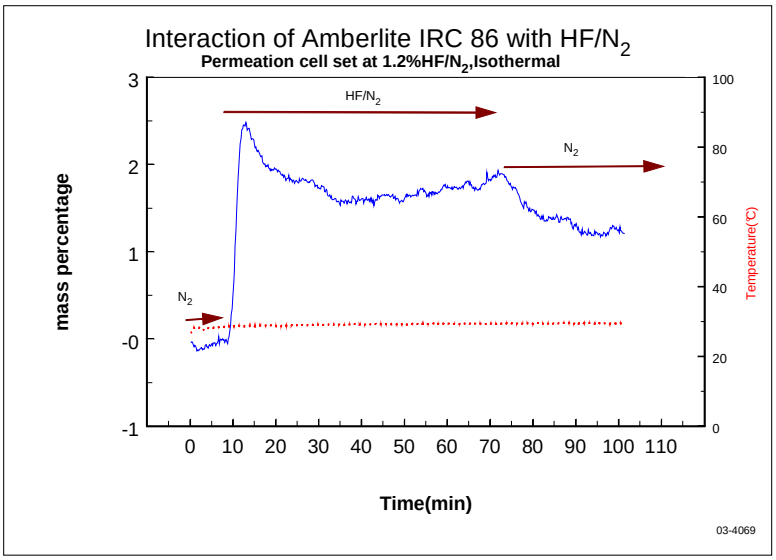


Figure 3.67: Thermogravimetric curve of Amberlite IRC 86 from a 1.2% HF/N_2 mixture

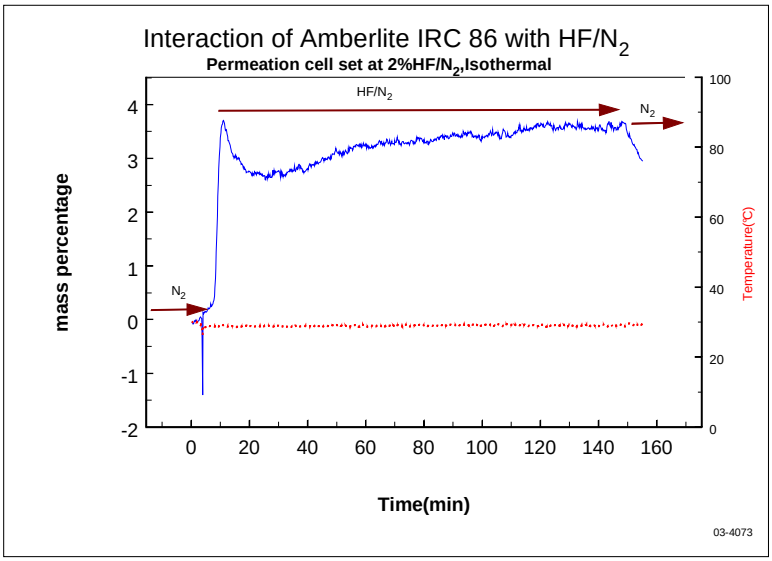


Figure 3.68: Thermogravimetric curve of Amberlite IRC 86 from 2% HF/N_2 mixture

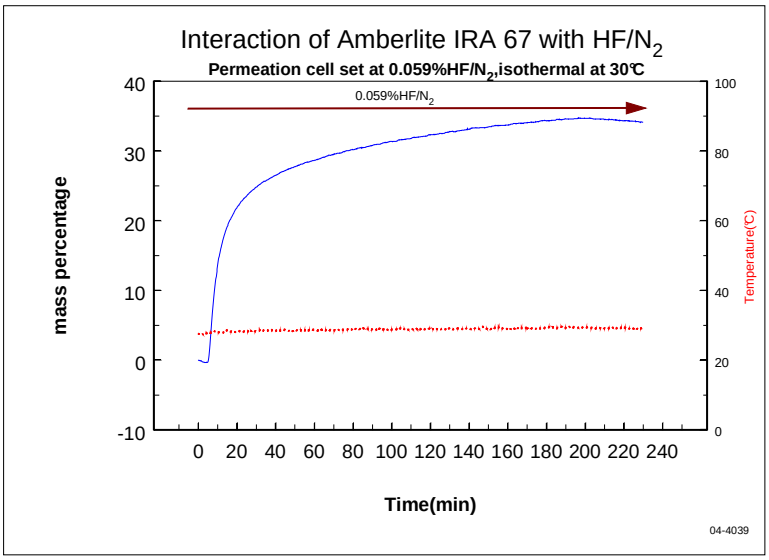


Figure 3.71: Thermogravimetric curve of the uptake of HF by Amberlite IRA 67 from 0.059% HF/N_2 mixture

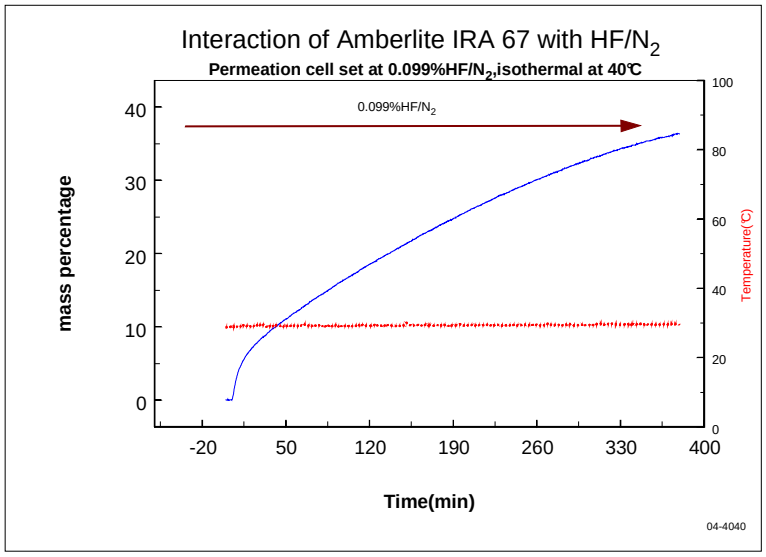


Figure 3.72: Thermogravimetric curve of Amberlite IRA 67 from 0.099% HF/N_2 mixture

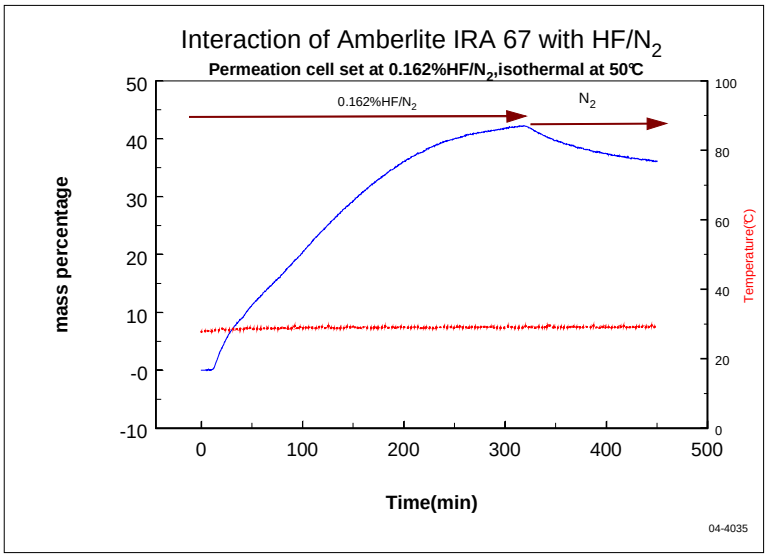


Figure 3.73: Thermogravimetric curve of Amberlite IRA 67 from 0.162% HF/N_2 mixture

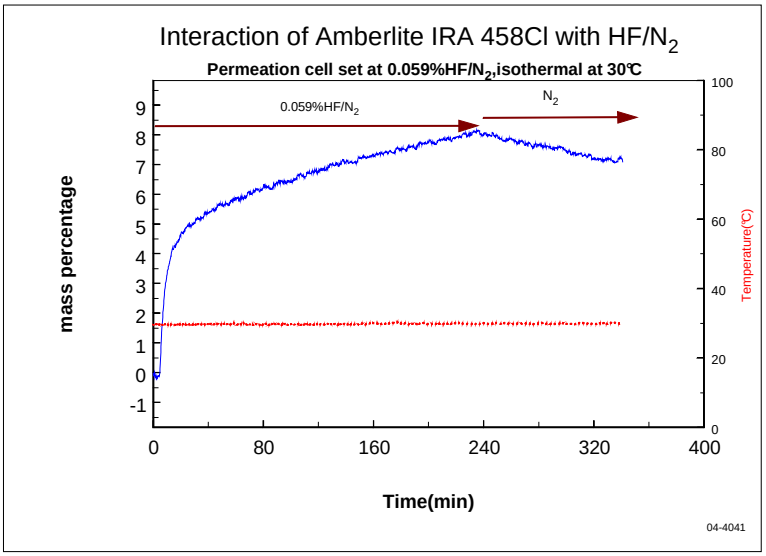


Figure 3.74: Thermogravimetric curve of Amberlite IRA 458Cl from a 0.059% HF/N_2 mixture

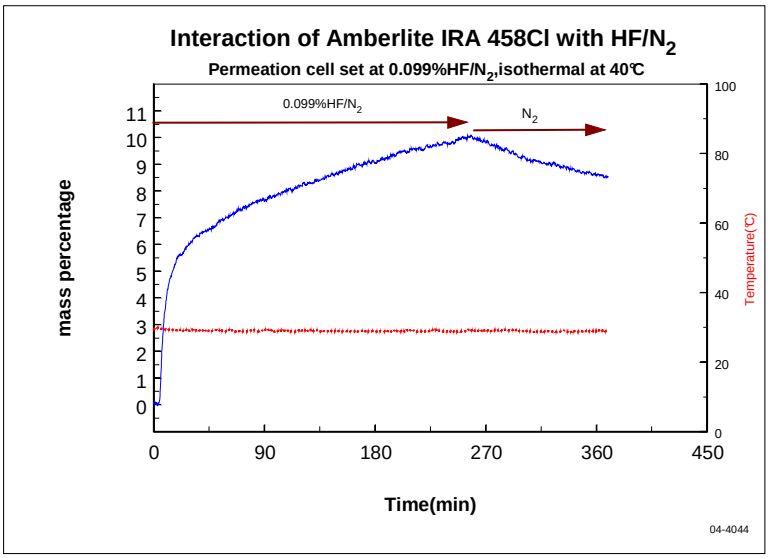


Figure 3.75: Thermogravimetric curve of Amberlite IRA 458Cl from a 0.099% HF/N_2 mixture

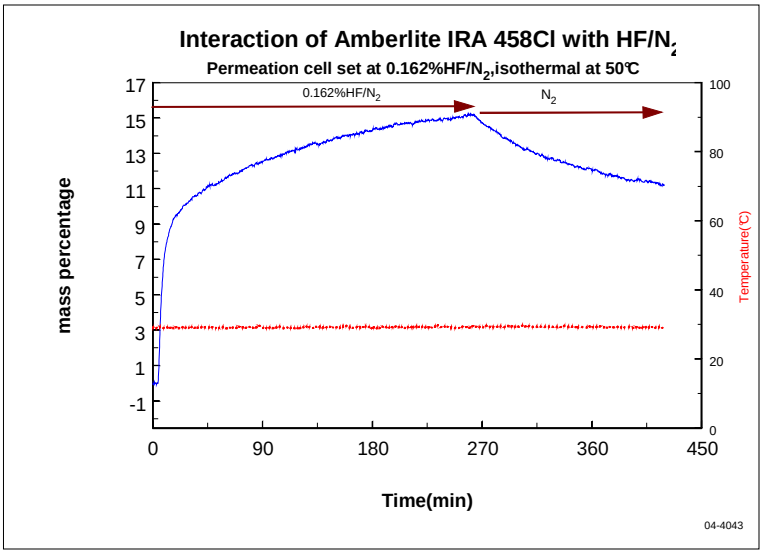


Figure 3.76: Thermogravimetric curve of Amberlite IRA 458Cl from a 0.162% HF/N_2 mixture